

Volcanism, Hydrothermal Processes and Faunal Communities at Shallow Submarine Volcanoes, Bransfield Back-Arc, Antarctica

CRUISE REPORT
RV SONNE CRUISE SO-155
(BMBF FK 03G0155A)

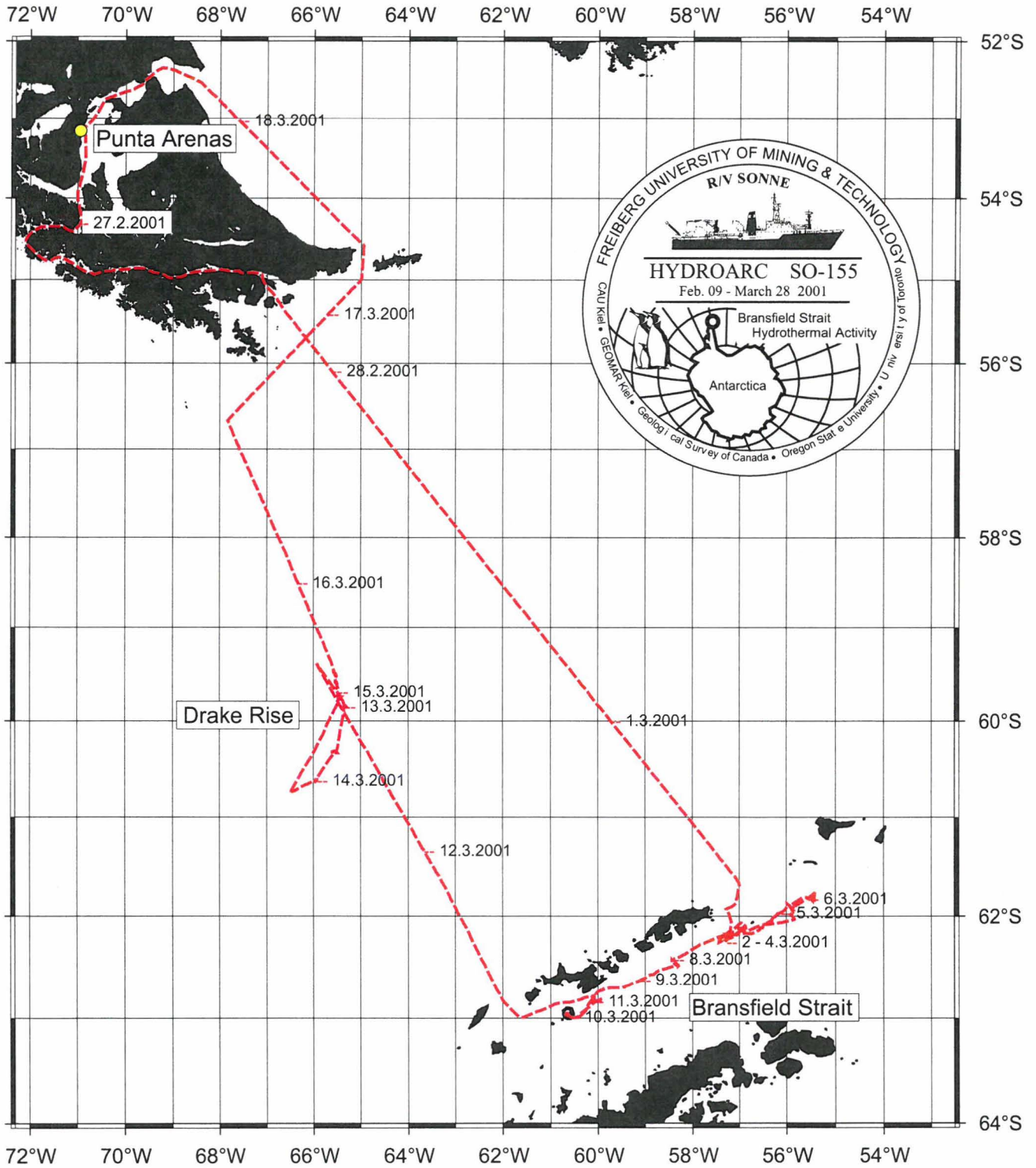
February 09 – March 28, 2001
Balboa (Panama) – Valparaiso (Chile) – Punta Arenas (Chile) –
Valparaiso (Chile)

Peter M. Herzig, Peter Stoffers, Mark D. Hannington, Sven Petersen
Yannick Beaudoin, Klaus-Peter Becker, Claudia Buley, Anke Dählmann, Leander Franz,
Susanne Fretzdorff, Roger Hekinian, Bernd Höppner, Ian R. Jonasson, Randy Keller,
Alexander Konschak, Thomas Kuhn, Claudia Reimann, Heiko Sahling, Rolf Schmaljohann,
Ulrich Schwarz-Schampera, Thomas Seifert, Kurt Stammer,
Jörg Sühling, Manuela Wagner, Tim Worthington

April 2001
Freiberg University of Mining and Technology

Cruise Track SO-155

Leg Punta Arenas - Punta Arenas



Volcanism, Hydrothermal Processes and Faunal Communities at Shallow Submarine Volcanoes, Bransfield Back-Arc, Antarctica

CRUISE REPORT
RV SONNE CRUISE SO-155
(BMBF FK 03G0155A)

Project Leader and Chief Scientist:

Prof. Peter M. Herzig

Institute of Mineralogy

Department of Economic Geology and
Leibniz-Laboratory for Applied Marine Research
Freiberg University of Mining and Technology
Brennhausgasse 14
D-09596 Freiberg, Germany

Tel. +49-3731-39-2662/2626

Fax. +49-3731-39-2610

email: herzig@mineral.tu-freiberg.de

www.mineral.tu-freiberg.de/econgeology/index.html

In Cooperation with

Institute of Geosciences, University of Kiel
GEOMAR, University of Kiel
Institute of Marine Research, University of Kiel
Geological Survey of Canada, Ottawa
University of Toronto, Canada
Oregon State University, U.S.A.

CONTENT

1. Summary	3	P.Herzig, S. Petersen
2. Participants.....	4	M. Wagner
3. Daily Report	9	P. Herzig
4. Introduction and Objectives	18	P. Herzig, S. Petersen
5. Geological Setting.....	19	P. Herzig, S. Petersen
6. Alteration and Mineralization	28	M. Hannington, I. Jonasson, U. Schwarz-Schampera, A. Konschak
7. Petrography of Porphyry Rocks	41	L. Franz, A. Konschak
8. Petrology	44	T. Worthington, R. Hekinian, P. Stoffers, S. Fretzdorff, L. Franz, R. Keller, Y. Beaudoin
9. OFOS Observations	57	S. Petersen, M. Hannington, C. Buley
10. Hydro Bottom Station	73	T. Kuhn, K. Stammer
11. Pore Water Geochemistry,..... Microbiology, and Macrofauna	78	H. Sahling, A. Dählmann, C. Reimann, R. Schmaljohann, J. Süling, P. Stoffers, T. Kuhn, S. Fretzdorff
12. XFR and XRD Analyses	106	K.-P. Becker
13. Whale Monitoring	107	M. Wagner
14. Station List	108	M. Wagner
15. Hydrosweep Mapping	113	S. Petersen
Appendix 1: Rock Descriptions		
Appendix 2: OFOS and TV-grab Protocols		

1 SUMMARY

Cruise SO-155 of R/V SONNE was dedicated to the study of volcanism, hydrothermal activity and faunal communities at shallow submarine volcanoes of the Bransfield Strait, Antarctica. Major results of this cruise include the first comprehensive rock sampling in the Eastern Bransfield Basin and the discovery of a spectacular suite of intrusive rocks with disseminated and vein-type pyrite and chalcopyrite which resemble a porphyry-style of alteration and mineralization so far only known from subaerial copper porphyry deposits at active continental margins and in island arcs. It is suggested that the Gibbs Seamount area represents a transition from volcanic magmatic activity to tectonic rifting of pre-existing arc or remnant arc crust which has exposed arc-related porphyry-style mineralization and alteration. It is currently not known whether the porphyry environment has actually formed within the subaerial arc or at the seafloor during periods of arc rifting. A TV-grab station recovered a 25x15 cm fragment of barite-sphalerite mineralization from the crater of Hook Ridge in the Central Bransfield Basin. Here, sediment temperatures of up to 23°C were measured in gravity cores on deck, clearly indicating that Hook Ridge is currently hydrothermally active. A camera survey of Viehoff Seamount confirmed that the crater is volcanically and hydrothermally inactive. Difficult weather conditions with gale force storm, drift ice, fog and snow severely hampered further work in the Central Bransfield Strait. A detailed investigation of the 9x5km caldera of Deception Island to the southwest indicated weak hydrothermal activity with fumaroles and hot springs in particular close to and at the shore. Due to drift ice which blocked the narrow caldera exit of Deception Island, SONNE had to brake some of the ice and to displace smaller icebergs in order to return to the open sea. However, at this stage it became obvious that, due to the accumulation of drift ice as a result of an intense storm, about 75% of the study area were inaccessible for a non-icebreaker. In order to avoid any risk of becoming enclosed by ice, it was decided to leave the Bransfield Strait premature. A dredging program at the Drake Rise completed the research program of cruise SO-155 on March 15, when SONNE left the Drake Passage for the Atlantic Passage of the Magellan Strait to avoid the next gale force storm south of Cape Horn.

Acknowledgements

Principal funding for the SO-155 cruise HYDROARC was provided by the German Federal Ministry for Education and Research (BMBF FK 03G0155A) to Freiberg University of Mining and Technology. We thank Master Andresen and the officers and crew of the R/V SONNE for their expert seamanship and their excellent cooperation during this cruise which took place under the extremely difficult weather and ice conditions of Antarctica.

2 PARTICIPANTS

Shipboard Scientific Party

01. Herzig, P., Prof. Dr.	Chief Scientist	Freiberg University
02. Petersen, S., Dr.	Co-Chief Scientist	Freiberg University
03. Schwarz-Schampera, U., Dr.	Economic Geology	Freiberg University
04. Becker, Klaus, Dipl.-Min.	Geochemistry	Freiberg University
05. Höppner, B., Dipl.-Chem.	Geochemistry	Freiberg University
06. Seifert, T., Dr.	Geology	Freiberg University
07. Franz, L., PD Dr.	Petrology	Freiberg University
08. Kuhn, T., Dr.	HBS, Alteration	Freiberg University
09. Konschak, A., cand. geol.	Station Work	Freiberg University
10. Buley, C., cand. geol.	Station Work	Freiberg University
11. Wagner, M.	Station Work	Freiberg University
12. Stoffers, P., Prof. Dr.	Petrology	Kiel University, IfG ¹
13. Worthington, T., Dr.	Petrology	Kiel University, IfG ¹
14. Fretzdorff, S., Dr.	Petrology	Kiel University, IfG ¹
15. Hekinian, R., Prof. Dr.	Petrology	Kiel University, IFREMER Brest
16. Süling, J., Dr.	Microbiology	Kiel University, IfM ²
17. Schmaljohann, R., Dr.	Microbiology	Kiel University, IfM ²
18. Dählmann, A., Dr.	Pore Water Chem.	GEOMAR Kiel
19. Reimann, C., cand. geol.	Pore Water Chem.	GEOMAR Kiel
20. Sahling, H., Dipl.-Biol.	Biology	GEOMAR Kiel
21. Stammer, K.	HBS Electronics	RTB Hambühren
22. Keller, R., Dr.	Petrology	OSU ³ , Corvallis, USA
23. Beaudoin, Y., M.Sc.	Economic Geology	University of Toronto, Canada
24. Hannington, M., Dr.	Economic Geology	Geological Survey of Canada
25. Jonasson, I., Dr.	Economic Geology	Geological Survey of Canada

¹ Institute of Geosciences

² Institute of Marine Research

³ Oregon State University

Cruise Report SO-155 (HYDROARC)

Herzig, Peter Prof. Dr.	TU Bergakademie Freiberg Lehrstuhl für Lagerstättenlehre und Leibniz-Labor für Angewandte Meeresforschung Brennhausgasse 14 D-09596 Freiberg Germany	herzig@mineral.tu-freiberg.de +49-3731-39-2626 +49-3731-39-2610
Petersen, Sven Dr.	TU Bergakademie Freiberg Lehrstuhl für Lagerstättenlehre und Leibniz-Labor für Angewandte Meeresforschung Brennhausgasse 14 D-09596 Freiberg Germany	sven.petersen@mineral.tu-freiberg.de +49-3731-39-2315 +49-3731-39-2610
Schwarz-Schampera, Ulrich Dr.	TU Bergakademie Freiberg Lehrstuhl für Lagerstättenlehre und Leibniz-Labor für Angewandte Meeresforschung Brennhausgasse 14 D-09596 Freiberg Germany	schwarz@mineral.tu-freiberg.de +49-3731-39-2315 +49-3731-39-2610
Becker, Klaus-Peter Dipl.-Min.	TU Bergakademie Freiberg Lehrstuhl für Lagerstättenlehre und Leibniz-Labor für Angewandte Meeresforschung Brennhausgasse 14 D-09596 Freiberg Germany	kpbecker@mineral.tu-freiberg.de +49-3731-39-3273 +49-3731-39-2610
Höppner, Bernd Dipl.-Chem.	TU Bergakademie Freiberg Lehrstuhl für Lagerstättenlehre und Leibniz-Labor für Angewandte Meeresforschung Brennhausgasse 14 D-09596 Freiberg Germany	hoepfner@mineral.tu-freiberg.de +49-3731-39-2315 +49-3731-39-2610
Seifert, Thomas Dr.	TU Bergakademie Freiberg Lehrstuhl für Lagerstättenlehre und Leibniz-Labor für Angewandte Meeresforschung Brennhausgasse 14 D-09596 Freiberg Germany	seifert@mineral.tu-freiberg.de +49-3731-39-3527 +49-3731-39-2610
Franz, Leander PD Dr.	TU Bergakademie Freiberg Lehrstuhl für Lagerstättenlehre und Leibniz-Labor für Angewandte Meeresforschung Brennhausgasse 14 D-09596 Freiberg Germany	lfranz@mineral.tu-freiberg.de +49-3731-39-2668 +49-3731-39-2610

Cruise Report SO-155 (HYDROARC)

Kuhn, Thomas Dr.	TU Bergakademie Freiberg Lehrstuhl für Lagerstättenlehre und Leibniz-Labor für Angewandte Meeresforschung Brennhausgasse 14 D-09596 Freiberg Germany	thomas.kuhn@mineral.tu-freiberg.de +49-3731-39-3398 +49-3731-39-2610
Konschak, Alexander cand. geol..	TU Bergakademie Freiberg Lehrstuhl für Lagerstättenlehre und Leibniz-Labor für Angewandte Meeresforschung Brennhausgasse 14 D-09596 Freiberg Germany	steinaxt@hotmail.com +49-3731-383101
Buley, Claudia cand. geol.	TU Bergakademie Freiberg Lehrstuhl für Lagerstättenlehre und Leibniz-Labor für Angewandte Meeresforschung Brennhausgasse 14 D-09596 Freiberg Germany	buley@merkur.hrz.tu-freiberg.de +49-3731-449202
Wagner, Manuela	TU Bergakademie Freiberg Lehrstuhl für Lagerstättenlehre und Leibniz-Labor für Angewandte Meeresforschung Brennhausgasse 14 D-09596 Freiberg Germany	wagnerm@mineral.tu-freiberg.de +49-3731-39-2662 +49-3731-39-2610
Stoffers, Peter Prof. Dr.	Universität Kiel Institut für Geowissenschaften Olshausenstraße 40 D-24118 Kiel Germany	pst@ghi.uni-kiel.de +49-431-880-2850 +49-431-880-4376
Worthington, Tim Dr.	Universität Kiel Institut für Geowissenschaften Olshausenstraße 40 D-24118 Kiel Germany	tw@ghi.uni-kiel.de +49-431-880-2854 +49-431-880-4376
Fretzdorff, Susanne Dr.	Universität Kiel Institut für Geowissenschaften Olshausenstraße 40 D-24118 Kiel Germany	sf@ghi.uni-kiel.de +49-431-880-2085 +49-431-880-4376
Hekinian, Roger Prof. Dr.	Universität Kiel Institut für Geowissenschaften Olshausenstraße 40 D-24118 Kiel Germany	rh@ghi.uni-kiel.de +49-431-880-2085 +49-431-880-4376
Dählmann, Anke Dr.	BIOLAB c/o GEOMAR Kiel Wischhofstraße 1-3 D-24148 Kiel Germany	adaehlmann@geomar.de +49-431-600-2609 +49-431-600-2960

Cruise Report SO-155 (HYDROARC)

Reimann, Claudia cand. geol.	GEOMAR Kiel Wischhofstraße 1-3 D-24148 Kiel Germany	stu37323@mail.uni-kiel.de
Sahling, Heiko Dipl.-Bio.	GEOMAR Kiel Wischhofstraße 1-3 D-24148 Kiel Germany	hsahling@geomar.de +49-431-600-2600 +49-431-600-2928
Süling, Jörg Dr.	Universität Kiel Institut für Meereskunde Düsternbrookerweg 20 D-24105 Kiel Germany	jsuehling@ifm.uni-kiel.de +49-431-597-3849 +49-431-567876
Schmaljohann, Rolf Dr.	Universität Kiel Institut für Meereskunde Düsternbrookerweg 20 D-24105 Kiel Germany	rschmaljohann@ifm.uni-kiel.de +49-431-597-3849 +49-431-597-3994
Stammer, Kurt	RTB Anlagenplanung GmbH Kleine Hög 2 D-29313 Hambühren Germany	RTBGMBH@aol.com +49-5084-5499 +49-5084-1563
Keller, Randy Dr.	College of Oceanic and Atmospheric Sciences Oregon State University 104 Ocean Admin Building Corvallis OR 97331-5503 USA	rkeller@oce.orst.edu +1-541-737-2354 +1-541-737-2064
Beaudoin, Yannick M.Sc.	University of Toronto Department of Geology 22 Russell St. Toronto, Ontario, M5S 3B1 Canada	beaudoin@geology.utoronto.ca +1-416-918-0665 +1-416-918-3938
Hannington, Mark D. Dr.	Geological Survey of Canada Mineral Resources Division 601, Booth Street Ottawa, Ontario K1A 0E8 Canada	mhanning@nrcan.gc.ca +1-613-996-4865 +1-613-996-9820
Jonasson, Ian R. Dr.	Geological Survey of Canada Mineral Resources Division 601, Booth Street Ottawa, Ontario K1A 0E8 Canada	ijonasso@nrcan.gc.ca +1-613-996-2766 +1-613-996-9820

Ship's Crew

01. Andresen, H.	Master	RF GmbH Bremen
02. Mallon, L.	Chief Mate	RF GmbH Bremen
03. Löffler, J.	1 st Mate	RF GmbH Bremen
04. Sturm, W.	Radio Officer	RF GmbH Bremen
05. Walther, A.	Surgeon	RF GmbH Bremen
06. Hartig, V.	Chief Engineer	RF GmbH Bremen
07. Guzman-Navarrete, W.	2 nd Engineer	RF GmbH Bremen
08. Rex, A.	2 nd Engineer	RF GmbH Bremen
09. Rieper, U.	Electrician	RF GmbH Bremen
10. Duthel, R.	Chief Electron. E.	RF GmbH Bremen
11. Angermann, R.	Electro. Engineer	RF GmbH Bremen
12. Grigel, J.	System Manager	RF GmbH Bremen
13. Wenz, C.	System Manager	RF GmbH Bremen
14. Stenzler, J.	Fitter	RF GmbH Bremen
15. Lange, G.	Motorman	RF GmbH Bremen
16. Parchow, K.	Motorman	RF GmbH Bremen
17. Fitzthum, R.	Motorman	RF GmbH Bremen
18. Isbrecht, F.	Motorman	RF GmbH Bremen
19. Tiemann	Chief Cook	RF GmbH Bremen
20. Braatz, W.	2 nd Cook	RF GmbH Bremen
21. Wege, A.	Chief Steward	RF GmbH Bremen
22. Grübe, G.	2 nd Stewardess	RF GmbH Bremen
23. Götze, R.	2 nd Steward	RF GmbH Bremen
24. Hadamek, P.	Boatswain	RF GmbH Bremen
25. Hoffmann, W.	A.B.	RF GmbH Bremen
26. Hänel, B.	A.B.	RF GmbH Bremen
27. Vor, H.-J.	A.B.	RF GmbH Bremen
28. Gundera, M.	A.B.	RF GmbH Bremen
29. Bosselmann, K.	A.B.	RF GmbH Bremen

3 DAILY REPORT

February 9-20, 2001

Cruise SO-155 of R/V SONNE started in Balboa, Panama with a transit to the port of Valparaiso, Chile which was reached on February 18. A scientist and a technician of Freiberg University embarked the ship on February 20 to oversee loading of two containers and arrival of air freight.

February 20-25, 2001

During transit from Valparaiso to Punta Arenas, South Chile, which was guided by two Chilean pilots, SONNE passed through spectacular fjord scenery. At this time the HBS system was set up and checked, the computer system was prepared and adapted to the needs of the cruise, and the two containers were partly unloaded.

February 26, 2001

After arrival on February 25, 23 scientists from Freiberg University, Kiel University (Institute of Geosciences, Institute of Marine Research, GEOMAR), the Geological Survey of Canada, the University of Toronto, and Oregon State University embarked the ship which left port at 15.18LT heading for Antarctica. A safety training session was directed by the chief mate, followed by a short science meeting at which the scientists were introduced to each other by the chief scientist. The unloading of the containers was completed and the labs were set up by the respective scientific groups.

February 27, 2001

SONNE continued her journey through the fjords of southern Chile and Argentina and reached the open sea after passing through the Beagle Channel. The two pilots were dropped off at the port of Paso Richmond at 15.54LT. Under calm seas and sunny skies SONNE set course to Bransfield Strait with an ETA of March 01, 11.00LT. A second science meeting was held to acquaint the shipboard scientific party with the scientific objectives of the cruise and to discuss the strategy for the first survey stations. In the late afternoon, SONNE passed the latitude of Cape Horn. The master had first contacts with the meteorologists onboard POLARSTERN who are supposed to provide a regional weather and ice forecast for the study area. Additional weather information is expected from the BSH.

February 28, 2001

The seas remained calm during the first night of transit to Bransfield Strait and the weather forecast continued to be good. During the day, the weather was unusually favourable for Drake Passage with very calm seas, blue skies and sunshine. Contrary to the agreement which had been reached with the Federal Environmental Agency (FEA) on February 22 by phone, no fax information regarding restrictions for the use of Hydrosweep and Parasound has been received by noon of this day. In the afternoon, the chief scientist contacted the FEA by fax asking for immediate further instructions and announced that the research program would be carried out according to the plan and schedule submitted to the FEA, as long as no new information is received. Another science meeting took place in the afternoon to up-date the scientific party and to introduce everyone to the scientific objectives of the petrology group. At 21.04LT, SONNE crossed latitude 60° and entered the waters of Antarctica.

March 01, 2001

At restricted visibility conditions due to fog, the first icebergs up to 30 m height were seen in the morning while passing around the NE shores of King George Island. Later on the weather conditions improved while SONNE was passing through fields of drift ice and icebergs of varying size. Since no new information was received from the FEA, a short Hydrosweep survey of Hook Ridge was commenced to determine the off-set to the existing bathymetric maps. A short Parasound survey indicated that the sediment thickness in the hinge area and the crater of Hook Ridge is in the range of 15 m and thus suitable for sampling by piston corer and/or multicorer. An OFOS traverse (01-OFOS) which crossed the crater of Hook Ridge indicated an area (150x50m) of hydrothermal precipitates (Fe oxyhydroxides, amorphous silica, and perhaps sulfides) close to the southern wall of the crater at about 1.050 m water depth. Several temperature anomalies were recorded with the CTD mounted on the OFOS. This initial OFOS run continued to an area SE of the crater where a ZAPS survey carried out during a cruise of R/V PALMER in 1999 had indicated the presence of a hydrothermal plume. Due to an iceberg in the area of interest, the track had to be slightly changed, however no signs of fluid venting were discovered. The night program consisted of two dredge hauls (02-DR, 03-DR) which were targeted at Edifice G and recovered talus and dropstones. A science meeting in the morning of that day introduced the scientific party to the scientific objectives of the pore

water geochemists and the microbiologists. Finally, a fax from the FEA was received that day, giving us permission to carry out the planned research program except for the use of the hydroacoustic systems Hydrosweep and Parasound. It was indicated by the FEA that the use of these systems is to be restricted to certain traverses which total about 15-20 hours for the entire cruise depending on the speed of the ship. The FEA has directed that one hour before Hydrosweep and Parasound surveys commence, a visual and acoustic monitoring for the presence of marine mammals has to be performed, and must continue during the entire survey. When marine mammals are being located, either acoustically or visually, the survey has to be suspended for at least 20 minutes. Hydrosweep and Parasound cannot be used at night or at bad visibility as this would restrict the monitoring program. The results of this monitoring must be documented in a protocol for submission to the FEA not later than 8 weeks after the cruise end. Seabed sampling, as well as the use of OFOS, HBS or CTD rosette sampler, is not restricted. A copy of the FEA letter will be faxed to BEO Warnemünde.

March 02, 2001

Three dredge hauls were successfully carried out at Edifice G which is located NE of Hook Ridge and contained both olivine basalt and feldspar-phyric dacite. During the day, two TV-grab stations in the crater of Hook Ridge recovered hydrothermally affected sediment. Measurements onboard revealed a maximum temperature of 16°C in the sediment, indicating a higher in-situ temperature before cooling by bottom water at a temperature of only -1.6°C. One of the TV-grabs (06-GTVA) contained a 25x15cm fragment of barite-sphalerite mineralization which is the first of this kind recovered from Hook Ridge. In the late afternoon, the wind and sea states changed and station work had to be suspended due to the risk of hitting icebergs which become difficult to locate in wave troughs.

March 03, 2001

Since the weather had improved over night, two further TV-grab stations were carried out to sample hydrothermal precipitates and massive sulfides in the crater of Hook Ridge at about 1.000m depth. The first of these two grabs recovered hydrothermally altered hyaloclastite, whereas the second grab failed to sample hydrothermal material. Two deployments of the multicorer in the sedimented part of the Hook Ridge crater were unsuccessful with respect to sediment recovery but returned a piece of fresh, glassy lava. Finally, a gravity corer was placed into the crater of Hook Ridge and returned more than

4m of homogeneous hemipelagic sediment which contained a single pumice layer. Maximum temperature in the sediment was 23°C which again clearly indicates elevated heat flow due to hydrothermal activity within the sedimentary column covering the volcanic rocks in this area. A dredge haul targeted at the hydrothermal precipitates at Hook Ridge returned empty. Following a 2 hour transit to Bridgeman Ridge which is located in the westernmost part of the Eastern Bransfield Basin, a comprehensive 2 days dredging program was initiated. Three dredge hauls were directed at sampling different areas of Bridgeman Ridge which, similar to the rest of the Eastern Bransfield Basin, are largely unknown with respect to volcanic petrology and hydrothermal activity. These dredge hauls (13-DR, 14-DR, 15-DR) returned a collection of dropstones, glacial erratics, and basalt fragments. The dropstones and the glacial erratics document the complex geological history of this particular part of Antarctica, while the basalts are the first volcanic rocks to be recovered from the area of Bridgeman Ridge.

March 4, 2001

The next phase of dredging at Bridgman Ridge commenced during the day. The first dredge haul at the central section of Bridgeman Ridge recovered a full load (several hundred kilograms) of olivine-rich basalt and aphyric, strongly vesicular basalt fragments together with a large (1 m diameter) basalt pillow. Meanwhile the first methane data for the sediments recovered from the crater of Hook Ridge (11 SL) became available and indicate that there is a continuous supply of methane from the volcanic basement into the overlying sediments. Dredge hauls 16-DR and 17-DR recovered several pillow fragments of black, vesicular olivine basalt. After a short transit, dredging commenced at the north end of Spanish Ridge at 61°52.4'S/55°59.0'W but then had to be abandoned due to drift ice in the area.

March 5, 2001

Dredging continued throughout the day in the Eastern Bransfield Basin further to the northeast at Gibbs Seamount, close to Gibbs Island. Dredge hauls 20-DR and 21-DR recovered a spectacular suite of intrusive rocks including fine-grained felsic subvolcanic intrusions with disseminated and vein-type pyrite and chalcopyrite which resembles a porphyry style of alteration and mineralization. The samples mainly consist of feldspar-phyric subvolcanic intrusions of dacitic to andesitic composition. Some of these samples are brecciated and strongly altered to chlorite+epidote and pyrite+hematite as well as K-

feldspar. It is suggested that the Gibbs Seamount area represents a transition from volcanic magmatic activity to tectonic rifting of pre-existing arc or remnant arc crust which has exposed arc-related porphyry-style mineralization and alteration. It is currently open to question whether the porphyry environment has actually formed within the subaerial arc or at the seafloor during periods of arc rifting. These samples, however, represent the first copper porphyry style mineralization recovered from the modern seafloor and resemble similar mineralization in the subaerial island arcs of the western Pacific (Philippines, Papua New Guinea etc.). Dredge haul 22-DR at the uppermost flank of Gibbs Seamount sampled a variety of dropstones, and also fresh diabase, gabbro, microdiorite, and a breccia consisting of arc-rock fragments. Dredge haul 23-DR which targeted a scarp northeast of Gibbs Seamount mainly returned plagioclase-rich andesite and some dolerite. Both dredges confirmed that volcanic activity in the Eastern Bransfield Basin is restricted to the area southwest of Gibbs Seamount, whereas the northern part of the Eastern Basin is dominated by rifting.

March 6, 2001

Dredging commenced after a short transit to Spanish Ridge which was reached at 03.00LT and continued during most of the day which was foggy with some snowfall at temperatures of -1°C and a wind speed of 10 m/sec. A total of 4 dredge hauls targeted the various seamounts in the area and, with the exception of 27-DR and 28-DR which returned slightly weathered basalt, sampled a great variety of dropstones. These display a cross section of the geology of this part of Antarctica and include sandstone, pumice, mica schist, granite, and gneiss. Following this major dredging program, the zodiac was used to take an ice sample of several kilogram from a nearby iceberg for environmental studies. The shipboard scientific party agreed that the petrological sampling program in the Eastern Bransfield Basin was successfully completed due to the particular efforts of the group from Kiel University (Institute of Geosciences) with 16 dredge hauls at Bridgeman Ridge, Spanish Ridge, and Gibbs Seamount of which only 2 dredge hauls did not recover rocks.

March 7, 2001

After a 4 hours transit from Spanish Ridge back to Hook Ridge, a sediment sampling program mainly involving the groups of GEOMAR and the Institute of Marine Research at Kiel University was completed during the night in the crater of Hook Ridge under difficult weather and ice conditions. A total of seven deployments of the multicorer resulted in

recovery of several series of sediment samples for porewater geochemistry and microbiology. Some of the push corers contained Fe-oxyhydroxide crusts, but all samples had relatively low temperatures reaching a maximum of only 4.5°C. The multicorer sampling was followed by the deployment of a gravity corer which recovered about 4 m of sediment. Temperature measurements in the core revealed a maximum temperature of 36.6°C which clearly indicates that the crater area of Hook Ridge is hydrothermally active. Two dredge hauls were directed towards sampling of hydrothermal precipitates in the crater of Hook Ridge, one of which returned hydrothermally altered sediment impregnated with crystalline native sulfur. Due to increasing drift ice and an accumulation of icebergs in the area of Hook Ridge, the transit to Viehoff Seamount (about 3.5 hours southwest of Hook Ridge) began at 04.00pm. At arrival, OFOS (41 OFOS) was deployed to survey the 3.5 km diameter crater of Viehoff. Except for a few weak temperature anomalies, no signs of hydrothermal activity were recorded and Viehoff is considered to be both volcanically and hydrothermally inactive. Arrival of a gale force storm caused station work to be abandoned at 01.00LT.

March 8, 2001

Since the weather conditions had not improved over night, it was decided that SONNE would continue to shelter in the area of Viehoff Seamount, which remained free of drift ice and major fields of icebergs. The wind during the day reached force 11 (75 km/h) with snowfall and fog. Due to increasing winds, drift ice and bad visibility in the afternoon it was decided to sail to the southwest towards Three Sisters where SONNE sheltered over night.

March 9, 2001

As the weather had improved over night, SONNE left the area of Three Sisters at 07.00LT and sailed towards Deception Island, which was reached at 09.00LT. After we had passed the entrance to the 9x5km caldera, which is one of the larger worldwide, a planned HBS survey had to be suspended due to an instrument failure. Instead, the gravity corer was deployed three times in the eastern crater but recovered only sediment in the core catcher. The OFOS system was used to survey a sediment Mn anomaly which was detected several years ago by a Spanish group. No signs of hydrothermal activity or Mn precipitates were encountered. A second OFOS deployment was directed to survey an inferred NE-SW trending fault array in the central caldera of Deception volcano.

March 10, 2001

A night mapping and temperature survey program was carried out with the Hydro Bottom Station (47-HBS) in several areas of the Deception caldera. At several locations, temperatures of up to 50°C were measured in the sediments. Calibration of the instrument after the station, however, indicated that an internal instrument drift was responsible for these high values and that these values do not represent the outflow of high temperature fluids at the seafloor (see chapter 11 for details). It is therefore not surprising that subsequent sampling of the caldera floor with the multicorer (3 deployments) recovered only cold sediment from 100-150 m depth. During the day, the HBS survey was extended to areas closer to shore in the vicinity of hot springs visible at the shore line (51-HBS) to detect hydrothermal activity which may be related to the ring fractures of Deception Island, the focus of volcanic activity around 1970. The zodiac was then used to take samples for microbiological purpose at hot springs and fumaroles of Fumarole Bay. At the same time, a series of rock samples including pre-volcanic basement and fresh lavas of the 1970 eruption were collected. In the afternoon, it was decided to leave Deception Island for the working areas of the submarine volcanoes Axe and Three Sisters. Approaching the narrow caldera exit it was realized that drift ice had accumulated in that area and partly blocked the passage. In a very slow approach, SONNE broke some of the ice cakes and displaced some of the smaller icebergs in order to reach the open sea of the Bransfield Strait. SONNE then headed for The Axe. In the late afternoon, however, it became obvious that this area was heavily covered by loose pack ice and floes and thus was not accessible for a non- icebreaker. The intense storm of March 8 with southeasterly winds up to force 11 was obviously responsible for the extremely rapid accumulation of ice. According to the radar image and observations on the bridge, the area of closed pack ice and iceberg accumulation blocked the journey to the northeast and covered large areas of the Bransfield Strait. In order to avoid any risk of becoming enclosed by ice during the next storm, it was decided to shelter close to Livingston Island for the night and to leave the Bransfield Strait as soon as possible.

March 11, 2001

In the morning, the ship moved further to the southeast and discovered that the passage around Deception Island was still open and largely free of ice. SONNE then set course for the Drake Passage to alternatively map and sample the Drake Rise, which is the failed ocean ridge linked to the South Shetland trench, arc, and back-arc (Bransfield Strait)

system. Smith and Sandwell maps were produced by the system operators in order plan the Hydrosweep survey. It was decided to map the two northernmost segments of Drake Rise close to the Chile Trench. During the night the weather turned stormy resulting in a large swell and rougher seas.

March 12, 2001

Since most of the important mapping and sampling targets of the Drake Rise are located within the 200 nm zone of Chile, the Chief Scientist contacted the German Embassy in Santiago de Chile by phone and fax seeking help in obtaining a work permit from the Chilean authorities. Meanwhile, a dredging program started at those segments of Drake Rise which are situated immediately south of the 200 nm limit. The FEA was informed by fax that some of the dredging would take place just south of latitude 60°S, as this area was not part of the original work program in Antarctica. Out of two dredge hauls at the second segment (segment 2) north of the Hero Fracture Zone, one returned empty, but the other contained strongly chloritized (+smectite+illite) and partly silicified hyaloclastites and pillow breccias, in addition to some pillow fragments with fresh glass, indicating that volcanism may not have completely ceased in the area as previously thought. A repeat of the empty dredge haul at segment 2 recovered some glassy pillow fragments and a variety of older volcanic rocks which are partly coated by manganese and Fe-oxyhydroxide (55-DR).

March 13, 2001

Dredging commenced at 07.30LT after permission by the FEA was received for a 24 h sampling program south of latitude 60°. Three dredge hauls (56, 57, 58-DR) were directed at the southernmost segment of the Phoenix Ridge which is intersecting the Hero Fracture Zone and located about 45nm south of latitude 60°S. Dredge hauls 56 and 57 recovered olivine and plagioclase phyric basalt.

March 14, 2001

During the night, a strong swell had developed in the working area which made dredging difficult. After tensions of up to 15 tonnes, dredge 58-DR returned upside down with broken weaklink and empty at 08.00LT and thus dredging south of latitude 60°S finished within the 24 hour limit given by the FEA. A fax message received from the German Embassy in Santiago de Chile informed us that the Chilean authorities have given us a research permit at short notice. However, one of the pre-requirements was to take a

Chilean observer on board in Punta Arenas. As the transit would take about 5 days, this was no option. It was decided to return to segment 2 of the Phoenix Ridge to further investigate the area where (hydrothermally altered) strongly chloritized rocks were recovered in dredge haul 53-DR. On arrival at site a strong swell had developed due to a large low pressure area with gale force wind in the western Drake Passage. As station work was not possible at these conditions, R/V SONNE was on stand-by waiting for the swell to decrease.

March 15, 2001

As the weather conditions did not improve over night and since the weather forecast indicated another gale force storm with large swells, it became obvious that station work would not be possible for the next few days. Chief Scientist and Master agreed that it would be wise to leave the Drake Passage as soon as possible to avoid the storm. At 13.00LT R/V SONNE finally set sail for Punta Arenas with a premature ETA of March 18, 15.00LT.

March 16, 2001

During the night SONNE had to pass through heavy seas with large swells which at times allowed a speed of only 6 kn. Since the aftdeck was closed by the Master for security reasons with respect to the strong pitch and roll of the ship, the containers could not be loaded. Instead, the labs were cleaned up and preparation of the cruise report commenced. In the afternoon, R/V SONNE sailed the Pacific-Atlantic passage around Cape Horn from west to east and headed for the Atlantic entrance of the Magellan Strait where the pilots are on stand-by for March 18, 07.00LT.

March 17, 2001

SONNE continued her journey along the east coast of South America at rough seas and sunshine. Despite the swell, loading of the containers for GEOMAR Kiel, the University of Kiel, and FU Berlin (HBS container) began in the morning. Preparation of the cruise report proceeded as all groups agreed to have this document finished by the time the ship docks. In the evening, a reception was held at which the Chief Scientist addressed the shipboard scientific party as well as the crew and thanked all participants for their support. In particular Master Andresen and his officers was thanked for their professional seamanship and safe guidance of the SONNE through all difficulties encountered during this cruise.

March 18, 2001

At 07.00LT SONNE met two Chilean pilots at the entrance to the Magellan Street who guided the ship savely the remaining 90 nm through the fjords of Chile and Argentina to Punta Arenas. Port was reached at 15.00LT (two days earlier than originally scheduled) and 22 scientists disembarked the ship which left Punta Arenas the next day for Valparaiso where cruise SO-155 ended on March 28, 2001.

4 INTRODUCTION AND OBJECTIVES

Evidence for hydrothermal activity in the Bransfield Strait was first deduced from anomalous heat flow values (Nagihara & Lawver, 1989, Lawver et al., 1995) and the occurrence of thermogenic hydrocarbons in altered sediments in the King George Basin (Whiticar et al., 1985; Brault and Simoneit, 1990). Elevated concentrations of hydrothermal tracers such as Mn and ^3He , high particle concentration in the water column as well as the occurrence of Fe-Zn-Cu-sulfides, Zn-chlorides, and Fe- and Zn-oxides in hydrothermally influenced sediments clearly indicated hydrothermal activity in the vicinity of several volcanic edifices (Schlosser et al., 1988, Lawver et al., 1995). A detailed investigation of the water column identified three sites of hydrothermal activity at Hook Ridge (Edifice F), Three Sisters (Edifice D), and Little Volcano (Edifice C; Klinkhammer et al., 1996; Chin et al., 1996). Hydrothermal venting was also located within the sunken caldera of Deception Island (Chin et al., 1996; Rey et al., 1997).

In December 1997, areas of hydrothermal activity were located and sampled at Hook Ridge during cruise ANT/2 of R/V Polarstern (Bohrmann et al., 1999). A follow-up cruise of R/V N. B. Palmer (Klinkhammer et al., 1999; Klinkhammer et al., in prep.) confirmed this style of hydrothermal activity and discovered additional sites of low-temperature venting in a central depression at Hook Ridge and at Three Sisters (Petersen et al., 2000). In addition to Hook Ridge and Three Sisters, a detailed bathymetric map of Vielhoff Seamount was produced during this cruise.

The SO-155 HYDROARC cruise of R/V Sonne aimed at a detailed investigation of hydrothermal sites and occurrences in the Bransfield Strait including Hook Ridge, Viehoff

Seamount, Three Sisters, The Axe, and Deception Caldera using a deep-towed camera system (OFOS), a TV-guided grab sampler, the HBS (Hydro Bottom Station), as well as conventional dredges and sediment corer. In addition to the mineralogy, geochemistry and isotope geochemistry of hydrothermal precipitates (Freiberg University), pore water and sediment geochemistry (GEOMAR Kiel) were involved to further constrain the specific characteristics of hydrothermal activity in a pre-rifting back-arc system underlain by either continental crust or an accretionary prism. Furthermore, a comprehensive rock sampling program was carried out at Bridgeman Ridge, Spanish Ridge and Gibbs Seamount in the Eastern Bransfield Basin to study the volcanic evolution and the petrogenetic relationships in this largely unknown area of the Bransfield Strait (Kiel University, Institute of Geosciences and Freiberg University). A microbiological program aiming at DNA identification of microorganism and the analysis of production rates (Kiel University, Institute of Marine Research) as well as a biodiversity and wale observation study (GEOMAR Kiel) completed the research program.

Due to strongly increasing drift ice and iceberg accumulation, only Hook Ridge, Viehoff Seamount, and Deception Island were investigated in some detail before R/V Sonne had to leave the Bransfield Strait premature on March 11, 2001. An alternative dredging program was then carried out at two segments of the Phoenix Ridge (Drake Rise/Drake Passage) which is the failed ocean ridge linked to the South Shetland trench, arc, and back-arc system.

References

- Bohrmann, G., Chin, C.S., Petersen, S., Sahling, H., Schwarz-Schampera, U., Greinert, J., Lammers, S., Rehder, G., Daehlmann, A., Wallmann, K., Dijkstra, S., and Schenke, H.W. (1999) Hydrothermal activity at Hook Ridge in the Central Bransfield Basin, Antarctica. *Geo-Marine Letters* 18: 277-284.
- Brault, M., and Simoneit, B.R.T., 1990, Mild hydrothermal alteration of immature organic matter in sediments from the Bransfield Strait, Antarctica. *Appl. Geochem.* 5: 149-158.
- Chin, C.S., Klinkhammer, G.P., Wilson, C., Lawver, L.A., and Lupton, J.E. (1996) Hydrothermal activity in a nascent basin: the Bransfield Strait, Antarctica. *Eos* 77(46): 413.
- Klinkhammer, G.P., Chin, C.S., Wilson, C., Rudnicki, M., Keller, R.A., Fisk, M.R., and Lawver, L.A. (1996) Results of a search for hydrothermal activity in the Bransfield Strait, Antarctica. *EOS*, Nov.7: 710.
- Klinkhammer, G.P., Chin, C.S., Keller, R., Daehlmann, A., Sahling, H., Sarthou, G., Petersen, S., Smith, F., and Wilson, C. (1999) Discovery of Hydrothermal Vent Sites in Bransfield Strait, Antarctica. *EOS* 80(46): 1174.
- Lawver, L.A., Keller, R.A., Fisk, M.R., and Strelin, J.A. (1995) Bransfield Strait, Antarctic Peninsula: Active extension behind a dead arc. In B. Taylor (ed.), *Backarc Basins: Tectonics and Magmatism*. Plenum Press, New York: 315-342.
- Nagihara, S., and Lawver, L.A. (1989) Heat-flow measurements in the King-George Basin, Bransfield Strait. *Antarctic Journal* 23: 123-125.

- Rey, J., Somoza, L., Martinez-Frias, J., Benito, R., and Martin-Alfageme, S. (1997) Deception Island (Antarctica): a new target for exploration of Fe-Mn mineralization? In Nicholson, K. et al. (eds) *Manganese Mineralization: Geochemistry and Mineralogy of Terrestrial and Marine Deposits*. Geological Society Special Publication 119: 239-251.
- Petersen, S., Schwarz-Schampera, U., Herzig, P.M., Bohrmann, G., and Klinkhammer, G. (2000) Hydrothermal precipitates from shallow-submarine volcanoes in the Bransfield Strait, Antarctica. In Gemmell, J.B., and Pongratz, J., (eds) *Volcanic Environments and Massive Sulfide Deposits, SEG/CODES Field Conference, Hobart, Tasmania*: 149-151.
- Schlosser, P., Suess, E., Bayer, R., and Rhein, M. (1988) ^3He in the Bransfield Strait waters: indication for local injection from back-arc rifting. *Deep-Sea Research* 35: 1919-1935.
- Whiticar, M.J., Suess, E., and Wehner, H. (1985) Thermogenic hydrocarbons in surface sediments of the Bransfield Strait, Antarctic Peninsula. *Nature* 314: 87-90.

5 GEOLOGICAL SETTING

The Bransfield Strait (62° - 54° W and 61° - 64° S) represents a marginal basin which separates the Mesozoic-Cenozoic South Shetland Island Arc in the northwest from the Mesozoic Antarctic Peninsula to the southeast. It is located at the southwestern end of the Scotia Arc (Grácia et al., 1997). The present-day plate configuration to the north of the Antarctic Peninsula and the Scotia arc region is shown in Figure 5.1. Bransfield Strait extends for more than 400 km from Low Island in the southwest to Clarence Island in the northeast, and is commonly between 30 and 38 km wide with a maximum water depth of more than 2.000 m.

The Bransfield Strait consists of three subbasins formed by early stages of rifting within a continental volcanic arc (Lawver et al., 1995). Oceanic lithosphere originating from the Antarctic-Phoenix spreading center (Drake Rise or Phoenix Ridge) in the South Pacific was subducted along the western margin of the Antarctic Peninsula for the past 200 Ma (Tanner et al., 1982; Barker et al., 1991; Pankhurst, 1983; Hole et al., 1991, Grunow et al., 1992). The Antarctic Peninsula and the South Shetland Islands are the result of accretion of oceanic crust and fore-arc basin sedimentary material, which subsequently formed a large accretionary prism. At about 4 Ma, the Antarctic-Phoenix spreading center was abandoned and the remnant Phoenix plate became part of the Antarctic plate.

Island-arc volcanism along the South Shetland Islands can be traced back as far as 145 Ma (Elliot et al., 1983) and was probably episodic (Birkenmajer et al., 1986). No arc-related magmatism younger than 20 Ma has been found in the South Shetland Islands, even though subduction must have continued until 4 Ma (Barker, 1982). Pankhurst and

Smellie (1983) have shown that magmatism becomes younger northeastward, along the length of the arc.

Accretion of Antarctic-Phoenix spreading center segments to the western Antarctic Peninsula occurred over the last 50 Ma (Barker, 1982). Magnetic lineations and dating of volcanic rocks associated with the collision of ridge segments clearly show a northeastward younging series of collision events (Fig. 5.2). Segments of the ridge were subducted to the southeast, until about 4 Ma, when the spreading center immediately southwest of the Hero fracture zone reached the trench (Barker, 1982). The last segments of the Antarctic-Phoenix spreading center (between the Hero and Shackleton fracture zones) were then abandoned offshore of the trench and the last remnant of the Phoenix plate was attached to the Antarctic plate. Plate reconstructions suggest that at least a thousand kilometers of Phoenix plate have been subducted beneath Bransfield Strait since 50 Ma (Barker, 1982; Mayes et al., 1990). At about 4 Ma, the subducting plate was detached from the overriding plate as the lower Phoenix Plate continued to slide beneath the upper Antarctic Plate. As segments of the Phoenix-Antarctic spreading center were accreted onto the western Antarctic Peninsula, the leading slab continued to sink, leaving a slab window (Hole and Larter, 1993).

This plate tectonic configuration facilitated the upwelling of relatively primitive, undersaturated alkali basalts (which are geochemically very similar to ocean island basalts and some continental alkali basalts) from the asthenosphere into the incipient void and the formation of trench-proximal volcanoes and seamounts. After 4 Ma, ridge-push forces along the northeastern extension of the Antarctic-Phoenix ridge declined. The cessation of subduction beneath the South Shetland trench resulted in extension in the Bransfield Strait, as the subducting slab continued to cool and sink (Barker and Dalziel, 1983). Relative aseismicity is a peculiar characteristic of the South Shetland trench and the Bransfield Strait (Pelayo and Wiens, 1989). At present, the subducted slab can be traced beneath the South Shetland Islands dipping at an angle of 25° to the southeast (Grad et al., 1993).

To explain the low seismicity of the subducting slab, slow, aseismic descent or even stationary rest of the subducted slab (slab-pull) beneath the South Shetland Islands and Bransfield Strait are invoked. The resulting slab rollback and the South Shetland trench

retreat have presumably led to extension in the upper plate and to opening of Bransfield Strait. A simplified model of the present day setting of the Central Bransfield Strait is depicted in Figure 5.3.

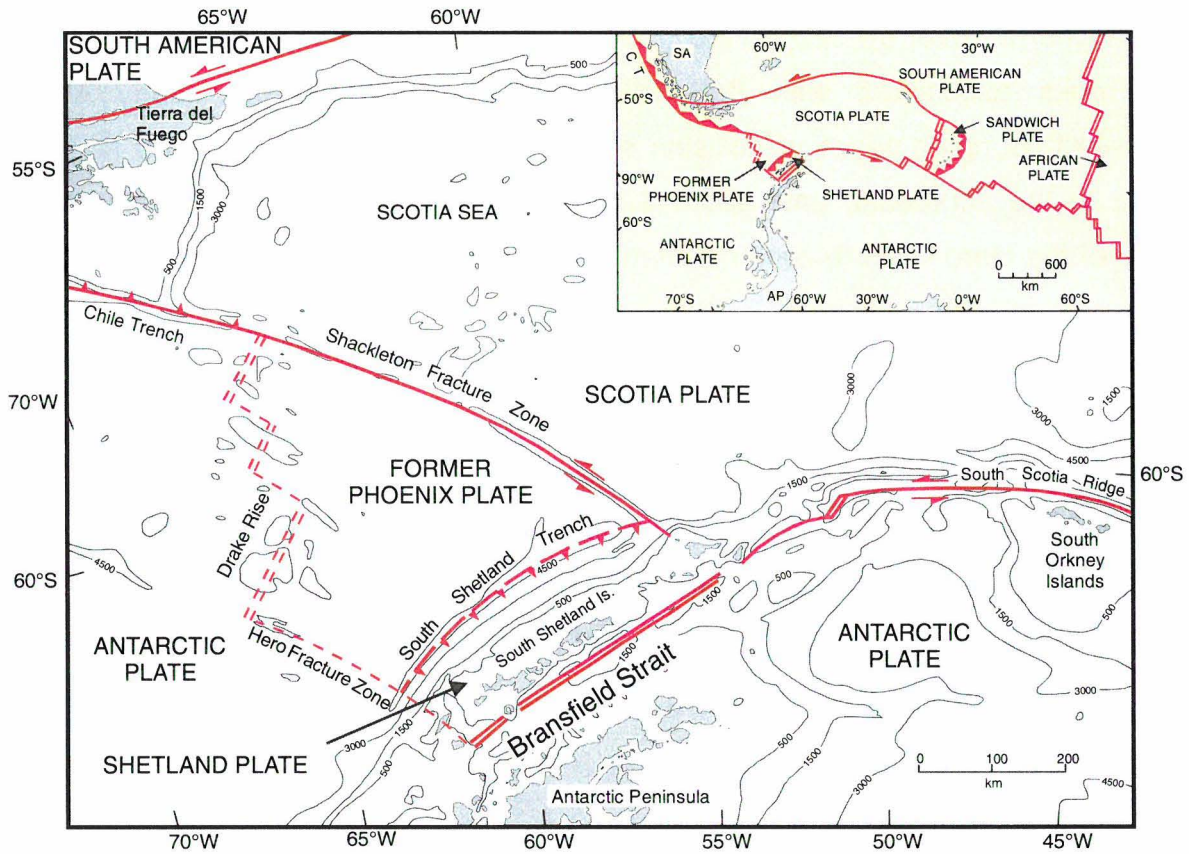


Fig. 5.1. Present-day plate configuration to the north of the Antarctic Peninsula and of the Scotia arc region (modified from Klepeis and Lawver, 1995).

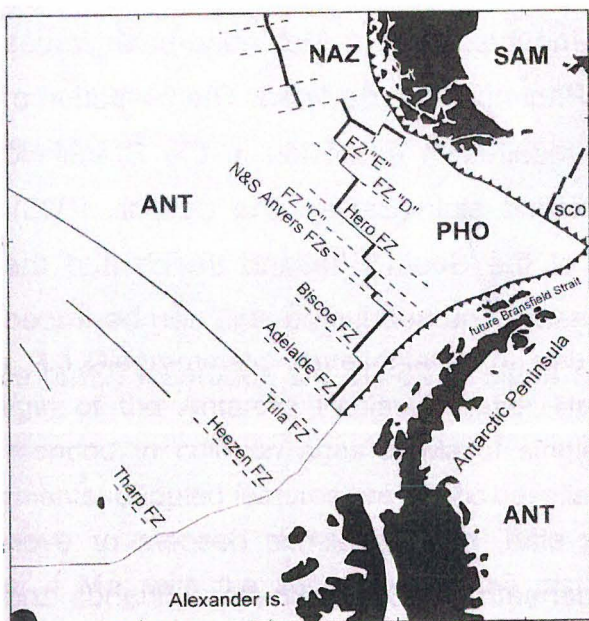


Fig. 5.2. Modified plate reconstruction of the southeastern Pacific and the Antarctic Peninsula region for 20 Ma (after Lawver et al., 1995). Abbreviations for the major plates are ANT=Antarctic, NAZ=Nazca, SAM=South American, PHO=Phoenix, and SCO=Scotia plate. Antarctic-Phoenix spreading centers collided with western Antarctic Peninsula prior to 20 Ma.

Fossil evidence from King George Island indicates that a marine basin in the position of the modern Bransfield Strait existed as early as the lower Eocene (Birkenmajer, 1992). Incipient rifting began during the late Oligocene (26 to 22 Ma) after regional uplift above sea level. The actual age of initiation of rifting in the Bransfield Strait is difficult to constrain. First evidence for extension comes from a system of antithetic faults cutting upper Oligocene and older rocks along the margin of the rift. Following arc tension during early Miocene, several stages of basaltic to andesitic dike intrusions occurred at 22 Ma, 20 Ma, and at 14 Ma (Birkenmajer, 1992). The initiation of the alkaline to calc-alkaline volcanism along the modern Bransfield rift occurred during the Pleistocene.

Bathymetric and satellite-derived gravity data allow the subdivision of the Bransfield Strait into three subbasins: the southern (western), central, and northern (eastern) basin. The central Bransfield Basin is located between longitudes 60°30'-56°50'W, and its southern and northern extent is defined by the heights of Deception Island and Bridgeman Island. The basin is ca. 30-38 km wide, ca. 230 km long and has a maximum depth of 1.950 m (Grácia et al., 1997). All subbasins are characterized by low gravity anomalies (Lawver et al., 1995). The sketch map of the central and eastern Bransfield Strait (Fig. 5.4) shows numerous bathymetric features representing volcanic ridges and seamounts. At least four different parallel lines of active and incipient volcanic edifices can be distinguished. The most westerly, located within the shelf area of the South Shetland Islands, includes Penguin Island, an active cinder cone just off King George Island, and Melville Peak. At least six to eight circular structures from a few tens of meters to a couple of hundred meters in height define the second line in the King George Basin. The third line represents the main rift axis and includes the subaerial edifices of Deception and Bridgeman Islands as well as several large submarine volcanoes (edifices A, C, D, and F in Fig. 5.4) that are aligned parallel to the basin axis showing consistent trends around N059°. The fourth volcanic lineation is defined by a ridge located southeast of the major rift. It shows the highest heat flow in the King George Basin, and a very recent extrusion at 57°W (Lawver et al., 1995). The trend of magmatic activity is thought to have shifted from the diapiric rift zone to the now active neovolcanic rift.

Detailed bathymetric surveys of the Bransfield Strait were performed by Oregon State University in 1995 and 1999 (Fig. 5.5), and the results clearly outline the morphological features of the basin. The central and eastern Bransfield basin both show a progressive

deepening toward the northeast, with Bridgeman Island marking the boundary between the central and eastern Bransfield basins. The central Bransfield Basin is characterized by a smooth, step-like topography and shallow water depths.

Volcanic activity in the Bransfield Strait is confined by K-Ar dating to the last 300 k.y. Volcanic centers are represented by recently active volcanoes (Deception, Bridgeman, and Penguin islands; Weaver et al., 1979), and by seamounts and ridges of the central volcanic rift axis between Deception and Bridgeman Islands (Fisk, 1990; Keller et al., 1991). The Bransfield volcanic rocks appear to be products of <5% to 15% melting of mantle that contained 0.5% to 2% of a subducted component. The products of volcanism are classified as mainly subalkaline olivine basalts and basaltic andesites. Deception Island is the only volcano which produced a complete basalt to trachydacite evolutionary suite (Keller et al., 1991). The seamounts consist of fresh, glassy, highly aphyric to olivine-plagioclase-phyric, vesicular, tholeiitic basalts, and basaltic andesites (Fisk, 1990; Keller and Fisk, 1992).

The volcanic rocks principally have higher Na, K, Rb, Sr, and Ba concentrations and less of an Fe enrichment trend (Fisk, 1990; Keller et al., 1991) than typical mid-ocean ridge tholeiites. Trace element concentrations generally are slightly to moderately enriched relative to N-MORB. Niobium shows negative anomalies (Lawver et al., 1995), typical for island arc calc-alkaline basalts. There are striking similarities in the major and trace element compositions between the arc volcanism and volcanism in Bransfield Strait. Island-arc affinities and hybrid compositions of arc and mid-ocean ridge basalts as well as similar isotope patterns may imply similar magma sources (Fisk, 1990). The Bransfield Strait volcanic rocks have a slightly negative Nb anomaly, and are moderately enriched in alkalis relative to MORB as typical of back-arc basin basalts suggesting a minor contribution from the subducted slab.

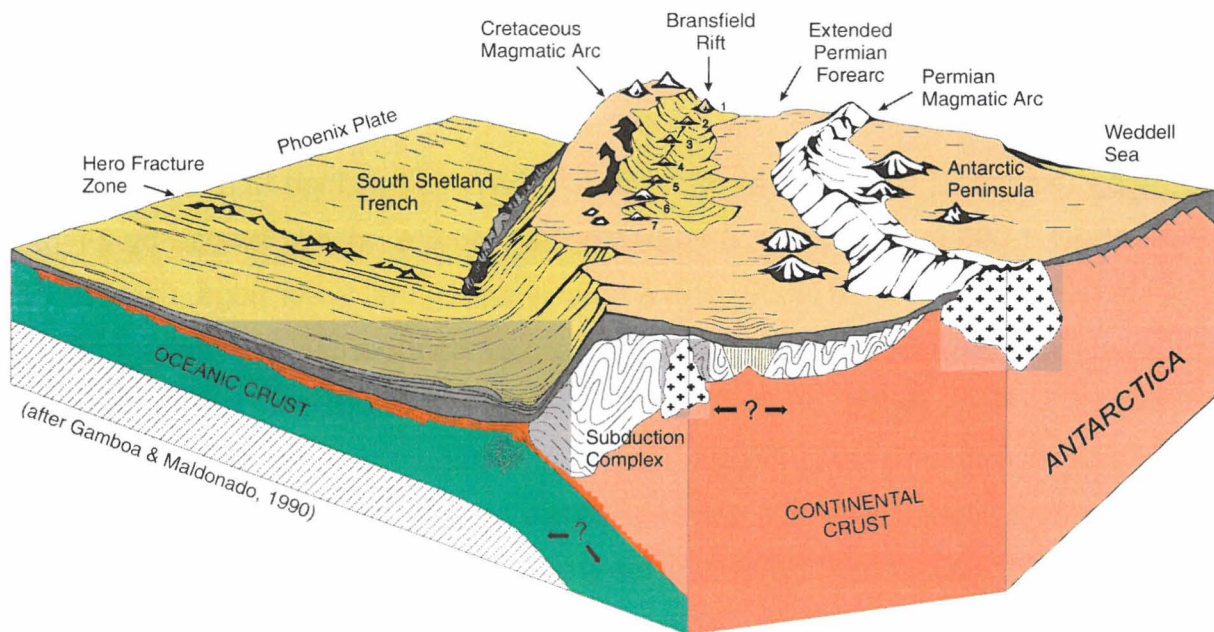


Fig. 5.3. Three-dimensional sketch of the Bransfield Strait (modified from Gamboa and Maldonado, 1990).

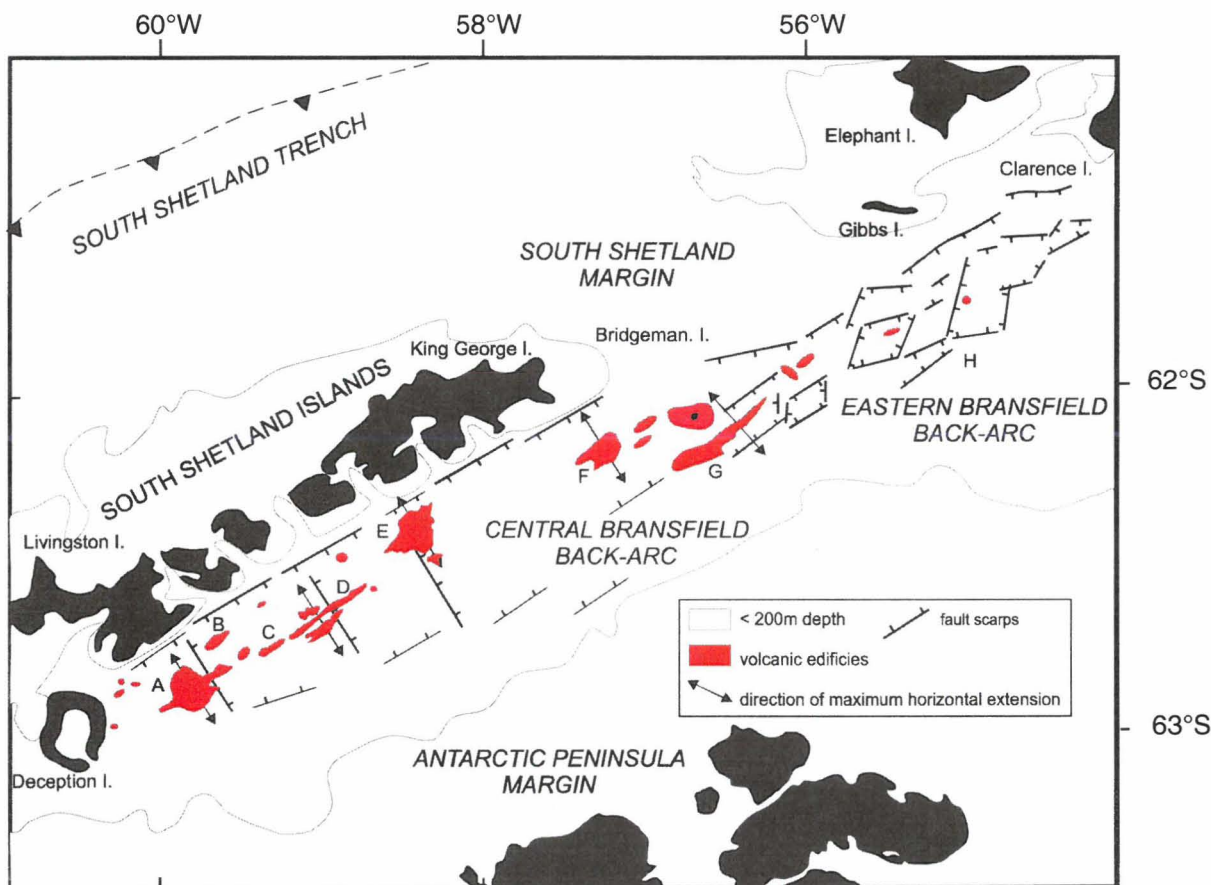


Fig. 5.4. Structural sketch map of the central and eastern Bransfield Basin (after Gracia et al., 1997). Letters A to G were used by Gracia et al. (1997) to name major submarine volcanic edifices in Bransfield Strait.

The volcanic edifices which were supposed to be targeted during the HYDROARC cruise include (from northeast to southwest) :

Hook Ridge (edifice F) is located at 62°11'S, 57°15'W, 550 m high and rises to a water depth of about 1.000 m (Fig. 5.6a). It is a composite edifice, mainly formed by an 18 km long, 4 km wide ridge oriented N059° and a roughly orthogonal lower ridge, rising to 1.200 m and trending N160°. Small secondary ridges are present parallel to the main ridge. To the northeast of Hook Ridge, on the submerged flanks of Bridgeman Island, there are a series of parallel ridges trending N060°. The most prominent of these ridges is more than 15 km long and aligned with the volcanic edifice of Hook Ridge. The larger volcanic edifices are all located above the transverse-trending steps separating the four different levels of the central Bransfield Basin. This indicates that volcanism is likely concentrated at the intersection between longitudinal and transversal structures. The structures are consistent with extension oriented perpendicular to the basin margins with a minor left-lateral component (Grácia et al., 1997).

Viehoff Seamount (edifice E) is a largely unknown seamount with a 3.5 km crater diameter located at 62°26'S, 58°25'W and the volcanic feature closest to King George Island (Fig. 5.5). The flanks of Viehoff Seamount are at a water depth of about 600 m.

Three Sisters is a composite volcanic ridge to the southwest of Viehoff Seamount. Middle Sister, the largest and longest of the three volcanic ridges is located at 62°39'S, 59°00'W. The edifice is 450 m high and rises to a water depth of 975 m (Fig. 5.6b). The lower part of Middle Sister is sedimented, while the upper part and the steeper slopes are almost free of sediment and are characterized by large lava pillows often reaching 1 m in diameter.

The Axe (edifice A) is a split volcano located almost half way between Three Sisters and Deception Island at 62°24'S, 59°45'W about 12 nm southeast of Livingston Island. Bathymetric data on The Axe are currently not available.

Deception Caldera is a currently inactive volcano with a large (9 x 5 km), partly submerged caldera. The last eruptions at Deception occurred in 1967 and 1970 with significant ash fall and hot spring activity. The caldera floor at 100-150 m water depth is covered with volcanoclastic sediments which are overlain by a thin blanket of pelitic sediments. Some areas which are related to ring fractures are known to have hot spring and fumerole activity.

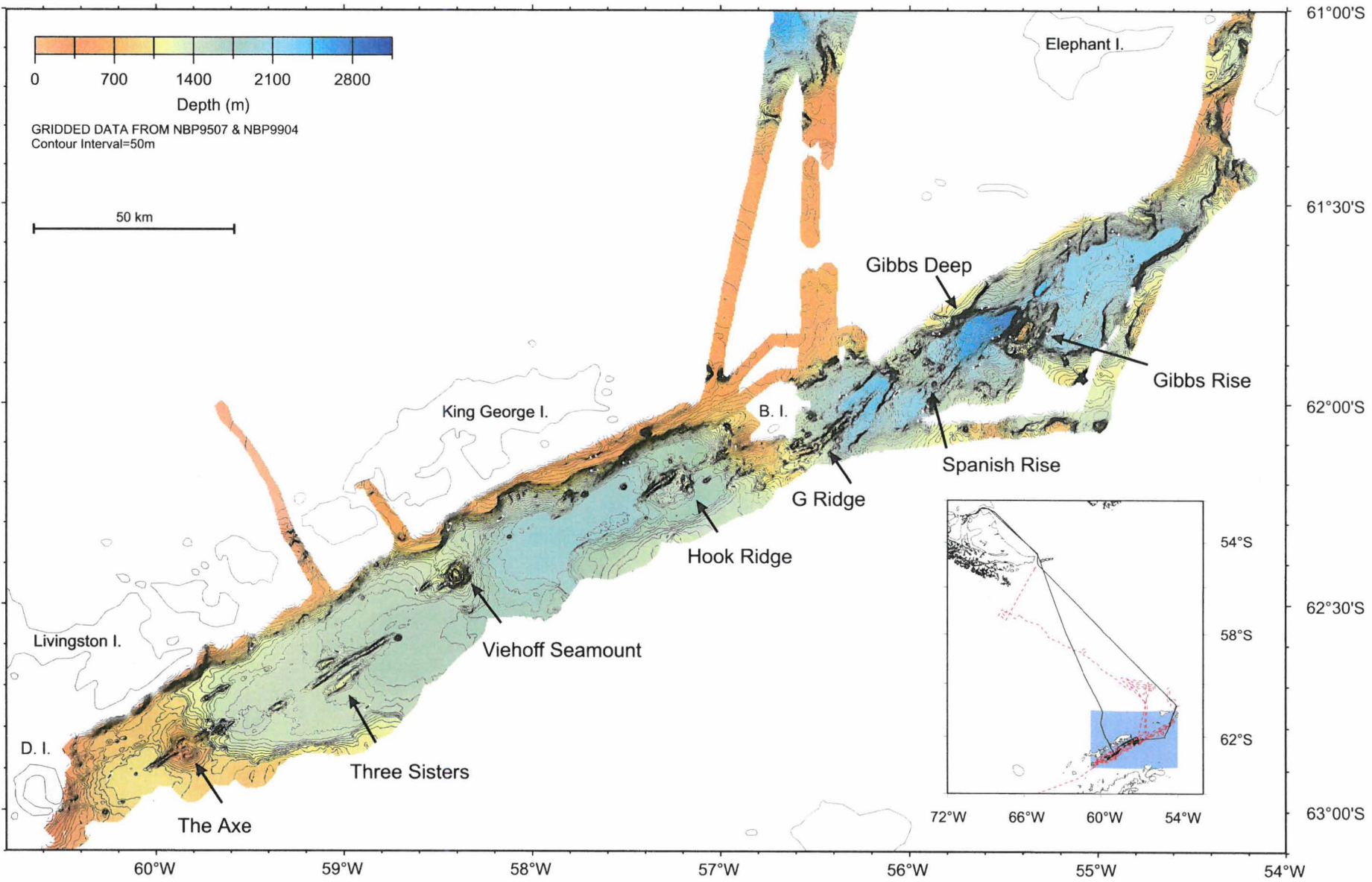


Fig. 5.5. Detailed bathymetric map of the Bransfield Strait showing the location of major volcanic edifices in the Central Bransfield Basin and other features in the East Bransfield Basin (bathymetry courtesy of Oregon State University).

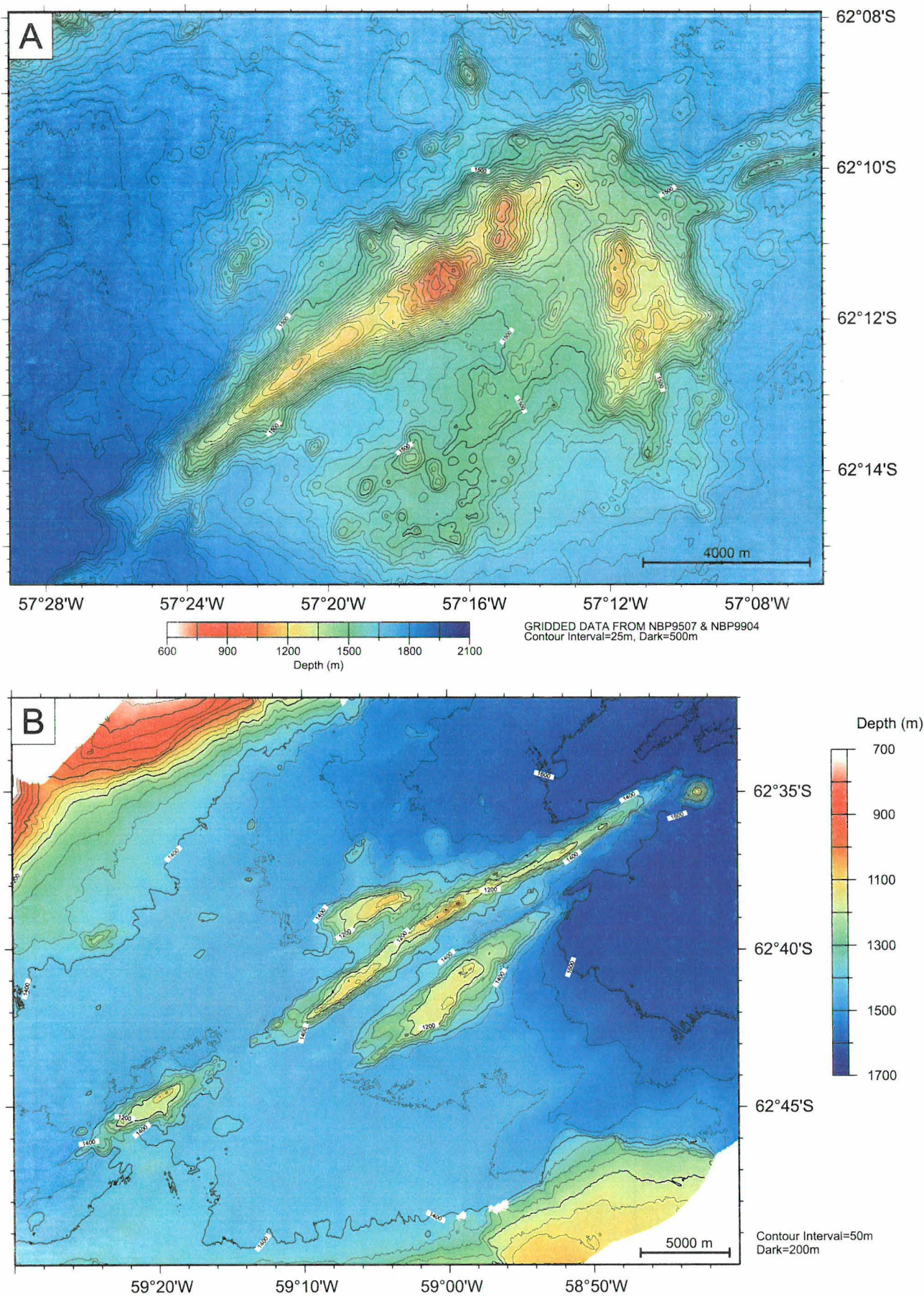


Fig. 5.6. Detailed bathymetric map of A) Hook Ridge and B) Three Sisters in the Central Bransfield Basin (bathymetry courtesy of Oregon State University).

References

- Barker, P.F. (1982). The Cenozoic subduction history of the Pacific margin of the Antarctic Peninsula: Ridge crest-trench interactions. *Journal of the Geological Society of London* 139: 787-801.
- Barker, P.F., and Dalziel, I.W.D. (1983) Progress in geodynamics of the Scotia Arc region. in: R. Cabre (ed), *Geodynamics of the Eastern Pacific Region, Caribbean and Scotia Arc*. *Geodyn. Series* 9: 137-170.
- Barker, P.F., Dalziel, I.W., and Storey, B.C. (1991) Tectonic development of the Scotia Arc region; in: R.J. Tingey (ed), *The geology of Antarctica*. Oxford, UK, Oxford University Press: 215-248.
- Birkenmaier, K. (1992) Evolution of the Bransfield Basin and rift, West Antarctica. In Yoshida, Y, et al. (eds) *Recent Progress in Antarctic Earth Science*, Tokyo: 405-410.
- Birkenmaier, K., Delitala, M.C., Narebski, W., Nicoletti, M., and Petrucciani, C. (1986) Geochronology of Tertiary island-arc volcanics and glacial deposits, King George Island, South Shetland Islands (West Antarctica). *Polish Academy of Sciences, Earth Sciences* 34: 257-273.
- Elliot, D.H., Dupre, D.D., and Gracianin, T.M. (1983) The age and geochemistry of some rocks from the South Shetland Islands. In *Antarctic Earth Science*, University Press, Cambridge: 357.
- Fisk, M.R. (1990) Back-arc volcanism in the Bransfield Strait, Antarctica. *Journal of South American Earth Science* 3: 91-101.
- Gamboa, L.A.P., and Maldonado, P.R. (1990) Geophysical investigations in the Bransfield Strait and in the Bellingshausen Sea – Antarctica. In St. John, B. (ed) *Antarctica as an Exploration Frontier – Hydrocarbon Potential, Geology, and Hazards; AAPG Studies in Geology* 31: 127-141.
- Gracia, E., Canals, M., Farran, M.-L., Sorribas, J., and Pallas, R. (1997) Central and eastern Bransfield basins (Antarctica) from high-resolution swath-bathymetry data. *Antarctic Science* 9(2): 168-180.
- Grad, M., Guterch, A., and Janik, T. (1993) Seismic structure of the lithosphere across the zone of subducted Drake plate under the Antarctic plate, West Antarctica. *Geophysical Journal International* 115: 586-600.
- Grunow, A.M., Dalziel, I.W.D., Harrison, T.M., and Heizler, M.T. (1992) Structural geology and geochronology of subduction complexes along the margin of Gondwanaland: New data from the Antarctic Peninsula and southernmost Andes. *Geological Society of America Bulletin* 104: 1497-1514.
- Hole, M.J., and Larter, R.D. (1993) Trench-proximal volcanism following ridge crest-trench collision along the Antarctic Peninsula. *Tectonics* 12: 897-910.
- Hole, M.J., Smellie, J.L., and Marriner, G.F. (1991) Geochemistry and tectonic setting of Cenozoic alkaline basalts from Alexander Island, Antarctic Peninsula. In Thomsen, M.R.A. et al., (eds) *Geological Evolution of Antarctica*, Cambridge: 521-526.
- Keller, R.A., and Fisk, M.R. (1992) Quaternary marginal basin volcanism in the Bransfield Strait as a modern analogue of the southern Chilean ophiolites. In Parson, L.M. et al., (eds) *Ophiolites and their Modern Analogues*. Geological Society of London Special Publication 60: 155-170.
- Keller, R.A., Fisk, M.R., White, W.M., and Birkenmajer, K. (1991) Isotopic and trace element constraints on mixing and melting models of marginal basin volcanism, Bransfield Strait, Antarctica. *Earth and Planetary Science Letters* 111: 287-303.
- Klepeis KA, and Lawver LA (1996) Tectonics of the Antarctic-Scotia plate boundary near Elephant and Clarence Islands, West Antarctica. *Journal of Geophysical Research* 101: 20,211-20,231.
- Lawver, L.A., Keller, R.A., Fisk, M.R., and Strelin, J.A. (1995) Bransfield Strait, Antarctic Peninsula:

- Active extension behind a dead arc. In B. Taylor (ed.), *Backarc Basins: Tectonics and Magmatism*. Plenum Press, New York: 315-342.
- Mayes, C.L., Lawver, L.A., and Sandwell, D.T. (1990) Tectonic history and new isochron chart of the South Pacific. *Journal of Geophysical Research* 95: 8543-8568.
- Pankhurst, R.J. (1983) Rb-Sr constraints on the ages of basement rocks in the Antarctic Peninsula. In, Oliver, R.L., James, P.L., and Jago, J.B., (eds) *Antarctic Earth Science*, Australian Academie of Science, Canberra and Cambridge University Press: 367-371.
- Pankhurst, R.J., and Smellie, J.L. (1983) K-Ar geochronology of the South Shetland Islands, Lesser Antarctica: Apparent lateral migration of Jurassic to Quarternary island arc volcanism. *Earth and Planetary Science Letters* 66: 214-222.
- Pelayo, A.M., and Wiens, D.A. (1989) Seismotectonics and relative plate motion in the Scotia Sea region. *Journal of Geophysical Research* 94: 7293-7320.
- Tanner, P.W.G., Pankhurst, R.J., and Hayden, G. (1982) Radiometric evidence for the age of the subduction complex of the South Orkney and South Shetland Islands, West Antarctica. *Journal of the Geological Society of London* 139: 683-690.
- Weaver, S.D., Saunders, A.D., Pankhurst, R.J., and Tarney, J. (1979) A geochemical study of magmatism associated with the initial stages of back-arc spreading. The Quaternary volcanics of Bransfield Strait, from South Shetland Islands. *Contributions to Mineralogy and Petrology* 68: 151-169.

6 ALTERATION AND MINERALIZATION

Samples of altered and mineralized volcanic rocks collected during SO-155 reflect the wide range of geological environments that have developed during the Mesozoic-Cenozoic evolution of the continental margin of the Antarctic Peninsula. Altered and mineralized samples were recovered from 5 different settings within the South Shetland Microplate and on the adjoining Phoenix Plate. These include (i) the small volcanic crater on Hook Ridge, in Central Bransfield Basin, (ii) the flanks of Bridgeman Ridge (Edifice G), a large volcanic high separating the Eastern and Central Bransfield Basins, (iii) the flank of Gibbs Seamount, an older volcanic edifice or foundered block of arc crust in the central part of the Eastern Bransfield Basin, (iv) the sediment and ash-filled caldera of Deception Island, and (v) a segment of the extinct Phoenix Ridge spreading center on the Drake Rise.

Samples collected from these settings represent a spectrum of different styles of alteration and mineralization, including (i) hydrothermally altered and cemented dacite breccias erupted at several locations along the axis of the Central Bransfield Basin (Hook Ridge, Edifice G), (ii) barite-sphalerite mineralization in the crater of a sedimented rift volcano (Hook Ridge), (iii) hydrothermally altered glacial sediments and ash from the caldera of a rifting volcano at the southern end of the basin (Deception Island), (iv) stockwork-like

quartz+/-pyrite mineralization in hydrothermally altered andesite porphyry from the Eastern Bransfield Basin (Gibbs Seamount), and (v) strongly chloritized and silicified basalt breccias from the fossil spreading ridge on the adjacent oceanic plate (Phoenix Ridge).

6.1 Central Bransfield Basin: Hook Ridge Crater

Altered and mineralized samples: 05-GTVA, 06-GTVA, 07-GTVA, 39-DR, 37-SL, 30 MUC, 31-MUC, 32-MUC, 33-MUC

Recent extension in the Central Bransfield Basin has occurred along an axial volcanic lineament close to the South Shetland Islands. The present location of the neovolcanic zone implies that intrusive activity and associated volcanism in the basin was initiated only after substantial opening of the Bransfield Strait (i.e., initial rifting occurred close to the Antarctic Peninsula, with progressive opening towards the southwest). Hook Ridge is among the most youthful features on the present volcanic lineament, with fresh dacite recovered from a small, 1-km diameter volcanic crater at the summit of the ridge.

Samples recovered from this location include massive barite crusts with up to 20% sphalerite, silica sinter, baked mud with pyrite-marcasite lining silicified burrows, and semi-lithified muds with native sulfur filling cavities and lining dessication cracks. These samples are similar to hydrothermal precipitates first collected from this site in 1999 by R/V N. B. Palmer). The barite crusts are associated with diffuse, low-temperature venting (ca. 60°C) through the sediments near the southern wall of the crater, where white patches of native sulfur and amorphous silica are common. Relatively fresh, glassy dacite is exposed on the walls of the crater, on both the northern and southern sides of the volcano, and is associated with extensive Fe-oxide staining, baked muds, and silica sinter-like deposits. These volcanic rocks are presumably the most recent extrusive manifestation of a subvolcanic heat source beneath Hook Ridge.



Fig. 6.1. Porous massive barite with minor sphalerite (dark) and amorphous silica. Sample 06-GTVA-1. Scale = 1 cm

6.2 Bridgeman Ridge: Edifice "G"

Altered and mineralized samples: 03-DR, 04-DR

Intensely altered, glassy dacite breccias and hyaloclastite were recovered from two volcanic features on the flank of Bridgeman Island, at the northeastern extension of the neovolcanic zone of the Central Bransfield Basin. The breccias are similar to the glassy dacite recovered from the Hook Ridge crater and are cemented by clay-altered glass, amorphous silica, nontronite, and Fe-oxides, with minor amounts of baked mud mixed with the hyaloclastite.

6.3 Eastern Bransfield Basin: Gibbs Seamount and Spanish Ridge

Altered and mineralized samples: 20-DR, 21-DR, 22-DR

The area of Gibbs Seamount and Spanish Ridge comprises a series of asymmetric subbasins and linear NE and NW trending ridges, from 2.000 m depth to less than 1.300 m. The distinctive horst and graben morphology bears a closer resemblance to the westernmost transtensional segment of the South Scotia Ridge, than to the rest of the Bransfield Basin. Several of the ridges may be tectonized blocks associated with the fragmentation of the arc crust during opening of the Bransfield Strait (i.e., a foundered block of old arc crust). A continuation of the volcanic activity in the Central Basin was not observed, and evidence for seafloor spreading in the deeper parts of the basin was not found (i.e., magma supply may be low and the lava flows are old). However, the fact that relatively little sediment has accumulated in the deeps is evidence of recent tectonic disruption of the basin floor. Extensive faulting and fragmentation of the basement in the Eastern Bransfield Basin has exposed distinctive porphyritic lavas and shallow intrusive rocks with alteration that resembles that of arc-related porphyry hydrothermal systems.

Although basaltic lavas were recovered from several of the ridges in the Eastern Basin, older arc-related material was also dredged from these locations (especially at Spanish Ridge). The volcanic suite from the flanks of Gibbs Seamount is dominated by altered porphyritic andesite and intrusive rocks. The samples include (i) fine-grained diabase, (ii) relatively fresh feldspar porphyritic andesite, (iii) leucogabbro/diorite (iv) vesicular basalt, (v) hematized diabase and feldspar porphyry, (vi) weakly altered, chloritized porphyry, (vii) strongly altered, epidotized porphyry, and (viii) intensely silicified and brecciated porphyry with stockwork-like quartz+/-pyrite veining. Traces of chalcopyrite were found in at least one sample. Rocks dredged from the top of Gibbs Seamount included medium-coarse

grained diorite, black medium-fine grained intrusive rocks, and fine-grained vesicular basalt (probable extrusive equivalent of the diorite).

The coarse-grained porphyritic andesite may represent the extrusive equivalent of a shallow subvolcanic intrusion (e.g., exposed carapace breccia of an intrusive dome). These rocks are undeformed, only slightly weathered, and include very fresh examples of the parent porphyry, suggesting that the dredged material may have formed in place (i.e., products of submarine intrusive activity and volcanism). The quartz-rich stockwork veining in these rocks bears a strong resemblance to continental porphyry-style alteration and mineralization and is typical of that what might be expected in high-level porphyry systems on the adjacent island arc. It is unclear whether these samples are part of a submarine volcanic dome or a tectonic remnant of an arc-related intrusive/extrusive complex from the South Shetland Islands. The abundant epidote may be an indication of interaction with hydrothermal seawater. Dating of the porphyry and the alteration (^{39}Ar - ^{40}Ar) and isotopic characterization of the alteration minerals (O, H, and $^{87/88}\text{Sr}$) will help to resolve this.

6.4 Deception Island

Altered and mineralized samples: 42-SL, 43-SL, 48-MUC, 49-MUC, 50-MUC, 51-MUC

A survey of the caldera floor at Deception Island showed that onshore hot springs extend into the submerged part of the caldera along a NE-SW trending structural lineament that has controlled the most recent volcanic activity on the island. Although the caldera has traditionally been considered a collapse structure, there is evidence for extensional faulting across the volcanic complex that is roughly colinear with the axial rift in Bransfield Basin.

Bottom photographs of this area revealed mainly sediment and ash, however, temperature anomalies of up to 60°C in the sediments and local white patches indicate ongoing geothermal activity within the central portion of the caldera. Fe and Mn-enriched sediments (up to 1.310 ppm Mn) were previously documented in the southern part of the caldera, close to the location of a small volcanic cone (Stanley Patch: Rey et al., 1995), but no visible manifestation of hydrothermal activity was found in this area.

Hydrothermally altered muds were recovered in gravity cores from the caldera floor along buried faults that correspond to the NE-SW trending structures onshore. Temperatures in the sediment recovered on deck were up to 4.5°C . The highest temperatures were located

close to known hot springs along the shores of Fumarole Bay. The cores contained dark altered sediment and ash, but hydrothermal precipitates were not found. White patches on the seafloor in this area resemble the sulfur- and silica-rich patches at Hook Ridge, and cores in the vicinity of the white patches recovered floccular material from the sediment surface which may be either bacterial in origin or fine native sulfur. A strong smell of sulfur was evident at the near-shore hot springs, suggesting that H₂S is likely venting on the floor of the caldera as well.

6.5 Drake Rise: Phoenix Ridge

Altered and mineralized samples: 53-DR

The prevailing tectonic model for the South Shetland microplate implies that subduction of the Phoenix plate was blocked as a result of oblique ridge-trench collision, beginning about 15-20 Ma ago. The segment of the plate between the Hero and Shackleton fracture zones has since become pinned beneath the Antarctic margin. Based on magnetic lineations, spreading at the Phoenix Ridge is thought to have ceased or decreased to a very slow rate at about 4 Ma, bringing an end to subduction-related volcanism in the South Shetland Islands. However, a few deep earthquakes suggest that slow subduction could be continuing along the South Shetland Trench. Sampling of the fossil spreading center along the two southernmost segments on the Phoenix Ridge was carried out to better constrain the age of the ridge and to evaluate whether spreading may continue to influence the Phoenix Plate.

Dredged basalt from the ridge showed variable alteration, including well-preserved glass and a notable lack of thick Mn encrustations, suggesting that the volcanism could be younger than 4 Ma. Samples dredged from the wall of the ridge included strongly chloritized and silicified autobreccias and hyaloclastite, similar to stockwork alteration associated with high-temperature hydrothermal activity at other mid-ocean ridges (e.g., Galapagos Rift). These samples raise the possibility that fossil ridge-crest sulfide deposits and associated stockwork mineralization might be found on the walls of the median valley, similar to the sulfide deposits exposed on the walls of the slow-spreading Mid-Atlantic Ridge (e.g., MIR zone at 26°N). It is noteworthy that the much younger deposits on the Mid-Atlantic Ridge (100,000-500,000 years old) show extensive seafloor weathering that was not evident in the samples from the Phoenix Ridge. Dating of these rocks will provide critical evidence for the age of the most recent spreading and may have important

implications for interpretation of the ongoing volcanic, tectonic and hydrothermal activity in the Bransfield Basin.

6.6 Summary and Synthesis

The Mesozoic to Recent evolution of the continental margin of the Antarctic Peninsula has involved at least four distinct lithotectonic elements: an incipient back-arc rift characterized by axial volcanic lineaments and intrusions (Central Bransfield Basin), a tectonically deformed marginal basin associated with transtension along the South Scotia Ridge (Eastern Bransfield Basin), actively rifting volcanoes on the inner margin of the South Shetland Arc (Deception Island), and an offshore oceanic plate with a fossil (dormant?) mid-ocean ridge spreading center (Phoenix Plate).

The Central Bransfield Basin is thought to developed by step-wise rifting close to the Antarctic Peninsula and progressive opening towards the southwest, with volcanic and intrusive activity occurring only at a relatively late stage during the most recent increment of extension. Small volcanoes along the length of the basin have erupted along a series of axial volcanic lineaments (e.g., en echelon fissures), presumably controlled by basement faults associated with crustal thinning and fracturing of the continental basement. The ongoing volcanism at Deception Island occurs along a NE-SW trending structure which appears to be colinear with the nearby volcanic lineaments in the adjacent Central Bransfield Basin (e.g., at the Axe and Three Sisters). Deception may be undergoing rifting in response to extension of the older arc crust, similar to other volcanoes in the basin. The Eastern Bransfield Basin is more strongly influenced by transtension at the northern boundary of the microplate, near the intersection with the Shackleton Fracture Zone and South Scotia Ridge. Hydrothermally altered and mineralized intrusive and extrusive volcanic rocks from this part of the basin (andesite prophyry) may represent fragments of older arc crust that have been dropped into the basin by recent tectonic activity or may be products of early submarine intrusive activity associated with the opening of the strait.

Despite the evidence for anomalous heat flow in the Bransfield Basin and widespread hydrothermal activity associated with the most recent volcanism, the volume of magma erupted is small by comparison with other large back-arc rifts. Although intrusive dikes and sills in the sediments of the basin have been detected by seismic reflection, the low volume of magma associated with the volcanoes suggests that a large heat source is not

present beneath the basin and that convective circulation of seawater at a large scale may be limited. The further development of a back-arc basin in this area and the possibility of Bransfield Basin becoming an important setting for seafloor massive sulfides depends on renewed magmatic activity and rifting, possibly in response to continued subduction of the Phoenix Plate.

6.7 Sample Descriptions

03-DR SW Flank of Edifice G

- edifice "G", southwest of Bridgeman Island
- moderately to strongly altered andesite/dacite breccias
- two main types: (i) grey-white, glassy dacite/andesite breccia clasts in a matrix of clay, baked muds, and amorphous silica, (ii) dark grey mafic breccias with vesicular to scoriaceous basalt clasts
- the matrix of the breccias is typically cemented hyaloclastite and clay-altered glass with minor disseminated pyrite

03-DR-19

- grey-white, poorly sorted clast-rich breccia with clay-rich matrix of altered glass with minor disseminated pyrite
- 75% grey-white, clay-altered lapilli (0.5-1 cm)
- 25% dark grey, moderately altered, angular clasts (2-3 cm)
- one piece (1 kg)

03-DR-20

- grey-white, poorly sorted, clay-altered volcanic breccia with mixed clasts, similar to sample 19
- fine grained mafic clasts, vesicular mafic clasts, rare feldspar-phyric clasts, rare glassy dacite clasts
- 2-3% fine-grained pyrite in the clay-rich matrix, rimming clasts
- weakly silicified
- 3 pieces (3 kg)

03-DR-21

- medium dark grey, moderately altered basalt/andesite breccia
- 50% vesicular basalt clasts (1-3 cm)
- 25% coarser, porphyritic basalt clasts (3-4 cm)
- matrix of clay-altered glass and fine, mm-sized fragments
- one piece (1 kg)

03-DR-22

- dark grey to black, coarse mafic volcanic breccia
- 80-90% poorly sorted, angular basalt clasts (1-5 cm) with weakly clay-altered rims; very fine disseminated pyrite in the rims of the basalt clasts
- framework supported, with a sandy matrix of clay-altered glass and mm-sized fragments (up to 0.5 cm)
- one piece (2 kg)

03-DR-23

- weathered/oxidized coarse mafic volcanic breccia
- rounded basalt clasts of vesicular basalt/scoria (up to 5 cm) in an Fe oxide- and clay-rich matrix; 50% Fe-stained clasts, 50% fresh clasts
- one piece (1 kg)

03-DR-24

- massive, light grey, intensely clay-altered basalt/andesite
- cut by a fracture with a distinctive, 1 cm-wide selvage of green clay
- 2-3% fine disseminated pyrite
- one piece (1 kg)

03-DR-25

- medium-grey basalt breccia
- 40-60% med-coarse, Fe-stained, vesicular to scoriaceous basalt clasts (1-3 cm) in a hard, clay-silica matrix
- similar to sample 21 but with Fe-stained clasts and minor disseminated pyrite in the matrix
- one piece (1 kg)

03-DR-26

- miscellaneous vesicular to scoriaceous, feldspar-phyric basalt and basalt breccia
- mostly Fe-stained, one less weathered feldspar porphyritic sample
- 4 cut pieces (1 kg each), 5 small uncut pieces

04-DR Volcanic Cone NW of Edifice G

- small cone on north flank of edifice "G"
- dominantly pale green, chlorite-altered andesite
- two main sample types: (i) pale green, fine-grained, chloritized andesite, and (ii) light grey clay-altered tuff with 2-3 cm thick bed of coarser ash (lapilli up to 0.5 cm)
- the altered ash is cut by a network of fine quartz-filled fractures, locally with abundant disseminated pyrite
- three large pieces (10-15 kg)

05-GTVA Hook Ridge Crater

- in small crater on main volcanic feature of Hook Ridge
- area of white patches at base of southern crater wall

05-GTVA-01

- two irregular pieces of light grey, baked and weakly silicified mud with black, sulfide-coated worm burrows
- only sample recovered

06-GTVA Hook Ridge Crater

- in small crater on main volcanic feature of Hook Ridge
- area of white patches at base of southern crater wall

06-GTVA-01

- massive barite crust with silica and sphalerite; one piece (1-2 kg) from large grab of mud
- coarse crystalline, grey to black barite (crystals up to 3 mm)
- narrow band (0.5-1 cm) of darker sulfide (?) on one side of sample; possible sphalerite
- mud in the grab is up to 16°C, with local black streaks (probably hydrocarbon as no obvious smell of sulfur was noticed)

06-GTVA-02

- two small pieces of soft silica sinter crust

07-GTVA Hook Ridge Crater

- in small crater on main volcanic feature of Hook Ridge

- rugged outcrops and talus near base of southern crater wall

07-GTVA-01

- black, glassy dacite lava with clay- and silica-cemented hyaloclastite
- large block (ca. 100 kg) of black glassy dacite and hyaloclastite
- weakly cemented flow breccia or carapace breccia - most clasts are 25-30 cm
- one larger block of massive glassy, vesicular dacite covered by a thick crust of cemented hyaloclastite
- hyaloclastite dominated by 2-3 cm angular clasts, cemented by baked mud, amorphous silica, minor yellowish nontronite (?) and trace Fe-oxides

07-GTVA-02 - cemented hyaloclastite

- 80-85%, poorly sorted breccia clasts (1-2 cm) ; 15-20% fine-grained, weakly clay-altered matrix of glassy shards
- several pieces (1 kg each)

07-GTVA-03 - fresh glassy dacite block (1 kg)

- hard glassy dacite with 10-15% deformed vesicles (3-5 mm)
- local 1-2 cm xenoliths of altered/baked mud and some less-altered clasts of basalt (?)

20-DR NW Flank of Gibbs Seamount (Lower Section)

- large tectonic block (Gibbs Seamount) in Eastern Bransfield Basin
- highly altered dacitic/andesitic porphyry dredged from base of seamount
- 20-25% coarse 1-3 mm feldspar phenocrysts, typical of arc crust
- chlorite-altered breccia with fine fractures lined by pyrite+chalcopyrite
- several small pieces (10 kg)

21-DR NW Flank of Gibbs Seamount (Middle Section)

- large tectonic block (Gibbs Seamount) in Eastern Bransfield Basin
- suite of fresh to highly altered, porphyritic dacite/andesite breccia dredged from middle of seamount
- possible carapace breccia of extrusive dome (?)

21-DR-01

- grey, med-to-fine grained dolerite (diabase); relatively unaltered

21-DR-02

- fine-grained, weakly hematized diabase with minor hematite spots and hematite-lined fractures

21-DR-03

- grey, med-grained feldspar porphyritic andesite (2-4 mm feldspar phenocrysts)

21-DR-04

- weakly altered, chloritized feldspar porphyry with clay-altered feldspar phenocrysts and trace of pyrite

21-DR-05

- coarse, porphyritic andesite breccia with large rim-altered, hematized porphyritic clasts (1-5 cm) in a feldspar porphyry matrix

21-DR-06

- chlorite-altered feldspar porphyry with hematite±pyrite bands/alteration fronts
- weak epidotization in matrix

21-DR-07

- strongly altered feldspar porphyry breccia with intensely epidotized fragments and chlorite-epidote altered matrix

21-DR-08

- intensely silicified feldspar porphyry breccia with stockwork-like quartz veins and pyrite-rimmed/dusted clasts
- relict epidote in larger clasts, with intensely clay-altered feldspar phenocrysts possibly altering to Kspar

21-DR-09

- fine-grained chloritized, aphyric tuffaceous rocks
- carbonate-filled cavities and veins

21-DR-10

- chlorite-altered, fine-grained volcanic wacke, with minor epidote

22-DR NW Flank of Gibbs Seamount (Upper Section)

- large tectonic block (Gibbs Seamount) in Eastern Bransfield Basin
- highly altered dacitic/andesitic porphyry and intrusive rocks dredged from top of seamount

22-DR-01

- medium-grained leucogabbro

22-DR-02

- massive, medium-coarse grained diorite

22-DR-03

- fine-grained black diabase intrusive rocks

22-DR-04

- fine-grained, vesicular black rock, probable basaltic extrusive equivalent of DR-03

22-DR-05

- poorly-sorted, medium grained heterolithologic breccia with 0.5-1cm clasts of volcanic fragments, black cherty sediment, chlorite-altered fragments, hematized fragments and quartz crystals (?) in a fine-grained siliceous and clay-rich matrix with minor fine disseminated pyrite

39-DR Hook Ridge Crater

- baked and altered sediment with abundant native sulfur infilling cavities and lining dessication cracks in sediment (ca. 100 kg)

53-DR Drake Rise (Second Segment N of Hero Fracture Zone)

- central segment of Drake Rise (Phoenix Ridge), marginal high
- all samples, fresh and altered, appear to be basalts; the most altered samples (21-30) represent brecciated or jointed massive flows, glassy pillow flow tops, and glassy hyaloclastite (possibly formed by autobrecciation during extrusion)
- altered basalt breccias have clasts of mm to 10s of cm, with patchy and variable alteration rinds; larger pieces commonly show an alteration zonation from glassy tops(?), through microlitic zones, to holocrystalline interiors
- intensely altered clasts have chlorite-smectite outer margins and more silicified +/- hematitic interiors
- devitrification spherulites and silica/hematite(?) bearing varioles are common in the inner silicified portions
- the alteration textures and mineralogy are strongly reminiscent of altered basalt and andesite lavas from the East Galapagos Rift at 85.5°W (see Embley et al., 1988, Canadian Mineralogist)

53-DR-21

- relatively fresh spheroidal, glassy basalt breccia with a supporting matrix of finer glass that has altered to yellow smectite (?)

- spheroidal texture may represent small lobes or pillow buds

53-DR-22

- weakly devitrified lava with distinctive spherulitic texture
- minor silica and chlorite alteration; blotchy grey to pale brown appearance

53-DR-23

- more pervasively silicified massive lava with "fuzzy" spherules now consisting of silica and minor hematite (?)
- blotchy net-textured appearance

53-DR-24

- intensely silicified basalt with coalescing devitrification spots (spherules) grading into isolated patches of individual and poorly-formed varioles
- groundmass is fine-grained and chloritized, pale green to pale brown

53-DR-25

- pieces of lava flow top
- in situ glassy hyaloclastite rinds are strongly chloritized (smectite?), grading into siliceous and weakly hematized interiors
- fine-grained microlitic interiors display weak chlorite, smectite, and hematite alteration with abundant, well-formed varioles and devitrification spots (spherules)
- varioles appear to be cored by silica and hematite

53-DR-26

- intensely altered, glassy flow top with green and white alteration patches/zones consisting of chlorite and smectite
- interiors or samples are fragmental, rather than massive, and siliceous with minor hematite(?) -cored varioles

53-DR-27

- massive hyaloclastite with 3-5 cm size altered spheroidal clasts (pillow buds?) and abundant altered glass shards as matrix
- pervasive, zoned chlorite and smectite alteration of fragments
- likely a product of autobrecciation during lava extrusion (sample 21 may be an unaltered analog)

53-DR-28

- one sample - example of concentrically-zoned alteration of basalt fragment with an outer chlorite-dominant rim, an inner smectite-dominant zone, and grey 'least-altered' siliceous (?) core
- similar samples described above

53-DR-29

- single fragment of a sugary-textured, equigranular intermediate or felsic(?) rock with altered mafic minerals
- may be a strongly silicified basalt

53-DR-30

- two pieces of cherty material
- one pale brown jasper samples; one jaspilitic breccia that may represent fragments of jasper veins or breccia cement
- relationship to other rocks in the dredge is unknown

7 PETROGRAPHY OF PORPHYRY ROCKS

The dredge hauls 20-DR and 21-DR at the lower and upper slope of the Gibbs Deep in the eastern basin of the Bransfield Strait revealed a sequence of pristine and altered magmatic rocks with affinities to porphyry systems as well as their probable, low-grade metamorphic host rocks.

Four different types of rocks including magmatites and paragenic host rocks can be classified:

1. Relatively pristine and weakly altered dolerites

These fine- to medium grained, mainly blue-grey rocks display mm-sized, euhedral plagioclase crystals and minor mafic minerals (pyroxene/hornblende). Magnetite, which is often replaced by hematite, is accessory. Oxidation processes affected part of the samples resulting in an overall brownish staining and hematite-filled microfractures. Furthermore, calcite- and quartz-filled veins appear in the fresh as well as in the altered rocks.

The following samples were taken:

- 21-DR-1, 1a, 2a and 3b are pristine, dark bluish dolerites with a fine grained, equigranular texture and rare, quartz-filled veins.
- 21-DR-1b and 2b are weakly and moderately oxidized dolerites with fine- to medium-grained textures and inhomogeneously distributed grainsizes. They commonly reveal hematite- and calcite-filled microfractures.

2. Dolerites with distinct, very low- to low-grade metamorphic overprint

These fine grained, bluish to greenish rocks display different stages of secondary alteration. They show equigranular and more often porphyric textures with plagioclase and clinopyroxene in a dense matrix. Alteration is mainly recognizable by the chloritisation of the pyroxenes and green staining of the matrix (i.e. probable chloritisation and epidotisation).

The following subgroups of samples were classified:

- 20-DR-2, 3 and 7 are micro-porphyric, green dolerites with an olive-green matrix and patchy, cm-sized quartz mobilisates. Quartz-veins incorporate mm-wide druses filled

with euhedral chalcopyrite and sphalerite crystals. A distinct impregnation of sulfides is made up with round and angular pyrite aggregates (up to 5 mm in diameter) in the matrix and small chalcopyrite-filled veins (<1 mm).

- 21-DR-4 is a porphyric dolerite with numerous, 2-4 mm long plagioclase tablets and minor, anhedral mafic minerals. The matrix and part of the mafic minerals are affected by a transformation to chlorite and epidote. Sulfide impregnation and veining are absent.
- 21-DR-6 closely resembles the foregoing sample with the exception of a cm-wide impregnation zone of tiny, disseminated pyrite crystals and rare pyrite aggregates. In these zones, oxidation has started to decompose the sulfide leading to a reddish rock colour.
- 21-DR-9 yields the highest degree of secondary alteration with completely chloritised mafic minerals, saussuritised plagioclase and a dense, green matrix. Remarkable are cm-sized calcite patches, which are in part aligned along fractures.

3. Magmatic rocks with breccia-textures

These are hypabyssal rocks, which are characterized by fragments of granitoid rocks (up to 7 cm in diameter) incorporated within a medium grained dolerite of intermediate geochemical character. All samples display moderate to strong secondary alteration including chloritisation, epidotisation, patchy quartz segregation and veining as well as sulfide impregnation. Especially within the weakly altered rocks of this suite it becomes evident that the granitoid fragments are xenoliths, which were incorporated by a later pulse of magma. In the strongly altered samples, tectonic deformation is evident by disruption of the primary texture, turning the rock into a tectonic breccia.

The following samples were chosen for investigation:

- 21-DR-5 is a moderately altered dolerite which bears several xenoliths of granitoid material as well as K-feldspar xenocrysts. The magmatic matrix is characterized by chloritisation and epidotisation, which also affected the rim sections of the xenoliths. Rare calcite veins are present in the host dolerite.
- 21-DR-7a, b, c, d, e, and f are distinctly altered, xenolith bearing, hypabyssal rocks. They show a strong, penetrative epidotisation and chloritisation of both matrix and xenoliths, often leading to halos of epidote and chlorite around the xenoliths. Veining is absent in these rocks and there is either no sulfide impregnation. Remarkable is a

discrete section of the rock, which probably displays K-feldspar metasomatism, well visible by its yellow-greyish colour (sample 21-DR-7e). The largest sample (21-DR-7f) was selected for zircon separation.

- 21-DR-8 shows the strongest metasomatic overprint of all samples. Matrix and xenoliths are tectonically disrupted to porphyroclasts displaying cataclastic features. They are penetratively transformed to chlorite and epidote, while yellow-brownish blasts are probable K-feldspar crystals, which formed by K metasomatism. The space in between the porphyroclasts as well as the fractures in the rock are filled by patchy quartz aggregates and disseminated sulfide.

4. Host rocks of the porphyry-type magmatites

Graphite-phyllites, marly schists, gneisses and meta-greywackes were dredged together with the porphyry-type magmatites. These rocks are probably not dropstones, which is evident by their angular shape and their relatively fresh appearance. Textures and mineral assemblages of these rocks give evidence for lower greenschist-facies metamorphic conditions. A penetrative metamorphic foliation with isoclinal, intafolial microfolds is developed in the schists and gneisses.

The following samples were taken:

- 20-DR-15 is a fine-grained, dark grey graphite-phyllite with a penetrative foliation and microfolding. The rock is mainly composed of white mica, quartz and minor amounts of graphite.
- 20-DR-16 is a marly schist, which shows compositional layering of fine-grained and slightly coarser grained sections. The greenish colour testifies to a high modal amount of chlorite and epidote while small mafic, anhedral minerals could be amphibole.
- 20-DR-17 is a paragneiss, which shows several mm-thick, quartz/feldspar- and mica-rich layers and intensive isoclinal folding.
- 20-DR-18 and 21-DR-10 are pale green metagreywackes, which are characterised by their compact, unfoliated texture. Quartz, feldspar and a large amount of chlorite show a homogeneous distribution in the rocks

8 PETROLOGY

8.1 Introduction

Previous scientific expeditions to the Central and Eastern Bransfield Basins (CBB and EBB respectively) have identified seven large seamounts, a series of prominent high-standing ridges that bisect these seamounts, and numerous smaller seamounts between Deception Island and the NE termination of Bransfield Strait (Fig. 8.1; Lawver et al., 1996; Gracia et al., 1996; 1997). Seismic profiling has revealed that both the CBB and the EBB are subdivided along strike into a series of small basins and troughs, each separated by NW-trending normal faults that downstep to the NE. In the CBB, these NW-trending faults separate heavily sedimented sub-basins and have no surface expression. The large seamounts of the CBB are located where the Bransfield Basin axis intersects these NW-trending faults. In the EBB, the NW-trending faults are associated with broad, complex, high-standing „rises“ that separate 2 km-deep troughs. Both Bridgeman and Gibbs Rise have large seamounts at their intersection with the Bransfield Basin axis, whereas the central peak on Spanish Rise has less relief.

Young lavas have been recovered from most of the seamounts and ridges of the CBB (Keller and Fisk, 1991; Keller et al., submitted; Gracia, pers. comm.). These lavas show a progressive geochemical gradation along the CBB from relatively MORB-like in the SW to relatively arc-like in the NE (Keller et al., submitted). However, the two largest volcanic constructs (Deception and Bridgeman Islands) have similar geochemistry, despite being located at opposite ends of the CBB, and both are arc-like. The prevailing model for volcanism in the CBB involves an initial phase of focussed volcanism to generate large conical volcanoes, followed by progressive rifting of these volcanoes and development of NE-SW propagating volcanic ridges (Gracia et al., 1996). The propagating ridges have been interpreted to mark the transition from rifting to incipient seafloor spreading (e.g., Keller et al., submitted).

The evolution of volcanism in the EBB is less clear and only one small seamount had been sampled prior to SO 155. The EBB is wider, contains far deeper troughs between the NW-trending normal faults, but lacks obvious conical volcanoes of the type found in the CBB. Seismic profiles across the EBB suggest it is in a more advanced stage of rifting than the CBB, and that rifting in Bransfield Basin has propagated from NE to SW. These studies

also suggest that sediment cover in the EBB troughs is thin, and that they may be flooded by young pillow and sheet flows (e.g., Gracia et al., 1996; 1997).

There are several problems with the current understanding of volcanism in the CBB and EBB. For example, if rifting has progressed from the EBB to the CBB, then the gradation from arc-like lavas at the EBB/CBB boundary to MORB-like lavas at the SW end of the CBB is the opposite of that expected. Are the geochemical trends from NE to SW along the propagating ridges of the CBB matched by similar trends in the older large conical volcanoes of the CBB? What is the age relationship of the ridges to the cones in the CBB? What is the nature of the unsampled volcanism in the EBB? Do the geochemical trends in the CBB lavas continue to the NE in the volcanic ridges and presumed sheet flows of the EBB?

These issues were discussed at a shipboard meeting of the SO 155 Petrology Group on 28 February. The following priority and target list was set for hard rock sampling during SO 155 (see Fig. 8.1):

1. Top priority was to obtain the first comprehensive set of samples from the EBB. The areas of the EBB selected for dredging were Bridgeman Rise (3 stations), G Ridge (5 stations), Spanish Rise (5 stations), Gibbs Deep (1 station) and Gibbs Rise (4 stations).
2. Second priority was to obtain samples from the 1967-70 eruption sequence at Deception Island for isotopic studies.
3. Third priority was to obtain new samples from the CBB that fill gaps in the existing sample coverage. The areas of the CBB selected for dredging were Hook Ridge (2 stations), Viehoff (3 stations), Three Sisters (4 stations) and Axe (2 stations).

The first and second priorities had been met in full by the end of the Bransfield Basin program. Unfortunately, severe weather and ice conditions prevented dredging at most of the lower priority targets in the CBB. A total of 252 samples were collected from 26 petrology stations in the EBB and on Deception Island (Table 8.1). Of these, 214 were considered *in situ* and the remainder erratics (glacial dropstones). A total of 83 were selected and prepared for initial geochemical studies (major and trace elements) back in Germany.

An unexpected consequence of adverse sea conditions in Bransfield Strait was the opportunity to obtain samples from Aluk Ridge. Aluk Ridge is a segmented paleo-spreading centre that separated the Antarctic and Phoenix Plates and was active from at least 50 Ma until 3 Ma (Fig. 8.2; Barker, 1982; note that the Phoenix Plate is also referred to as Drake Plate in early literature). The full spreading rate at the ridge was 6 cm per year, similar to that at the mid-Atlantic Ridge, from 20 to 6.7 Ma. However, the ridge segments were progressively subducted at the South Shetland Trench until only 4 segments remained at 6.7 Ma. Following subduction of the Anvers segment, the spreading rate at the remaining segments declined and probably ceased at either 3.5 or 2.4 Ma, dependent upon the identification of poorly-known seafloor magnetic lineations. There are no published analyses of lavas from Aluk Ridge.

The age at which spreading ceased on Aluk Ridge is a key issue in the debate about the origin of Bransfield Basin. Most published models hold that subduction at the South Shetland Ridge ceased when Aluk Ridge became inactive, and that Bransfield Basin has only opened since that time in response to passive, slow, slab rollback at the trench (e.g., Gracia et al., 1996; Keller et al., submitted). Therefore, the age at which spreading ceased on Aluk Ridge is critical to an understanding of the evolution of Bransfield Basin.

Equally important is whether spreading has truly ceased, or continues at some reduced rate, or was even re-activated at some more recent time. Other outstanding questions that can be addressed by studies of Aluk Ridge concern the geochemical consequences of spreading ridge death (i.e., are the last lavas derived from a progressively more depleted mantle source)?

The two western segments of Aluk Ridge were dredged at the conclusion of the Bransfield Basin program. International treaty obligations and further adverse weather in Drake Passage prevented any work on the two eastern segments. A total of 67 samples were collected from 6 petrology stations on Aluk Ridge (Table 8.2). Of these, 57 were considered *in situ* and the remainder erratics. A total of 24 were selected and prepared for initial geochemical studies (major and trace elements) back in Germany.

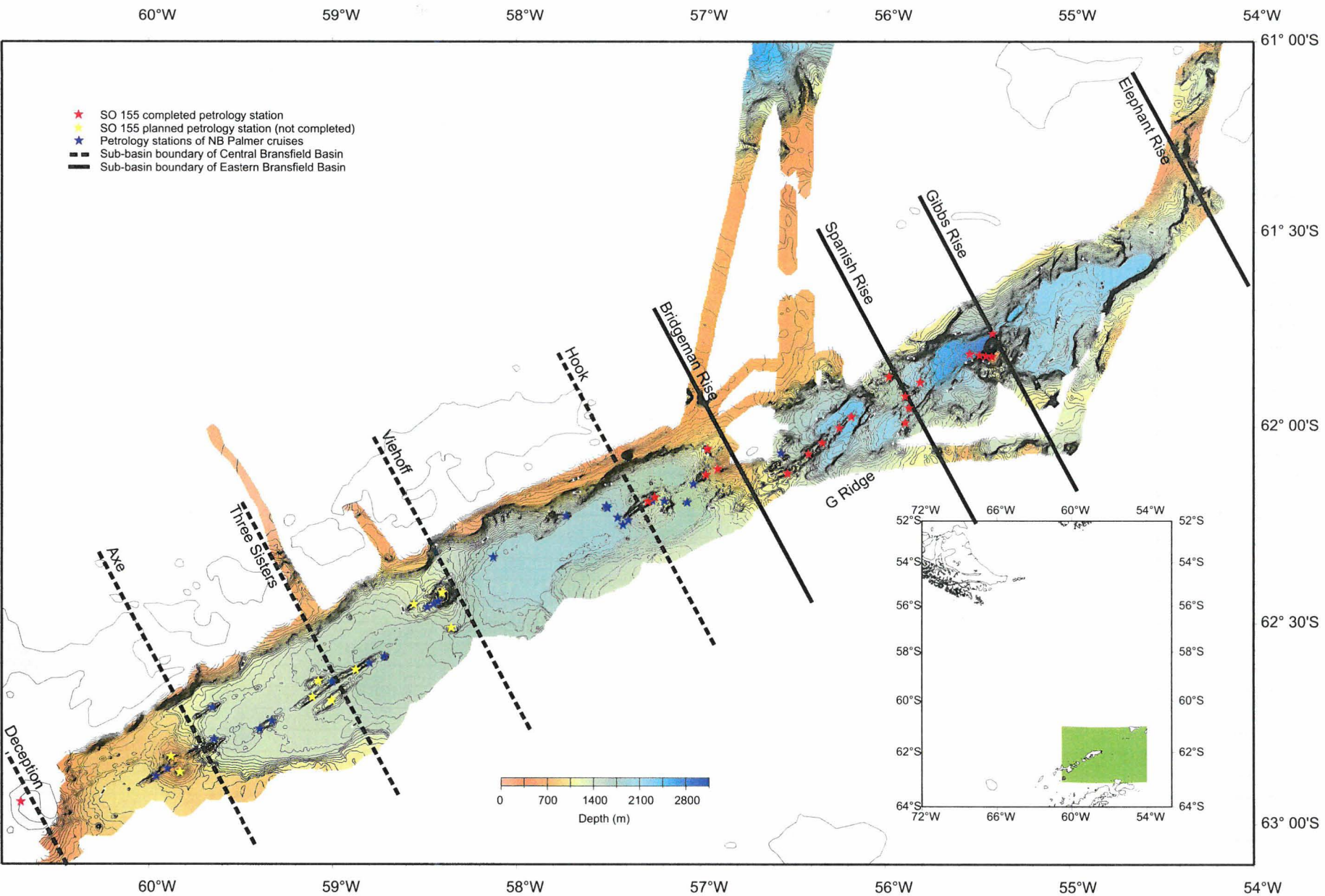


Fig. 8.1. Bathymetric map of the Bransfield Strait showing the location of petrology stations and subbasin boundaries (bathymetry courtesy of Oregon State University).

Table 8.1: Recovered samples and lithologies from the Bransfield Basin

Station	N	N (in situ)	Geo anal.	Aph. BA	OI BA 5-15%	OI BA >15%	Px BA 5-15%	PI BA 5-15%	PI BA >15%	OI-PI BA	Px-PI BA	Aph. DA	PI DA 5-15%	PI DA >15%	Brec.	Volc. SST	Dol/Gab.	Wack	Ash
02-DR	18	15	5	X															
03-DR	18	18	11	X		X	X	X		X		X		X					
04-DR	14	14	7	X				X	X										
07-GTV	4	4	1									X							
09-MUC	1	1	1									X							
12-DR	-	-	-																
13-DR	11	9	3	X															
14-DR	9	7	3		X	X				X									
15-DR	9	9	3		X														
16-DR	12	11	4	X				X											
17-DR	11	11	3		X														
18-DR	12	11	4	X	X	X													
19-DR	-	-	-																
20-DR	18	14	4	X					X		X				X				
21-DR	13	13	2	X					X		X						X	X	
22-DR	10	-	3																
23-DR	13	13	5						X		X		X				X		
24-DR	10	1	-													X			
25-DR	11	7	4	X	X														
26-DR	9	8	3	X	X		X									X			
27-DR	5	5	1					X											
28-DR	10	10	3		X												X		
38-DR	7	6	2									X							
39-DR	1	1	-										X						
40-DR	5	5	3									X							X
52-BIO	21	21	8	X				X							X				
Stn: 26	252	214	83	11	7	3	2	5	4	2	3	5	2	1	2	2	3	1	1

Abbreviations: N - total number of samples; N (in situ) - total number of *in situ* samples (i.e., excluding erratics)
 Geo anal. - number of samples selected and prepared for geochemical analysis

Lithological: Aph. - aphyric, BA - basalt to andesite, DA - dacite, OI - olivine, Px - pyroxene, PI - plagioclase, Brec. - breccia, Volc. SST - volcanoclastic sandstone-siltstone (including hyaloclastite), Dol/Gab. - dolerite/gabbro, Wack - wacke.

Table 8.2: Recovered samples and lithologies from Aluk Ridge

Station	Np	N (in situ)	Geo anal.	Aph. BA	OI BA 5-15%	OI BA >15%	Px BA 5-15%	PI BA 5-15%	PI BA >15%	OI-PI BA	Px-PI BA	Aph. DA	PI DA 5-15%	PI DA >15%	Brec.	Volc. SST	Dol/ Gab.	Wack	Ash
53-DR	20	20	5	X				X	X						X				
54-DR	-	-	-																
55-DR	19	19	8	X	X										X		X		
56-DR	25	17	10	X	X	X											X		
57-DR	3	1	1						X										
58-DR	-	-	-																
Stn: 6	67	57	24	3	2	1	-	1	2	-	-	-	-	-	2	-	2	-	-

Abbreviations: N - total number of samples
 N (in situ) - total number of *in situ* samples (i.e., excluding erratics)
 Geo anal. - number of samples selected and prepared for geochemical analysis

Lithological: Aph. – aphyric, BA – basalt to andesite, DA – dacite, OI – olivine, Px – pyroxene, PI – plagioclase, Brec. – breccia, Volc. SST – volcanoclastic sandstone-siltstone (including hyaloclastite), Dol/Gab. – dolerite/gabbro, Wack. – wacke.

49

Table 8.3: Total recovered samples and lithologies

Stations	N	N (in situ)	Geo anal.	Aph. BA	OI BA 5-15%	OI BA >15%	Px BA 5-15%	PI BA 5-15%	PI BA >15%	OI-PI BA	Px-PI BA	Aph. DA	PI DA 5-15%	PI DA >15%	Brec.	Volc. SST	Dol/ Gab.	Wack	Ash
Bran: 26	252	214	83	11	7	3	2	5	4	2	3	5	2	1	2	2	3	1	1
Aluk: 6	67	57	24	3	2	1	-	1	2	-	-	-	-	-	2	-	2	-	-
Total: 32	319	271	107	14	9	4	2	6	6	2	3	5	2	1	4	2	5	1	1

Abbreviations: N - total number of samples
 N (in situ) - total number of *in situ* samples (i.e., excluding erratics)
 Geo anal. - number of samples selected and prepared for geochemical analysis

Lithological: Aph. – aphyric, BA – basalt to andesite, DA – dacite, OI – olivine, Px – pyroxene, PI – plagioclase, Brec. – breccia, Volc. SST – volcanoclastic sandstone-siltstone (including hyaloclastite), Dol/Gab. – dolerite/gabbro, Wack. – wacke.

In total, the Petrology Group collected 319 samples from 32 petrology stations in Bransfield Basin and on Aluk Ridge, of which 271 were regarded as *in situ* and 107 were prepared for geochemical analysis (Table 8.3). A detailed description of each petrology station and the rocks recovered is given in Appendix 2.

8.2 Glacial Dropstones

Boulders dropped by melting icebergs („erratics“) were recovered from almost every dredge station. In general, these erratics can be recognised by their well-rounded to sub-rounded nature, their disparate lithologies compared to the expected volcanics, and their more weathered character. The adopted policy on erratics was to collect only exceptional specimens or, where recovery of *in situ* lavas was minimal, to collect a representative suite for archive purposes. In cases of doubt (e.g., weathered sub-rounded lavas that could be native to Bransfield Strait or erratics from the outcropping calc-alkaline volcanics on the South Shetland Islands), the recovered specimens were treated as *in situ* samples and retained for further examination in Germany.

The recovery of erratics at each dredge station varied irregularly, both as an absolute number and as a proportion of the total dredge haul. No correlation was observed between station location and either the number or the proportion of recovered erratics. For example, Station 13-DR recovered 10 erratics representing <5 % of a moderate dredge haul, whereas the nearby Station 14-DR (<10 km to the northeast and in water only 200 m deeper) recovered ~1000 kg of erratics representing >70 % of a large dredge haul. The maximum size of the erratics correlated roughly with the number of erratics, and those larger than 15 cm across were usually restricted to stations with large volumes of erratics.

The predominant erratic lithologies were:

1. Micaceous schists. These ranged from finely laminated biotite-bearing schists to those in which the lamellae were isoclinally folded with wavelengths of 5-10 cm and cut by numerous <1 mm wide quartz veins. The schists were often recovered as large (>20 cm across) rectangular to platy blocks, broken from their outcrops along joint planes, and were seldom rounded. These schists were probably derived from the mid-Cretaceous greenschist-blueschist metamorphic rocks that outcrop on Elephant Island, and they were noticeably more common at the northeastern EBB stations.

2. Plutonic rocks. A wide variety of coarse grained gabbros, diorites, granodiorites and granite, together with fine grained dolerite, were recovered at most stations, and these were the dominant erratic lithology at Aluk Ridge. These lithologies were usually well rounded and seldom exceeded 10 cm in diameter in Bransfield Strait, although at Aluk Ridge some were angular and nearly 1 m in length. They were probably derived from the mid- to late Cretaceous calc-alkaline plutonics outcropping on the South Shetland Islands (in particular Livingstone to King George Islands), although similar plutonics also outcrop on Trinity Peninsula.
3. Sedimentary rocks. A few well-rounded boulders of weathered shale, greywacke and quartz wacke, often cut by <1 mm wide quartz veinlets, were recovered at many stations. These closely resemble the late Carboniferous to Triassic sedimentary sequence found on the South Shetland Islands, especially the Miers Bluff Formation on Livingstone Island.
4. Alkali feldspar-bearing lavas. A few small weathered, well-rounded trachyte and trachybasalt erratics were recovered at some stations. These may have been derived from the Erebus-Terror and related alkaline volcanics of the Ross Sea, but trachytic lavas are widespread around coastal Antarctica.

Overall, the provenance of the erratics in Bransfield Basin is consistent with glacial plucking from the South Shetland Islands followed by southwestward movement of calved icebergs across Bransfield Strait. None of the recovered lithologies require a Trinity Peninsula source. Similarly, the erratics at Aluk Ridge may have been dropped by icebergs calving from the northern shore of the South Shetland Islands and drifting northeast across the Antarctic Sea.

8.3 Hook Ridge

Fresh lavas were recovered from 5 of 6 petrology stations on Hook Ridge (4 dredges, 1 TV-grab, 1 multicorer). The prime objective of these stations was to obtain altered rocks and sediment from the hydrothermal system located on the southern flank of the summit crater on the principal NW-SE trending ridge (Fig. 8.1). Previous cruises of the NB Palmer had obtained fresh aphyric rhyolite and rhyodacite from this area (Keller et al., submitted).

The rocks recovered from stations 07 GTV, 09 MUC, 38-DR and 40-DR had pillow forms and were black glassy aphyric dacites (or rhyodacites) with sub-conchoidal fracture and

weakly developed flow alignment of vesicles. All were extremely fresh and unweathered. In contrast, a weakly weathered plagioclase-bearing dacite was recovered from station 39-DR, where it was associated with widespread native sulfur and grey clays.

The aphyric Hook Ridge samples closely resemble the aphyric rhyodacites recovered by the NB Palmer cruises and are almost certainly the same unit. The presence of pillow forms and flow alignment textures suggest the summit of Hook Ridge is largely covered by this aphyric dacite flow sequence. The dacite/rhyodacite is clearly young (maximum age of several hundred years, probable age of a few hundred years). A dark green coarse ash layer >4 cm thick and consisting of fresh glass often embedded in fresh black aphyric dacite fragments was recovered at station 40-DR, and probably represents either waning pyroclastic activity associated the dacite flows or a younger small pyroclastic eruption. In contrast, the plagioclase-bearing dacite at station 39-DR appears to be a much smaller localised lava flow and is older in appearance, although its association with diffuse hydrothermal venting may cause faster weathering.

8.4 Bridgeman Rise

Bridgeman Rise is a broad high-standing region that separates the Central and Eastern Bransfield Basins (Fig. 8.1). The rise separates the 1500 m-deep Hook Basin of the CBB from the 2500 m-deep Trough 1 of the EBB, and consists of two central high-standing volcanic constructs: Bridgeman Island to the east and an unnamed edifice to the west. Both of these are flanked to the north and south by axial valleys trending sub-parallel to Bransfield Strait.

A narrow ridge protrudes from the unnamed central western edifice, trends towards Hook Ridge, and may be continuous with Hook Ridge. Dredging on the mid-slope of this feature (station 02-DR) recovered fresh to weakly weathered dark grey aphyric andesite with well-developed glassy pillow crusts, flow banding, and minor orange surface staining. These rocks were thickly coated with grey mud when dumped on the deck. Dredging on the slopes of Bridgeman Rise above the western ridge (station 03-DR) returned a wide variety of lavas ranging from fresh black glassy aphyric dacite to a series of fresh coarse-grained plagioclase-rich dacites, weakly weathered pillow lavas consisting of dark grey olivine and olivine-plagioclase basalt, and a more weathered sequence of block jointed plagioclase and pyroxene-bearing basalt and andesite. The western ridge is clearly the site of

relatively recent volcanism of similar character to that at Hook Ridge (i.e., young aphyric and plagioclase-bearing andesite-dacite), and has apparently broken through the western flank of Bridgeman Rise. In contrast, the upper part of Bridgeman Rise appears to consist of significantly older olivine and plagioclase-bearing jointed lavas.

The third dredge station on Bridgeman Rise was a small seamount located in the axial valley to the north of the unnamed central western edifice (station 04-DR). This returned a series of fresh black plagioclase-bearing and aphyric pillow basalts with well-developed glassy crusts, together with a more weathered aphyric basalt. The axial seamount is apparently also a site of relatively recent volcanism.

8.5 G Ridge

The G Ridge is a 30 km-long narrow ridge extending from the top of the southern axial valley on Bridgeman Rise into the 2 km-deep Trough 1 of the EBB (Fig. 8.1). The lower half of G Ridge bisects the axis of Trough 1, and this ridge has been likened to a developing spreading centre in previous geophysical and morphological studies (e.g., Gracia et al., 1996). Therefore, it was expected to be covered by very young lavas. A series of 5 stations were dredged on the ridge, in descending bathymetric order from near Bridgeman Rise to where the ridge disappears into Trough 1 (stations 13-DR to 17-DR).

Weakly weathered vesicular aphyric black andesite was recovered from the highest part of G Ridge adjacent to Bridgeman Rise (station 13-DR). These lavas are clearly young, and some have thin coatings of Fe-stained silica. In marked contrast, the second to highest station (14-DR) recovered an older series of weakly weathered vesicular olivine- and plagioclase-bearing basalts in which some of the vesicles were infilled with soft clay. Nevertheless, the olivines were fresh and green, and there was no development of MnOx crusts. The central station (15-DR) recovered a weakly weathered olivine basalt with a well developed but largely palagonised glassy pillow crust. The second to lowest station (16-DR) recovered rather fresher black aphyric and plagioclase-bearing basalts with minor glass development on pillow crusts. The lowest station at the NE-foot of G Ridge (17-DR) recovered weakly weathered olivine basalt with well-developed but often palagonised glass pillow crusts very similar to that at the central G Ridge site.

The results from G Ridge were not as expected. Although recent volcanism has occurred at the top of the ridge and near the second to lowest station, the remaining stations provide clear evidence that much of G Ridge has not been re-surfaced in several hundreds or, more probably, several thousands of years. Sufficient time has elapsed for clays to infill vesicles in these lavas, weak weathering rinds to develop, and for glassy pillow crusts up to 2 mm thick to be almost completely palagonised. This result is at odds with the predictions of Gracia et al. (1996). It is patent that G Ridge is not an active spreading centre, nor has it been the site of much volcanism for a long time.

8.6 Spanish Rise

Spanish Rise is a broad high-standing region similar in structure to Bridgeman Rise, and separates Troughs 1 and 3 of the EBB (Fig. 8.1). A geophysical profile across the EBB passes through Spanish Rise, and Gracia et al. (1996) interpreted the southern axial valley as the locus of active seafloor spreading, flanked to the north and south by older volcanic constructs. Five dredge stations were completed on the most prominent topographic features of Spanish Rise; the northern flank, the central and middle slopes of the central high, the southern axial valley, and the southern flank (stations 18-DR and 25 to 28-DR).

The northern flank dredge (station 18-DR) recovered weakly weathered olivine-bearing basalts with well-developed but generally palagonised glassy pillow crusts, together with a moderately weathered block-jointed aphyric andesite. Both dredges in the mid and upper slopes of the central high (stations 25-DR, 26-DR) recovered moderately weathered olivine-bearing basalts, some with thin quartz veinlets or other evidence of alteration, although most of the olivine remained green and fresh. A weathered aphyric basalt was also sampled from station 25-DR, and a weathered plagioclase andesite at station 26-DR. In contrast to these samples, fresh black plagioclase basalts with autobrecciating crusts were recovered from a seamount in the southern axial valley (station 27-DR). The southern flank of Spanish Rise (station 28-DR) returned moderately weathered olivine basalt with a well-developed glassy pillow crust.

The southern axial valley of Spanish Rise appears to be a site of relatively recent volcanism, but the flanking highs and central high have clearly not been active for a long time. Again, these results are contrary to those expected and indicate that the magma flux has been low at Spanish Rise for a considerable time.

8.7 Gibbs Deep

Two attempts were made to obtain samples from a small 300 m-high seamount located in the Gibbs Deep to the southwest of Gibbs Rise (stations 19-DR, 24-DR). The models of Gracia et al. (1996) and others had suggested this seamount and the surrounding Trough 3 plain could be composed of young pillow and sheet flows. No rocks were recovered on the first attempt, although several weak „bites“ were noted on the dredge log. The second attempt, dredging from the opposite direction, recovered numerous erratics together with a well-compacted volcanoclastic sandstone-siltstone. The seamount is interpreted as a very old structure buried by a considerable thickness of sediment. In light of this result, it is reasonable to assume that the flat Trough 3 plain surrounding the seamount is also composed of thick sediments.

8.8 Gibbs Rise

Gibbs Rise is a broad high-standing region similar in structure to Bridgeman Rise, and separates Troughs 3 and 4 of the EBB (Fig. 8.1). The central high has the form of a large conical seamount that has been truncated on its northwestern flank. Unlike Bridgeman and Spanish Rises, the northern axial valley is far better developed and deeper than the southern axial valley. Four stations were located on Gibbs Rise (stations 20 to 23-DR); three of these sampled the lower, middle and upper flanks of the central high, whereas the remaining dredge sampled the northern axial valley.

The lower and mid-flanks of the central high (stations 20-DR, 21-DR) returned a series of altered, mostly plagioclase-bearing, lavas and a few fine grained block-jointed dolerites. All of these have been chloritised, silicified and hematized to varying extents, and commonly contain disseminated pyrite and/or other sulfides. Quartz veins and veinlets were often present. These lavas have been more thoroughly described by the hydrothermal and sulfide working groups. Only erratics were recovered from the upper flanks of the central high (station 22-DR). Dredging of the northern axial valley (station 23-DR) recovered a deeply weathered plagioclase andesite with clay-filled vesicles together with a quartz-veined dolerite containing disseminated pyrite.

The rocks recovered from Gibbs Rise are completely unlike those recovered from elsewhere in the EBB. Their plagioclase-rich character, old age, outcrops of dolerites and intrusive rocks, and extent of hydrothermal alteration are all consistent with Gibbs Rise

being an old arc-related volcano or area of arc-generated crust. The alteration may or may not have occurred during dissection and tectonism associated with the opening of the EBB. There is no evidence of recent volcanism at any of the stations on Gibbs Rise.

8.9 Deception Island

Samples from the beach at Fumarole Bay were recovered during a visit by the biologists and the Chief Scientist. The principal lithology sampled was fresh black vesicular aphyric basalt from the 1967-1970 eruption sequence. Also recovered were a series of red and black aphyric lavas from the older post-caldera sequence on top of the ridge behind Fumarole Bay, and some pre-caldera lavas and clasts from the the Yellow Tuff Series pyroclastic flows (complete with palagonised glassy matrix).

8.10 Aluk Ridge

Following the early termination of the Bransfield Basin program, the Smith and Sandwell (1997) inferred bathymetry for Aluk Ridge was re-interpreted by the Shipboard Scientific Party. Four ridge segments were identified, but International Treaty obligations and sea conditions restricted our attention to only the two southwestern segments (Fig. 8.2). The key aim of the six dredge stations on these segments was to recover samples from both flanks of these two ridge segments. The samples will be analysed and dated back in Kiel. There are no published high resolution bathymetric maps of Aluk Ridge, and no published analyses of rocks from the ridge.

Six dredge stations were completed on the two southwestern segments of Aluk Ridge (stations 53-DR to 58-DR). A wide variety of lavas were recovered from both segments, mostly consisting of grey aphyric and plagioclase-bearing pillow basalts with Fe-stained irregular fractures and vesicles rimmed by soft clays or zeolite (stations 53-DR and 56-DR), grey olivine basalts in which some of the olivines have begun to alter and are now colourless (stations 55-DR and 56-DR), and a distinctive plagioclase-rich basalt (station 57-DR). Many of these lavas have adhering pieces of palagonised hyaloclastite. A series of pervasively chloritised and silicified lavas grading through to apple green chlorite-smectite-silica rock retaining an original hyaloclastite texture were also recovered from station 53-DR, and have been described in more detail by the hydrothermal working group. All of these lavas are moderately to deeply weathered, and many have 1-2 mm of MnOx

crust on top of an orange clay layer that rests on palagonised glassy pillow crusts (especially station 56-DR).

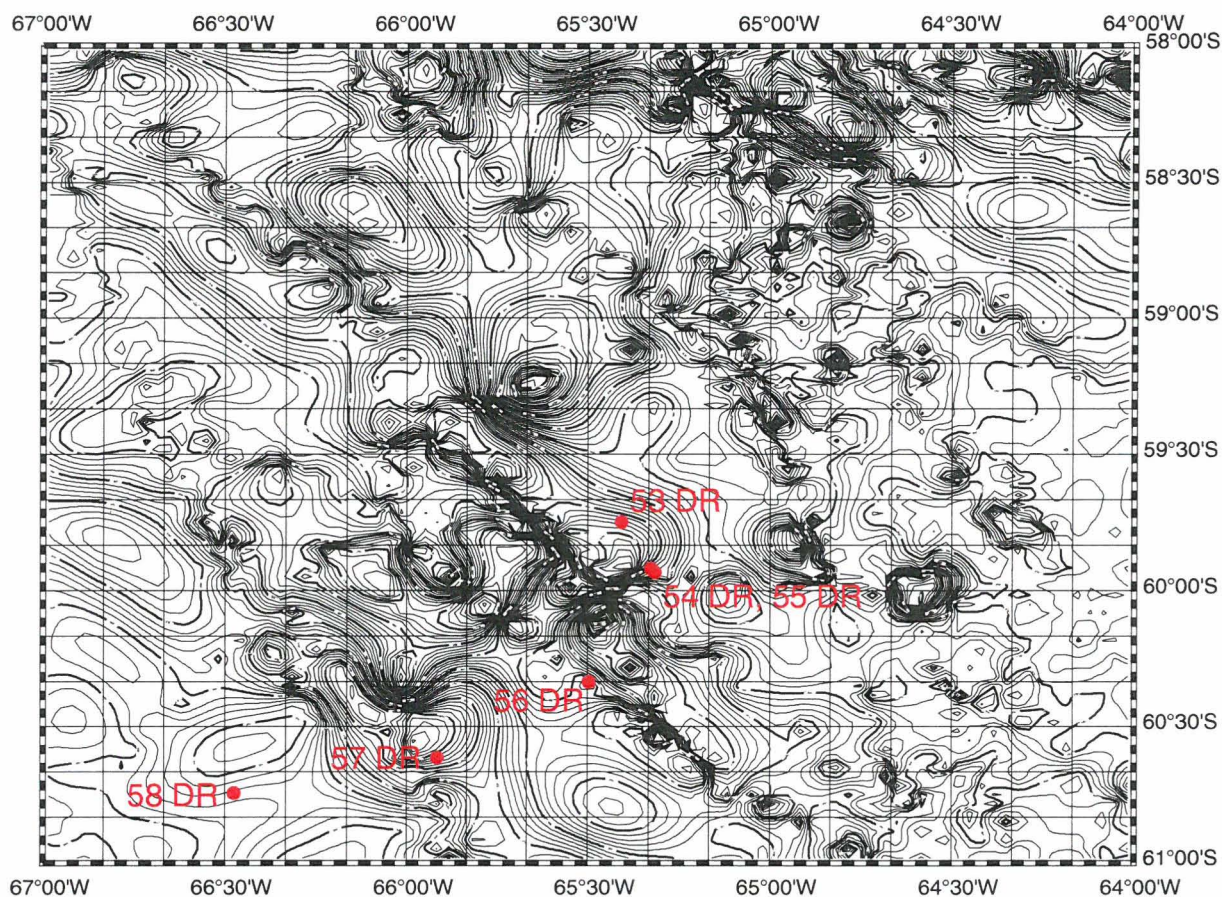


Figure 8.2. Predicted seafloor bathymetry and location of dredge Stations along the two southern segments of Aluk (Phoenix) Ridge. Predicted bathymetry from Sandwell and Smith.

The rocks from Aluk Ridge are clearly more weathered and older than any recovered from the EBB, with the possible exception of Gibbs Rise. The thin MnOx crusts and partial alteration of olivine phenocrysts is consistent with the expected 2.5 – 3.4 Ma age of the lavas (Barker, 1982). Nothing was seen to suggest that either of the two ridge segments has been active since that time.

9 OFOS Observations

Locations given in this report are usually coordinates derived from the subpositioning system deployed on the OFOS, however, station 46-OFOS was deployed without the subpositioning system because of the very shallow water depth within the crater of Deception Island (<170 m) preventing a large offset between ship and towed instrument. The detailed protocols for all 4

stations can be found in Appendix 2.

Table 9.1: Summary of OFOS stations

Station (date)	Area	time on bottom [UTC]	Lat. [S]	Long- [W]	depth	comment
01-OFOS (03.01. - 03.02)	Hook Ridge crater and „hinge area“	on bottom 19:09 – 22:36 and 00:11 – 01:47	on bottom 62°11.016 off bottom 62°12.894	on bottom 57°16.930 off bottom 57°15.919	on bottom 1215 m off bottom 1531 m	422 slides; 2 BW & 2 color video tapes; 2 subprofiles
41-OFOS (03.08. - 03.09)	Viehoff Seamount	on bottom 23:22 – 03:30	on bottom 62°24.980 off bottom 62°26.009	on bottom 58°23.937 off bottom 58°24.388	on bottom 918 m off bottom 1048 m	750 slides; 2 BW & 2 color video tapes; 2 subprofiles
45-OFOS (03.09. - 03.10)	Deception crater	on bottom 22:30 - 00:40	on bottom 62°58.995 off bottom 62°58.938	on bottom 60°38.124 off bottom 60°37.130	on bottom 91 m off bottom 120 m	443 slides; 1 BW & 1 color video tape
46-OFOS (03.10)	Deception crater	on bottom 01:16 – 02:38	on bottom 62°58.008 off bottom 62°57.405	on bottom 60°39.044 off bottom 60°38.979	on bottom 120 m off bottom 170 m	250 slides; 1 BW & 1 color video tape

01-OFOS Hook Ridge

Objectives: This station was carried out in order to relocate the area of hydrothermal precipitates within the crater of Hook Ridge and also to observe a plume site in the “hinge“ area to the southeast of the crater. The crater of Hook Ridge was sampled during Nathaniel B. Palmer cruise NBP99-04 in 1999 using a TV-guided grab and hydrothermal precipitates recovered from the crater in 1999 included altered sediment with vesicles lined by native sulfur and one piece of massive Zn-Ba-rich sulfide talus.

The OFOS started at 62°11.016'S / 57°16.930'W at the northern flank of Hook Ridge in a water depth of 1215 m (Fig. 9.1). During lowering a potential small plume was detected by the CTD-system at a water depth of approximately 1000 m which corresponds with the crest height of Hook Ridge (Fig. 9.2). The OFOS reached the bottom at 19:09 [UTC] at the northern flank of the ridge close to the entrance to the crater. The seafloor in this area is covered with thick sediment with some brittle stars. The instrument was then towed in a southeasterly direction towards the hydrothermal area. The number of brittle stars clearly increased when the rim was approached. Abundant Fe-oxyhydroxides were observed close to the outer rim of the crater covering large areas of rocky outcrop and also the

upper parts of smaller terraces (Fig. 9.3a). It is not clear whether these Fe-precipitates are related to oxidation of primary high-temperature sulfide assemblages, low-temperature diffuse flow, or to the cooling of individual lava flows resulting in Fe-oxide staining of the lava surface. The area of Fe-oxyhydroxides was followed by heavily sedimented seafloor reaching all across the crater until the OFOS reached the southern wall of the crater. Here white, siliceous (?) patches appeared on the seafloor sometimes in close association with minor amounts of Fe-oxyhydroxides. These hydrothermal areas are not extensive and sediment ponds lie in between them. Small conical depressions and even larger circular features with a flat bottom and a several cm high coarse rim are the dominant shapes of these proposed fluid exit sites (Fig. 9.3a,b). Small outcrops associated with these vent sites are often devoid of background sediment, probably because of fluid upflow through the rubble thereby preventing sedimentation. The main geological features observed during this first part of the station are presented in Figure 9.4. Potential temperature anomalies up to 0.15°C were recorded in areas of white hydrothermal precipitates (Fig. 9.5a) and were associated with an increase in conductivity. Three additional tracks were run parallel to the first track line in this hydrothermally influenced area in order to map the areal extent of the hydrothermal field at the southern wall. Several other potential temperature and conductivity anomalies have been recorded near the southern wall of the crater (Fig. 9.5b).

It was then decided to bring up the OFOS to 850 m and to relocate the ship and the OFOS system to the „hinge“ area slightly SE of the crater. The upcast ($62^{\circ}11.461'\text{S}/57^{\circ}16.645'\text{W}$) started at 22:36 [UTC] and is characterized by a small bottom anomaly and shows an overall irregular temperature versus depth correlation when compared with the downcast (Fig. 9.6) which might indicate the influence of hydrothermal activity to the lower part of the water column above the crater.

After relocation of the ship to the “hinge“ area the OFOS was lowered back to the seafloor at 00:11 [UTC]. This „hinge“ area was surveyed during cruise NBP99-04 in 1999 and a nephelometer and Mn anomaly was detected at $62^{\circ}12.50'\text{S}/57^{\circ}14.80'\text{W}$ (station ZAPS 22) on top of a bathymetric high. During the lowering of the OFOS to the seafloor (at $62^{\circ}12.310'\text{S}/57^{\circ}16.211'\text{W}$) on the northwestern flank of this structure two small plume signals were recorded by the CTD in different water depths (Fig. 9.7). The upper plume was recorded at a water depth of 1000 m and a larger, deeper plume was recorded at water depths between 1250 m and 1350 m. The OFOS was targeted in a southeasterly

direction towards the location of ZAPS 22, however an iceberg prevented the ship from reaching its target position and so the OFOS track was skirting the bathymetric high at its southwestern flank. The area is heavily sedimented and no evidence for hydrothermal activity was observed and no anomalies were recorded by the CTD (Fig. 9.7). The geological features observed during this subprofile are given in Figure 9.8. The station ended at 01:47 [UTC] and during the upcast a much smaller „plume“ signal was recorded in the water column at 1200 – 1150 m (Fig. 9.9).

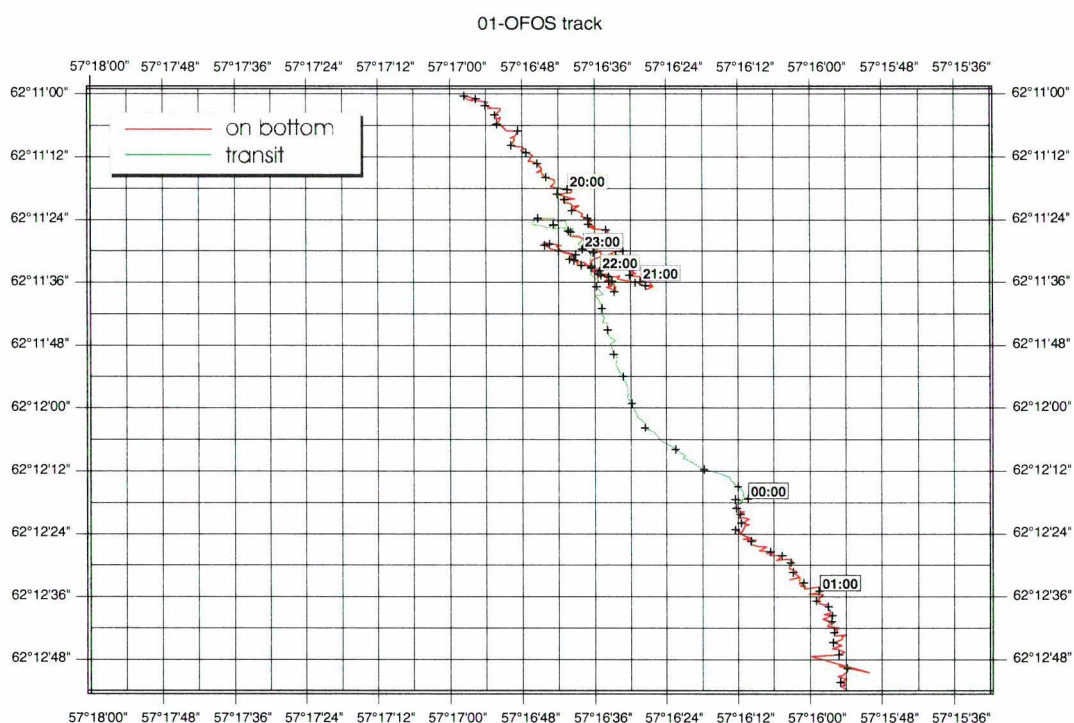


Fig. 9.1: Track plot for station 01-OFOS.

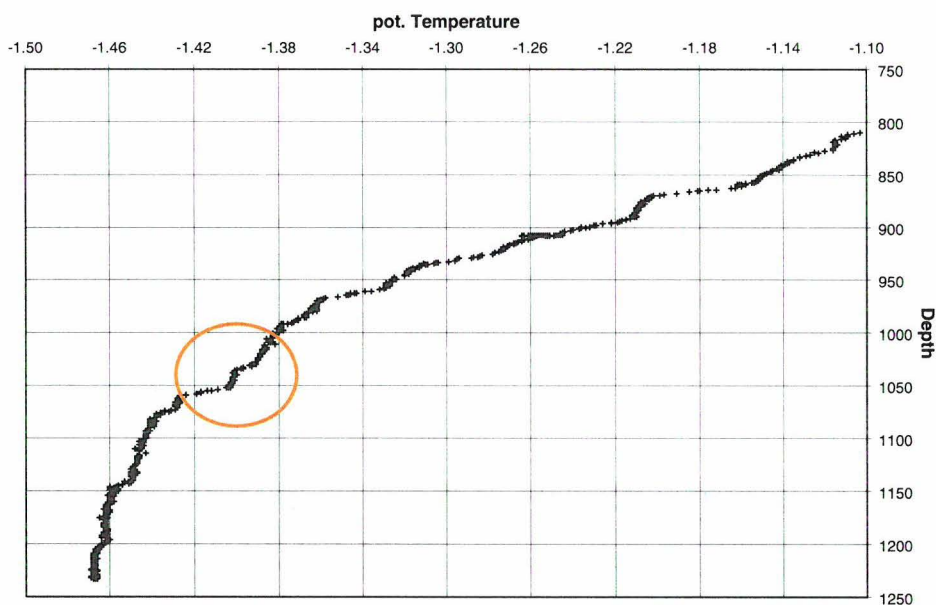


Fig. 9.2: Pot. temperature versus depth for the down-cast (62°11.020'S / 57°16.965'W) at the northern flank of Hook Ridge crater.

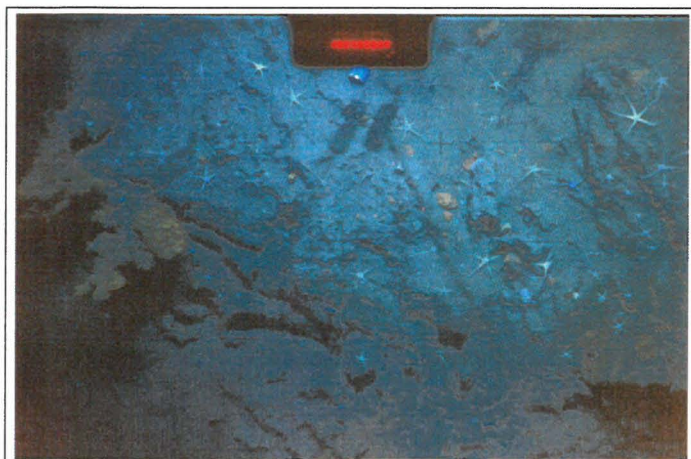


Fig. 9.3: Bottom photographs obtained during station 01-OFOS.

a) Fe-oxyhydroxides near the northern crater rim. It is not clear if these Fe-oxyhydroxides are low-temperature coatings on basalt outcrops or related to oxidizing massive sulfides. A weak temperature anomaly over a wider area is associated with these Fe-oxyhydroxides.

Slide 047; time: 19:27:23; depth 1154 m
OFOS position: 62°11.084'S / 57°16.864'W



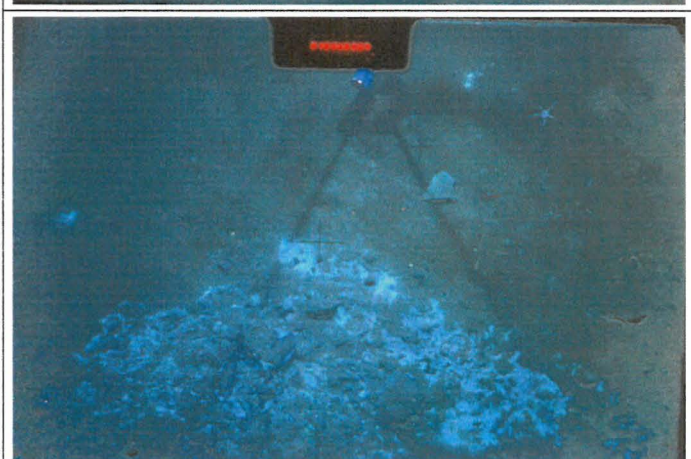
b) White patches of amorphous silica (?) protruding through the sediment close to the southern wall of the crater. There is no temperature anomaly associated with this exposure.

Slide 158; time: 20:36:17; depth 1063 m
OFOS position: 62°11.480'S / 57°16.543'W



c) Circular depressions within the sediment lined with hydrothermal precipitates. There is no temperature anomaly associated with this feature.

Slide 277; time: 21:28:11; depth 1038 m
OFOS position: 62°11.522'S / 57°16.653'W



d) Small rock pile devoid of sediment due to the diffuse venting of hydrothermal fluids (?). There is a weak temperature anomaly associated with this outcrop.

Slide 307; time: 21:59:56; depth: 1056 m
OFOS position: 62°11.564'S / 57°16.587'W

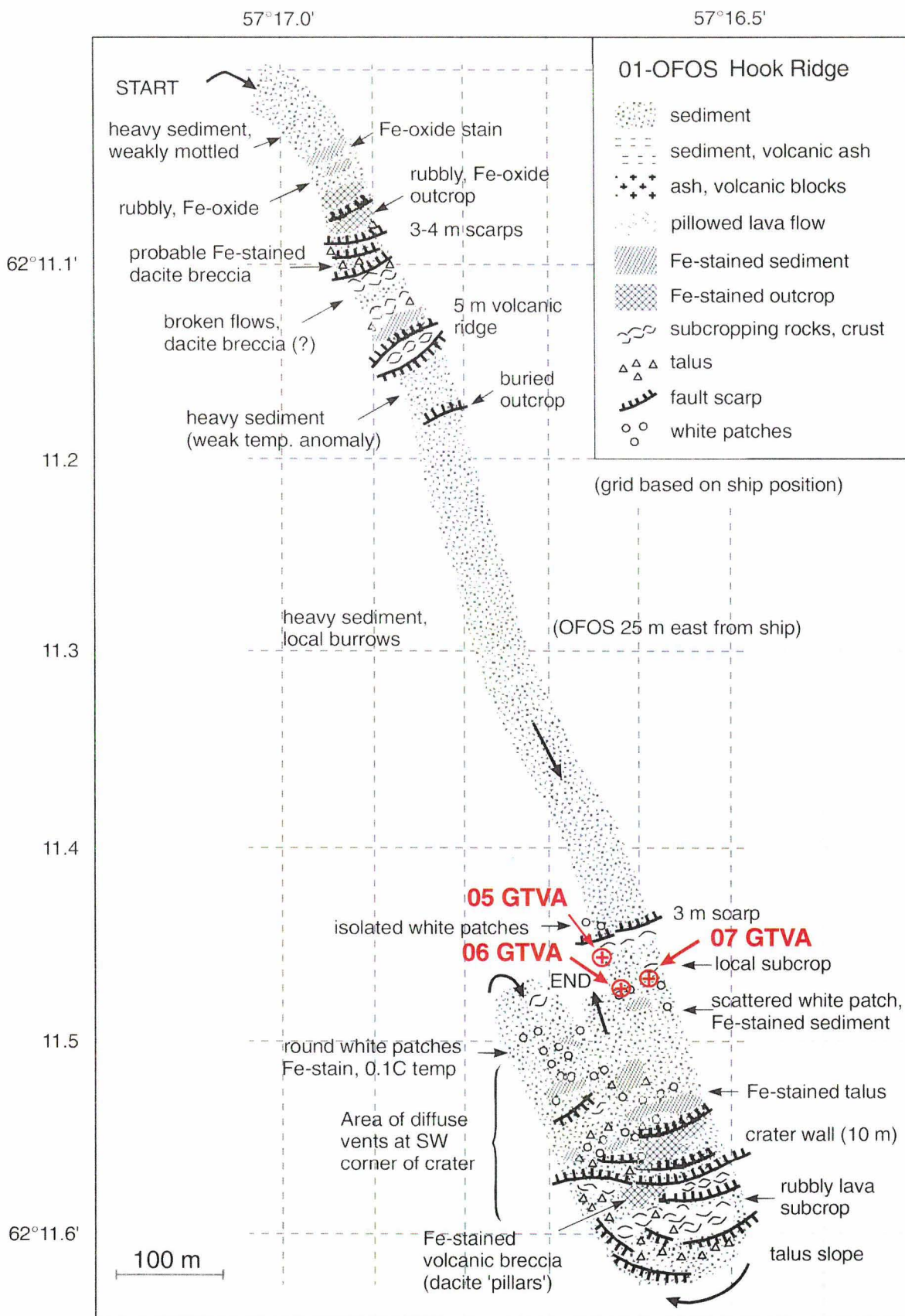


Fig. 9.4: Simplified geological map for subprofile 1 at Hook Ridge crater. The location of TV-grab samples is also given for information.

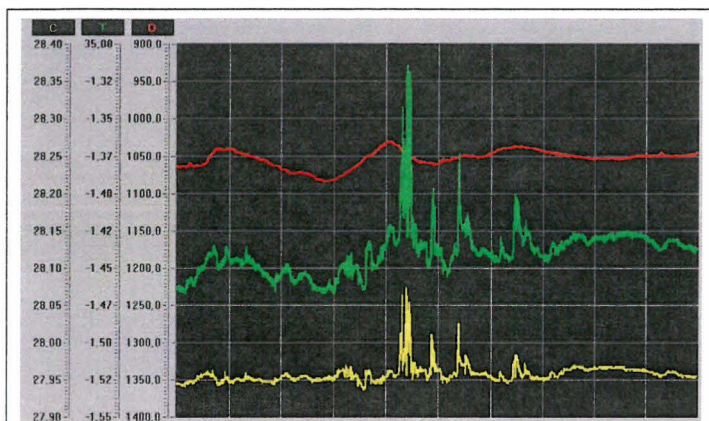


Fig. 9.5a: Pot. temperature (green) and conductivity (yellow) anomalies recorded during station 01-OFOS near the first approach of the southern crater wall. The red line is the water depth as calculated from the pressure sensor of the CTD.

Instrument location at the time of the highest peak (time: 21.15 UTC; 0.15°C) was 62°11.591'S 57°16.558'W at a water depth of 1048 m (calculated from the pressure sensor of the CTD).

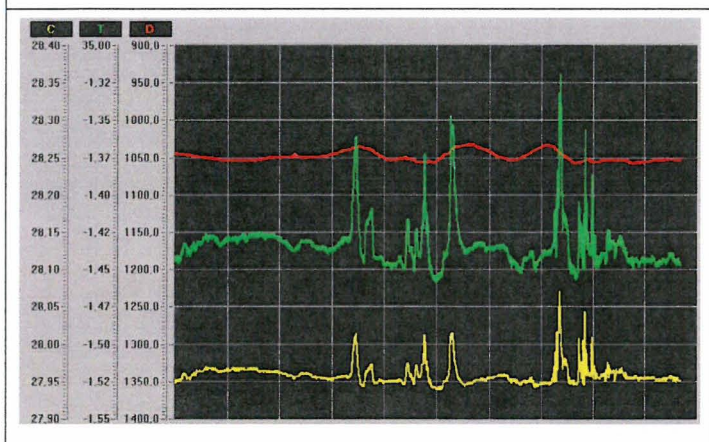


Fig. 9.5b: Additional pot. temperature anomalies recorded during three tracklines passing through the area of hydrothermal activity at the southern wall of the crater.

Instrument locations for the two highest peaks on this picture are:

peak 1; time: 22.03 UTC; 0.12°C; 62°11.572'S 57°16.581'W depth = 1041 m

peak 2; time: 22.15 UTC; 0.15°C; 62°11.595'S 57°16.551'W depth = 1044 m

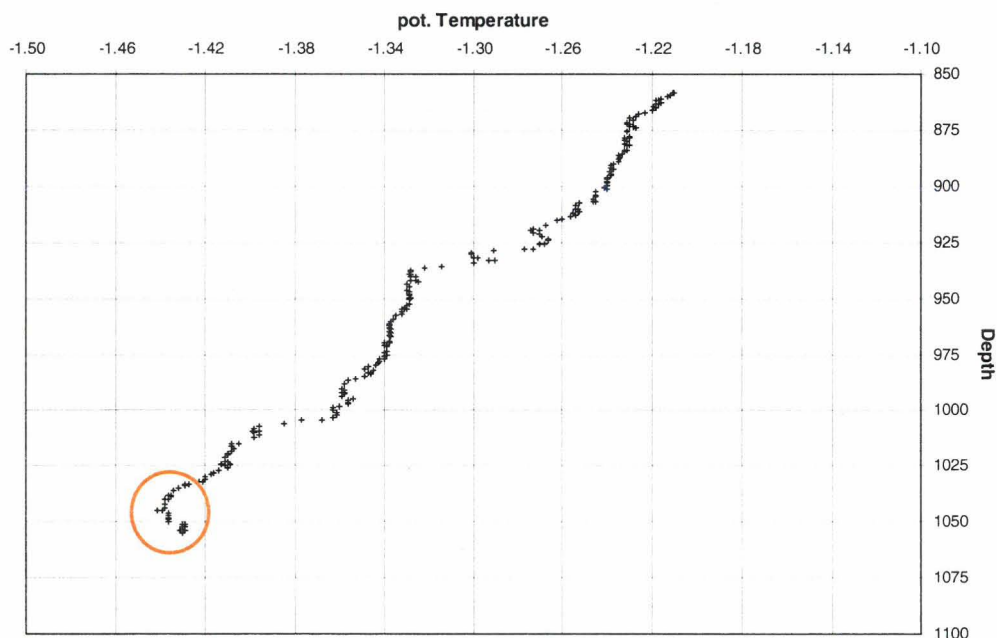


Fig. 9.6: Pot. temperature versus depth for the upcast (62°11.461'S / 57°16.645'W) at the southern wall of Hook Ridge crater. Note the bottom anomaly and the overall irregular shape of the curve.

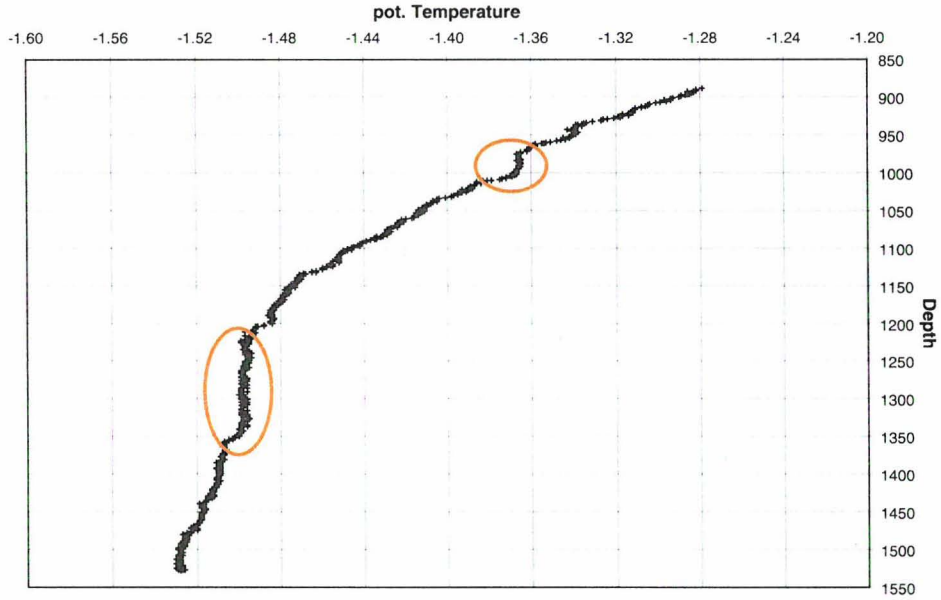


Fig. 9.7: Pot. temperature versus depth for the downcast ($62^{\circ}12.310'S / 57^{\circ}16.211'W$) in the “hinge” area. The downcast location is northwest of the plume station ZAPS 22 of NBP99-04 in 1999.

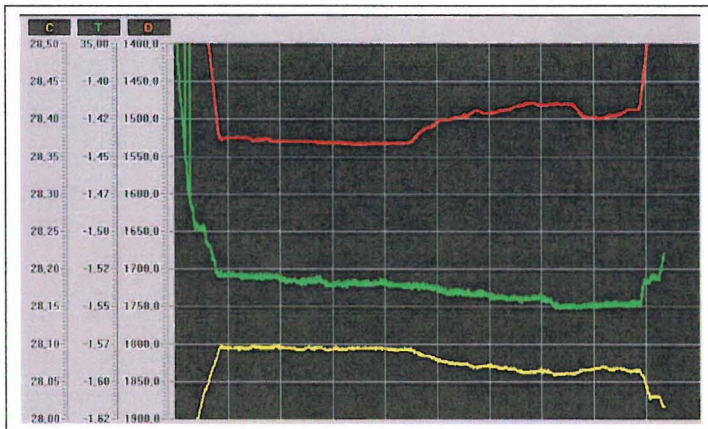


Fig. 9.8: CTD recordings for the second part of station 01-OFOS in the „hinge“ area.

Red line is water depth. Green line is pot. temperature and yellow line is conductivity.

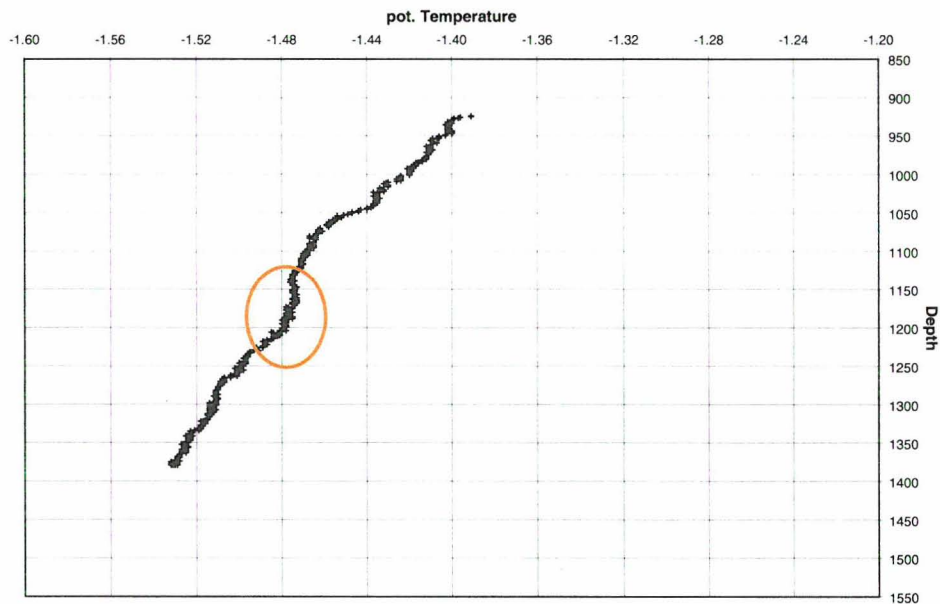


Fig. 9.9: Pot. temperature versus depth for the upcast ($62^{\circ}21.536'S / 57^{\circ}26.452'W$) in the “hinge” area.

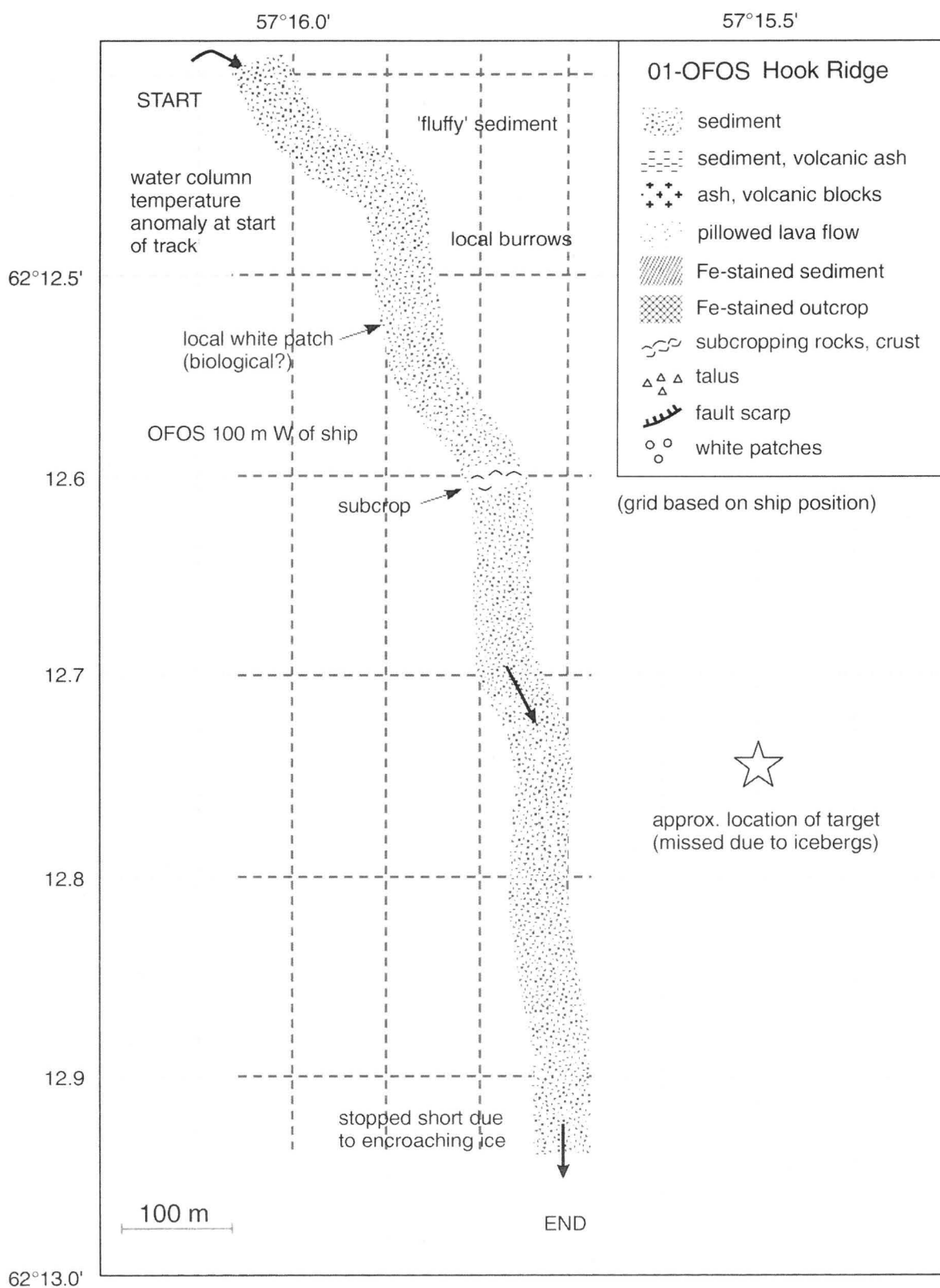


Fig. 9.10: Simplified geological map of the second subprofile during station 01-OFOS in the “hinge” area.

41-OFOS Viehoff Seamount

Objectives: This station was carried out in order to survey the rim and crater of Viehoff Seamount, a large volcano with a caldera measuring 3.5 km in diameter. The caldera walls rise to a water depth of approximately 600 m while the caldera floor is at a water depth of 1180 m. The seafloor within Viehoff Seamount was investigated by two OFOS-subprofiles. The first profile started at the northern rim (Fig. 9.11) and was targeted in a southerly direction towards the caldera floor. During the tow a small pot. temperature anomaly was observed at a water depth of ~ 1000 m (Fig. 9.12). The northern rim of Viehoff Seamount is characterized by sedimented lapilli and ash. The northern wall is almost vertical in relief and consists of several terraces with large vertical scarps showing offsets up to 40 m in height (Fig. 9.13). Pillow lavas are locally exposed along the walls, however, talus formation and sedimentation are strong all along the wall. The crater floor is covered by thick sediment with only local subcropping volcanics. The OFOS was brought up above the rim of the crater and ship and instrument were relocated to the southern wall. The second subprofile was run in a northerly direction to investigate the bulge area at the intersection of the crater floor and the southern wall. During the descend it became apparent that the crater rim in this area consists of meter-sized irregular blocks (Fig. 9.13). The southern slope is more gentle than the northern slope and is dominated by volcanoclastic material. The topographic high within the crater is a large talus pile (75 m high) consisting of large blocky, disrupted lava surrounded by an apron of talus material. The crater floor consists of similar thick sediment with local subcropping volcanics.

There are no visual indications of present or past hydrothermal activity anywhere at Viehoff Seamount. A small temperature anomaly in a water depth of 1000 m, that was observed during both subprofiles might be related to different water masses.

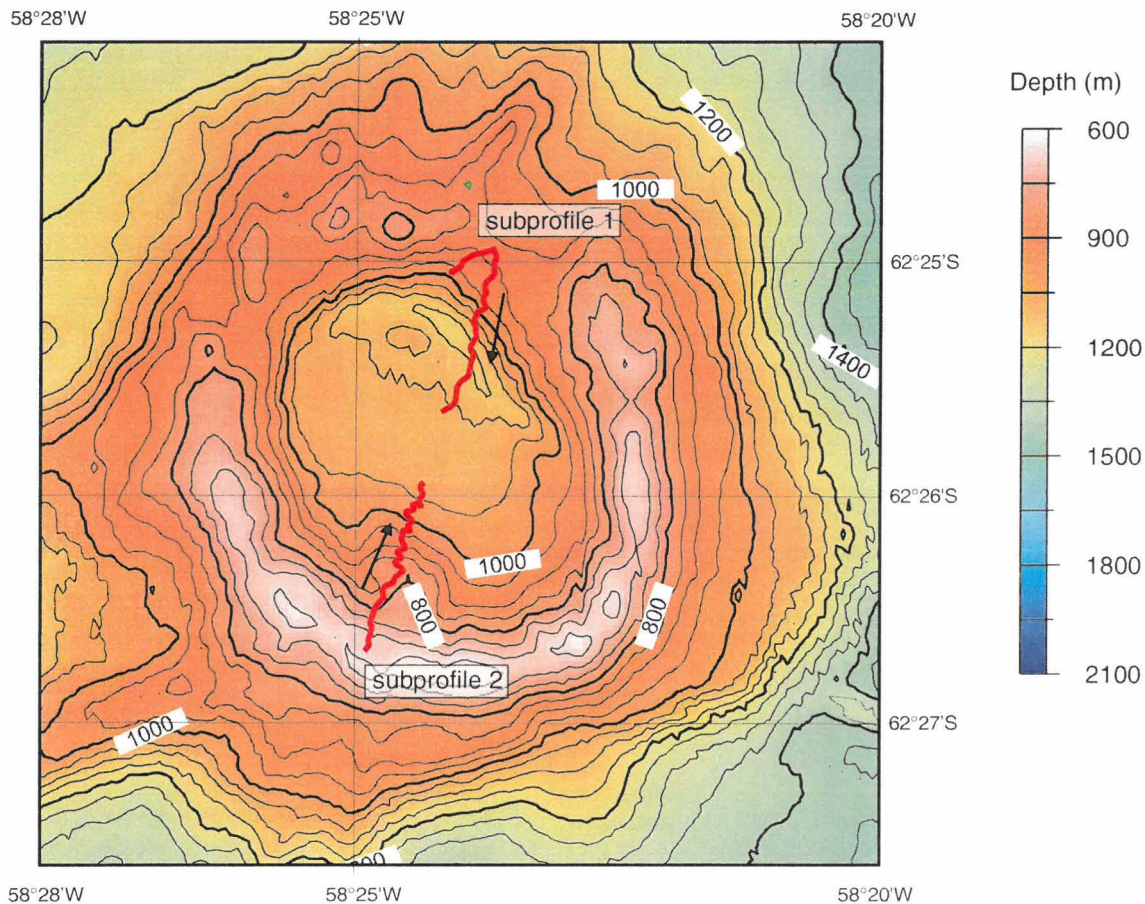


Fig. 9.11: Ship's track during station 41-OFOS.

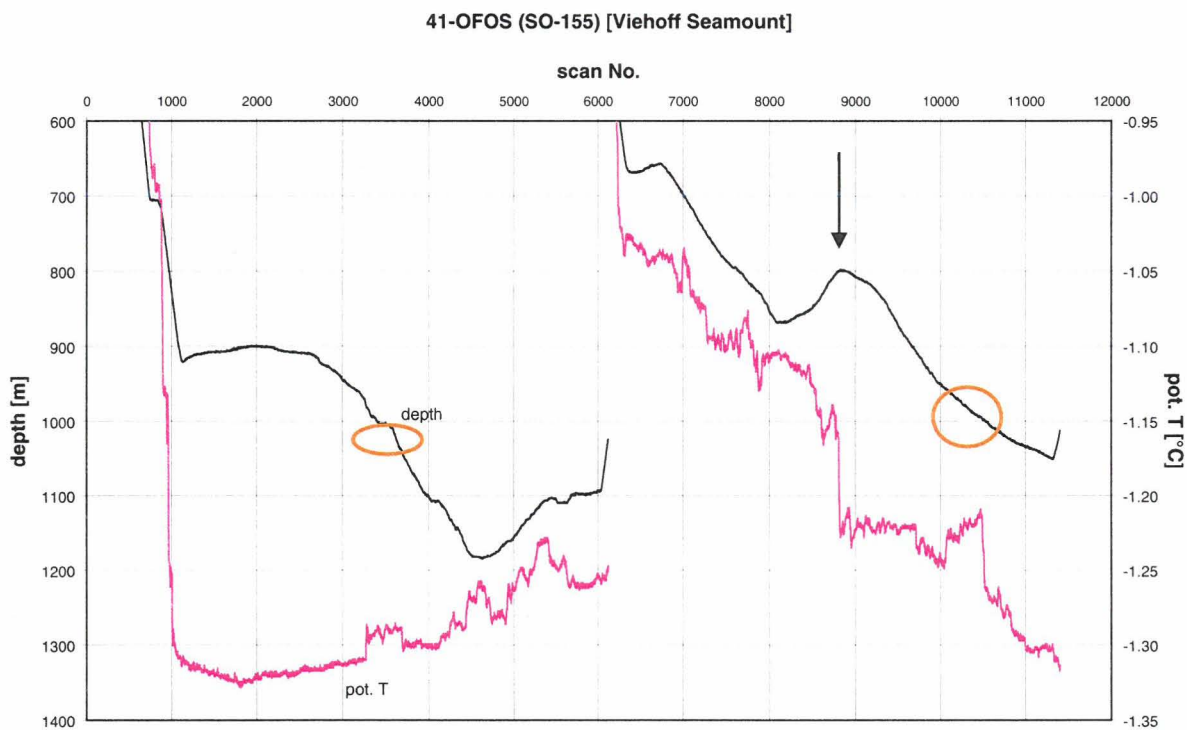


Fig. 9.12: Depth and pot. temperature recordings during the two subprofiles run at station 41-OFOS. Note the small temperature anomaly observed at a waterdepth of ~ 1000 during both tows and the actual drop in pot. temperature (arrow) while climbing the blocky talus pile during the second subprofile.

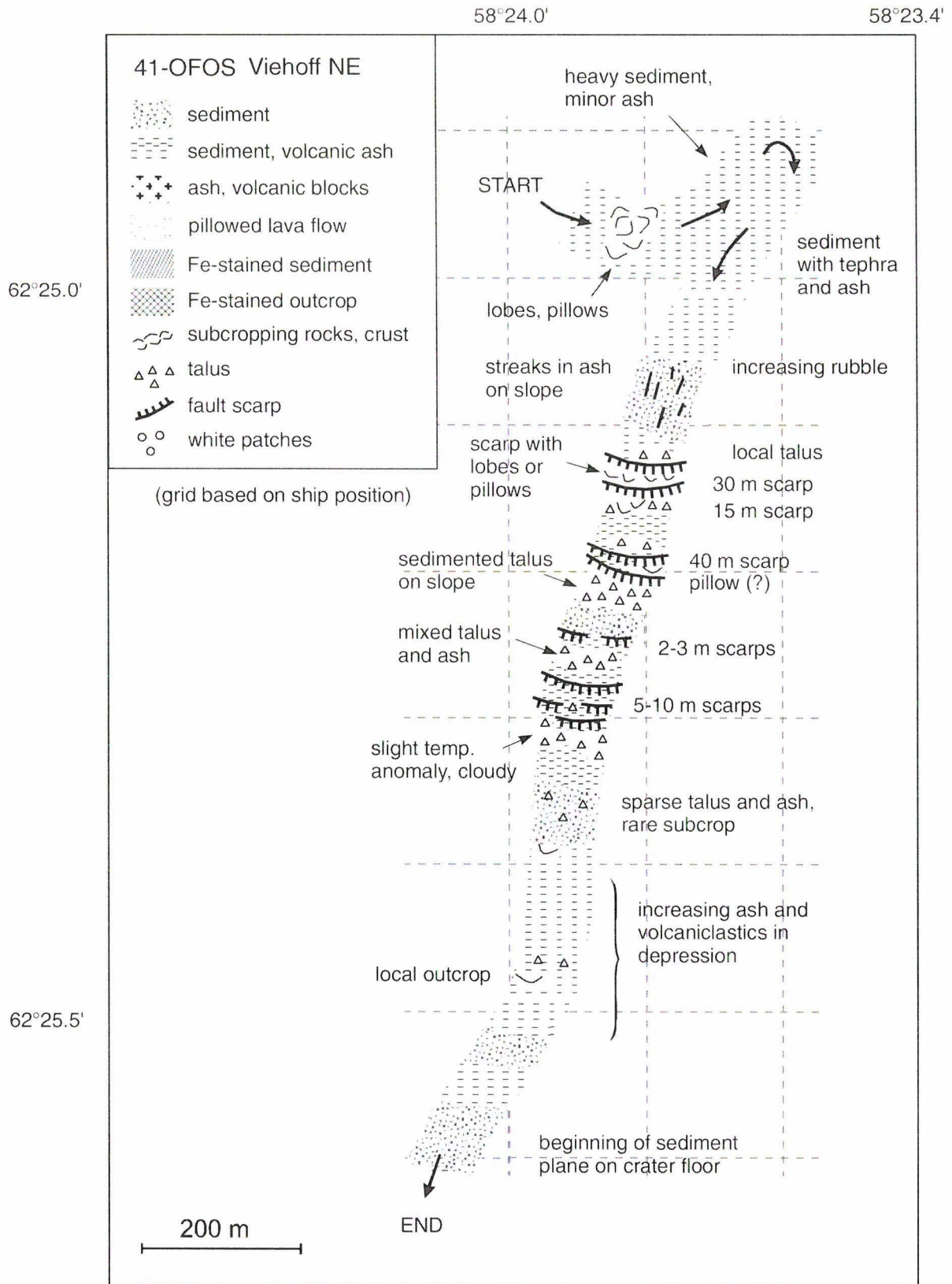


Fig. 9.13: Simplified geological map of the first subprofile during station 41-OFOS at the northern rim of Viehoff Seamount.

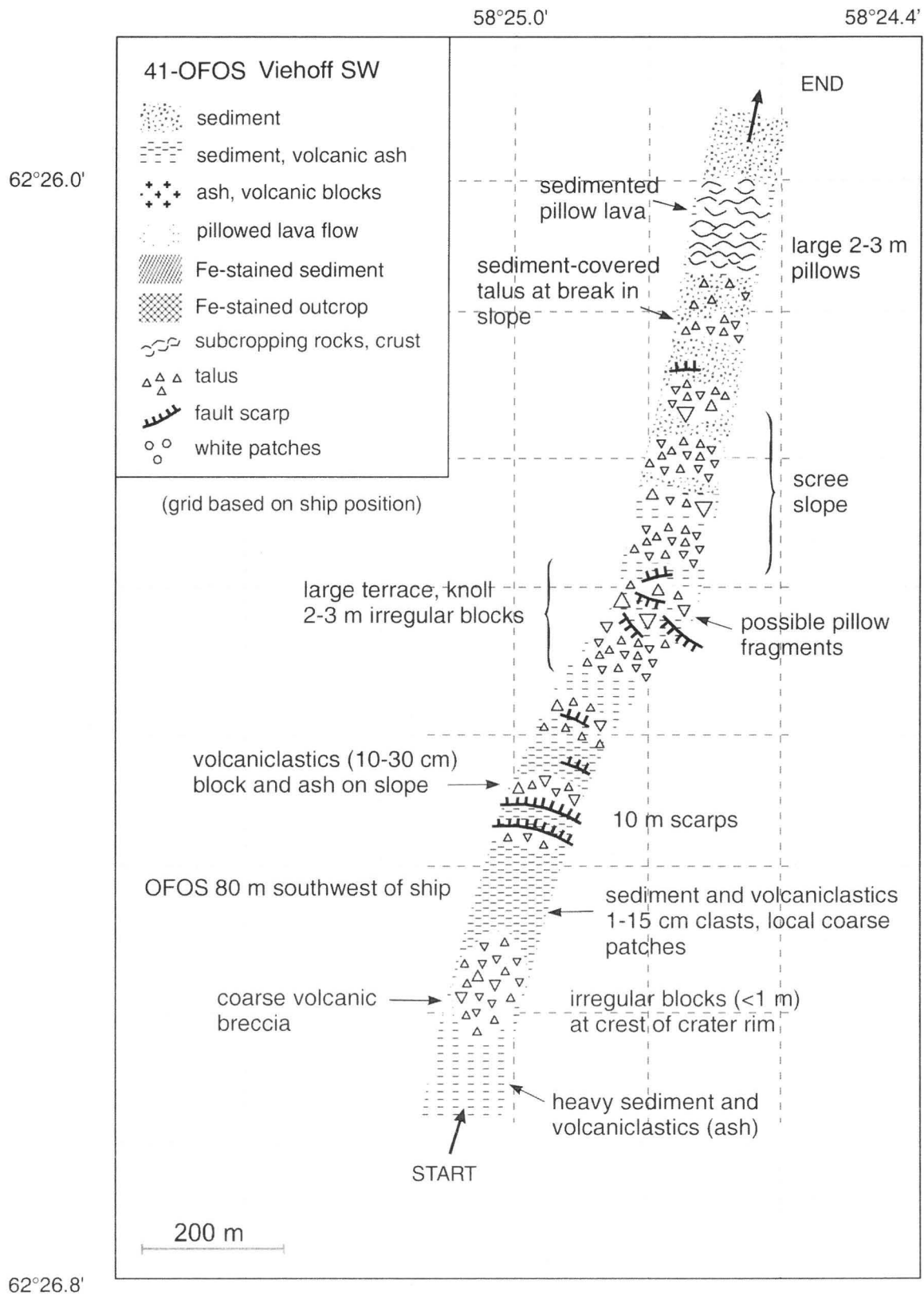


Fig. 9.14: Simplified geological map of the second subprofile during station 41-OFOS starting at the southern rim of Viehoff Seamount and heading to northeast.

45-OFOS / 46-OFOS Deception Island

Two OFOS profiles (stations 45-OFOS and 46-OFOS) were run in the crater of Deception Island to investigate areas of possible hydrothermal influence. Station 45-OFOS was located in an area where Rey et al. (1997) found enrichments in Ba, Mn, etc in the sediments and was targeted in a east-west direction. The station was started in a water depth of approx. 90 m and the instrument touched down in thick sediment accumulations with abundant fauna. The instrument then followed a gentle downslope until it reached a slightly undulating seafloor at 110 m water depth with small hills possibly indicating buried fault scarps (Fig. 9.15, Fig. 9.16). The maximum depth reached during this station was 120 m. There is abundant macrofauna all over the crater floor, however, no visual indications for hydrothermal activity were found. The OFOS instrument was brought up and relocated to the second target area where we hoped to find evidence for hydrothermal activity.

The target area for station 46-OFOS is located in the deepest part of the caldera and lies between the subaerial hydrothermally active sites Pendulum Cove and Fumarole Bay. The location of the site is based on the location of an inferred NW-SE trending fault system connecting the hydrothermally active sites. The instrument reached bottom in a water depth of 142 m and was towed down a gentle, stepped, and heavily sedimented slope to a water depth of 170 m. The water depth of 170 m marks the flat bottom of the crater and stayed constant for the rest of dive (Fig. 9.17). The CTD recorded highly variable pot. temperatures most likely indicating incursions of cold freshwater (Fig. 9.18). Similar to station 45-OFOS makro fauna is very abundant throughout the dive. The water column was characterized by the presence of abundant particulate matter strongly reducing visibility. Similar to station 45-OFOS no indications for hydrothermal activity were found.

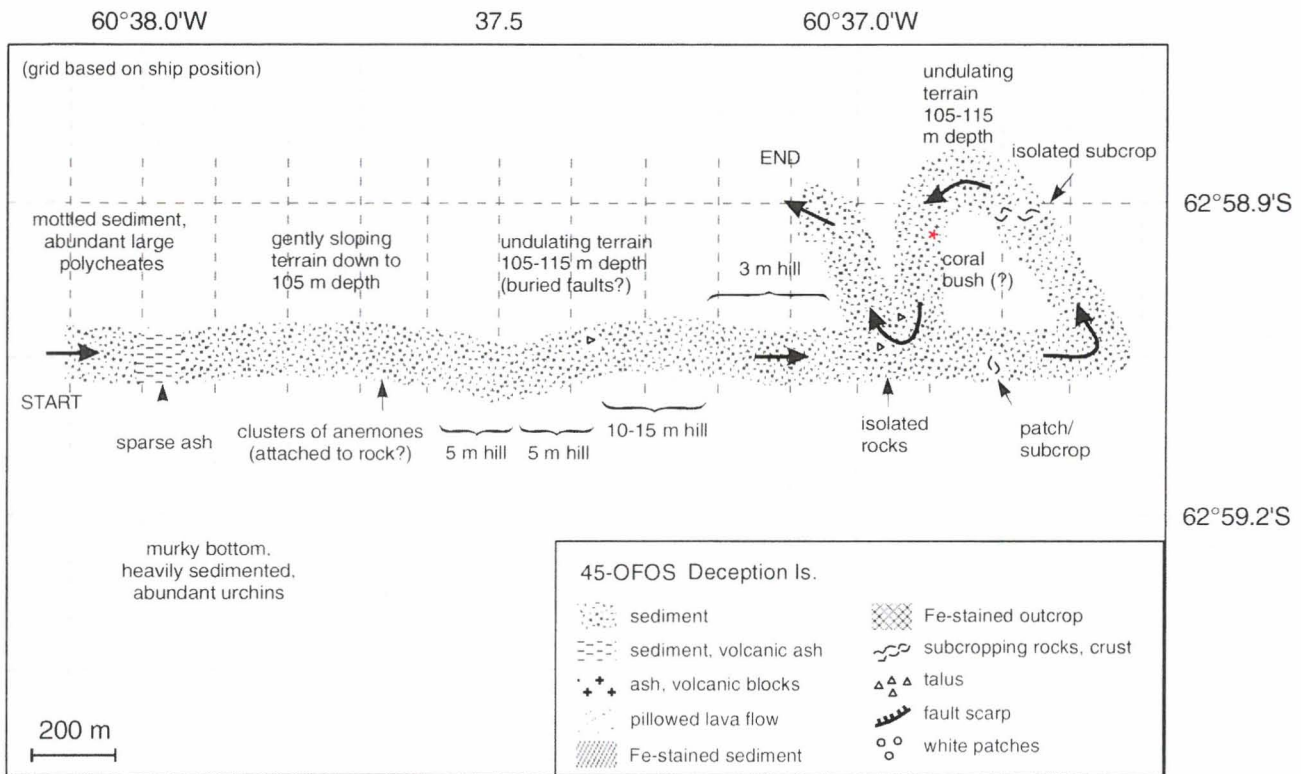


Fig. 9.15: Simplified geological map of the crater floor within Deception Island based on observations obtained during station 45-OFOS.

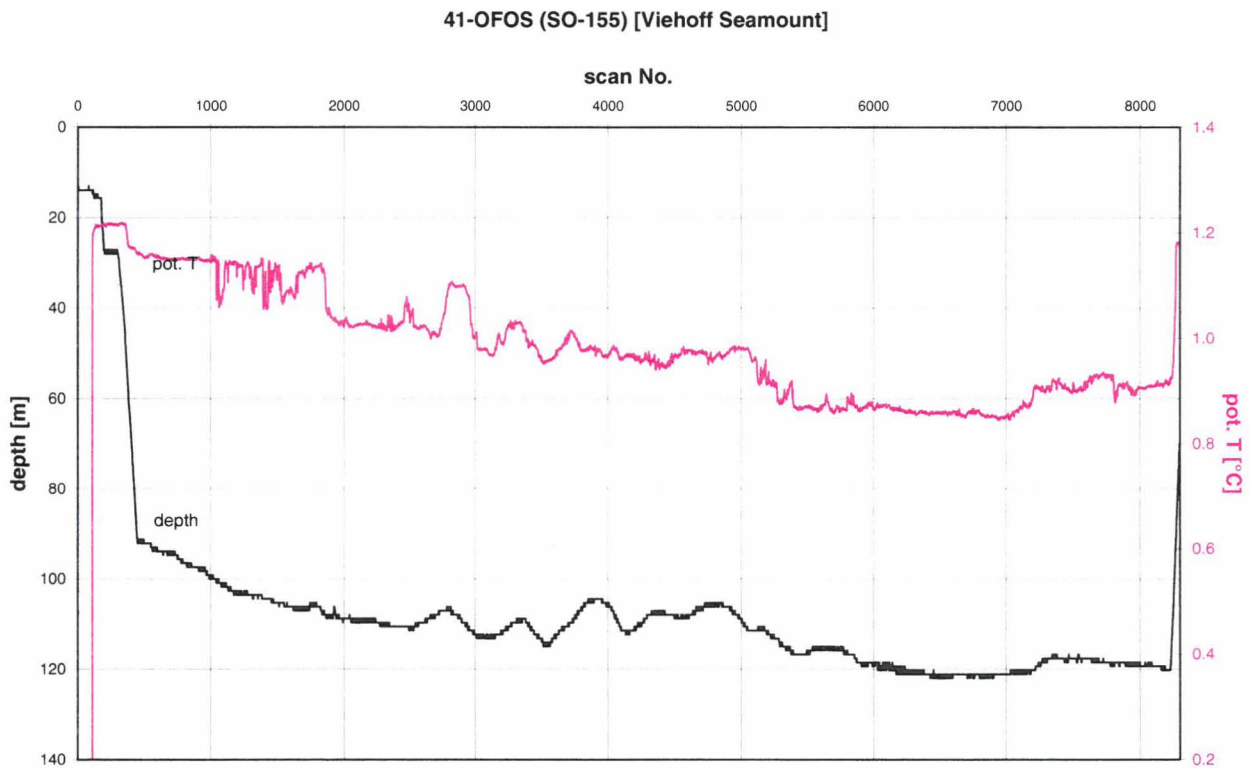


Fig. 9.16: Depth and pot. temperature recordings during station 45-OFOS.

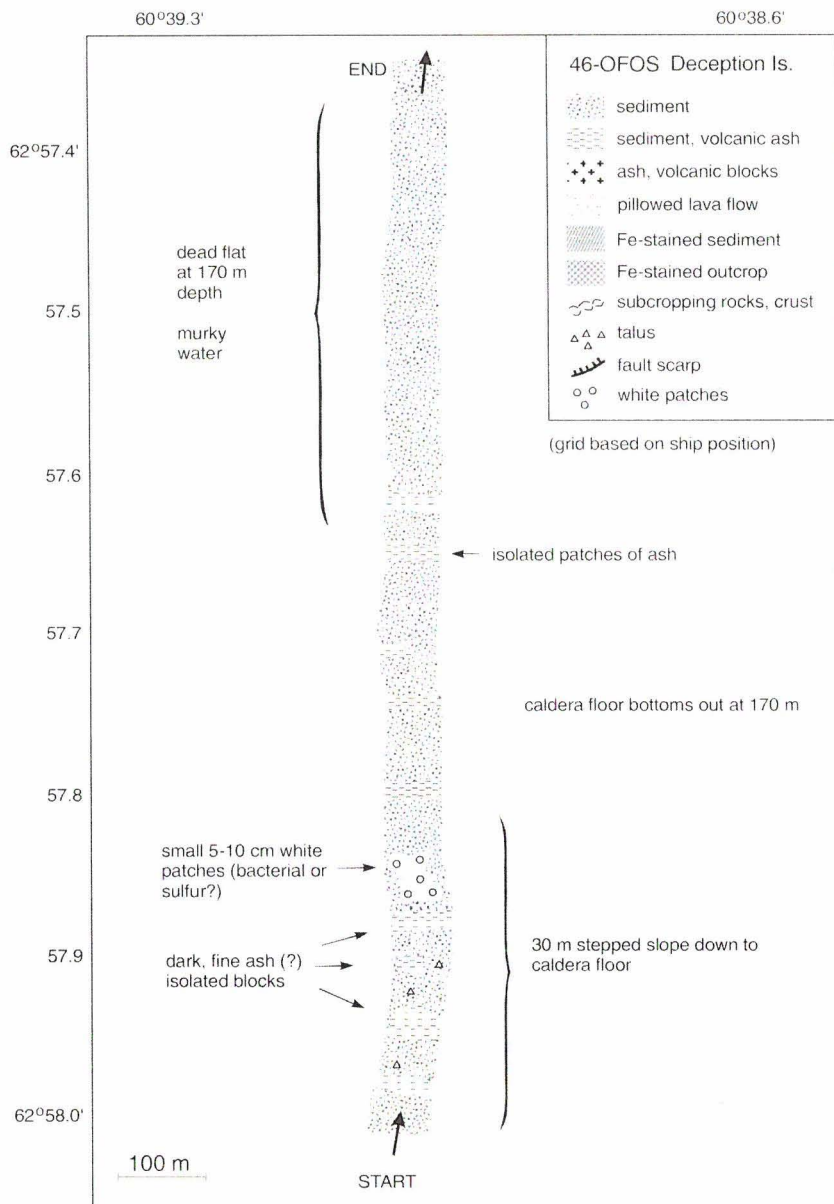


Fig. 9.17: Simplified geological map of the crater floor within Deception Island based on observations obtained during station 46-OFOS.

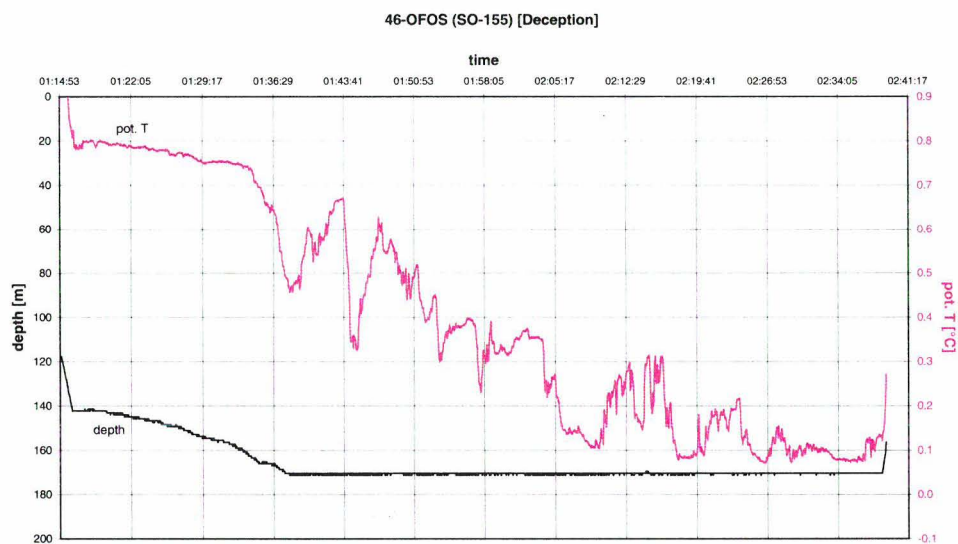


Fig. 9.18: Depth and pot. temperature recordings during station 46-OFOS. Note the irregular pattern of the pot. temperature possibly indicating cold freshwater incursions.

10 Hydro Bottom Station

The Hydro-Bottom-Station (HBS) is a tool for sampling and measuring diffuse hydrothermal fluids. It consists of the following six main parts (Kuhn and Halbach, 1999):

- instrumental frame
- telemetry and optical cable units
- on-line sensor package measuring temperature, pressure, Eh, pH, dissolved oxygen, carbon dioxide partial pressure, conductivity and H₂S
- water sampling system with vertically movable lance (hydrolance) and 12 sampling bags
- sediment sampling unit (geolance)
- on-line camera system with b/w camera and two colour cameras

HBS is always deployed on a coaxial or an optical cable. It is towed one or two meters over the seafloor with the ship moving along a given track. The on-line cameras enable a video-controlled lowering of the system at places of interest.

10.1 Sensor calibration

During SO-155, the two temperature sensors as well as pH, oxygen and CO₂ sensors could be calibrated. The H₂S and conductivity sensors were precalibrated before delivery by the respective manufacturer. The pressure sensor was out of order whereas the Eh sensor could not be calibrated due to lack of calibration solution. It was run with previously done settings.

The owner of HBS (Free University of Berlin) delivered a new software for calculating the raw data (mV values) into true data. However, it turned out that this software does not work at all. Therefore, some Excel Makros were written to do the calculations in Excel spreadsheets. Calibration of the pH sensor was done with three different pH values between 3 and 8. Temperature sensors were calibrated at several temperatures between 0 and 20 °C. All three sensors turned out to work reliably during the calibration procedure (Fig. 10.1). A single point calibration was done with the oxygen sensor with oxygen saturated water (9.61 mg O₂/l at the given conditions) since all other parameters were preset by the manufacturer. A two point calibration was carried out with the CO₂ sensor. At concentrations of 5 and 25 mmol CO₂/l, the sensor measured a difference of 461 mV (2210 mV and 2761 mV). However, the in-situ CO₂ measurements showed concentrations

larger than the calibration concentration. Therefore, the calculated CO₂ content were too high and can only be correctly calculated after another calibration was carried out in the home lab. Long time measurements onboard showed that pH has a drift of ~ 0.4 units within eleven hours, O₂ of ~1 mg/l and Eh of about 20 mV whereas T cell was rather constant.

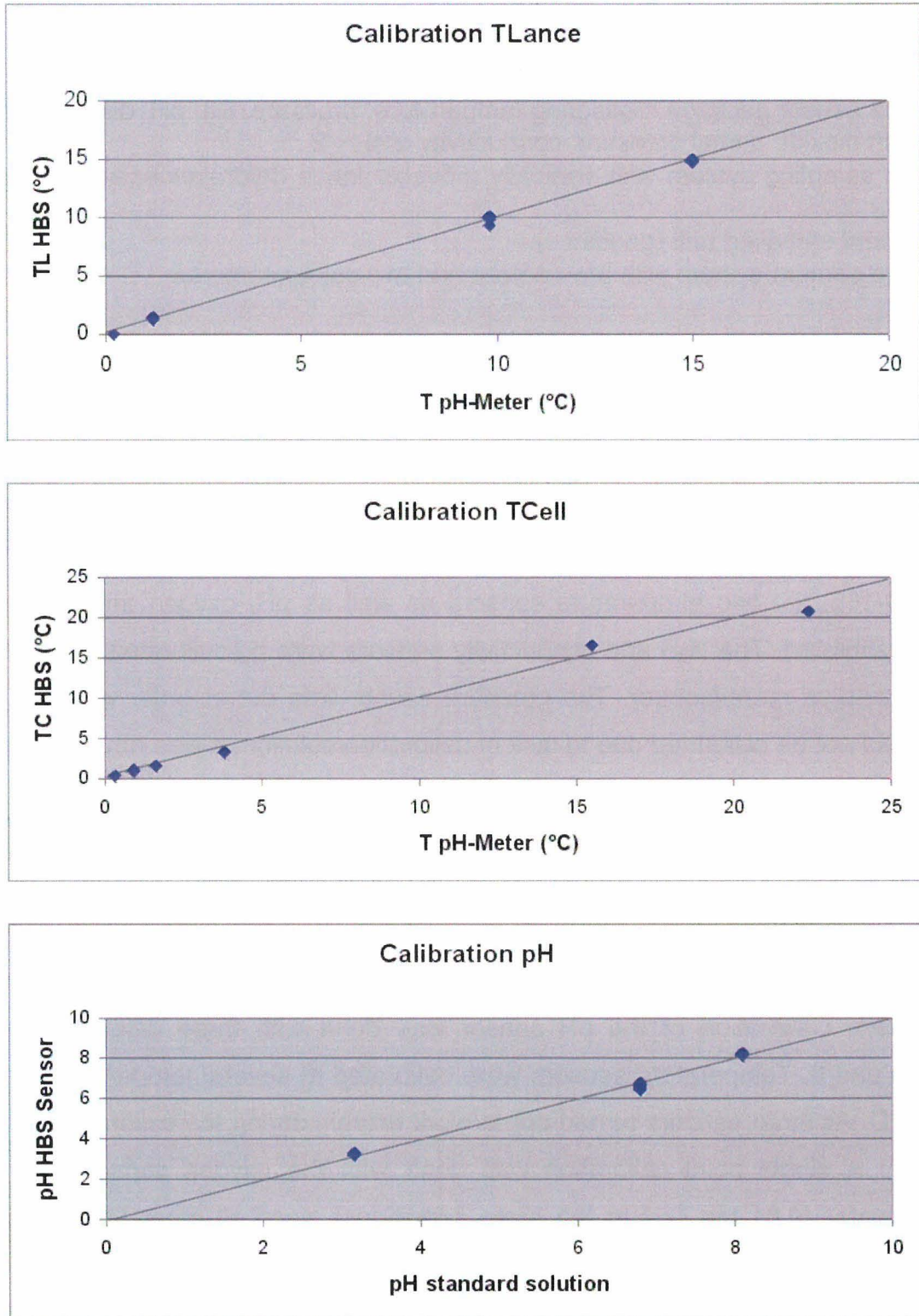


Fig. 10.1: Calibration of the temperature and pH sensors.

10.2 Deployment

HBS was only deployed twice during SO-155. Both stations were situated in the Deception Island caldera. Two other deployments had to be cancelled due to electronic problems with HBS and a breakdown of the optical cable.

Station 47-HBS was carried out in the deeper NW part of the Deception Island caldera in about 160 to 170 m water depth. It should follow the inferred strike of NE-SW oriented normal faults which are linked to the postcollapse episode and present volcanism (Rey et al., 1995, 1997). Hot, As-rich springs at Fumarole Bay and Pendulum Cove are the subaerial expression of present hydrothermal activity bound to the normal faults.

The seafloor of the deepest part of the caldera is characterized by a thin cover (only some centimeters) of brownish sediments which is underlain by blackish sediments. Multicorer stations later showed that both are fluffy layers rich in diatoms which may represent the last summer bloom in the water body. The black layer is due to reduced conditions in the sediments as a consequence of the decay of organic matter. This succession was more or less observed over an area of about 4 km² in the deep, central part of the caldera. In most western part of the profile (62°57.700'S & 60°40.290'W) the seafloor was furthermore characterized by white patches which looked like bacterial mats probably growing on hard rocks which stick through the sediments. Getting further to the east and northeast, these white patches were less abundant but not totally absent. Any sign of hydrothermal activity as precipitates, shimmering emanating water or characteristic biology could not be seen during the station. Unfortunately, the sensors measured reasonable values only within the first two hours of the station. Afterwards they got a strong drift or showed large unrealistic variations. These are probably due to synchronization errors between the HBS-UW-telemetry and the HBS-control unit which largely occurred during the usage of the optical cable but did not occur during tests with coaxial cable onboard. Furthermore T lance, pH, and conductivity showed peaks when the hydrolance was moved. These peaks had to be skipped, too. Eventually, only the cell temperature, oxygen concentration, Eh, and H₂S concentration could be used for interpretation. Except a small temperature anomaly of 0.2 °C at 62°57.72'S and 60°40.22'W (Fig. 10.2) no signs of hydrothermal activity could be detected.

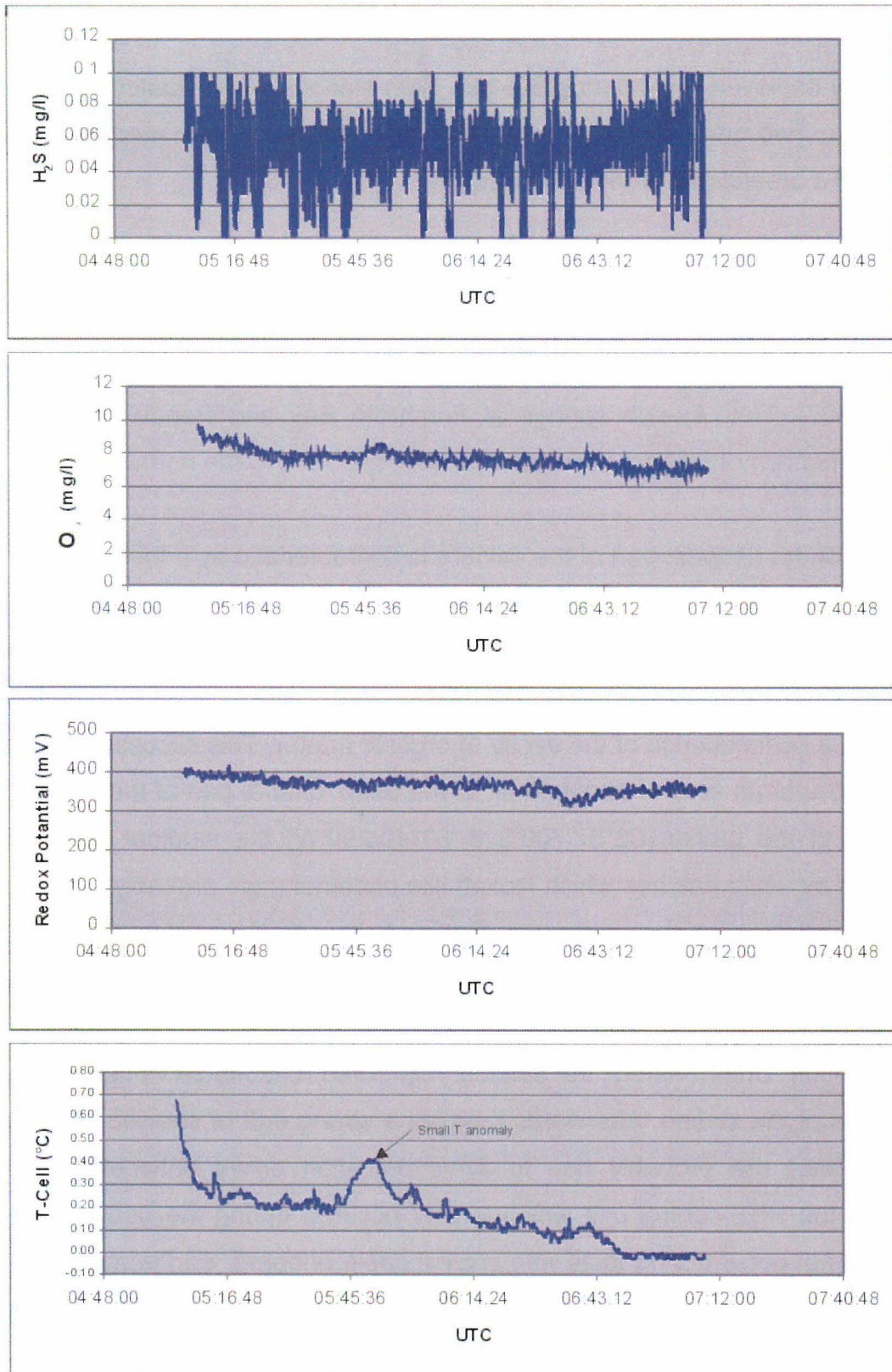


Fig. 10.2: Results of in-situ measurements of some water parameters during station 47HBS in the Deception Island caldera. Except for a small T-anomaly no signs of hydrothermal activity were detected. Small variations in the H_2S recordings may be due to exhalation from sediments when HBS touches the seafloor.

The oxygen and H₂S concentrations remained near saturation value and detection limit (about 8 mg/l O₂ and 0.05 mg/l H₂S). Small H₂S variations could be due to exhalation of H₂S from sediments as concluded from multicorer samples of that area which had a H₂S smell.

Station 51-HBS was run parallel to the shore of Fumarole Bay just 100 m offshore. The shore itself is characterized by black volcanic lapilli and some spots emanating hot gases rich in CO₂, CH₄ and steaming water. However, no precipitates were found around these sites. The seafloor consists of the same sediment as in the central part of Deception caldera (station 47-HBS) but is to a much higher degree covered by clusters of holothurians, seastars and urchins. As in the central part of the caldera, no signs of hydrothermal activity as temperature anomalies, hydrothermal precipitates or typical biology could be detected during station 51-HBS.

10.3 References

- Kuhn, T. and Halbach, P., 1999. The technical setup of the Hydro-Bottom-Station: a system for monitoring and sampling of diffuse hydrothermal fluids. In: C. Wilson (Editor), *InterRidge Workshop Long-Term Monitoring of the Mid-Atlantic Ridge (MOMAR)*. InterRidge, Lisbon, pp. 84-85.
- Rey, J., Somoza, L. and Martinez-Frias, J., 1995. Tectonic, volcanic, and hydrothermal event sequence on Deception Island (Antarctica). *Geo-Marine Letters*, 15: 1-8.
- Rey, J., Somoza, L., Martinez-Frias, J., Benito, R. and Martin-Alfageme, S., 1997. Deception Island (Antarctica): a new target for exploration of Fe-Mn mineralization? In: K. Nicholson, J.R. Hein, B. Bühn and S. Dasgupta (Editors), *Manganese Mineralization: Geochemistry and Mineralogy of Terrestrial and Marine Deposits*. The Geological Society, London, pp. 239-251.

11 PORE WATER GEOCHEMISTRY, MICROBIOLOGY, AND MACROFAUNA

11.1 Introduction

At Hook Ridge, hydrothermal activity was discovered during previous cruises with RV Polarstern (ANT XV/2) (Bohrmann et al., 1999) and RV N. B. Palmer (NBP 99-04) (Klinkhammer et al., submitted). Venting of Si-rich hydrothermal fluids through the sediment column causes precipitation of Si-crusts on the sediment surface. During the previous cruises these precipitates were recovered with sediments which had temperatures of up to 48 °C measured in the TV-grab on deck. The pore fluids extracted from this grab showed a decrease in Cl concentrations, probably indicating phase separation in a reaction zone below Hook Ridge (Daehlmann et al., submitted). The acidic vent fluids at Hook Ridge are methane- and sulfide-rich. Besides Si-precipitates, Fe-oxyhydroxide precipitates are commonly observed. No vent-typical macrofauna has yet been discovered on Hook Ridge. The only chemoautotrophic macrofauna discovered earlier was a species of pogonophoran tube worm belonging to the family Sclerolinidae.

Deception Island is well known for its hydrothermal activity. The fumaroles in shallow waters are situated along major fault systems (Rey et al., 1995). Geophysical and geochemical investigations proposed hydrothermal venting also in deeper waters (Rey et al., 1995).

During this cruise, an interdisciplinary approach was used to investigate hydrothermal fluids and their influence on the benthic system. A set of chemical constituents of pore waters and solid phases will be determined on the same samples as the microbial composition and activity, as well as the composition of macrofaunal species.

11.2 Sampling strategy and sample recovery

11.2.1 Introduction

During cruise SO-155 a TV-guided grab (GTVA), a gravity corer (SL) and a multicorer (MUC) were used to collect hydrothermally influenced sediment samples. The samples were used for investigations of sediments, pore water chemistry, microbial composition and activity, and macrofaunal assemblages. The target areas for the sediment sampling program were defined based on camera surveys conducted by OFOS and HBS. Samples

were taken in two investigation areas: Hook Ridge Crater and Deception Island Caldera (Table 11.1).

Table 11.1: Summary of sediment stations during SO-155.

Station No.	Tool	Lat	Long	Depth	Subsamples					Foto	TU	GPI	T _{max} °C	HF mWm ⁻²	Comments
					PW	CH ₄	PP	Mac	Mic						
<i>Hook Ridge Crater</i>															
05	GTVA				-	-	-	-	-	-	-	-	-	-	few sediment, grab opened on deck
06	GTVA	62°11,550'	57°16,623'	1025	x	x	x	-	x	x	-	16	20570	trying to grab rocks failed, sediments warm	
07	GTVA	62°11,55'	57°16,55'	1046	x	x	x	-	x	x	-	13.4	19800	grabbing basalt rock, sediments warm	
08	GTVA	-	-	-	-	-	-	-	-	-	-	-	-	no sample	
09	MUC	62°11,544'	57°16,563'	1053	-	x	?	-	x	-	-	-	-	winch failure when MUC was near bottom, several ground-touches, 1 core 10 cm	
10	MUC	62°11,519'	57°16,559'	1072	-	-	-	-	-	-	-	-	-	not released, no samples	
11	SL	62°11,581'	57°16,518'	1059	x	x	x	-	x	x	x	22.3	4400	4.48 m warm sediments	
30	MUC	62°11,538'	57°16,649'	1049	C	-	-	BDE	A	ACE	x	-0.2	-	6 cores, ca. 20 cm, Fe-oxyhydroxides on top of muddy sediment	
31	MUC	62°11,523'	57°16,654'	1045	-	-	-	BC	-	-	-	1.4	-	7 cores, 30-50 cm, soft muddy sediment	
32	MUC	62°11,535'	57°16,664'	1042	A	C	C	DH	E	A	x	3.8	-	6 cores, ca. 20 cm, Fe-oxyhydroxides on top, sulfide smell, Pogonophoran tube worms on surface (Sclerolinidae)	
33	MUC	62°11,538'	57°16,681'	1043	G	G	G	ADE	B	-	-	4.5	-	6 cores, ca. 20 cm, Fe-oxyhydroxides near top, Pogonophoran tube worms on surface (Sclerolinidae)	
34	MUC	62°11,567'	57°16,737'	1047	-	-	-	4 cores	-	-	-	-1.5	-	8 cores, 35 cm, few Fe-oxyhydroxides on soft muddy sediment	
35	MUC	62°11,563'	57°16,698'	1053	-	-	-	-	-	-	-	-	-	rope under MUC arm, disturbed muddy sediments without temp anomaly	
36	MUC	62°11,518'	57°16,703'	1038	-	-	-	-	-	-	-	-	-	not released, probably fallen over	
37	SL	62°11,535'	57°16,647'	1040	-	x	x	-	x	x	-	36.6	22100	2.52 m sediments	
39	DR				-	-	-	-	-	x	-	-	-	indurated S-rich sediments	
<i>Deception Island Caldera</i>															
42	SL	62°57,752'	60°38,035'	153	-	-	-	-	-	-	-	-	-	15 cm dark muddy sediment	
43	SL	62°57,696'	60°38,106'	153	-	-	-	-	-	-	-	-	-	5 cm dark muddy sediment	
44	SL	62°57,784'	60°38,170'	154	-	-	-	-	-	-	-	-	-	5 cm dark muddy sediment	
48	MUC	62°57,447'	60°38,626'	162	-	-	-	GFDB C	-	x	-	-	-	6 cores, ca. 20 cm, with Diatom-fluff	
49	MUC	62°57,382'	60°38,723'	159	-	-	-	CDE	-	x	-	-	-	4 cores, ca. 30 cm, with Diatom-fluff	
50	MUC	62°57,687'	60°39,118'	163	F	D	D	BCG H	e	F	x	-	-	7 cores, ca. 40 cm, 2 cm thick black soupy layer with fresh brown layer on top all consisting of Diatom-fluff	
52	BIO	Fumarole Bay beach			water										

PW = pore water chemistry, Letter indicate subcore; CH₄ = Methane concentration; PP = water content; Mac = Macrofauna; Mic = Microbiology; TUBAF = Geochemistry (XRD, XRF) on sediment and Fe-oxyhydroxid; GPI = Geochemistry (microprob) on ash; T_{max} = Maximal temperature of core measured on board ship; HF = Calculated heatflow based on temperature differences between depth intervals (k=1.1 W/mK).

11.2.2 Methods

Beside samples from TV-guided grabs sediment cores were taken by conventional gravity corer and multicorer without TV-control. The gravity corer was equipped with a core of 4.5 or 5.75 m length, with 12 cm inner diameter and a weight of 2 metric tonnes. The sediment filled liner was cut in 1 m sections and halved into a work and an archive half. The multicorer was equipped with 8 cores, each 10 cm in diameter and 50 cm long. Temperature of sediment at the base of the cores were measured as soon as possible

after core retrieval. Subsequent sample processing was conducted at room temperature of about 16-18 °C. Although generally the subcores of one MUC did not differ significantly in temperature or stratigraphic appearance, small scale heterogeneity had to be taken into account when discussing parallel cores taken at one station.

11.3 Results and Discussion

11.3.1 Hook Ridge Crater

Venting activity at Hook Ridge Crater was mapped in detail during station 01-OFOS (Fig. 11.1). Based on the distribution of Si-crusts and temperature anomalies recorded by the CTD mounted on OFOS most vigorous venting activity was thought to occur near the SW crater wall.

Stations 05-, 06-, 07-, 08-GTVA were conducted to grab hydrothermal precipitates other than Si-crusts in the area of Hook Ridge Crater. However, two of these grabs (06-, 07-GTVA) only recovered considerably warm sediments from the terrace-like area of the SW crater wall which were sampled for pore water and microbiological work (Fig. 11.1, Tab. 11.1). A comparison of the temperatures measured in sediments sampled by the TV-guided grab during the NBP 9904 and SO 155 cruises confirmed that the hottest fluids were found in sediments with Si-crusts just inside the crater wall, with values of 42.6 - 48.6°C (NBP 99-04: TVG 68, 69), while the sediments on the crater wall, which had no obvious Si-crusts, had lower values of 13.4 - 16°C (SO 155: 06-, 07-GTVA).

For the deployment of MUC and SL without TV-guidance, a target area with a high density of Si-crusts on the sediment surface was chosen as indicated in Fig. 11.1. A total of 09-MUC and 02-SL were deployed within this area, with 06-MUC and 02-SL stations recovering sediments. These sediments were influenced by hydrothermal venting to various degrees. Highest temperatures were measured in 37-SL with maximum temperatures of 36.6°C at 1.52 mbsf. The temperature maximum of 22.3 °C at a depth of 4.4 mbsf in 11-SL indicated less hydrothermal influence.

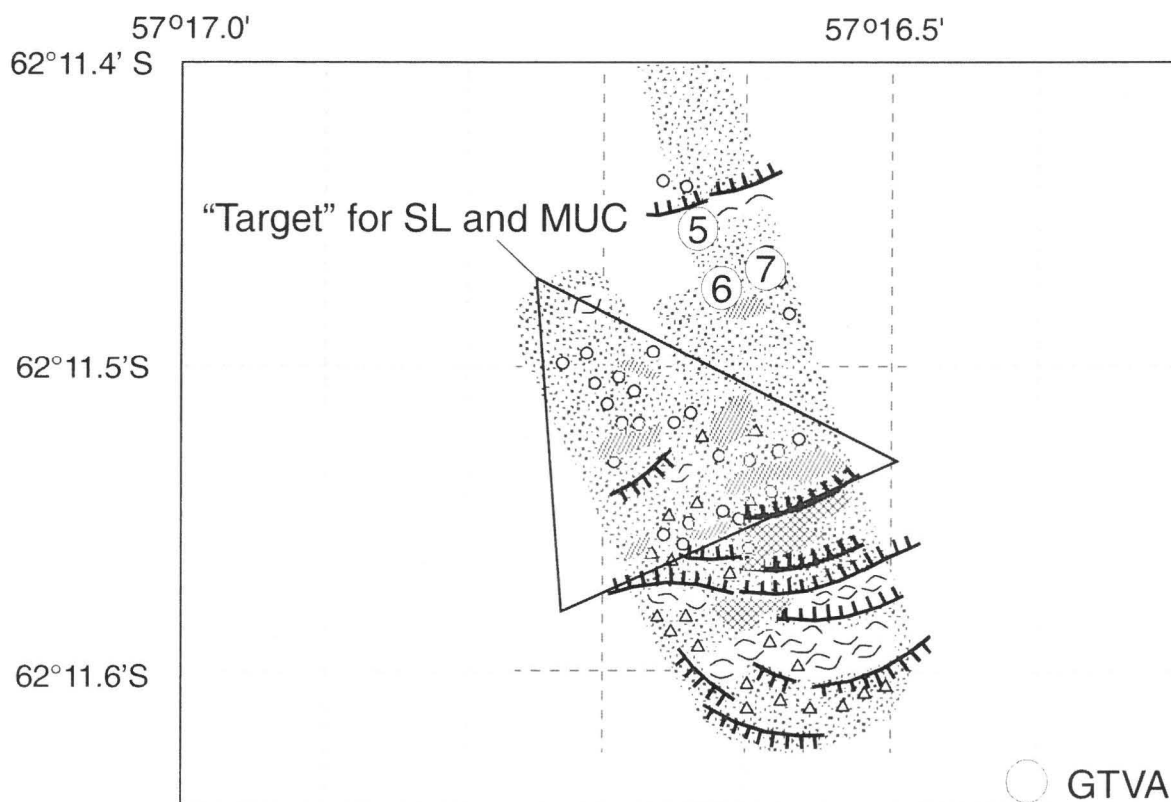


Fig. 11.1: Close-up view of the geological map of the SW crater area of Hook Ridge (see Fig. 9.4). The target area for SL and MUC deployments is indicated as well as GTVA sample locations.

Temperatures at the base of the cores recovered by MUC were probably significantly cooled in the water column. The maximum temperature of 4.5°C at 35 cmbsf in station 33-MUC thus indicated a strong influence of warm hydrothermal vent fluids *in situ*. Fe-oxyhydroxide crusts were found at or near the sediment surface of 4 MUC stations, ranging from the coldest to the hottest sediments. The crusts were sometimes covered by a thin layer of sediment. All sediments, with or without Fe-oxyhydroxides, consisted of soft grayish-green mud. No Si-crusts, indicative of the hottest fluid flow areas, were found on top of any of the sediment cores. Two multicorers (32-, 33-MUC) contained living pogonophoran tube worms of the family Sclerolinidae (see chapter 11.6). This species was recovered earlier during cruise ANT XV/2 but its relation to hydrothermal venting is not known. The presence of specimens in two out of 5 MUC deployments suggests a wide distribution in the venting area of Hook Ridge Crater.

11.3.2 Deception Island Caldera

Three gravity cores (42-, 43-, 44-SL) were deployed in the caldera of Deception Island to

sample hydrothermally influenced sediments (Fig. 11.2). At the time of deployment, no seafloor observations were available neither from OFOS nor from HBS. The gravity cores were located in an area where geophysical surveys indicated fault systems (Rey et al., 1995). All three gravity cores recovered only dark-muddy sediments in the core catcher. No temperature anomaly and no smell of sulfide was detected.

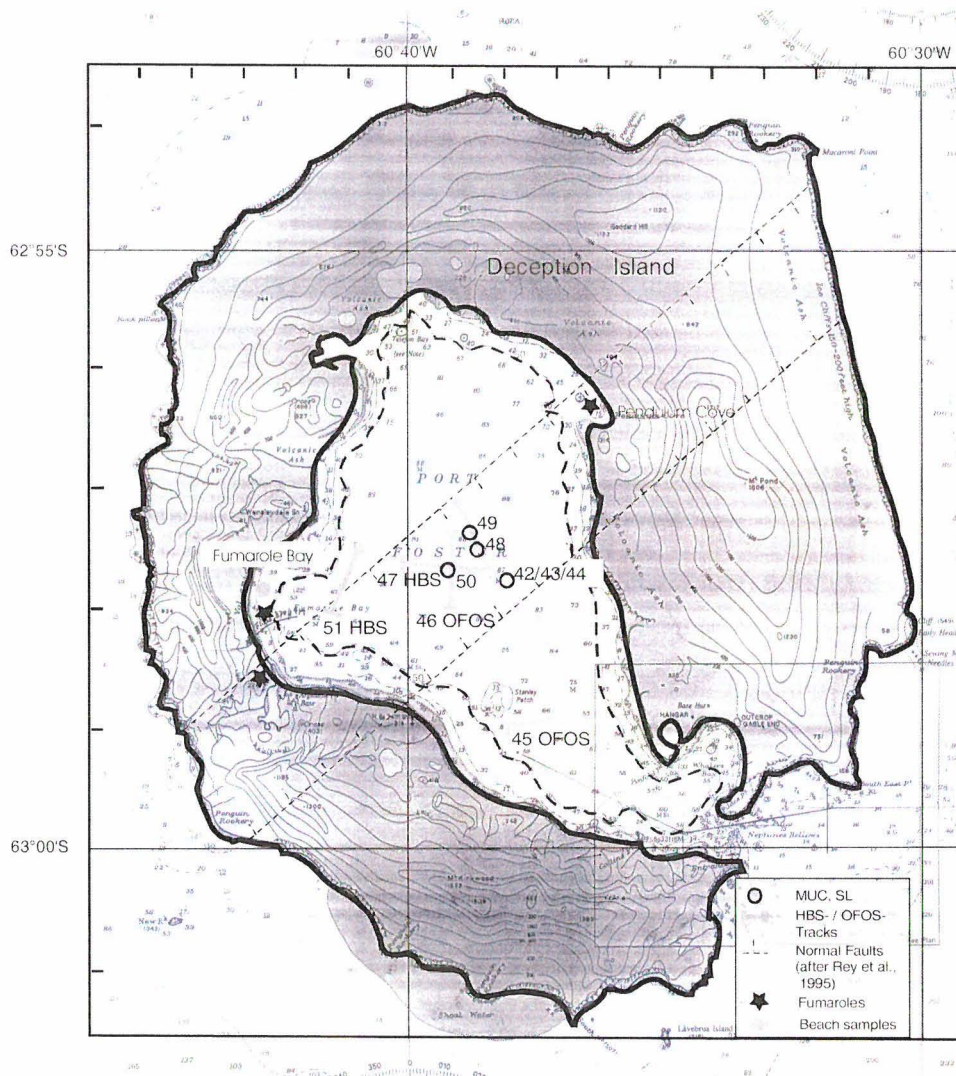


Fig. 11.2: Overview of Deception Island Caldera with the location of OFOS, HBS, MUC, and SL stations.

Three multicores (48-, 49-, 50-MUC) were deployed in the caldera of Deception Island at sites with alleged temperature anomalies observed during 47-HBS. The temperature in the surface sediments at these sites was supposed to be several tens of °C elevated with respect to ambient bottom water (see chapter HBS). However, all three deployments recovered muddy gray-green sediments without temperature anomalies. All sediment cores had a brown fluffy layer on top consisting of centric diatoms in an unidentified organic matrix. Additionally, the cores of 50-MUC had a 2-3 cm thick black soupy layer

overlaying the sediments, which in turn was overlaid by patches of fresh brown fluff. After storing the cores for some hours in the eluminated cold room, the brownish fluffy patches had disappeared from the surface. Microscopy of the mostly black fluffy layer revealed abundant centric diatoms, brown in color, few formed chains of 2-3 cells. No ash particles were found in the black fluffy layer. We assume that chain-forming diatoms very recently settled from surface waters, form these fluffy layers. The layers were black because of anaerobic conditions, which were determined by a weak smell of sulfide within the dark fluffy layer of some subcores. The cores contained abundant living macrofaunal species.

Water and seafloor samples were taken at a fumarole on the beach at the northern end of Fumarole Bay. Fumarole activity was concentrated at 3 focussed spots with a diameter of 1 to 3 m, that were characterized by emission of steam to the atmosphere and hot surface temperatures. Diffuse outlets of gas and elevated temperatures were found throughout the beach, which was free from snow in contrast to the adjoining area. Numerous small gas seeps also occurred in the shallow water zone, where water temperatures of 5 to 7°C and varying sediment temperatures up to more than 60°C were measured. The beach at the fumaroles area consisted of coarse-grained basalt particles.

Samples for the analysis of the bacterial community were taken from beach areas with different temperatures and also from shallow water sediments. Water samples for the determination of bacterial activities and chemical parameters were taken directly close to the bubble stream of small seeps. Because of the coarse structure of the sediment it was not possible to obtain sediment cores of more than a few centimeters. Furthermore the methane and hydrogen content of the emitted gas bubbles was measured, resulting in values of 14.8 ppm H₂ and 136.3 ppm CH₄.

11.4 Sedimentology

Two gravity cores (11-, 37-SL) were deployed in the Hook Ridge Caldera in water depths of 1040 and 1059 m. Both recovered warm sediments with max. 22.3 and 36.6°C, respectively. Starting at the bottom, they were cut into pieces of 1 m in length, halved into a working and an archive half and sampled immediatly for pore water and microbiological analyses. The archive half was used for description

In station 11-SL (Fig. 11.3) we recovered 448 cm of generally homogeneous olive-green, diatomaceous mud, including three layers of coarse grained volcanic ash and spots of blackish material, sometimes coarse grained. An additional ca. 6 cm long section consisting of more greyish mud with some coarse grained greenish spots is found at 395 to 391 cm depth.

Core 37-SL (Fig. 11.4), with a total recovery of 256 cm, consists in most parts of light olive-green diatomaceous mud. The first 10 cm were hardly recovered, due to handling on deck. From 110 to 123 cm the core is badly disturbed, due to lithofied crust material. This core also contains three coarse grained ash layers, few dark grey or greenish spots and lithofied layers and fragments. One of the ash layers (40 – 44 cm) also contains rock and shell fragments. From 148 up to 156 cm the sediment consists of olive-green mud, followed by ca. 50 cm of light olive-green mud, then turning to a generally light grey mud with abandoned patches of dark grey and green (205 to 232 cm). The last 10 cm consist of light olive-green mud.

In both archive halves the core catcher sediment (~15 cm) is missing.

11.5 Pore Water Chemistry

11.5.1 Introduction

In general, pore waters of hydrothermally influenced sediments are a mixture of diagenetic pore water components produced during the degradation of organic matter and of hydrothermal fluids, advectively or diffusively transported from deeper sequences. The distinction between diagenetic and hydrothermal components is made by considering specific tracers. Diagenetic parameters (ammonia, phosphate, total alkalinity) are generally high in the study area, because of the high primary productivity in the southern ocean.

Methane and silica are pore water components that increase with depth either due to diagenetic or hydrothermal processes. The processes causing high methane concentrations are methanogenesis during anaerobic degradation of organic matter and thermally induced cracking of organic matter, respectively.

The Si sources are dissolution of diatoms in the sediment and Si-rich fluids advecting from

below, respectively. Whereas for methane the source is the organic matter of the sediment in both cases, the Si source might be not only sediment-derived but also rock-derived in case of intense hydrothermal processes within the crust. A distinction between both sources can be made by isotopic analysis of methane, which will be done later on, and by a correlation of Si to Cl, the latter being a distinct tracer for hydrothermal processes within the crust.

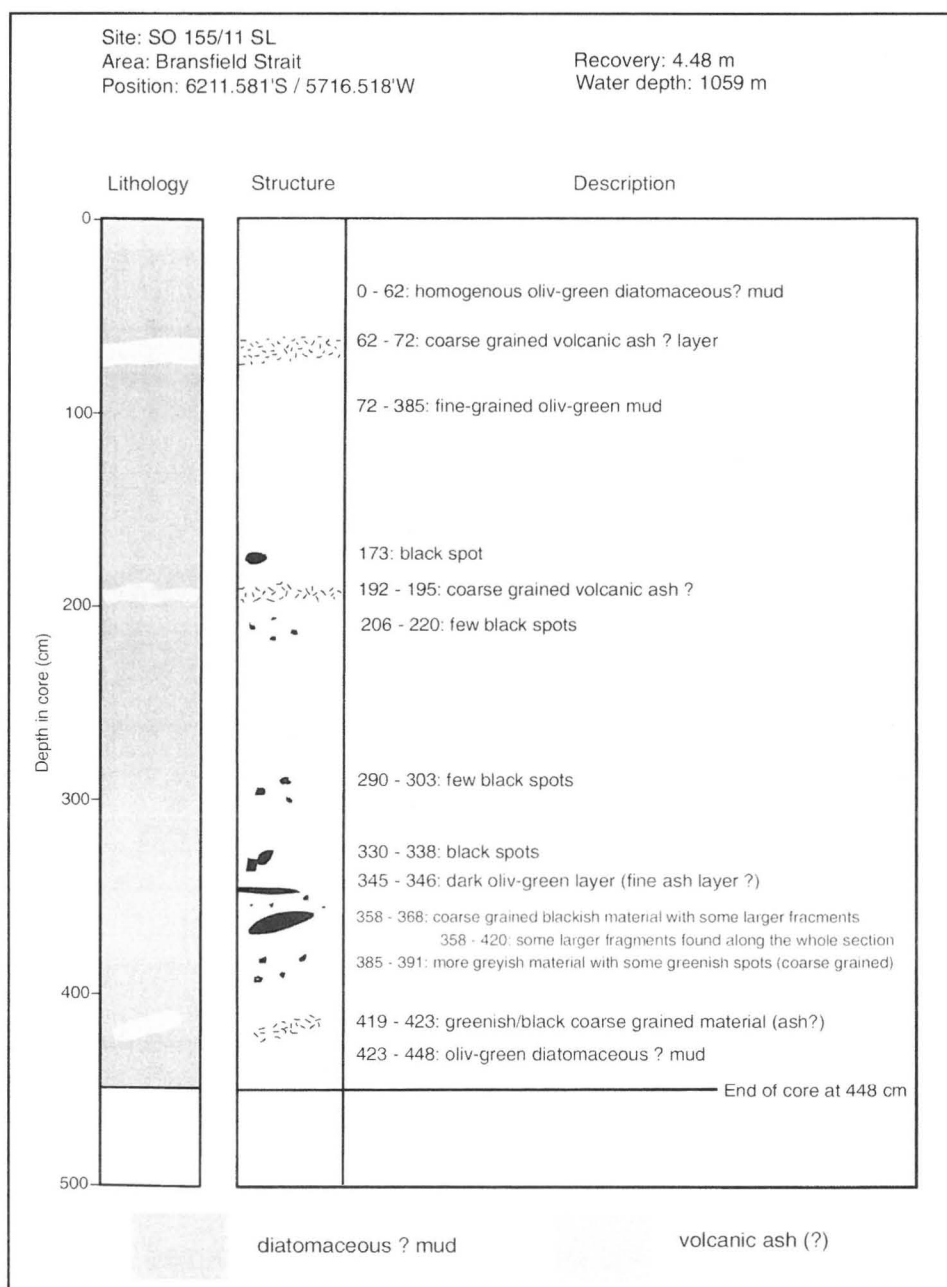


Fig. 11.3: Core description of gravity core 11-SL.

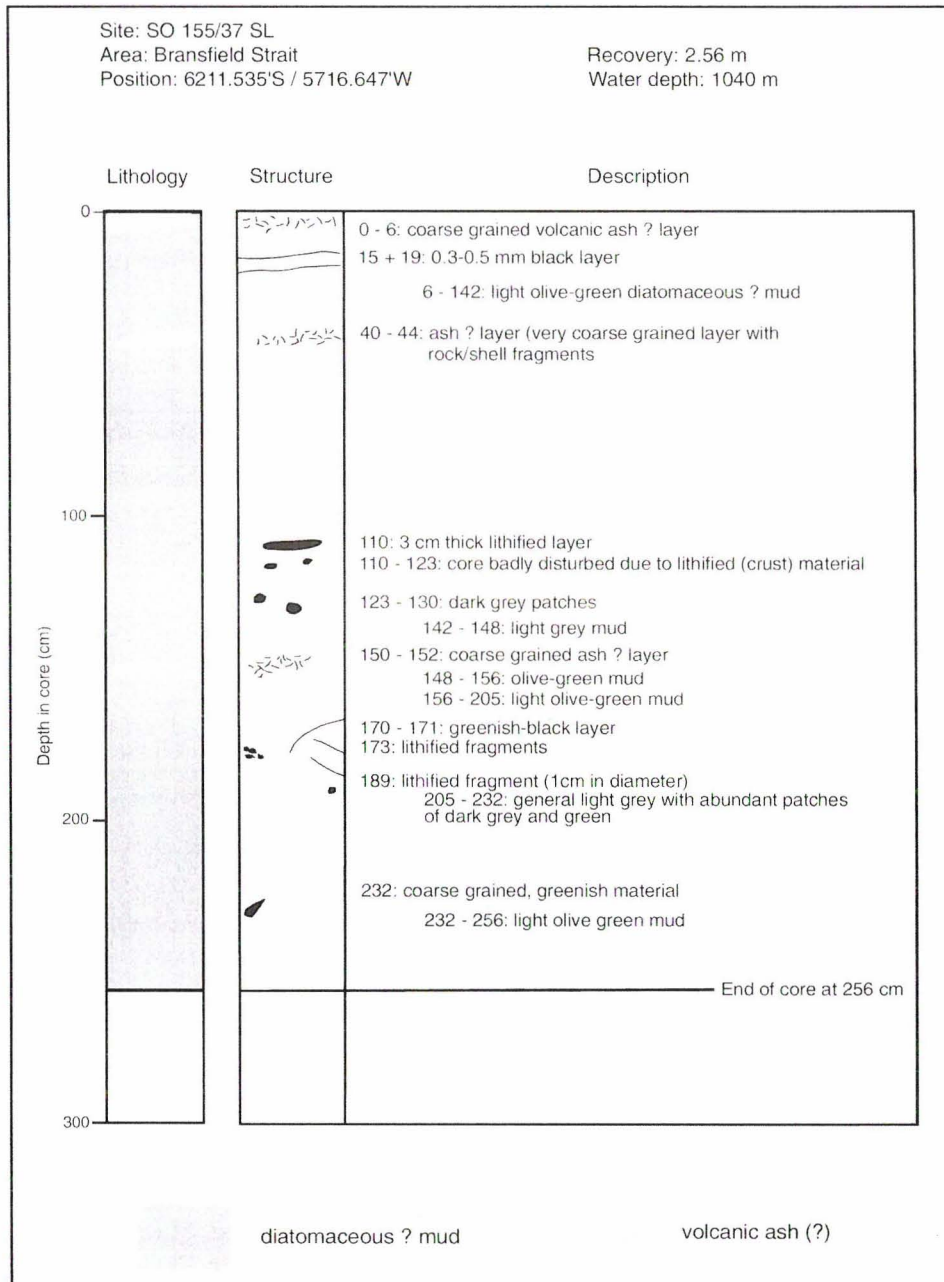


Fig. 11.4: Core description of gravity core 37-SL.

From previous studies it is known that - besides the temperature - pH and Cl concentration may serve as tracers for hydrothermal activity. Since pH values are generally low in hydrothermal fluids, a decrease of this parameter clearly indicates the presence of a hydrothermal component within the pore fluid. Cl is an indicator of hydrothermal processes if phase separation occurs within the crusts. Hot sediments sampled at Hook Ridge taken by the TV-grab during cruise NBP 99-04 (max. 48°C) were extremely depleted in Cl (min. 442 mM), whereas fluids sampled with a SL corer SW of Hook Ridge during cruise ANT XV/2, show a Cl enrichment up to 579 mM at 6 m depth. Detailed studies on these pore water samples revealed that phase separation takes place underneath Hook Ridge, with

the vapor phase emanating at Hook Ridge crater and the Cl-rich liquid phase remaining at depth and being transported diffusively to the surface (Dählmann et al., *subm.*).

In order to get closer to the concentration of the hydrothermal endmember the main objective for pore water analyses during cruise SO-155 was therefore to sample hotter sediments with a stronger Cl depletion at Hook Ridge (vapor phase endmember) as well as to recover longer cores next to the venting area with a stronger increase in Cl (liquid phase endmember). By using the MUC we also wanted to sample a more undisturbed sediment surface than it is possible with the TV-grab that was used solely during the preceding cruises.

11.5.2 Sampling procedure

During Cruise SO-155 a total of 8 sediment cores were analyzed for pore water chemistry. Apart from sediments taken with the multicorer (MUC) and the gravity corer (SL) two additional subcores of a TV-guided grab (GTVA), deployed for sampling of precipitates, were subsampled. Subcores taken with the MUC were separated into 1 to 3 cm thick slices with the higher resolution at the surface. The overlying bottom water was also sampled and analyzed. The gravity cores were cut along their longitudinal axes and sediment samples were taken approximately every 25 cm by means of 50 ml syringes. The second half of the core is stored as archive. Two GTVA were sampled by cutting plexiglas boxes out of the retrieved loads which were subsampled with syringes. An overview of all cores with the analyses done aboard as well as subsamples taken for home lab analysis is given in Table 11.2.

Each sediment sample was placed in a segment of the pore water squeezer. Each plate was equipped with a coarse plastic mesh upon which a 0.2 μm membrane filter was placed. The plate was then covered with parafilm and separated from the next segment by a rubber gasket. Plastic tubes connected each segment to vials receiving the pore water. The chambers were pressurized with nitrogen at a pressure of up to 5 bar until no more fluid was extracted. By this procedure a maximum of 30 ml pore water was received from each sediment sample. Pore water squeezing was carried out at room temperature, since most samples were warmer than 10°C. The remaining squeeze cakes were packed into plastic bags and stored for further analyses.

SL and GTVA cores were squeezed in a glove bag under inert gas atmosphere (nitrogen) to prevent oxidation of trace elements which may cause artefacts in fixed and dissolved amounts by precipitation/dissolution. For trace elements analysis, an aliquote of 4 ml was subsampled immediately within the glove bag into a bottle that contained 4 μ l of suprapur HCl (30%). The squeezer plates used within the glove bag were made of teflon to prevent the contamination of trace element samples. For trace element squeezing in the glove bag we used acid-cleaned Durapore membrane filters, also surfactant-free cellulose acetate membrane filter (SFCA) were used.

11.5.3 Analytical methods

The pH was measured in wet sediment samples prior to squeezing by means of a pH electrode calibrated using BIS and 2-Aminopyridine buffers (pH 7 to 9) prepared in artificial seawater (Dickson 1993) and a commercially available buffer of pH 3,16 (SWS scale, KSI, Meinsberg). Photometric analyses of silicate, ammonia, phosphate, and hydrogen sulfide were based on methods given in Grasshoff et al. (1983). Total alkalinity was measured by titration of 1 ml of pore water with 0.02 N HCl in an open cell (Ivanenkov and Lyakhin 1978). The method was standardized using IAPSO seawater solution (TA = 2.325 mM). A mixture of methylene blue and methyl red was used as indicator (pH at the end point is 5.4-5.5). This method is especially suited for samples containing H₂S and those with TA values largely exceeding 2.3 mM as H₂S and CO₂ are removed during the titration by a continuous stream of nitrogen through the samples. Chloride titration was done following the procedure developed by ODP (Gieskes et al. 1991). All samples will be analyzed for major elements by ICP-OES at GEOMAR. Bromide and sulfate will be measured by ion chromatography. Subsamples were taken for trace element analysis with ICP-MS as well as for analysis of dissolved inorganic carbon (DIC) and $\delta^{13}\text{C}$ of DIC (refer to tab. 11.2).

11.5.4 Results and discussion

A synopsis of all cores recovered, analyses for pore water chemistry on board, and subsamples taken for home lab analysis is given in Table 11.2. All data from pore water analyses performed on board are given in Table 11.3 und 11.4.

Hook Ridge Crater

With MUC and SL we were able to sample hydrothermally influenced sediments taken in the SW crater area of Hook Ridge just inside the crater wall (Fig. 11.1), with the highest

temperature of 36.6°C in ~1.5 m depth of 37-SL. Unfortunately no hot surface sample with Si precipitates could be sampled. The maximum temperature of MUC sediments was 4.5°C. Comparison of pore water profiles of MUC and SL (Fig. 11.4) clearly show that the surface sampled with the MUC corresponds to the deeper section sampled with the SL corer, i.e. the MUC sediments represent the surface sediments missing in the SL cores. The higher the hydrothermal influence (i.e. temperature) in the MUC sample (33-SL > 32-SL > 30-SL) the better is the fit to 37-SL that shows a very strong hydrothermal imprint. Both MUC and SL profiles exhibit diagenetic reactions partly overprinted by advecting or diffusively transported hydrothermal fluids as can be seen for ammonia, phosphate, and total alkalinity (diagenetic parameters) and pH, and Cl (hydrothermal tracers), respectively. GTVA subcore data is similar to MUC, but not presented here in detail (ref. tab. 11.3).

Table 11.2: Summary of all cores recovered, analyses for pore water chemistry performed on board, and subsamples taken for home lab analyses.

station SO 155 /	no. of subcores / max. length [cm]	T max. [°C]	subcore for PW analysis	length of analyzed subcore [cm]	N	shipboard analyses							No. of samples for analyses			sampling strategy
						Si	PO ₄	NH ₄	H ₂ S	Cl	TA	pH	SE	HE	DIC	
Hook Ridge																
05 GTVA	0															
06 GTVA	1/44	16.1			6	x	x	x	x	x		x		6	syringes	
07 GTVA	1/45	13.4			6	x	x	x	x	x	x			6	6	syringes
09 MUC	0															
10 MUC	0															
11 SL		22.3		432	22	x	x	x	x	x	x	x	22	22	11	syringes, GB
30 MUC	6/21	-0.2	C	18	12	x	x	x	x	x	x	x		12		1-3 cm slices
31 MUC	7/54	1.4														
32 MUC	6/26	3.8	A	24	13	x	x	x	x	x	x	x		13	11	1-3 cm slices
33 MUC	6/27	4.5	G	27	13	x	x	x	x	x	x	x		13	13	1-3 cm slices
34 MUC	8/-25	-1.6														
35 MUC	8	-1.1														
36 MUC	0															
37 SL		36.6		256	14	x	x	x	x	x	x	x	14	14	10	syringes, GB
Deception Island																
42 SL				15												
43 SL				5												
44 SL																
48 MUC	6/20	0.1														
49 MUC	4/-30	0.3														
50 MUC	7/-30	-0.2	F	27	15	x		x	x	x	x	x		15	11	1-3 cm slices
Beach					2	x	x	x		x	x	x		2	2	filled into bottles in situ

subsamples taken for analysis in home lab:

SE: acidified pore water for trace element studies

HE: acidified pore water for major element studies

DIC: pore water for dissolved inorganic carbon

sampling procedure:

GB: squeezed in nitrogen atmosphere (Glove Bag)

Within the sediment surface sampled by MUC (Fig. 11.5) ammonia, phosphate, hydrogen sulfide, and total alkalinity signify diagenetic processes by an increase with depth. The visual appearance of the cores with a brownish Fe-oxyhydroxide layer on top and grayish-

green sediment below ca. 7 cm is reflected by the highest phosphate concentration just below this horizon, representing the zone of intense degradation of organic matter.

The pH decreases with depth to almost 5.0, which indicates an increasing amount of the hydrothermal component within the pore water. Chlorine as an indicator of hydrothermal influence decreases with depth. The warmest core (33-MUC) exhibits the largest gradient, although even in samples with bottom water temperature (-0.2°C , 30-MUC) a decrease in Cl is evident. The increase in CH_4 with depth is remarkable in both cores (32-, 33-MUC). The linearity of the profile (especially in station 32-MUC) may indicate a diffusion-controlled transport of CH_4 generated at depth. The question whether methane is of microbial or thermogenic origin can only be answered by isotopic analysis of CH_4 onshore. The coincidental presence of H_2S and CH_4 suggests that H_2S is probably produced by anaerobic methane oxidation / sulfate reduction.

Silica increases with depth either due to Si-rich fluids advecting from below or due to diagenetic dissolution of diatoms in the sediment. According to laboratory experiments (Van Cappellen & Qiu 1997) the saturation concentration of dissolved silica in equilibrium with biogenic silica is approximately $600\ \mu\text{M}$ at -1.5°C (bottom water) and $750\ \mu\text{M}$ at 4.5°C (temperature maximum on deck in 33-MUC). Much more elevated Si concentrations within the cores (up to $1500\ \mu\text{M}$) can therefore be explained by either higher *in situ* temperatures – enhancing opal dissolution – or by an admixture of additional silica dissolved under hydrothermal conditions in deeper sediment sections or even from the rocks underneath the sediment cover. Assuming a cooling of $\sim 20^{\circ}\text{C}$ will result in a concentration of $\sim 1400\ \mu\text{M}$ silica in equilibrium with biogenic silica at an *in situ* temperature of 25°C .

An exceptional Si profile is observed in station 33-MUC: A crust of amorphous silica at the end of this core results in a sharp decrease in dissolved Si in the pore water, this crust probably serving as a precipitation nucleus. As silica crusts do only precipitate at the sediment surface when warm, Si-rich fluids emanate into the cold bottom water, this crust most likely represents a former surface layer that has been sedimented up to a depth of about 20 cm at present.

Table 11.4: Data from methane analyses (in $\mu\text{mol/l}$) in wet sediment performed on board.

station	06-GTVA	07-GTVA	09-MUC	32-MUC	33-MUC	50-MUC	11-SL	37-SL
depth [cm]							depth [cm]	depth [cm]
0.5			3.35	0.27	0.46	0.28	15	5
1.5				0.23	0.29	0.26	35	25
2.5				0.40	0.65	0.29	55	45
3.5				0.31	3.17	0.35	75	65
5.0				0.73	5.35	0.27	95	85
6.5		4.80					115	105
7.0				0.67	7.92	0.30	135	125
9.0	0.37			1.15	11.08	0.35	155	145
11.0				1.68	13.96	0.37	175	165
13.5				2.06	13.60	0.43	195	185
15.0							215	205
16.5				2.44	13.81	0.51	235	225
19.0	0.41						255	
19.5				3.91	13.61	0.52	275	
20.0		8.13					295	
22.5				5.52	10.90	0.62	315	
25.0							335	
25.5				6.98		0.65	355	
28.5				8.17		1.01	375	
33.0		9.33					395	
35.0							415	
37.0	0.36						430	
41.0		8.69						

Both diagenetic and hydrothermal influence is also shown in profiles of the gravity core taken at the same location (Fig. 11.4). In station 11-SL intense degradation of organic carbon commences below a prominent ash layer (60-75 cm), as can be seen by increasing ammonia, phosphate, and total alkalinity. Sulfide concentration is below detection limit in this core. In core 37-SL, however, no such strong diagenetic reactions are observed. High silica concentrations, very low pH and the presence of H_2S are more probably due to a hydrothermal fluid component. The stronger hydrothermal influence in 37-SL was first obvious by higher temperature measured directly after the retrieval (max. 36.6°C in 37-SL compared to 22.3°C in 11-SL).

Large differences between the two cores are also observed for the Cl profiles: In 11-SL the Cl concentration stays rather constant at about 525 mM, whereas the smallest concentration in 37-SL is 480 mM (considering the value of 421 mM at 212 cm a sampling artefact, as it is not a fault in Cl analysis). The difference in the pore water chemistry between these two cores is also very pronounced in the pH and methane concentration. In core 11-SL the pH decrease is only from about 7.4 in the uppermost sample to 6.1 in the lowermost (418 cm).

Cruise Report SO-155 (HYDROARC)

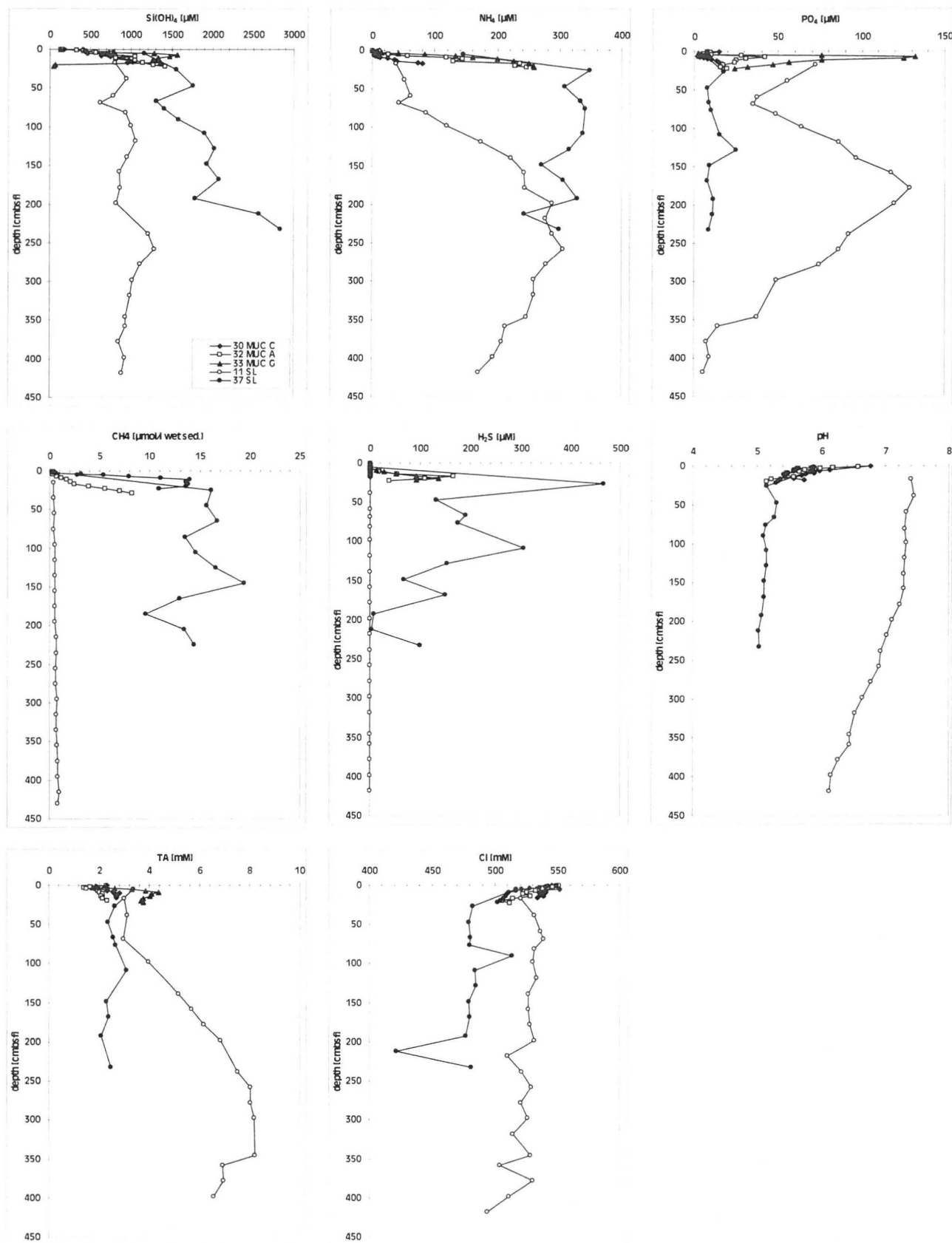


Fig. 11.4: Pore water profiles of all MUC and SL stations at Hook Ridge analyzed for pore water chemistry

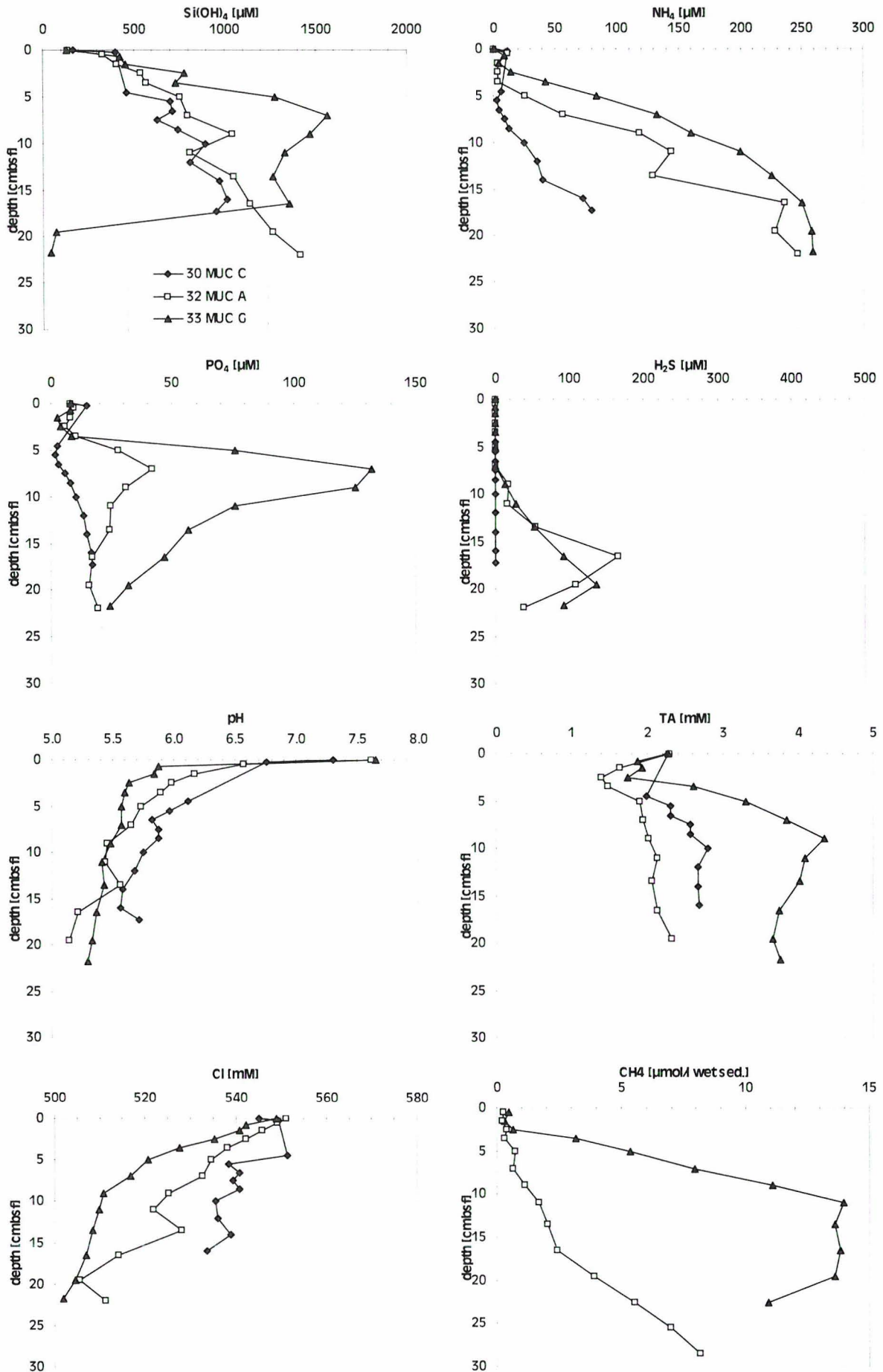


Fig. 11.5: Detailed pore water profiles of all MUC stations at Hook Ridge analyzed for pore water chemistry

In core 37-SL, however, a (constant) pH of about 5.0 is already achieved at 26 cm depth. Methane shows elevated concentrations of 10 to 20 $\mu\text{mol/l}$ (in wet sediment) in 37-SL, whereas in 11-SL the concentrations are not much higher than 1 $\mu\text{mol/l}$. Both pH and CH_4 show sharp gradients in the surface sediment that are in good accordance with the results obtained within the MUC cores.

Silica concentrations in core 11-SL do not exceed 1500 μM , i.e. they are partly even lower than the maximum concentrations measured in the surface samples of the MUC cores. In contrast, Si increases to almost 3000 μM in 2.3 m depth in 37-SL. The Si concentration in 11-SL can be explained by diagenetic dissolution of biogenic silica. The same is true for core 37-SL if cooling of $\sim 20^\circ\text{C}$ (i.e. the same as discussed for 33-MUC) is assumed to have taken place during recovery of the gear. According to Van Cappellen & Qiu (1997) the equilibrium concentration at 55°C is $\sim 3000 \mu\text{M}$. Also, hydrothermally induced dissolution from either deeper sediments or rocks has to be considered as an additional source for Si.

Figure 11.6 shows the Si-Cl correlation of all analyzed pore waters, excluding the two samples from the Si crust layer in 33-MUC. The strong negative correlation ($r^2=0.77$) suggests that the pore waters are mixtures of two endmembers, a high Si / low Cl and a low Si / high Cl. Since low Cl fluids result from phase separation in the deeper crust (vapor phase), it can be assumed that the high Si concentration of this endmember originates from the same source, i.e. is rock-derived. The second endmember, low in Si and high in Cl, is mostly of seawater composition with slightly enhanced Si concentration (550 mM Cl and 500 μM Si, compared to $\sim 150 \mu\text{M}$ Si in bottom water).

Deception Island Caldera

Pore water was extracted and analyzed from a core containing a 2 cm thick black fluffy layer on top of gray-green muddy sediment. Furthermore, water samples from a 60°C hot fumarole taken on the beach of Fumarole Bay were analyzed. The hot water samples from the fumarole was characterized by low pH and low Cl concentrations (Fig. 11.7). No hydrothermal vent influence was detected in the core of 50-MUC, neither the temperature in the sediments after retrieval was anomalous nor the pH was decreased. The slight decrease in chlorinity towards the sediment surface may indicate a change in chlorinity of

the bottom water during time. This is likely to occur during the summer season, due to significant input of fresh water by melting ice.

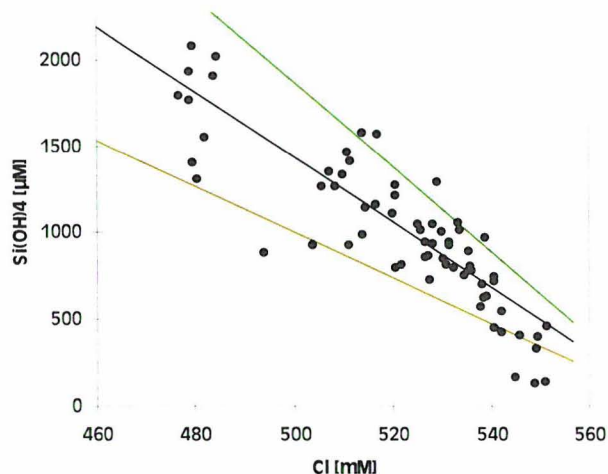


Fig. 11.6: Si-Cl correlation of all pore waters at Hook Ridge, excluding the two samples from the Si crust layer in 33-MUC. Although two other data points with high Si concentrations (37-SL) are not plotted, their values are included in the data set taken for regression. The two lines surrounding the regression line and covering almost all samples represent a deviation of 30% relative to the mean calculated by the least square fit.

One motivation for the pore water studies of core 50-MUC was to identify the influence of the fluffy layer, consisting of diatoms and an organic matrix, on the porewater chemistry. Therefore, the bottom water and the water of an upper and a lower section of the fluffy layer were sampled separately. It is interesting to notice, that the gradient in nutrient concentration (Si, NH_4) between bottom water and pore water was almost the same as the gradient found between the two sections of the fluffy layer.

This finding suggests that the fluffy layer, although soupy and unconsolidated, was present for time periods long enough to establish this gradient. It is most likely that the chain forming centric diatoms on the sediments settled from the surface water and are subject to remineralization at present. Such an onset of remineralization may be indicated by a very high phosphate concentration in the fluffy layer, compared to the pore water concentrations. The remineralization may not be completed, as the Si and NH_4 concentrations were not elevated.

Cruise Report SO-155 (HYDROARC)

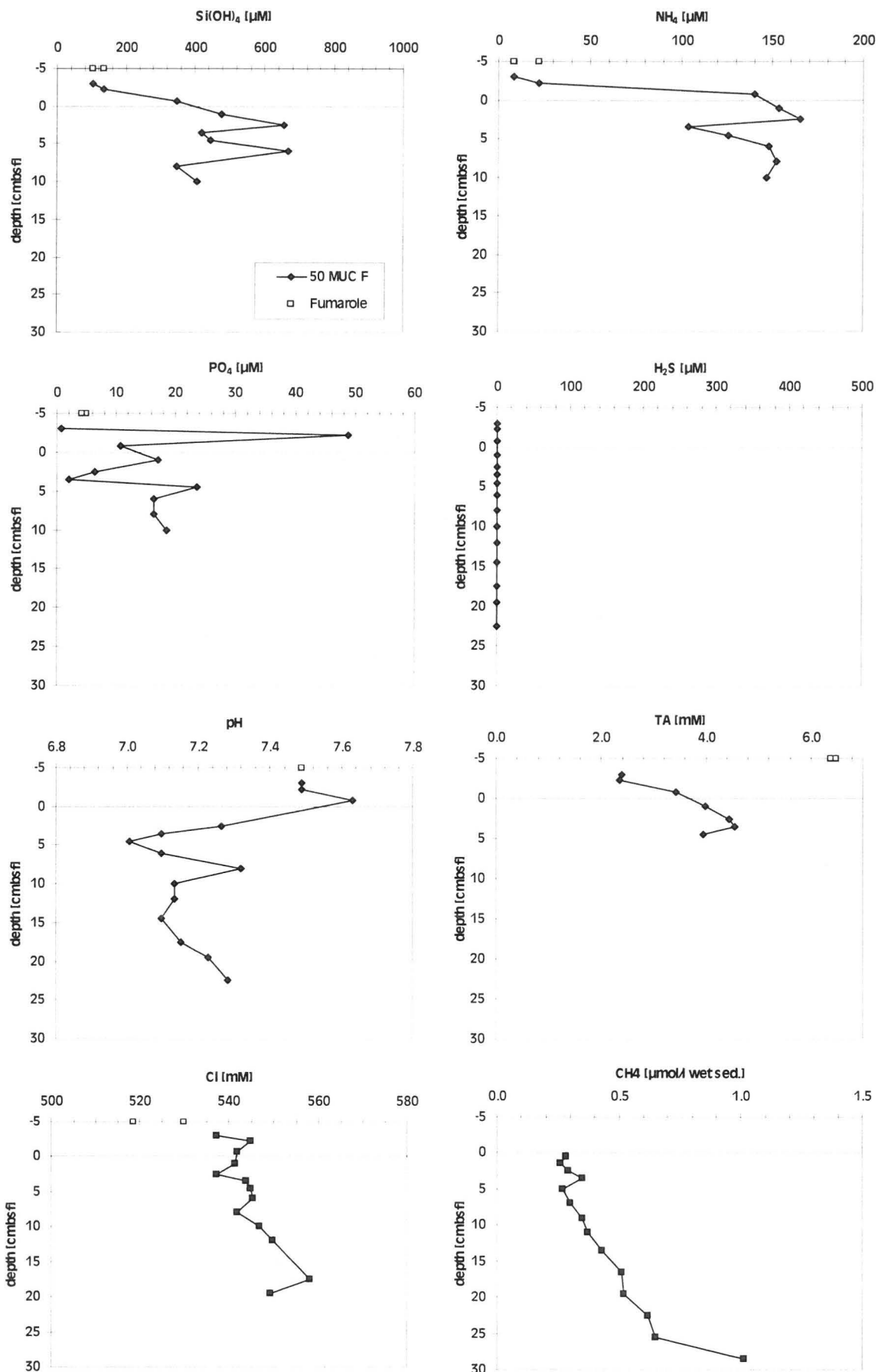


Fig. 11.7: Pore water profiles of station 50-MUC taken in Deception Island Caldera and two samples of surface water taken in Fumarole Bay.

11.6 Microbiology

11.6.1 Introduction

Biological communities at hydrothermal vents have attracted considerable interest since their discovery in respect to the transfer of geochemical energy into biological forms of energy. Since then a number of studies on high-temperature hydrothermal vents were carried out, but relatively little is known on the microbiology of low-temperature hydrothermal sites. Especially sites in the Antarctic region have not been studied up to now and possibly are, because of their isolated geographical position and extreme environmental conditions, characterized by hitherto unknown bacterial community structures.

The focus of our investigations lies on oxidative processes of the sulfur and methane cycles. Molecular-genetic studies on the composition of the bacterial communities will be carried out at different sites and sediment depths. Additional information will be gained by the culture of bacteria in media selective for various physiological groups, and by morphological studies using light and scanning electron microscopy. The determination of chemoautotrophic and methanotrophic activities in sediment profiles will provide links to geochemical gradients.

The microbiological investigations started during this cruise cannot be completed on board ship, they all require a time-consuming post-processing in the home lab. Therefore in this report no microbiological results can be presented, but the applied methods will be described in the next section.

11.6.2 Methods and material

Fixation of sulfide by zincacetate:

To determine the sulfide concentration, sediment samples were fixed in zincacetate solution. 1 ml sediment samples were filled into 10 ml-polypropylene tubes containing 2 ml of 20% zincacetate. This mixture was shaken vigorously to obtain good contact of the solution to the sulfides within the complex matrix of sediment and stored at 4°C. Analyses will be done in the home laboratory.

Pore water nutrients and soluble sulfur compounds:

To get information about the general chemical background, samples were taken for

analysis of the major nutrients (sulfate, sulfite, thiosulfate, tetrathionate, nitrate, phosphate). For each depth 2 x 10 ml polypropylene tubes were filled with sediment and centrifuged at 3500 rpm (ca. 4000 x g) for 30' at 4°C. The pore water then was taken up with a 5 ml syringe fitted with a 0.2 mm Ø needle. The needle was replaced with a 0.2 µm SFCA (surfactant free cellulose acetate)-filter and the filtered pore water was collected into 2 ml Eppendorf reaction tubes, which were frequently rinsed with supra pure water, autoclaved and dried prior to use, and stored at -20°C. These samples will be used for the analysis of pore water nutrients and soluble unfixed sulfur compounds in the home laboratory.

Fixation of soluble sulfur compounds by monobromobimane derivatization:

As many of the sulfur compounds are unstable when in contact with oxygen at room temperature, sulfur compounds should be derivatized and/or stored at lower temperature. Derivatization was done according to Fahey and Newton. Briefly 50 µl HEPES buffer ((2(4-(hydroxyethylene)-1-piperazinylethansulfonic acid, 160mM; EDTA (ethylenedinitrilo-tetraacetic acid) 16mM) is added to 50 µl acetonitrile (gradient grade) and 10 µl monobromobimane reagent (96 mM, Thiolyt Reagent, Fluorescent Labelling Compound, Calbiochem) and shaken. Then 50 µl of filtered pore water is added mixed and stored in the dark at room temperature. After 30' 100 µl methanesulfonic acid (130mM) is added, mixed and stored at -20°C.

Methane concentrations:

Samples for the determination of methane concentrations in the sediment were taken from subcores of the TV grab or the multicorer. 5 ml aliquots of sediment were transferred into vials containing saturated NaCl solution, which were then quickly closed with a septum cap and shaken. By this procedure pore water methane was released into the gas phase. Methane in the headspace was measured on board using a gas chromatograph fitted with a solid-state semiconductor detector.

Water content:

5 ml samples of sediment were transferred into preweighed vials to determine wet weight and, after 24 h of drying at 100°C, dry weight and water content.



Sediment sampling for molecular biological community analysis:

Bacterial community structure will be determined by DGGE (denaturant gradient gel electrophoresis, Muyzer et al., 1993) pattern comparison of PCR (Mullis et al., 1987) amplified 16S rDNA gene fragments of DNA extracted from sediment samples. Further information will be gained by sequencing (Sanger et al., 1977) of cloned 16S rDNA genes and genes for sulfite oxidase (*sox*) and methane monooxygenases (particulate (*pmoA*) and soluble (*mmo*)) as indicators for sulfur oxidizing respectively methane oxidizing bacteria. Additional information will be gathered by enrichment cultures for bacteria using different substrates (sulfide, thiosulfate, organic compounds). Careful investigation of the corresponding biochemical pathways and biochemical potential will follow.

Sampled material was transferred into sterile 2 ml Eppendorf reaction tubes and stored at -20°C . This material will be used for molecular genetic analysis in the home laboratory.

Enrichment cultures:

Hydrothermally influenced sediments contain significant amounts of reduced inorganic compounds. Sulfide or other reduced sulfur compounds are used as energy source by autotrophic bacteria. For these organisms Pfennig's medium (KH_2PO_4 : 0.34 g/l; NH_4Cl : 0.34 g/l; $\text{MgSO}_4 \times 7 \text{H}_2\text{O}$: 0.5 g/l; $\text{CaCl}_2 \times 2\text{H}_2\text{O}$: 0.25 g/l; KCl : 0.34 g/l. Trace element solution SL12: 1 ml / l ; Vitamin solution: 1 ml / l (2 mg vitamin B12 in 100 ml aq. dest); 7.5% NaHCO_3 - solution.: 20 ml / l ; 10% $\text{Na}_2\text{S} \times 9 \text{H}_2\text{O}$ -solution: 4 ml / l) is used for enrichment cultures. Furthermore enrichment cultures for aerobically growing bacteria were made with TSB (Tryptone soy broth; 0.3g/l) as a complex medium. From this 2 subsamples were taken (TSB 0.3g/l; 20 mM NO_3^-) for enrichment of nitrate reducing bacteria and TSB 0.3g/l; 20 mM MoO_4^{2-} . Enrichments were incubated at 30°C except the Deception Island (Fumarole Bay) fumarole samples which were additionally incubated at 60°C . Approximately 50-100 mg sediment sample were applied as inoculum to the different media. After 7 days of incubation at 30°C growing enrichment cultures are transferred to fresh media and sulfide reduced media were replenished with 0.15 ml of a sulfide solution (28 g $\text{Na}_2\text{S} \times 9 \text{H}_2\text{O}$ /l). For enrichment and isolation of methanotrophic bacteria water and surface sediment samples were inoculated into liquid mineral culture media containing no organic compound other than methane. This medium is selective for an enrichment of methanotrophic bacteria, which subsequently can be isolated on agar plates and characterized by physiological methods and by 16S-rDNA sequencing.

Furthermore methanotrophic bacteria were isolated by direct plating of pore water on agar surfaces.

Total bacterial numbers, biomass, and morphological characterization of the bacterial community:

For the analysis of these parameters seawater samples (overlying water from MUC cores, fumarole water) and sediment samples were fixed with formaldehyde (1% final concentration). The determination of bacterial numbers and biomass will be done on acridineorange-stained samples by epifluorescence microscopy. Furthermore, bacterial communities in the water and on sediment and crust samples will be morphologically characterized by scanning electron microscopy.

Determination of bacterial activities in the sediment (Stations 32-MUC and 50-MUC):

Methane oxidation rates

Bacterial methane oxidation in sediments was determined using a radioactive tracer method. It is based on the ability of methanotrophic bacteria to oxidize ^{14}C -labelled methane injected into a sediment core to CO_2 and to incorporate a part of it into bacterial biomass. For this purpose, $^{14}\text{CH}_4$ is injected into a sediment subcore (surface to 18 cm sediment depth) with lateral silicone septa in 1 cm distance. After an incubation time of 12 h at estimated in-situ temperatures the subcores were cut into 1 cm slices and transferred into 1 N NaOH to stop the incubation. Samples will be further analyzed in the home lab for radioactivity in the produced CO_2 and in bacterial biomass.

CO_2 fixation rates

Though several metabolic pathways may contribute to a bacterial uptake and incorporation of CO_2 (bacterial primary production) it is generally assumed that the majority is due to chemoautotrophic processes, i.e. a fixation of CO_2 coupled with the oxidation of reduced anorganic compounds like sulfide, sulfur, thiosulfate, Fe^{2+} , Mn^{2+} , ammonia, nitrite or hydrogen. In analogy to the determination of methane oxidation rates, the CO_2 fixation rates were also determined using a radiotracer technique, but with ^{14}C -bicarbonate as a substrate. A solution of $\text{NaH}^{14}\text{CO}_3$ was laterally injected into sediment subcores (0-18 cm depth) taken from multicorers. These were subsequently incubated for 12 h at estimated in-situ temperatures, under atmospheric pressure and in darkness. After incubation the sediment was cut into 1 cm slices and washed with seawater to remove excess $\text{H}^{14}\text{CO}_3^-$

and subsequently centrifuged. Then the sediment was dried and transported to the home lab, where the determination of incorporated ^{14}C will be done by liquid scintillation counting.

Determination of bacterial activities in fumarole water (Deception Island):

As the methods used to determine bacterial activities in soft sediments (see above) could not be applied in the coarse-grained sediments of the beach of Fumarole Cove (Deception Island), at these sites seawater samples were taken a few centimeters apart from an outlet of gas bubbles.

Methane oxidation was measured in 100 ml water samples to which ^{14}C –labelled methane was added. After incubation of 4, 8, 12 and 16 h under temperatures of 5°C and 20°C the process was stopped by adding 10 N NaOH. $^{14}\text{CO}_2$ formed during the incubation was expelled by acidification of the medium and trapped with ethanolamine. ^{14}C incorporated into cell material was concentrated by subsequent $0.2\ \mu\text{m}$ membrane filtration. Both fractions of ^{14}C will be analyzed by liquid scintillation counting in the home lab. For determination of rates of CO_2 fixation in the fumarole water samples, these were incubated for 8 h at 5°C and 20°C , with addition of ^{14}C -bicarbonate solutions. The incubation was stopped by addition of formaldehyde, and after $0.2\ \mu\text{m}$ membrane filtration, incorporated ^{14}C activity will be determined by liquid scintillation counting.

Subsampling for long time storage:

For long time storage 10 ml sediment were transferred into sterile polycarbonate tubes and stored at -20°C (will be transferred at the IfM to -80°C).

Subsampling for enrichment cultures:

For additional enrichment cultures in the home laboratory 10 ml sediment were transferred into sterile polycarbonate tubes and stored at 4°C .

11.7 Macrofaunal composition

11.7.1 Introduction

At most hydrothermal vent and cold seep sites in the deep-sea symbiont-containing macrofauna occurs at high densities and biomass (Sibuet and Olu, 1998; Tunnicliffe, 1991). These macrofaunal species satisfy their nutritional demands by harvesting the

chemoautotrophically produced organic matter of their endosymbiotic bacteria. Most endosymbionts investigated so far rely on chemoautotrophy with sulfur-oxidation as the energy source (Fisher, 1990). Due to the chemoautotrophic primary production, which serves as additional food supply to the otherwise food-limited deep-sea, heterotrophic species are often attracted to the vent and seep sites. These specimens may prey on macro- or megafaunal species or feed on non-symbiotic chemoautotrophic micro-organisms. As the reduced chemical compounds in the vent and seep fluids serve as energy source for chemoautotrophic species, the concentration and flux of sulfide and/or methane is crucial in understanding distribution patterns of chemoautotrophic species.

Despite the fact that sulfide- and methane-rich hydrothermal fluids emanate at Hook Ridge, no vent-typical mega- or macrofaunal species were discovered during the former cruises ANT XV/2 and NBP 99-04. Several hypotheses may be proposed for the suspicious absence of characteristic vent taxa, such as geographical isolation, low temperature, or just misfortune in finding them, though none of these hypotheses can be tested at present. The only chemoautotrophic macrofaunal species recovered during cruise ANT XV/2 were pogonophoran tube worms belonging to the family Sclerolinidae (E. Southward, pers. comm.). All members of the class pogonophora studied so far live in symbiosis with autotrophic bacteria (Fisher, 1990). The megaepifaunal species at Hook Ridge showed a distribution pattern which was correlated to the morphology and/or the hydrothermally influenced sediments, based on preliminary results of extensive OFOS surveys conducted during cruise NBP 99-04. These results indicate increasing numbers of suspension feeding organisms (mainly Cnidaria) on the hard grounds around the hydrothermal vents as well as higher numbers of brittle stars (Ophiuroidea) around the vents compared to the central vent sites.

The OFOS observations and sediment sampling program at Hook Ridge will be used to answer the following questions: is there an influence of hydrothermal venting on the benthic mega- and macrofauna? Is the geochemical environment favorable for chemoautotrophic macrofaunal species?

11.7.2 Methods

Megaepifaunal species and larger macrofaunal species were observed during extensive OFOS surveys conducted during cruise NBP 99-04 and station 01-OFOS during this cruise. Photographic investigations of the slides will provide information about the

distribution patterns of these species in relation to the hydrothermal vent and/or other environmental parameters.

The sediments recovered by the TV-guided grab were qualitatively investigated for the occurrence of macrofaunal species. The surface sediments (ca. 10 cm) recovered by multicorer were processed quantitatively through 0.5 mm sieves. Macrofaunal specimens were preserved in buffered formaldehyd for taxonomic work or frozen for stable isotopic analyses.

11.7.3 Results and Discussion

Hook Ridge Crater

No vent-typical macrofaunal species were discovered in the crater area of Hook Ridge during this cruise SO-155. However, living pogonophoran tube worm species of the family Sclerolinidae were recovered in MUC sediment cores (32-, 33-MUC). The tubes are about 0.5 mm in diameter and up to 15 cm long. Their maximum abundance was about 10 individuals per core. The cores inhabited by Sclerolinidae had maximum temperatures of 4.5 °C when measured on deck, indicating a much higher temperature *in situ*. The sediments had Fe-oxyhydroxides on top of the muddy grayish green sediment. No specimens were found in warm sediments without Fe-oxyhydroxides (31-MUC) nor in cold sediments with Fe-oxyhydroxide (30-MUC). This finding may suggest, that active venting has occurred for periods of time, maybe long enough to cause Fe-oxyhydroxide precipitation. The size of the animals allows them to reach sediment depth (10-15 cmbsf) which contained significant methane, sulfide and ammonia concentrations in the porewater (32-, 33-MUC; Fig. 11.5).

From the sieving procedure it became evident that the numbers of macrofaunal species and specimens in the cores inhabited by pogonophoran tube worms were much lower compared to the numbers of species and specimens from the cores without pogonophorans (30-, 31-, 34-MUC).

Deception Island Caldera

The benthic macro- and megafauna in the caldera of Deception Island was observed by cameras during stations 45-, 46-OFOS and 47-, 51-HBS and sampled by 48-, 49- 50-MUC. Due to the shallow water depth, the faunal abundance and diversity is extraordinary

Appendix 1

Rock Descriptions

Appendix 1

Appendix 1: Petrology Stations and Rock Descriptions

- Notes:**
- Each different lithology recovered from a station is designated Unit A, Unit B, etc. These „units“ are for classification purposes at each station. Note that Unit A at 02 DR **IS NOT** the same as Unit A at 03 DR or any other station, etc.
 - This appendix only describes samples logged by the Petrology Group. At some stations additional samples have been collected and logged by other working groups (e.g., altered rocks recovered at 20 DR, 21 DR, 39 DR, etc). Those samples are described by those groups in different appendices.

Station Abbreviations: DR - Chain-bag dredge
 GTV - TV-Grab
 MUC - Sediment Multicorer
 BIO - Biology Sample Station

Station	Date / Time / Depth / Coordinates	Description
02 DR Lower western flank, Bridgeman Ridge	02.03.2001 on bottom: 04:40 h 1377 m 62°07.34' S 057°01.00' W off bottom: 06:03 h 1200 m 62°07.07' S 057°00.10' W	-1: 22 x 8 cm fresh grey andesite, banded with light grey vesicular and black glassy bands typically 1-5 cm in width, aphyric with trace of dark green pyroxene phenocrysts. Unit A. -2: 22 x 9 cm Unit A , as for 1 but with slightly orange stained weathered surfaces. -3: 16 x 9 cm Unit A. -4: 13 x 10 cm Unit A. -5: 14 x 7 cm Unit A. -6: 11 x 8 cm Unit A. Mostly one dark band 5 cm in width. -7: 12 x 7 cm Unit A. Slight orange staining on some surfaces. -8: 14 x 8 cm Unit A. Orange clay in vesicles on one side of clast. -9: 11 x 5 cm Unit A. -10: 11 x 6 cm agglutinate of Unit A clasts, each up to 1 cm across but averaging 3 mm across. -11: 9 x 4 cm Unit A. Slight orange staining. -12: 10 x 6 cm Unit A. -13: 10 x 5 cm Unit A , grading to agglutinated clasts (see 10) on one side. -14: 8 x 3 cm Unit A. Slight orange staining on one side, very glassy on the other side. -15: 15 small pieces of Unit A , mostly 8 x 3 cm each, with orange staining on three of them. Bulk sample. -16: 18 x 8 cm granodiorite, consisting of quartz, amphibole and plagioclase each about 3 mm across; a subrounded erratic. -17: 7 x 3 cm gabbro, consisting of two pyroxenes (dark green and black) and plagioclase, grain size averaging 2 mm across; a well-rounded erratic. -18: 9 x 4 cm olivine basalt, dense, fine grained matrix with olivine +/- pyroxene/spinel clusters up to 3 mm across, probably an erratic. Other rounded erratics comprising fine grained gabbro, diorite, chloritised conglomerate with chert clasts, and schist were recovered but not kept.
03 DR Upper western flank, Bridgeman Ridge	02.03.2001 on bottom: 08:24 h 640 m 62°07.32' S 056°53.93' W off bottom: 09:58 h	-1: 21 x 8 cm dark grey olivine basalt, 20 % fresh olivine phenocrysts up to 3 mm across, 10 % vesicles up to 1 mm across, columnar jointing within block. Unit A. -2: 17 x 13 cm dark grey olivine/plagioclase basalt, 10 % fresh olivine phenocrysts up to 2 mm across, 20 % plagioclase phenocrysts up to 2 mm across.

Appendix 1

Station	Date / Time / Depth / Coordinates	Description
	450 m 62°06.62' S 056°52.64' W	dense sub-rounded clast possibly from a pillow. Unit B. -3: 12 x 9 cm Unit B. Definitely a pillow fragment. -4: 19 x 7 cm Unit B. -5: 16 x 12 cm Unit B. -6: 12 x 10 cm dark grey plagioclase basalt, 5 % plagioclase phenocrysts up to 2 mm across, 5 % small vesicles, weathered orange on some surfaces. Unit C. -7: 16 x 5 cm black plagioclase dacite, 30 % plagioclase phenocrysts as laths up to 3 mm long set in a black glassy matrix. Unit D. -8: 15 x 6 cm black plagioclase dacite, 40 % plagioclase phenocrysts up to 6 mm long set in a black glassy matrix with conchoidal fracture. Medium grained variant of Unit D. -9: 11 x 6 cm black plagioclase dacite, 40 % plagioclase phenocrysts with stumpy form up to 5 mm long set in a black glassy matrix with conchoidal fracture. Coarse grained variant of Unit D. -10: 9 x 4 cm black glassy dacite, aphyric, a pillow fragment, possibly just a big glass fragment from the coarse grained variant of Unit D. -11: 11 x 9 cm dark grey plagioclase basalt, trace plagioclase phenocrysts, abundant (10 %) xenoliths of altered lavas and one gabbro up to 5 cm across (most 5 mm), blocky surfaces and possibly an erratic. Unit E. -12: 11 x 7 cm dark grey plagioclase basalt, as for Unit E but more weathered and with 20 % large (up to 3.5 cm long) pumiceous xenoliths. -13: 15 x 11 cm grey pyroxene andesite, 5 % small pyroxene phenocrysts and trace plagioclase phenocrysts, dense, weakly weathered block that may be an erratic. Unit F. -14: 15 x 7 cm aphyric basalt, 20 % vesicles up to 1 mm across. Unit G. -15: 16 x 6 cm Unit G, weathered. -16: 11 x 6 cm grey plagioclase andesite, 5 % small (<1 mm across) plagioclase phenocrysts, 10 % small vesicles, weakly weathered and possibly an erratic. Unit H. -17: 23 x 12 cm dark reddish grey aphyric basalt, vesicular with 40 % vesicles up to 1 cm across and flow aligned. Unit I. -18: 13 x 7 cm Unit I.
04 DR Small seamount, NW Bridgeman Ridge	02.03.2001 on bottom: 11:30 h 771 m 62°03.73' S 056°57.97' W off bottom: 12:17 h 635 m 62°03.38' S 056°57.68' W	-1: 20 x 10 cm black plagioclase basalt, 20 % large plagioclase phenocrysts up to 6 mm across set in a glassy black matrix, glassy rind up to 2 mm thick at the rim (probably a pillow), large irregular vesicles up to 5 mm long. Unit A. -2: 20 x 9 cm Unit A. Definitely a pillow fragment with a glassy rind 7 mm thick. -3: 13 x 8 cm Unit A. -4: 22 x 11 cm Unit A. -5: 24 x 12 cm Unit A. -6: 21 x 10 cm black basalt, traces of black pyroxene and plagioclase phenocrysts, rarer traces of green olivine phenocrysts, total phenocrysts about 5 % and up to 1 mm across, dense fine grained pillow but not

Appendix 1

Station	Date / Time / Depth / Coordinates	Description
		<p>glassy. Unit B.</p> <p>-7: 16 x 5 cm Unit B. Glassy in outermost 2 mm of pillow.</p> <p>-8: 10 x 5 cm grey basalt, 5 % plagioclase phenocrysts up to 1 mm across, trace black pyroxene phenocrysts, dense with irregular vesicles along flow planes, probably central part of a pillow. Unit C.</p> <p>-9: 14 x 7 cm Unit C.</p> <p>-10: 7 x 4 cm Unit C. Glassy 1 cm wide rind on one side, definitely a pillow.</p> <p>-11: 11 x 6 cm Unit C, as for 10.</p> <p>-12: 7 x 4 cm Unit C, as for 10.</p> <p>-13: 17 x 9 cm reddish grey aphyric basalt, vesicular with 20 % vesicles up to 2 cm long, weakly weathered, probably a pillow core. Unit D.</p> <p>-14: 6 x 4 cm Unit D, but dark grey.</p>
07 GTV Crater, Hook Ridge		<p>-1: 11 x 6 cm fresh black aphyric dacite, trace plagioclase phenocrysts, a few flow aligned small vesicles, dense, sub-conchoidal fracture, appears to be interior of a pillow. Unit A.</p> <p>-2: 9 x 4 cm Unit A.</p> <p>-3: 7 x 5 cm Unit A.</p> <p>-4: 11 x 6 cm Unit A. Grey and vesiculated on both sides suggesting the sample is part of a 6 cm wide glassy flow band.</p>
09 MUC Crater, Hook Ridge		<p>-1: 9 x 4 cm fresh black aphyric dacite, glassy, fracture planes are flow aligned, sub-conchoidal fracture. Unit A.</p>
12 DR Southern side of summit, NE-SW ridge, Hook Ridge	<p>04.03.2001 on bottom: 01:03 h 1099 m 62°11.38' S 057°16.65' W off bottom: 01:44 h 1194 m 62°11.73' S 057°16.58' W</p>	<p>No rock samples, a small amount of sediment.</p>
13 DR Highest seamount, SW end of G Ridge	<p>04.03.2001 on bottom: 02:30 h 1100 m 62°06.76' S 056°30.69' W off bottom: 04:37 h 977 m 62°06.66' S 056°31.10' W</p>	<p>-1: 15 x 8 cm black andesite autobreccia, clasts are highly vesicular aphyric andesite, sub-rounded and up to 1 cm across (average 3 mm across), breccia is clast-supported with minor Fe-stained silica deposited in the matrix near the surface. Autobreccia of Unit A.</p> <p>-2: 15 x 8 cm black aphyric andesite, 20 % small irregular vesicles up to 1 cm long, lava autobrecciates along vesicle flow planes, minor Fe-stained silica in the matrix. Unit A.</p> <p>-3: 10 x 7 cm Unit A. Relatively dense with no autobrecciation, 30 % vesicles up to 5 mm across but most are <1 mm across.</p> <p>-4: 10 x 7 cm Unit A, as for 3.</p> <p>-5: 9 x 6 cm Unit A, as for 3.</p> <p>-6: 8 x 5 cm black aphyric andesite, 30 % vesicles up to 3 mm across and regular, probably a denser variant of Unit A.</p> <p>-7: 12 pieces of Unit A (as for 3), each about 7 x 4 cm, bulk sample.</p> <p>-8: 2 pieces (9 x 3 cm, 8 x 4 cm) of black fine grained autobreccia, consisting of Unit A clasts, up to 2.5 cm across but most are sand-sized (<1 mm), fresh.</p>

Appendix 1

Station	Date / Time / Depth / Coordinates	Description
		<p>-9: 13 x 5 cm dark reddish grey aphyric basalt, dense, 5 % irregular vesicles up to 2 mm across now filled by silica, well-rounded boulder and probably an erratic.</p> <p>-10: 17 x 9 cm blue-grey anorthosite, 40 % plagioclase laths up to 6 mm long showing multiple twinning and Schiller effect, matrix is fine grained 2 pyroxene (black and green), large well-rounded boulder and definitely an erratic.</p> <p>-11: 14 x 6 cm Unit A autobreccia (as for 1), but with 1-2 mm wide layers of Fe-stained silica near the surface.</p>
14 DR Second highest seamount, SW end of G Ridge	<p>04.03.2001 on bottom: 06:47 h 1330 m 62°04.16' S 056°23.71' W off bottom: 10:50 h 1023 m 62°04.15' S 056°24.91' W</p>	<p>-1: 11 x 6 cm black plagioclase-olivine basalt, 5 % plagioclase phenocrysts, 10 % green olivine phenocrysts (both up to 3 mm across), 30 % vesicles up to 2 mm across, dense and fresh. Unit A.</p> <p>-2: 8 x 5 cm Unit A.</p> <p>-3: 12 x 6 cm Unit A, with clay in some vesicles.</p> <p>-4: 9 x 5 cm Unit A, with clay in some vesicles.</p> <p>-5: 8 x 4 cm Unit A, with clay in some vesicles.</p> <p>-6: 8 x 4 cm black olivine basalt, 10 % green olivine phenocrysts up to 2 mm across, 20 % large vesicles up to 1 cm across, clay in some vesicles. Unit B.</p> <p>-7: 8 x 4 cm black olivine basalt, 20 % small green olivine phenocrysts up to 2 mm across (most <1 mm), 10 % small vesicles up to 3 mm across, sub-rounded dense boulder and possibly erratic. Unit C.</p> <p>-8: 14 x 8 cm pyroxene-plagioclase basalt, 5 % small plagioclase phenocrysts up to 1 mm across, 5 % black pyroxene phenocrysts up to 1 mm across, dense, weathered surface with orange clay, sub-rounded boulder, an erratic.</p> <p>-9: 13 x 4 cm reddish grey plagioclase andesite, 30 % plagioclase laths up to 4 mm long with trachytic flow aligned texture, weathered, sub-rounded boulder, an erratic- Erebus volcanics?</p>
15 DR Central seamount, centre of G Ridge	<p>04.03.2001 on bottom: 09:20 h 2068 m 62°02.43' S 056°19.24' W off bottom: 12:00 h 1600 m 62°02.46' S 056°19.99' W</p>	<p>-1: Very large complete pillow ~2 m in diameter, broken with hammers on the deck (most shipped to Freiberg in crate). Black olivine basalt, 5 % green olivine phenocrysts up to 1 mm across, 20 % vesicles up to 3 mm across, palagonised glassy rind 2 mm wide on surface of pillow. Unit A.</p> <p>-2: 16 x 4 cm Unit A, fresh pillow core only with no glass.</p> <p>-3: 17 x 7 cm Unit A, as for 2.</p> <p>-4: 20 x 8 cm Unit A, as for 2.</p> <p>-5: 11 x 6 cm Unit A, as for 2.</p> <p>-6: 16 x 11 cm Unit A. As for 1, but is a pillow fragment with palagonised glassy rind up to 2 mm thick on the surface.</p> <p>-7: 19 x 14 cm Unit A, as for 6.</p> <p>-8: 19 x 8 cm Unit A, as for 6.</p> <p>-9: 17 x 9 cm Unit A, as for 6.</p>
16 DR Lower NE flank of G Ridge	<p>04.03.2001 on bottom: 18:08 h 2250 m 62°00.01' S 056°13.73' W off bottom: 19:22 h 2000 m 62°00.09' S 056°14.56' W</p>	<p>-1: 8 x 5 cm black aphyric basalt, numerous small pull-apart structures, dense, fresh and angular with rough surface. Unit A.</p> <p>-2: 15 x 5 cm black aphyric basalt, 30 % small vesicles <1 mm across, fresh, darker glassier surfaces up to 2 mm wide, possibly a vesicular variant of Unit A. Unit B.</p> <p>-3: 9 x 5 cm Unit B.</p> <p>-4: 11 x 4 cm Unit B.</p>

Appendix 1

Station	Date / Time / Depth / Coordinates	Description
		<p>-5: 8 x 5 cm Unit B.</p> <p>-6: 8 x 5 cm Unit B, weakly weathered to grey and clay in some vesicles.</p> <p>-7: 11 x 7 cm Unit B, weathered along pull-apart structures and somewhat less vesicular, midway variant between Units A and B but these are almost certainly all the same lithology.</p> <p>-8: 9 x 5 cm Unit B, clay in some vesicles.</p> <p>-9: 16 x 7 cm Unit B, as for 7 but autobrecciating along one surface to small fragments.</p> <p>-10: 11 x 6 cm Unit B, as for 7 but more weathered.</p> <p>-11: 7 x 3 cm black plagioclase andesite, 5 % plagioclase phenocrysts up to 2 mm across set in a black glassy matrix, several flow planes, smooth upper and lower surfaces to clast, possibly an erratic. Unit C.</p> <p>-12: 8 x 5 cm black aphyric lava (basalt?), extremely fine grained, sub-rounded boulder, probably an erratic.</p>
<p>17 DR Lower NE end of G Ridge</p>	<p>04.03.2001 on bottom: 21:53 h 2430 m 61°58.34' S 056°09.87' W off bottom: 23:00 h 2234 m 61°58.54' S 056°11.79' W</p>	<p>-1: 10 x 4 cm black olivine basalt, 5 % green olivine phenocrysts up to 2 mm across, 5 % large vesicles up to 5 mm across, 10 % small vesicles <1 mm across, pillow fragment. Unit A.</p> <p>-2: 14 x 9 cm Unit A, with a 3 mm thick glassy rind on the pillow surface.</p> <p>-3: 11 x 4 cm Unit A.</p> <p>-4: 7 x 6 cm Unit A, with a 2 mm thick palagonised glassy pillow surface.</p> <p>-5: 11 x 8 cm Unit A, more weathered.</p> <p>-6: 10 x 5 cm black olivine basalt, as for 1 but extremely fresh and with a 3 mm thick glassy black rind on both the upper and lower surfaces, maybe Unit A but more likely a similar younger unit. Unit B.</p> <p>-7: 8 x 5 cm Unit B.</p> <p>-8: 19 x 12 cm Unit A, pillow fragment with well-developed 3 mm thick glassy rind.</p> <p>-9: 16 x 11 cm Unit A, pillow fragment with 2 mm thick glassy rind.</p> <p>-10: 23 x 11 cm Unit A, perfect pillow fragment with well-developed 3 mm thick glassy rind.</p> <p>-11: 27 x 7 cm Unit A, perfect pillow surface (only) with well-developed 3 mm thick glassy rind.</p>
<p>18 DR Seamount, NW end of Spanish Rise</p>	<p>04.03.2001 on bottom: 22:28 h 1542 m 61°52.97' S 055°58.96' W off bottom: 23:57 h ~1300 m 61°52.59' S 055°59.01' W</p>	<p>-1: 15 x 8 cm black olivine basalt, 5 % green olivine phenocrysts up to 3 mm across, 10 % flow aligned vesicles up to 1 cm long, probably a pillow core. Unit A.</p> <p>-2: 11 x 8 cm Unit A, palagonised glass on one surface, a pillow fragment.</p> <p>-3: 13 x 9 cm Unit A, as for 2.</p> <p>-4: 17 x 9 cm black olivine basalt, 10 % small green olivine phenocrysts up to 1 mm across, 10 % flow aligned vesicles up to 1.5 cm long, possibly a textural variant of Unit A. Unit B.</p> <p>-5: 17 x 8 cm Unit A.</p> <p>-6: 12 x 6 cm black olivine basalt, 20 % green olivine phenocrysts mostly about 1 mm across but some clusters (xenoliths) up to 5 mm across, 2 % flow aligned vesicles up to 5 mm across. Unit C.</p> <p>-7: 7 x 5 cm Unit C, with a 3 mm thick weathered palagonised glassier crust on one surface.</p> <p>-8: 17 x 6 cm Unit A, with a 3 mm thick glassier crust on one surface.</p>

Appendix 1

Station	Date / Time / Depth / Coordinates	Description
		<p>-9: 16 x 7 cm grey aphyric andesite, 5 % small vesicles <1 mm across, numerous flow planes spaced at 3 mm intervals, weathered to yellow clay along both surfaces for several cm, especially the upper surface which has pillow-type fractures, but otherwise fresh. Unit D.</p> <p>-10: 12 x 7 cm Unit A, with fresh interior but up to 1 cm of weathered yellow clay on the upper surface of the pillow.</p> <p>-11: 16 x 3 cm Unit A, as for 10 but only weakly weathered on the upper surface.</p> <p>-12: 14 x 6 cm brecciated black aphyric basalt, trace small plagioclase phenocrysts, matrix black and silicified, the few vesicles are infilled with silica, a 1 mm thick MnOx crust, probably an erratic.</p>
19 DR Seamount, Gibbs Deep	05.03.2001 on bottom: 03:57 h 2670 m 61°48.83' S 055°31.47' W off bottom: 05:00 h 2500 m 61°48.79' S 055°32.39' W	No recovered rocks and only a few small bites during the dredge; interpreted as thick sediment cover on old seamount.
20 DR Lower western flank, Gibbs Rise	05.03.2001 on bottom: 07:06 h 2809 m 61°48.32' S 055°28.56' W off bottom: 08:35 h 2200 m 61°48.96' S 055°28.58' W	<p>-1: 10 x 4 cm red aphyric basalt, 10 % vesicles up to 6 mm long and often filled with soft clay, rock is hematized and moderately weathered, possibly an erratic. Unit A.</p> <p>-2: 12 x 7 cm green-grey pyroxene-plagioclase andesite, 20 % plagioclase phenocrysts up to 2 mm across, 5 % black pyroxene phenocrysts up to 1 mm across, pyroxene altered to chlorite and locally pseudomorphed by pyrite, silicified matrix. Unit B.</p> <p>-3: 16 x 7 cm green-grey plagioclase-pyroxene andesite, as for Unit B but with 10 % plagioclase and 20 % pyroxene up to 2 mm across, and trace pyrite only. Unit C.</p> <p>-4: 14 x 5 cm Unit B, no pyrite.</p> <p>-5: 11 x 5 cm Unit B, but 5 % of the pyroxene is green (epidote?).</p> <p>-6: 10 x 4 cm Unit B, no pyrite.</p> <p>-7: 9 x 9 cm chloritized andesite, as for Unit B but the matrix is pervasively chloritized to dark apple green, disseminated pyrite, and one <1 mm wide chalcopyrite veinlet. Unit D.</p> <p>-8: 15 x 7 cm chloritized andesite, 30 % plagioclase phenocrysts up to 5 mm across in a dark green pervasively chloritized matrix, trace of dark grey pseudomorphed mafics (pyroxene?). Unit E.</p> <p>-9: 12 x 8 cm Unit E, but plagioclase only up to 3 mm across.</p> <p>-10: 12 x 6 cm Unit B, cut by 3 mm wide quartz vein with epidote halo, chloritized with disseminated fine grained pyrite.</p> <p>-11: 11 x 5 cm Unit E, with a >4 cm wide dark grey pervasively silicified zone.</p> <p>-12: 10 x 7 cm breccia, pervasively chloritized and silicified with abundant 1 mm thick quartz veinlets.</p> <p>-13: 9 x 3 cm breccia of altered andesite clasts, some hematized, some chloritized, typically 1.5 cm across.</p>

high. The observations and samples will be used to enlarge the understanding of benthic communities from the caldera of Deception Island.

11.8 References

- Bohrmann, G., Chin, C., Petersen, S., Sahling, H., Schwarz-Schampera, U., Greinert, J., Lammers, S., Rehder, G., Daehlmann, A., Wallmann, K., Dijkstra, S., and Schenke, H.-W., 1999, Hydrothermal activity at Hook Ridge in the Central Bransfield Basin, Antarctica: *Geo-Marine Letters*, v. 18, p. 277-284.
- Daehlmann, A., Wallmann, K., Sahling, H., Sarthou, G., Bohrmann, G., Petersen, S., Chin, C., and Klinkhammer, G., submitted, Hot vents in an ice-cold ocean: Indications for phase separation at the southernmost area of hydrothermal activity, Bransfield Strait, Antarctica: *Earth and Planetary Science Letters*.
- Dickson, A.G. (1993): pH buffers for sea water media based on the total hydrogen ion concentration scale, *Deep-Sea Research I*, 40, 107-118.
- Fahey, R.C. and Newton, G.L. (1987): Determination of low-molecular-weight thiols using monobromobimane fluorescent labeling and high-performance liquid chromatography. *Meth. Enzymol.* (Jakoby, W.B., Griffith, W.B., eds). Academic Press Inc. London, 143: 85-96.]
- Fisher, C.R., 1990, Chemoautotrophic and methanotrophic symbioses in marine invertebrates: *Reviews in Aquatic Sciences*, v. 2, p. 399-436.
- Gieskes, Garno, and Brumsack (1991): *Chemical Methods For Interstitial Water Analysis Aboard Joides Resolution*, Ocean Drilling Program Technical Note No. 15.
- Grasshoff, K., Ehrhardt, M., and Kremling, K. (1983): *Methods of Seawater Analysis*, VCH Weinheim.
- Ivanenkov, V.N., and Y.I. Lyakhin (1978): Determination of total alkalinity in seawater, In: O.K. Bordovsky and V.N. Ivanenkov (eds.): *Methods of hydrochemical investigations in the ocean*, Nauka Publ. House, Moscow, 110-114 (in Russian).
- Klinkhammer, G.P., Chin, C.S., Keller, R.A., Dählmann, A., Sahling, H., Sarthou, G., Petersen, S., Smith, F., and Wilson, C., submitted, Discovery of hydrothermal vent sites in Bransfield Strait, Antarctica: *Earth and Planetary Science Letters*.
- Muyzer et al. (*Appl. Environm. Microbiol.* 59, 695-700)
- Mullis, K.B. and F. Faloona (1987). Specific synthesis of DNA in vitro via a polymerase-catalysed chain reaction. *Methods Enzymol.* **155**:335-350
- Rey, J., Somoza, L., and Martinez-Frias, J., 1995, Tectonic, volcanic, and hydrothermal event sequence on Deception Island (Antarctica): *Geo-Marine Letters*, v. 15, p. 1-8.
- Sanger, F., Nicklen, S. and Coulson, A.R. (1977). DNA sequencing with chain-terminating inhibitors. *Proc. Natl. Acad. Sci. USA* **74**:5463-5467
- Sibuet, M., and Olu, K., 1998, Biogeography, biodiversity and fluid dependence of deep-sea cold-seep communities at active and passive margins: *Deep-Sea Research II*, v. 45, p. 517-567.
- Tunnicliffe, V., 1991, The biology of hydrothermal vents: ecology and evolution: *Oceanogr. Mar. Biol. Annu. Rev.*, v. 29, p. 319-407.
- Van Cappellen, P., Qiu, L., 1997, Biogenic silica dissolution in sediments of the Southern Ocean. I. Solubility: *Deep-Sea Research II*, v. 44 (5), p. 1109-1128.

12 XRF AND XRD ANALYSES

12.1 XRF

The XRF Spectrometer Philips PW 1480, equipped with a Rh-side-window tube to be operated at max. 100kV and 3kW, was calibrated for base metal ore samples. The program "ORE" included the following elements: Fe, Cu, Pb, Zn, S, Si, Al and uses straight line intensity vs concentration calibration. Program "TRACE" uses the element intensity ratioed against Rh-Compton radiation as a measure of concentration for the elements Pb, As, Se, Bi, Zn, Cu, Ni, Co, and Ba.

As one sample of massive barite plus sphalerite (06-GTVA-1) was recovered, Ba was included in the analytical program but due to a lack of high concentration standards the analyses were poor giving only 20% Ba with program "ORE" and 50% Ba with program "TRACE". Other elements detected are 0.8% Pb and 260 ppm Zn with all other trace elements below 30 ppm. For Cu, measured at 590 ppm, a special calibration on the $\text{CuK}\beta$ -line had to be made due to the overlap of the $\text{BaK}\alpha$ 4th order and the $\text{CuK}\alpha$ line. The absence of other main elements besides Ba and S was confirmed with scans over the whole wave length range of the spectrometer. From these scans the presence of some minor elements was detected and their content was estimated to about 1% Si, < 0.5% Al and Ca, < 0.3% Fe, Mn, K and Na and about 2% Sr.

Another sample of interest was a layer of coarse grained greenish gray material with fine white needles up to 1cm length in Core 11-SL, which was first described as pumice layer but was also questioned to be of biologic origin or to contain gypsum. The concentration measured with program "ORE", although not calibrated for that kind of material, were: 55% SiO_2 , 9% Al_2O_3 and 8% Fe_2O_3 with trace elements below the detection limit. The wavelength scan gave estimated concentrations of about 0.5% MnO, 1% TiO_2 , 7% CaO, 4% K_2O , 0.3% P_2O_5 , 2% MgO and 2% Na_2O as well as several hundred ppm of Zr and Sr and lesser Rb and Y concentrations. Thus it was proven that this material is of volcanic origin.

12.2 XRD

The Cu-Tube of the PW 1840 diffractometer was operated at 30 kV 40 mA. Samples were prepared as pressed powders in standard Philips sample holders. The only good spectrum obtained came from the barite sample 06-GTVA-1. It showed the distinct reflection pattern of barite and no other minerals were identified. Three sediment samples from 11-SL and 30-MUC as well as the pumice layer resulted only in a poor spectrum with no identifiable peaks and a constantly rising background. Although several attempts were made with different preparations and very long counting times, no spectra for identification could be obtained. The silicon standard delivered with the instrument and a quartz sample prepared in the same way as the other samples gave good spectra with expected peaks and intensities.

13 WHALE MONITORING

Name	Date	Time Period	Lat. [S] Long. [W]	N	Whale Type	Distance	Heading	Behavior	Comment
Mallon	01.03.01	21.45-21.48 Z	62°11.50 57°16.71	4	unidentified	300 m	090°	blowing to the surface, diving	good view
Löffler	03.03.01	08.35-08.45 Z	62°11.87 57°15.24	3	unidentified	0,2 nm	000°	blowing	good view
Löffler/ Stoffers	03.03.01	17.05-17.15 Z	62°11.62 57°16.58	1	Sei Whale	50 m	270°	blowing to the surface, diving	good view
Löffler/ Stoffers	04.03.01	08.34-08.35 Z	62°06.21 56°30.55	1	Humpback	0.1 nm	350°	blowing, jumping	restricted view
Bosselmann	04.03.01	08.42-08.50 Z	62°05.70 56.29.17	2	unidentified	0,2 nm	000°	blowing	restricted view
Sturm	04.03.01	11.11-11.17 Z	62°04.10 56°24.11	1	Humpback	0,2 nm	30°	blowing to the surface, diving	good view
Herzig	04.03.01	11.05-11.07 Z	62°04.08 56°25.11	2	unidentified	50 m	20°	blowing	good view
Löffler	04.03.01	16.33 Z	62°01.33 56°18.15	1	unidentified	1 nm	350°	blowing	good view
Wagner	04.03.01	17.02 Z	62°00.56 56.13.84	2	unidentified	700 m	340°	blowing	good view
Gudera/ Stoffers	05.03.01	06.45-06.50 Z	61°48.84 55°31.44	2	Humpback	30 m	90°	blowing to the surface, diving	snow flurry
Sturm	05.03.01	21.35-22.15 Z	61°45.55 55°24.63	2	Humpback	10-50 m	90°	blowing to the surface, diving	foggy, snow flurry
Mallon	06.03.01	09.05 Z	61°55.56 56°53.47	2	Humpback	1,5 nm	90°	blowing to the surface, diving	good view
Andresen	06.03.01	17.33 Z	62°00.73 55°51.30	1	Humpback	0,3 nm	270°	blowing to the surface, diving	good view
Sturm	10.03.01	21.15-21.25 Z	62°54 60°15	2	Humpback	50 fathon	90°	blowing to the surface, diving	very good view
Andresen	11.03.01	11.15 Z	62°47.49 60°11.19	2	Humpback	400 m	70°	blowing to the surface, diving	good view
Andresen	11.03.01	11.35 Z	62°48.67 60°20.74	8	Orka?	300-500 m	90°	blowing to the surface, diving	good view

Cruise Report SO-155 (HYDROARC)

Name	Date	Time Period	Lat. [S] Long. [W]	N	Whale Type	Distance	Heading	Behavior	Comment
Sturm	11.03.01	13.10-13.12 Z	62°53.37 61°03.05	1	Humpback	200 m	115°	blowing, diving	good view
Sturm	11.03.01	18:46 Z	62°15.49 62°37.37	2	unidentified	20 m	90°	blowing	good view
Mallon	15.03.01	14.07-14.53 Z	59°29.16 65°33.08	1	Sei Whale	30 m	different	circles the ship	good view

14 Stationlist

Abbreviations: DR = dredge, GTVA = TV-grab A, OFOS = deep-tow camera system, SL = gravity corer, MUC = multicorer, HBS = Hydro Bottom Station, BIO = land station for microbiology and petrology.

Coordinates (DGPS) given for TV grab, OFOS stations and HBS stations are instrument (sub)positions at first and last bottom contact. For dredges and sediment stations ship coordinates are given. Depths for OFOS stations are calculated from the pressure sensor for first and last bottom contact. Depth for TV-grab and HBS are the actual cable length at first and last bottom contacts. For dredge stations, the depth at first and last bottom contact is taken from the navigation echosounding system or Hydrosweep depth. The cable length at the sampling site is given as depth for multicorer and gravity corer.

station	area	location	depth	objectives	brief description
Hook Ridge					
01-OFOS	Hook Ridge crater	62°11.0158' S 57°16.9302' W to 62°12.8939' S 57°15.9185' W	1296 m to 1531 m	relocate hydrothermal activity and massive sulfides in the crater of Hook Ridge and in the "hinge" area	3 parallel lines in the crater area identified hydrothermal activity; OFOS moved to the "hinge" area; OFOS in "hinge" area never reached target point due to the presence of an iceberg right above the target
02-DR	SW flank of "G"	62°07.34' S 57°01.00' W to 62°07.07' S 57°00.10' W	1377 m to 1200 m	sample volcanic rocks at middle part of edifice "G"	10 kg of volcanic rocks, mainly vesicular dacites, glassy with numerous fractures; dropstones are granitoids, schists and gabbros
03-DR	SW flank of "G"	62°07.32' S 56°53.93' W to 62°06.62' S 56°52.64' W	640 m to 450 ? m	sample volcanic rocks at upper part of edifice "G"	250 kg of volcanic rocks, comprising andesites with glassy matrix as well as vesicular olivine basalts; granitoid dropstones
04-DR	Volc. cone NW of "G"	62°03.73' S 56°57.97' W to 62°03.38' S 56°57.68' W	770 m to 635 m	sample volcanic rocks	2000 kg of volcanic rocks; three types of volcanics: dacites or andesites with glassy sections, vesicular, porphyric andesites and strongly vesicular andesites; rounded volcanic dropstones
05-GTVA	Hook Ridge crater	62°11.56' S 57°16.65' W to 62°12.518' S 57°15.642' W	(1050 m)	sample hydrothermal precipitates at southern wall of the crater	200 kg of greyish-green fine-grained sediment

Cruise Report SO-155 (HYDROARC)

station	area	location	depth	objectives	brief description
06-GTVA	Hook Ridge crater	62°11.540' S 57°16.605' W to 62°11.55'S 57°16.623'W	(1050 m)	sample hydrothermal precipitates at southern wall of the crater	100 kg of sediment containing 1 piece (2 kg) of massive barite with minor sphalerite. Few cm-sized siliceous crusts
07-GTVA	Hook Ridge crater	62°11.514' S 57°16.656' W to 62°11.544'S 57°16.588'W	(1050 m)	sample hydrothermal spires on top of terrace at southern wall of the crater	one large block (60 kg) of autobrecciated basalt with silica and clay lining fractures; plus 50 kg sediment (13.6 °C)
08-GTVA	Hook Ridge crater	62°11.56 S 57°16.58 W	1054 m	sample barite chimneys at southern wall of Hook Ridge	no samples
0-MUC	Hook Ridge crater	62°11.51 S 57°16.61 W	(1050 m)	sample hot sediment in crater of Hook Ridge	problems with the rope; second deployment and sampling of 10 cm muddy sediment with a single dacitic rock in one of the liner
10-MUC	Hook Ridge crater	62°11.52 S 57°16.63 W	1072 m	sample hot sediment in crater of Hook Ridge	hydrothermally influenced sediment in one core liner
11-SL	Hook Ridge crater	62°11.54 S 57°16.62 W	1059 m	sample hydrothermal sediment	4 m of hydrothermally influenced sediment; temperatures: T0=22.3 °C at bottom of the core; T1=18.0°C, 1-2 m; T2=13.9°C, 2-3 m; T3=9.7°C, 3-4 m; T4=5.0°C, 4-5 m
12-DR	Hook Ridge crater	62°11.38 S 57°16.65 W to 62°11.68 S 57°16.02 W	1194 m	sample hydrothermal precipitates	no samples
13-DR	Edifice "G" propagator	62°06.76 S 56°30.69 W to 62°06.66 S 56°31.10 W	977 m	sample highest seamount to the SE of Bridgeman Ridge	black aphyric andesites and additional dropstones
14-DR	Edifice "G" propagator	62°04.16 S 56°23.72 W to 62°04.15 S 56°24.91 W	1023 m	sample second peak of Bridgeman Ridge	black plagioclase-olivine basalt plus dropstones
Eastern Bransfield Basin					
15-DR	Edifice "G" propagator	62°02.43 S 56°19.24 W to 62°02.46 S 56°19.99 W	2068 m to 1600 m	sample central Bridgeman Ridge	large complete pillow (1m) plus other olivine pillow basalts
16-DR	Bridgeman Ridge	62°00.01 S 56°13.73 W to 62°00.09 S 56°14.56 W	2250 m to 2000 m	sample northeast lower flank of Bridgeman Ridge	aphyric basalt and plagioclase andesite plus dropstones

Cruise Report SO-155 (HYDROARC)

station	area	location	depth	objectives	brief description
17-DR	Bridgeman Ridge	61°58.34 S 56°09.87 W to 61°58.54 S 56°11.79 W	2430 m to 2234 m	sample northeast end of Bridgeman Ridge	olivine basalt plus pillow fragments with glassy rims
18-DR	Spanish Ridge	61°52.97 S 55°58.96 W to 61°52.59 S 55°59.01 W	1540 m to 1300 m	sample northern seamount on Spanish Ridge	olivine basalt, some with thick glassy rims plus dropstones
19-DR	Gibbs Deep	61°48.83 S 55°31.47 W to 61°48.79 S 55°32.39 W	2670 m to 2500 m	sample seamount in Gibbs Deep	no samples
20-DR	Gibbs Deep	61°48.32 S 55°28.56 W to 61°48.96 S 55°28.58 W	2800 m to 2200 m	sample lower northwestern flank of Gibbs Seamount	red vesicular aphyric basalt, breccias of altered andesite plus abundant erratics
21-DR	Gibbs Deep	61°49.68 S 55°28.44 W to 61°50.13 S 55°28.37 W	1560 m to 1400 m	sample middle northwestern flank of Gibbs Seamount	plagioclase andesite, dolerite
22-DR	Gibbs Deep	61°50.47 S 55°26.48 W to 61°50.48 S 55°25.77 W	950 m to 860 m	sample upper northwestern flank of Gibbs Seamount	only dropstones (e.g. granodiorite and dolerite)
23-DR	Trough 3-4	61°45.93 S 55°25.32 W to 61°45.57 S 55°24.58 W	2600 m to 2200 m	sample northwestern scarp of Trough 3-4 rise	fine-grained dolerite, plagioclase andesite
24-DR	Gibbs Deep	61°49.24 S 55°33.65 W to 61°48.80 S 55°32.36 W	2700 m to 2500 m	sample seamount in Gibbs Deep	volcaniclastic sandstone, plus dropstones
25-DR	Spanish Ridge	61°53.67 S 55°49.30 W to 61°53.20 S 55°48.47 W	2170 m to 2100 m	sample seamount NE of Spanish Ridge	200 kg of olivine basalts and few dropstones
26-DR	Spanish Ridge	61°55.90 S 55°52.99 W to 61°55.26 S 55°53.67 W	1900 m to 1650 m	sample northern flanking seamount of Spanish Ridge	olivine basalt
27-DR	Spanish Ridge	61°57.80 S 55°52.29 W to 61°57.30 S 55°52.15 W	2000 m to 1600 m	sample seamount in axial deep of Spanish Ridge	plagioclase-phyric basalt
28-DR	Spanish Ridge	61°59.12 S 55°54.15 W to 61°59.44 S 55°53.53 W	2000 m to 1700 m	sample seamount on SW flank of axial deep of Spanish Ridge	olivine basalts, some of them with thick glassy crusts

Cruise Report SO-155 (HYDROARC)

station	area	location	depth	objectives	brief description
29 ICE	Spanish Ridge		0 m	sample ice from nearby drift iceberg for environmental studies	15 kg ice
Hook Ridge					
30 MUC	Hook Ridge crater	62°11.54 S 57°16.65 W	1049 m	sample hydrother-mally influenced sediment	half core liners; siliceous Fe-oxyhydroxide crusts with Mn-staining on top of sediment; Tmax = -0.2°C
31 MUC	Hook Ridge crater	62°11.52 S 57°16.65 W	1045 m	sample hydrother-mally influenced sediment	full core liners; Tmax = 1.4°C
32 MUC	Hook Ridge crater	62°11.54 S 57°16.66 W	1042 m	sample hydrother-mally influenced sediment	half core liners; Tmax = 3.8°C, H2S smell; few Fe-oxyhydroxide crusts
33 MUC	Hook Ridge crater	62°11.54 S 57°16.68 W	1043 m	sample hydrother-mally influenced sediment	half core liners; Tmax = 4.5°C, H2S smell; few Fe-oxyhydroxide crusts
34 MUC	Hook Ridge crater	62°11.57 S 57°16.74 W	1047 m	sample hydrother-mally influenced sediment	8 cores filled, no temperature anomaly, Tmax – 1.6°C
35 MUC	Hook Ridge	62°11.56 S 57°16.70 W	1053 m	sample hydrothermal vent sediments	cores empty, MUC tipped over
36 MUC	Hook Ridge	62°11.52 S 57°16.70 W	1038 m	hydrothermal vent sediments; sample target a bit north of former ones	not released
37 SL	Hook Ridge	62°11.54 S 57°16.65 W	1040 m	hydrothermally altered sediments in crater area of Hook Ridge	256 cm sediment core; ~ 0.5 m 16.5°C; ~1.5 m 36.6°C; ~2.5 m 35.1°C
38-DR	Hook Ridge	62°11.38 S 57°14.66 W to 62°10.11 S 57°14.12 W	1390 m to 1280 m	sample hydro-thermal material from Twin Peak area	200 kg of fresh, glassy, dense dacite
39-DR	Hook Ridge crater	62°11.43 S 57°16.59 W to 62°11.63 S 57°16.65 W	1064 m	sample hydro-thermal material from southern crater rim	plagioclase-bearing dacite and light grey clay with native sulfur lining cavities
40-DR	Hook Ridge crater	62°11.42 S 57°16.62 W to 62°11.66 S 57°16.69 W	1063 m	sample hydro-thermal material from southern crater rim	coarse ash layer, aphyric dacite

Cruise Report SO-155 (HYDROARC)

station	area	location	depth	objectives	brief description
Viehoff Seamount					
41-OFOS	Viehoff Seamount	62°26.65 S 58°24.87 W to 62°25.94 S 58°24.37 W	918 m to 1050 m	survey wall and crater floor of VS on two subprofiles	steep scarps at northern wall; thick sediment on crater floor, Viehoff Seamount shows no signs of hydrothermal activity (750 slides)
Deception Island					
42-SL	Deception Island	62°57.76 S 60°38.04 W	153 m	sample hydrothermally altered sediment in the crater	ca. 15 cm sediment (dark, muddy)
43-SL	Deception Island	62°57.70 S 60°38.11 W	153 m	sample hydrothermally altered sediment in the crater	5 cm sediment and one small rock piece
44-SL	Deception Island	62°57.78 S 60°38.17 W	154 m	sample hydrothermally altered sediment in the crater; Shorter core (~3,5 m)	no sediment
45-OFOS	Deception Island	62°58.98 S 60°38.08 W to 62°58.88 S 60°37.18 W	91 m to 120 m	survey area of Mn-anomalies in SE part of the crater	thick sedimented seafloor with no sign of hydrothermal activity or Mn-precipitates
46-OFOS	Deception Island	62°58.01 S 60°39.06 W to 62°57.40 S 60°38.97 W	120 m to 170 m	survey central part of the crater in area of assumed fault systems	thick sediment at crater floor; seafloor in this area is extremely flat with a water depth of 170 m; small undulations at the seafloor
47-HBS	Deception Island	62°57.70 S 60°40.30 W to 62°57.39 S 60°38.71 W	160 m to 170 m	survey central part of crater for hydrothermal activity	no visual signs of hydrothermal activity detected; only one small T anomaly (0.2°C); sediment consists of a thin muddy layer underlain by a black Mn-rich diatomaceous layer throughout the basin
48-MUC	Deception Island	62°57.45 S 60°38.63 W	162 m	sample T-anomaly observed during HBS station	6 core lines filled with up to ~25 cm sediment
49-MUC	Deception Island	62°57.38 S 60°38.72 W	159 m	sample hydrothermal influenced sediment in Deception Caldera	4 core lines ~30 cm, no temperature anomaly
50-MUC	Deception Island	62°57.69 S 60°39.12 W	163 m	sample hydrothermal influenced sediments in Deception Caldera	7 core lines; ~ 40 cm sediment filling (line A empty); T~0.3°C
51-HBS	Deception Island	62°58.16 S 60°41.97 W to 62°58.09 S 60°41.97 W	69 m to ??	locate temperature anomalies on the bottom of Deception Island Caldera	located area with bigger white patches (MUC-target?); no temperature anomalies

Appendix 1

Station	Date / Time / Depth / Coordinates	Description
		<p>-14: 15 x 8 cm light green breccia of pervasively chloritised andesite clasts up to 2 cm across set in a sand-sized chloritic matrix, possibly an altered pyroclastic unit.</p> <p>-15: 22 x 3 cm grey biotite schist, laminae are biotite (mica) and plagioclase-quartz, all <1 mm thick, with isoclinal folds seen in cross-section. Probably an erratic.</p> <p>-16: 11 x 3 cm grey phyllite, with 2-3 mm thick quartz-rich layers, no obvious folding, very fine grained. Probably an erratic.</p> <p>-17: 9 x 4 cm grey phyllite, as for 16 but quartz-rich layers up to 5 mm thick. Probably an erratic.</p> <p>-18: 10 x 3 cm grey metasandstone, sand-sized well-rounded grains of quartz, plagioclase, and chloritised rock fragments. Probably an erratic.</p>
<p>21 DR Middle western flank, Gibbs Rise</p>	<p>05.03.2001 on bottom: 13:39 h 1560 m 61°49.68' S 055°28.44' W off bottom: 14:33 h 1400 m 61°50.13' S 055°28.37' W</p>	<p>-1: 7 x 6 cm grey plagioclase andesite, 5 % small black partly chloritised pyroxene phenocrysts, 10 % plagioclase phenocrysts up to 2 mm across, least altered rock from 21 DR (hydrothermal log 1a). Unit A.</p> <p>-2: 20 x 15 cm reddish grey dolerite, 5 % small black pyroxenes, 5 % plagioclase laths up to 3 mm long, dense and very hard, hematized with small red spots that resemble (but aren't) garnet (hydrothermal log 1c and 2d). Unit B.</p> <p>-3: 19 x 11 cm Unit A (hydrothermal log 3a).</p> <p>-4: 11 x 6 cm green altered andesite, 30 % plagioclase up to 3 mm across set in a green pervasively chloritised matrix (hydrothermal log 4b). Unit C.</p> <p>-5: 19 x 11 cm chloritised andesite, 30 % plagioclase up to 2 mm across, 10 % dark chlorite (after pyroxene?), green chloritic matrix, numerous hematized xenoliths up to 3 cm across (hydrothermal log 5a). Unit D.</p> <p>-6: 10 x 7 cm pervasively chloritised andesite with no relic phenocrysts (hydrothermal log 7a). Unit E.</p> <p>-7: 11 x 8 cm Unit D, more chloritised and xenoliths <3 mm across (hydrothermal log 7b).</p> <p>-8: 18 x 8 cm pervasively chloritised andesite, no relic phenocrysts but relic patches of epidotised lava with brown K-spar overprint up to 4 cm across and disseminated pyrite (hydrothermal log 8a). Unit F.</p> <p>-9: 10 x 6 cm Unit E, but more chloritised and with quartz blobs up to 4 mm across (hydrothermal log 9).</p> <p>-10: 10 x 10 cm chloritised wacke, with well-rounded sand-sized quartz grains, silicified matrix, and a few <1 mm thick quartz veinlets (hydrothermal log 10a). Unit G.</p> <p>-11: 16 x 5 cm Unit D, pervasively chloritised matrix with pervasively hematized xenoliths (hydrothermal log 11).</p> <p>-12: 21 x 6 cm Unit G, but finer grained and really a silty wacke (hydrothermal log 13).</p> <p>-13: 15 x 4 cm Unit C, pervasively chloritised and possibly the protolith had only 20 % plagioclase phenocrysts (hydrothermal log 15).</p>
<p>22 DR Upper western flank, Gibbs Rise</p>	<p>05.03.2001 on bottom: 16:37 h 950 m 61°50.47' S</p>	<p>-1: 15 x 9 cm granodiorite, with quartz, plagioclase and hornblende up to 2 mm across, outermost 4 cm is weathered. An erratic.</p> <p>-2: 30 x 15 cm dolerite, with plagioclase, green and</p>

Appendix 1

Station	Date / Time / Depth / Coordinates	Description
	055°26.48' W off bottom: 17:47 h 860 m 61°50.48' S 055°25.77' W	black pyroxene up to 1 mm across. An erratic . -3: 17 x 8 cm black dolerite (?), very fine grained (<<1 mm), with plagioclase and maybe olivine (epidote?), cut by a few <1 mm quartz veinlets, well-rounded. An erratic . -4: 18 x 8 cm black olivine-plagioclase basalt, 5 % green olivine and 5 % plagioclase up to 2 mm across, 10 % vesicles up to 3 mm across, well-rounded. An erratic . -5: 15 x 6 cm breccia, chloritised, epidotised and hematized clasts up to 1 cm long in a pinkish silicified matrix, well-rounded. An erratic . -6: 12 x 6 cm black dolerite (?), very fine grained with plagioclase to 1 mm across, chlorite infilling vesicles or pseudomorphing pyroxene (or both). An erratic . -7: 9 x 5 cm black olivine-plagioclase basalt, 5 % green olivine phenocrysts and 10 % plagioclase phenocrysts up to 2 mm across, dense lava with one lighter grey surface that includes a glassier crust 1 mm thick. Probably an erratic . -8: 12 x 8 cm black metadolerite, very fine grained (<<1 mm) with numerous quartz veinlets and eyes up to 1 mm wide. An erratic . -9: 10 x 6 cm pinkish blue trachyte, 5 % K-spar phenocrysts up to 3 mm across set in a fine grained altered matrix. An erratic . -10: 9 x 5 cm gabbro, well-rounded. An erratic .
23 DR Centre of axial deep, Gibbs Rise	05.03.2001 on bottom: 20:22 h 2600 m 61°45.93' S 055°25.32' W off bottom: 21:52 h 2200 m 61°45.57' S 055°24.58' W	-1: 12 x 5 cm grey fine grained dolerite, plagioclase up to 1 mm across, black pyroxene, disseminated pyrite, hard, disrupted quartz vein 3 mm wide. Possibly an erratic. Unit A . -2: 11 x 6 cm black plagioclase andesite, 20 % large plagioclase phenocrysts up to 3 mm across, trace green olivine phenocrysts up to 2 mm across, 10 % vesicles up to 2 mm across, weathered with clay in some vesicles. Unit B . -3: 9 x 5 cm Unit B . -4: 13 x 6 cm Unit B , but a denser variant with only a few vesicles and nearly fresh. -5: 11 x 7 cm Unit B , with a fresh core and weathered exterior, and an increase to 30 % plagioclase phenocrysts. -6: 15 x 7 cm Unit B . -7: 16 x 8 cm Unit B . -8: 15 x 8 cm Unit B . -9: 16 x 10 cm Unit B . -10: 8 x 6 cm Unit B , denser non-vesicular variant with numerous flow planes and an increase to 30 % plagioclase phenocrysts. -11: 7 x 3 cm Unit B , as for 10 but a further increase to 40 % plagioclase phenocrysts. -12: 11 x 4 cm black plagioclase dacite, 10 % plagioclase phenocrysts up to 2 mm across, flow banded into light grey devitrified and black glassy layers 3-5 mm thick, and with a glassy pillow crust. Unit C . -13: 11 x 6 cm altered andesite, 20 % plagioclase phenocrysts up to 2 mm across, 5 % small black pyroxene phenocrysts altered to chlorite, locally epidote after pyroxene, numerous <1 mm wide quartz veinlets. Unit D .

Appendix 1

Station	Date / Time / Depth / Coordinates	Description
24 DR Seamount, Gibbs Deep	05.03.2001 on bottom: 21:13 h 2715 m 61°49.24' S 055°33.65' W off bottom: 22:44 h 2500 m 61°48.80' S 055°32.36' W	-1: 11 x 6 cm brown volcanoclastic sandstone-siltstone, moderately indurated, massive, with well-rounded weathered black lava grains and quartz/plagioclase grains. Unit A. -2: 6 x 4 cm vesicular aphyric dacite, pumiceous with 20 % vesicles up to 5 mm across, weathered brown-black surfaces, waterlogged. Probably an erratic. -3: 7 x 3 cm light grey plagioclase dacite, flow banded with grey vesicular and darker glassier bands 1-2 mm wide, pumiceous, trace plagioclase phenocrysts up to 2 mm across, weathered. Probably an erratic. -4: 21 x 5 cm diorite, interlocking plagioclase and hornblende crystals up to 2 mm across, with an 8 cm long fine grained mafic enclave. An erratic. -5: 11 x 1 cm biotite schist, alternating micaceous and quartz-plagioclase laminae 1 mm wide. An erratic. -6: 10 x 5 cm biotite schist, intruded by deformed white quartz veins up to 5 mm wide. An erratic. -7: 12 x 5 cm red sandstone, well-rounded. An erratic. -8: 9 x 4 cm dark grey siltstone. An erratic. -9: 8 x 3 cm greenish grey metawacke, quartz-rich. An erratic. -10: 7 x 4 cm greenish grey chloritised and silicified breccia with a few relic clasts 2-3 mm across. An erratic.
25 DR Seamount on NE flank, Spanish Rise	06.03.2001 on bottom: 01:50 h 2160 m 61°53.67' S 055°49.30' W off bottom: 03:00 h 2100 m 61°53.20' S 055°48.47' W	-1: 16 x 8 cm weathered black olivine basalt, 5 % green olivine phenocrysts up to 1 mm across, 10 % vesicles up to 3 mm across, a pillow fragment with a very weathered rim. Unit A. -2: 15 x 8 cm Unit A , somewhat less weathered. -3: 9 x 4 cm black basalt, trace olivine phenocrysts up to 2 mm across, 10 % vesicles up to 3 mm across, a pillow fragment, green epidotised rim but interior is fresh. Unit B. -4: 7 x 4 cm black aphyric basalt, 20 % vesicles up to 3 mm across, glassy rim on one surface. Unit C. -5: 8 x 3 cm Unit C. -6: 9 x 4 cm black dense aphyric basalt, weathered surface. Unit D. -7: 9 x 4 cm altered andesite, 10 % plagioclase phenocrysts, matrix silicified. Probably an erratic. -8: 8 x 4 cm chloritised olivine dolerite, well-rounded. An erratic. -9: 8 x 4 cm Unit D. -10: 12 x 4 cm metadolerite, with 1 mm wide hematitic patches and 1 mm wide quartz veinlet, well-rounded. An erratic. -11: 17 x 6 cm fine grained dolerite, well-rounded. An erratic.
26 DR Seamount, northern flank of axial deep, Spanish Rise	06.03.2001 on bottom: 05:46 h 1902 m 61°55.90' S 055°52.99' W off bottom: 06:58 h 1640 m 61°55.26' S 055°53.67' W	-1: 6 x 6 cm black basalt, fine grained with trace plagioclase phenocrysts up to 1 mm across, several <1 mm thick quartz veinlets, otherwise fresh in appearance. Unit A. -2: 10 x 3 cm black olivine basalt, 5 % green olivine phenocrysts up to 3 mm across, 20 % flow aligned vesicles to 5 mm across, weathered on one surface. Unit B. -3: 6 x 4 cm Unit B. -4: 4 x 2 cm Unit B. -5: 10 x 3 cm black plagioclase andesite, 10 %

Appendix 1

Station	Date / Time / Depth / Coordinates	Description
		<p>plagioclase phenocrysts up to 2 mm across, weathered 1 mm thick surface layer but fresh in interior. Unit C.</p> <p>-6: 18 x 5 cm weathered volcanoclastic, sand-sized clay and weathered rock fragments, poorly consolidated, 1 mm thick MnOx crust, probably a weathered hyaloclastite. Unit D.</p> <p>-7: 10 x 4 cm weathered volcanoclastic, most grains are finer than Unit D and silt to clay sized.</p> <p>-8: 13 x 5 cm breccia, clasts of fresh aphyric basalt, vesicular basalt and plagioclase basalt to 1.5 cm across, angular, and set in a sand-silt volcanoclastic matrix.</p> <p>-9: 4 x 3 cm weathered pumice, waterlogged. An erratic. Also a wide variety of erratics (95 % of half full dredge) consisting of: 50 % micaceous schists (biotite-bearing) with quartz veining that is often deformed or cross-cutting, and the remainder being a mix of diorites and gabbros, very fine grained chloritised dolerites, chloritised and hematised volcanics and breccias, silicified volcanics and breccias, and wacke and argillite.</p>
27 DR Seamount in axial deep, Spanish Rise	06.03.2001 on bottom: 12:00 h 2000 m 61°57.80' S 055°52.29' W off bottom: 13:30 h 1600 m 61°57.30' S 055°52.15' W	<p>-1: 12 x 8 cm black plagioclase basalt, 5 % small plagioclase phenocrysts up to 1 mm across, 20 % vesicles up to 3 mm across, mostly the dense central part of a pillow but with a 5 mm wide autobrecciating pillow surface on one side, fresh. Unit A.</p> <p>-2: 13 x 8 cm Unit A.</p> <p>-3: 15 x 4 cm Unit A.</p> <p>-4: 13 x 4 cm Unit A.</p> <p>-5: Four pieces of Unit A, each about 7 x 3 cm, as a bulk sample.</p>
28 DR Seamount, SW flank of axial deep, Spanish Rise	06.03.2001 on bottom: 15:17 h 2000 m 61°59.12' S 055°54.15' W off bottom: 16:47 h 1700 m 61°59.44' S 055°53.53' W	<p>-1: 11 x 6 cm black olivine basalt, 5 % green olivine phenocrysts up to 2 mm across, 20 % vesicles up to 7 mm across, outer 5 mm is weathered but interior is fresh. Unit A.</p> <p>-2: 10 x 7 cm Unit A.</p> <p>-3: 16 x 8 cm Unit A, a large pillow fragment with well-developed 3 mm thick glassy autobrecciating pillow surface.</p> <p>-4: 12 x 6 cm Unit A, as for 3.</p> <p>-5: 16 x 6 cm Unit A, as for 3.</p> <p>-6: 14 x 10 cm Unit A, as for 3.</p> <p>-7: 13 x 6 cm Unit A, as for 3.</p> <p>-8: 11 x 9 cm Unit A, as for 3.</p> <p>-9: 15 x 8 cm Unit A, as for 3.</p> <p>-10: 11 x 7 cm black dolerite, very fine grained fresh plagioclase-pyroxene dolerite, hard, flat on one surface but otherwise angular. Possibly an erratic. Unit B.</p>
38 DR Inner southern flank of NE-SW ridge, Hook Ridge	07.03.2001 on bottom: 09:50 h 1390 m 62°11.38' S 057°14.66' W off bottom: 13:43 h 1280 m 62°10.47' S 057°14.16' W	<p>-1: 13 x 6 cm black aphyric dacite, trace plagioclase phenocrysts up to 1 mm across, dense, extremely fresh (no weathering on any surfaces or fractures), glassy with sub-conchoidal fracture, a few vesicles along flow joints but otherwise none. Unit A.</p> <p>-2: 15 x 8 cm Unit A, grading to denser and greyer on one surface.</p> <p>-3: 15 x 6 cm Unit A.</p> <p>-4: 16 x 10 cm Unit A, weakly flow banded with 'woody' texture developing on uppermost surface.</p> <p>-5: 10 x 8 cm Unit A, as for 4.</p>

Appendix 1

Station	Date / Time / Depth / Coordinates	Description
		<p>-6: 10 x 6 cm Unit A, as for 4 and with small patch of <1 mm thick Fe-stained silica on one surface.</p> <p>-7: 7 x 4 cm blue-grey andesite, very fine grained and appears aphyric, 10 % vesicles to 3 mm across. Probably an erratic.</p>
39 DR Southern side of summit, NE-SW ridge, Hook Ridge	<p>07.03.2001 on bottom: 12:33 h 1074 m 62°11.43' S 057°16.60' W off bottom: 14:09 h 1070 m 62°11.43' S 057°16.58' W</p>	<p>-1: 8 x 5 cm black plagioclase dacite, 10 % plagioclase phenocrysts up to 2 mm across, 20 % vesicles up to 5 mm across, almost pumiceous and light weight with minor Fe-silica staining in patches on the surface, some faint internal colour changes suggest minor leaching by hot water. Unit A.</p> <p>Numerous pieces of light grey clay, some with well-developed sulfur crystals. Whole dredge has strong smell of sulfur. This material was sampled only by Freiberg.</p>
40 DR Southern side of summit, NE-SW ridge, Hook Ridge	<p>07.03.2001 on bottom: 15:11 h 1063 m 62°11.42' S 057°16.62' W off bottom: 15:40 h 1063 m 62°11.66' S 057°16.69' W</p>	<p>-1: 11 x 4 cm very dark green coarse ash layer with glass shards banded colourless to dark green, most about 2 mm long, some have perfect bubble walls and others are still welded into fragments of black aphyric dacite.</p> <p>-2: 8 x 4 cm black aphyric dacite, fresh and dense with traces of very small vesicles, glassy, unweathered surface. Unit A.</p> <p>-3: 9 x 5 cm dark grey aphyric dacite, 20 % small vesicles up to 2 mm across, fresh, probably a vesicular and less dense variant of Unit A. Unit B.</p> <p>-4: 13 x 9 cm Unit B.</p> <p>-5: Bulk sample of 5 small pieces of Unit A, each about 8 x 5 mm.</p>
52 BIO Beach at Fumarole Bay, Deception Island	<p>10.03.2001 on shore: 13:30 h 60°41.28' S 062°58.05' W off shore: 15:30 h 60°41.28' S 062°58.05' W</p>	<p>-1: 10 x 4 cm black aphyric basalt, 40 % vesicles up to 1 cm across (most 3mm), scoria from 1967-70 eruptions. Unit A.</p> <p>-2: 8 x 3 cm grey Unit A, but denser with 15 % vesicles to 3 mm across.</p> <p>-3: 10 x 3 cm Unit A, but vesicles mostly <1 mm across.</p> <p>-4: 4 x 3 cm Unit A, but vesicles mostly 1 mm across.</p> <p>-5: Bulk sample of 3 Unit A pieces (6 x 2 cm, 6 x 2 cm, 8 x 3 cm), with vesicles generally less regular and <1 mm across, and possibly these represent the second to last eruption in the sample area.</p> <p>-6: 7 x 4 cm red scoriaceous aphyric basalt, 20 % vesicles in 2 generations (1 mm and <1 mm across), several small (<5 mm across) plagioclase-hornblende xenoliths. Unit B.</p> <p>-7: 7 x 3 cm Unit B, but dark red with black streaks and denser.</p> <p>-8: 11 x 6 cm Unit B, but pumiceous and rather weathered.</p> <p>-9: Bulk sample of 7 small (<5 x 2 cm) Unit B pieces, as for 6.</p> <p>-10: 15 x 10 cm grey aphyric andesite, dense lava flow with numerous flow planes at 2 mm intervals, clearly rolled downslope to sample area and represents an old lava. Unit C.</p> <p>-11: 27 x 4 cm blue-grey plagioclase andesite, 10 % small plagioclase phenocrysts up to 1 mm across, dense and non-vesicular, part of a jointed lava flow, clearly rolled downslope to sample area and represents an old lava. Unit D.</p> <p>-12: 9 x 4 cm black aphyric andesite, dense sub-rounded boulder from an old lava flow, probably rolled a long</p>

Appendix 1

Station	Date / Time / Depth / Coordinates	Description
		<p>distance up the coast. Unit E.</p> <p>-13: 7 x 3 cm flow banded red and black aphyric andesite, flow bands are irregularly spaced and discontinuous, dense. Unit F.</p> <p>-14: 11 x 5 cm Unit C, but weathered to yellow-orange clay along its surfaces.</p> <p>-15: 9 x 2 cm blue-grey aphyric andesite, sub-rounded thin plate from a lava flow and probably rolled some distance up the coast. Unit G.</p> <p>-16: 9 x 1 cm Unit G.</p> <p>-17: 12 x 4 cm breccia, polymict with red, black and grey aphyric sub-rounded clasts set in a yellow-grey silty clay matrix, weakly weathered, probably represents the fine part of a thin surge deposit or a debris flow. Unit H.</p> <p>-18: 10 x 5 cm Unit H, but well consolidated and with a greenish matrix, the boulder is sub-rounded.</p> <p>-19: 15 x 3 cm Unit H, but well consolidated and the boulder is sub-rounded.</p> <p>-20: 6 x 3 cm Unit H, with a more weathered yellow matrix.</p> <p>-21: 18 x 5 cm breccia, polymict with rounded clasts of grey, red and black aphyric, plagioclase-bearing and olivine-bearing basalt/andesite, each up to 2 cm but most about 6 mm across, set in a yellow-orange palagonised clay matrix that includes some quartz veinlets, open void space in matrix is about 5 % but the boulder is clay-cemented, probably a pyroclastic flow from the Yellow Tuff sequence. Unit I.</p>
<p>53 DR Aluk Ridge; seg. 3</p>	<p>12.03.2001 on bottom: 17:49 h 3352 m 59°44.95' S 065°24.69' W off bottom: 20:23 h 3229 m 59°44.62' S 065°25.25' W</p>	<p>-1: 13 x 6 cm dark grey aphyric basalt, 5 % small vesicles <1 mm across often partly rimmed by pale blue zeolite or silica, Fe-staining along some irregular fractures, black glass up to 1 mm thick on some surfaces. Unit A.</p> <p>-2: 8 x 7 cm Unit A, less weathered with no Fe-staining, and up to 1 cm of palagonised hyaloclastite on the surface.</p> <p>-3: 11 x 6 cm Unit A, more weathered with Fe-stained fractures throughout, well developed glassy crust overlain by up to 1.5 cm of palagonised hyaloclastite.</p> <p>-4: 11 x 8 cm dark grey plagioclase basalt, 5 % plagioclase phenocrysts up to 2 mm across, 10 % small vesicles up to 1 mm across, 1 mm thick black glassy surface layer, some irregular fractures filled by clay. Unit B.</p> <p>-5: 9 x 7 cm Unit B, slightly more weathered.</p> <p>-6: 13 x 6 cm dark grey dense aphyric basalt (possibly fine grained dolerite), matrix is alternating dark green and black patches (pervasive chloritisation?), angular jointed block. Unit C.</p> <p>-7: 12 x 6 cm Unit C, more altered.</p> <p>-8: 8 x 5 cm dark grey plagioclase basalt, 10 % plagioclase phenocrysts up to 2 mm across, 20 % small vesicles up to 1 mm across, a fresh angular block. Unit D.</p> <p>-9: 12 x 4 cm Unit C.</p> <p>-10: 11 x 7 cm Unit D, with concentric weathering bands.</p> <p>-11: 14 x 8 cm Unit A, with chloritic clay and pale blue zeolite or silica in most vesicles.</p> <p>-12: 12 x 9 cm Unit C, pervasively chloritised.</p>

Appendix 1

Station	Date / Time / Depth / Coordinates	Description
		<p>-13: 12 x 8 cm altered basalt, 10 % dark grey chlorite pseudomorphing mafic phenocrysts (olivine?), matrix is greenish and weakly pervasively chloritised. Unit E.</p> <p>-14: 13 x 7 cm Unit C, but pervasively silicified except for numerous 1-10 mm ovoid patches.</p> <p>-15: 16 x 9 cm altered basalt, 20 % small very light green phenocrysts (epidotised plagioclase?) up to 2 mm across, 20 % dark grey chlorite infilling vesicles to 1 mm across, set in a pervasively silicified and chloritised matrix. Unit F.</p> <p>-16: 13 x 8 cm pervasively silicified, chloritised, aphyric lava, with dark red hematitic patches. Unit G.</p> <p>-17: 14 x 7 cm Unit G, breaking up into 2-3 mm variolitic ovoids of dark reddish hematitic silicified lava set in pale green chloritic clay along one side.</p> <p>-18: 12 x 6 cm Unit G, as for 17 but mostly variolitic and grading to green and white chlorite-smectite-illite clays with silica blobs on one side.</p> <p>-19: 8 x 5 cm chloritised hyaloclastite, with chlorite-smectite-illite replacing clasts up to 5 mm across (hyaloclastite) and local development of white silica blobs.</p> <p>-20: 15 x 4 cm hyaloclastite, with fresh clasts of Unit A up to 2 cm across (most 1 mm), often glassy, set in a yellow-brown matrix of palagonised glass.</p> <p>The sequence from 12 (and in particular 16) onwards is one of increasing chloritisation and silicification of the host lavas. There is a continuum from altered lava cores through variolitic textured lava to chloritised hyaloclastite (often seem in one boulder), or to cherty silicified hyaloclastite. There is an equivalent sequence of fresh cores to weathered lava to palagonised hyaloclastite for Unit A. More altered rocks were logged by the hydrothermal gang.</p>
54 DR Aluk Ridge; seg. 3	12.03.2001 on bottom: 23:46 h 3254 m 59°50.54' S 065°19.14' W off bottom: 01:34 h 3029 m 59°50.09' S 065°19.62' W	No samples recovered.
55 DR Aluk Ridge; seg. 4	13.03.2001 on bottom: 01:22 h 3156 m 59°50.49' S 065°19.51' W off bottom: 04:48 h 2948 m 59°50.32' S 065°20.11' W	-1: 10 x 9 cm black olivine basalt, 5 % green to pale green olivine phenocrysts up to 1 mm across and sometimes in clusters, 10 % small vesicles <1 mm across, black glassy rind up to 5 mm thick, pillow fragment. Unit A. <p>-2: 12 x 5 cm Unit A, a well formed pillow section with glass crust.</p> <p>-3: 15 x 7 cm Unit A, as for 2.</p> <p>-4: 16 x 6 cm Unit A, as for 2.</p> <p>-5: 15 x 8 cm Unit A, with particularly well developed 5 mm thick glass crust on one side.</p> <p>-6: 17 x 8 cm Unit A, but more fractured with yellow-orange clay infilling fractures, 1 mm thick MnOx crust on top of the thin glassy crust, and possibly represents an older olivine basalt sequence.</p> <p>-7: 15 x 9 cm Unit A, as for 6.</p>

Appendix 1

Station	Date / Time / Depth / Coordinates	Description
		<p>-8: 22 x 12 cm Unit A, as for 6.</p> <p>-9: 14 x 5 cm Unit A, as for 6.</p> <p>-10: 15 x 5 cm Unit A, as for 6 but blockier with poor pillow development.</p> <p>-11: 12 x 6 cm Unit A, but only a pillow top with 5 mm thick black glass.</p> <p>-12: 7 x 3 cm Unit A, an entire very small pillow wrapped in 3 mm thick black glass.</p> <p>-13: 15 x 7 cm dark grey olivine basalt, 10 % green olivine phenocrysts up to 2 mm across but most 1 mm across, often clustered, 15 % small vesicles up to 1 mm across, thick well developed black glass crust 5 mm thick capped by a few mm of orange clay-carbonate development. Unit B.</p> <p>-14: 13 x 7 cm Unit B, but no glass and the olivine phenocrysts are more weathered to colourless and incipient iddingsite.</p> <p>-15: 14 x 10 cm black aphyric basalt, 10 % vesicles up to 2 mm across and mostly rimmed by orange clay, several irregular fractures filled with orange clay, black glass crust up to 2 mm wide with overlying orange clay-carbonate and MnOx crust. Unit C.</p> <p>-16: 13 x 7 cm Unit C.</p> <p>-17: 15 x 7 cm palagonised hyaloclastite, clasts of fresh aphyric black basalt with glass crust, clasts up to 1.5 cm but most 2 mm across, set in a yellow-brown palagonised glass (clay) matrix. Unit D.</p> <p>-18: 30 x 8 cm gabbro, with plagioclase, black pyroxene, green pyroxene all about 2 mm across, disseminated traces of pyrrhotite +/- pyrite mostly around two <1 mm wide chlorite veinlets, a weathered jointed block. Unit E.</p> <p>-19: Glass chips from a very large (1 m diameter) Unit A (?) pillow broken on the back deck.</p>
<p>56 DR Aluk Ridge; seg. 4</p>	<p>13.03.2001 on bottom: 13:02 h 3448 m 60°19.93' S 065°29.88' W off bottom: 15:59 h 3075 m 60°19.29' S 065°34.36' W</p>	<p>-1: 13 x 5 cm dark grey olivine basalt, 5 % green olivine phenocrysts up to 1 mm across that are always leached to colourless in the pillow core, 10 % vesicles up to 2 mm across, black glassy pillow crust up to 1 mm thick, moderately weathered throughout. Unit A.</p> <p>-2: 12 x 6 cm Unit A.</p> <p>-3: 16 x 7 cm Unit A.</p> <p>-4: 11 x 7 cm dark grey olivine basalt, 10 % green olivine phenocrysts up to 2 mm across, 10 % vesicles up to 2 mm across, poorly developed black glassy pillow crust up to 1 mm thick, thin and intermittently developed MnOx crust over glass up to 1 mm thick, weakly weathered in outermost 1 cm. Unit B.</p> <p>-5: 9 x 6 cm Unit B.</p> <p>-6: 17 x 6 cm Unit B.</p> <p>-7: 15 x 8 cm Unit B.</p> <p>-8: 12 x 6 cm Unit B, with 1 cm of strongly weathered palagonised hyaloclastite around its margin.</p> <p>-9: 10 x 6 cm dark grey olivine basalt, 15 % green olivine phenocrysts up to 2 mm across, 15 % small vesicles up to 2 mm across, a pillow fragment with poorly developed 1 mm thick black glassy crust, weathered surface. Unit C.</p> <p>-10: 22 x 7 cm, as for Unit B but has additional population of small (<1 mm) green olivine microphenocrysts that</p>

Appendix 1

Station	Date / Time / Depth / Coordinates	Description
		<p>are typically arranged in arcs throughout the matrix, totalling 20 % olivine, more weathered than the other units. Unit D.</p> <p>-11: 10 x 5 cm black aphyric basalt, dense, nearly fresh, possibly an erratic. Unit E.</p> <p>-12: 18 x 9 cm dark grey aphyric basalt, trace olivine phenocrysts weathered to colourless and up to 2 mm across, 15 % vesicles up to 3 mm across rimmed with soft pale blue clay. Unit F.</p> <p>-13: 13 x 4 cm Unit F.</p> <p>-14: 13 x 8 cm, as for Unit F but the olivines are distinctly larger and up to 3 mm across, though still <5 %. Unit G.</p> <p>-15: 23 x 6 cm Unit G.</p> <p>-16: 17 x 6 cm dolerite, dark green and black pyroxene-plagioclase dolerite, crystals up to 1 mm across, sub-rounded boulder and possibly an erratic. Unit H.</p> <p>-17: 5 x 2 cm red aphyric basaltic scoria, 40 % vesicles up to 4 mm across and usually filled with soft yellow clay. Probably an erratic.</p> <p>-18: 7 x 4 cm black olivine basalt, 5 % green to colourless olivine phenocrysts up to 4 mm across, trace plagioclase phenocrysts up to 4 mm across, 5 % small vesicles up to 1 mm across, well developed 1 mm thick glassy pillow crust. Unit I.</p> <p>-19: 11 x 7 cm black olivine basalt, 10 % green olivine phenocrysts up to 1 mm across, 20 % vesicles up to 2 mm across, sub-rounded boulder with white zeolite in most vesicles. Probably an erratic.</p> <p>-20: 12 x 8 cm diorite, plagioclase and black hornblende (or pyroxene) up to 2 mm across, much pyrite pseudomorphing the mafic phenocrysts, well-rounded. An erratic.</p> <p>-21: 19 x 7 cm diorite, as for 20 but finer grained (crystals 1 mm across) and weakly foliated. An erratic.</p> <p>-22: 30 x 20 cm granite, with 4 mm across crystals of K-feldspar, plagioclase, quartz, and hornblende, weakly foliated. An erratic.</p> <p>-23: 13 x 6 cm gabbro, exposing a sheared intrusive contact between two gabbroic units. An erratic.</p> <p>-24: 11 x 5 cm volcanoclastic breccia, with a variety of altered volcanic clasts up to 5 mm across set in a green chloritic matrix. An erratic.</p> <p>-25: 20 x 7 cm silicified yellow rock, pervasively silicified and with sub-parallel quartz veins and veinlets up to 3 mm wide, the protolith could be a lava or a sedimentary rock. An erratic.</p> <p>A small greenschist erratic with isoclinal folding was also recovered but not kept.</p>
57 DR Aluk Ridge; seg. 4	13.03.2001 on bottom: 21:07 h 2227 m 60°36.98' S 065°55.18' W off bottom: 22:29 h 1970 m 60°36.74' S 065°56.40' W	-1: 50 x 30 cm blue-grey plagioclase andesite, 30 % large plagioclase phenocrysts up to 5 mm across and sometimes greenish, trace small vesicles, MnOx crust up to 1 mm thick, sub-rounded boulder and possibly an erratic. Unit A. <p>-2: 21 x 16 cm brown silty claystone, small curved dark markings up to 2 mm across that may be dissolved shells, sub-rounded boulder and probably an erratic.</p> <p>-3: 17 x 14 cm well-rounded diorite boulder. An erratic.</p>
58 DR Aluk Ridge; seg. 4	14.03.2001 on bottom: 02:33 h	Safety cable broke during this attempt to dredge in very heavy seas. Dredge recovered, but no samples.

Appendix 1

Station	Date / Time / Depth / Coordinates	Description
	3520 m 60°44.45' S 066°28.53' W off bottom: 06:53 h 2484 m 60°44.24' S 066°28.58' W	

Appendix 2

OFOS and TV-grab Protocols

SONNE - 155



138 Records

SO 155**01 OFOS****Donnerstag, 1. März 2001**

Ship Nr	Ship Latitude	Ship Longitude	Hydrosweep Depth [m]	Subl Latitude	Subl Longitude	Time [UTC]	CTD [m]	Remark
1	62° 11,0170' S	57° 17,0073' W	0	0° 0,0000' N	0° 0,0000' E	17:34:16	13	start operation
2	62° 11,0115' S	57° 16,9911' W	0	0° 0,0000' N	0° 0,0000' E	17:43:13	13	fieren to 900m, the winch operator switches to the geology lab, ship is on station, waterdepth is approx. 1300m,
3	62° 10,9945' S	57° 16,9861' W	1299	0° 0,0000' N	0° 0,0000' E	17:46:38	14	OFOS off deck
4	62° 11,0106' S	57° 16,9894' W	1292	0° 0,0000' N	0° 0,0000' E	17:52:34	13	OFOS in the water, temperature is measured in the weight
5	62° 10,9952' S	57° 16,9664' W	1296	62° 11,0093' S	57° 16,9386' W	18:03:13	61	problems with the winch camera have been resolved
6	62° 10,9949' S	57° 16,9445' W	1301	62° 10,9976' S	57° 16,9024' W	18:22:52	61	problems have not been resolved yet
7	62° 11,0327' S	57° 16,9995' W	1275	62° 11,0490' S	57° 16,9720' W	18:45:27	63	winch is operating now! obviously our camera is now taking pictures of blue water
8	62° 11,0091' S	57° 16,9972' W	1284	62° 11,0308' S	57° 16,9619' W	19:00:19	907	reached instrument depth of 900 m, winch operator is changing to the geology lab
9	62° 11,0050' S	57° 16,9895' W	1287	62° 11,0200' S	57° 16,9648' W	19:02:27	910	fieren with 1,0 to 1200m
10	62° 11,0019' S	57° 16,9906' W	1294	62° 11,0231' S	57° 16,9455' W	19:09:21	1208	reached 1200m, fiere to bottom contact
11	62° 10,9990' S	57° 16,9939' W	1296	62° 11,0158' S	57° 16,9302' W	19:09:45	1223	bottom contact at 1224 m waterdepth in heavily sedimented area, striped fish
12	62° 10,9975' S	57° 16,9870' W	1295	62° 11,0156' S	57° 16,9467' W	19:12:25	1238	video turned on
13	62° 11,0041' S	57° 16,9737' W	1293	62° 11,0078' S	57° 16,9537' W	19:13:16	1235	textured sediment, one seastar

Ship Nr	Ship Latitude	Ship Longitude	Hydrosweep Depth [m]	Subl Latitude	Subl Longitude	Time [UTC]	CTD [m]	Remark
14	62° 11,0234' S	57° 16,9493' W	1277	62° 11,0140' S	57° 16,9557' W	19:15:20	1229	increasing numbers of brittle stars, mottled texture
15	62° 11,0411' S	57° 16,9266' W	1253	62° 11,0201' S	57° 16,9107' W	19:18:07	1215	iron staining and Fe-oxyhydroxides close to the top
16	62° 11,0518' S	57° 16,9264' W	1243	62° 11,0362' S	57° 16,9012' W	19:20:02	1205	the whole area is covered with Fe-oxyhydroxides
17	62° 11,0698' S	57° 16,9230' W	1224	62° 11,0441' S	57° 16,8614' W	19:22:36	1191	red cliff
18	62° 11,0720' S	57° 16,9358' W	1227	62° 11,0599' S	57° 16,8482' W	19:23:41	1184	nice area to use the TV-grab !!!!!!!
19	62° 11,0833' S	57° 16,9175' W	1215	62° 11,0643' S	57° 16,8774' W	19:24:53	1178	oxide cliff with abundant brittle stars
20	62° 11,0963' S	57° 16,9191' W	1196	62° 11,0841' S	57° 16,8640' W	19:27:21	1154	Fe-oxide chimneys, sometimes on top of lava other critters as well as on the hard substrate
21	62° 11,1073' S	57° 16,9100' W	1189	62° 11,0821' S	57° 16,8443' W	19:29:26	1149	back to Fe-oxyhydroxides and brittle stars
22	62° 11,1202' S	57° 16,8895' W	1179	62° 11,0973' S	57° 16,8733' W	19:30:53	1142	sediment with abundant brittle stars, we are still going up the outer flank of Hook Ridge
23	62° 11,1352' S	57° 16,8628' W	1160	62° 11,1091' S	57° 16,8718' W	19:32:40	1131	slabs or crusts, Fe-staining, still abundant brittle stars (some of them are red)
24	62° 11,1515' S	57° 16,8793' W	1145	62° 11,1254' S	57° 16,8144' W	19:35:31	1107	big cliff, other animals, elongated lava flow or hydrothermal? Textures
25	62° 11,1666' S	57° 16,8545' W	1126	62° 11,1446' S	57° 16,8461' W	19:37:29	1094	flying a bit over the ground, back to sediment with Fe-oxyhydroxides
26	62° 11,1764' S	57° 16,8448' W	1118	62° 11,1453' S	57° 16,8221' W	19:39:15	1089	the temperature probe in the weight is recording slightly elevated temperatures (0,15°C; instrument is adjusted to -2°C)
27	62° 11,1967' S	57° 16,8328' W	1098	62° 11,1763' S	57° 16,7955' W	19:42:33	1067	still flying over the flanks of Hook Ridge
28	62° 11,2249' S	57° 16,8170' W	1082	62° 11,2087' S	57° 16,7675' W	19:46:37	1058	heavily sedimented, but the fauna is much less abundant here
29	62° 11,2388' S	57° 16,7888' W	1085	62° 11,2153' S	57° 16,7834' W	19:47:54	1059	animal tracks in the sediment, rarely sea lilies
30	62° 11,2495' S	57° 16,7889' W	1085	62° 11,2133' S	57° 16,7656' W	19:49:14	1052	small burrows and more tracks in heavily sedimented area
31	62° 11,2655' S	57° 16,7898' W	1080	62° 11,2424' S	57° 16,7600' W	19:51:40	1049	the absence of brittle stars is quite obvious, only sea lilies and stalked "balls"

Ship Nr	Ship Latitude	Ship Longitude	Hydrosweep Depth [m]	Sub1 Latitude	Sub1 Longitude	Time [UTC]	CTD [m]	Remark
32	62° 11,2809' S	57° 16,7657' W	1085	62° 11,2515' S	57° 16,7525' W	19:53:25	1052	still the same with more black dots, slide number 111
33	62° 11,2901' S	57° 16,7518' W	1088	62° 11,2565' S	57° 16,7292' W	19:54:26	1054	abundant animal tracks in 100% sediment
34	62° 11,3033' S	57° 16,7427' W	1087	62° 11,2860' S	57° 16,7159' W	19:57:42	1055	still the same
35	62° 11,3122' S	57° 16,7427' W	1089	62° 11,3026' S	57° 16,6821' W	20:00:49	1062	still heavily sedimented with animal tracks, burrows and traces
36	62° 11,3335' S	57° 16,7078' W	1090	62° 11,3208' S	57° 16,7042' W	20:05:12	1064	small group of anemones
37	62° 11,3264' S	57° 16,7382' W	1086	62° 11,3342' S	57° 16,6649' W	20:08:13	1067	still in sediment
38	62° 11,3573' S	57° 16,6943' W	1100	62° 11,3432' S	57° 16,6869' W	20:11:00	1069	slowly moving into the crater
39	62° 11,3708' S	57° 16,6918' W	1103	62° 11,3629' S	57° 16,6650' W	20:14:37	1071	still in sediment
40	62° 11,4010' S	57° 16,6602' W	1107	62° 11,3929' S	57° 16,6222' W	20:20:10	1073	we are almost in the center of the crater
41	62° 11,4091' S	57° 16,6616' W	1106	62° 11,4127' S	57° 16,6219' W	20:23:24	1074	very small temperature anomalies, still the same surrounding
42	62° 11,4291' S	57° 16,6382' W	1108	62° 11,4159' S	57° 16,6024' W	20:26:06	1075	sediment with anemones
43	62° 11,4519' S	57° 16,6148' W	1100	62° 11,4278' S	57° 16,5774' W	20:29:24	1069	still in the sedimented area, 150m to go to the hydrothermal area
44	62° 11,4546' S	57° 16,6171' W	1098	62° 11,4329' S	57° 16,5692' W	20:30:02	1065	small rock outcrop with anemones than back to sediment
45	62° 11,4637' S	57° 16,6023' W	1102	62° 11,4494' S	57° 16,5834' W	20:32:05	1058	another small outcrop, partially to completely sedimented with some brittle stars, numbers of brittle stars are increasing; temperature is decreasing although it is getting shallower
46	62° 11,4838' S	57° 16,5787' W	1099	62° 11,4780' S	57° 16,5472' W	20:35:47	1062	white patches with Fe-staining
47	62° 11,4905' S	57° 16,5750' W	1102	62° 11,4793' S	57° 16,5332' W	20:36:44	1062	talus pocking through the sediment
48	62° 11,4939' S	57° 16,5732' W	1102	62° 11,4757' S	57° 16,5310' W	20:37:20	1064	Fe-oxyhydroxides
49	62° 11,4963' S	57° 16,5737' W	1100	62° 11,4760' S	57° 16,5290' W	20:37:47	1067	sediment; no animals
50	62° 11,5065' S	57° 16,5896' W	1096	62° 11,4979' S	57° 16,5243' W	20:41:11	1070	sediment; approaching the entrance to the crater
51	62° 11,5436' S	57° 16,5276' W	1102	62° 11,5165' S	57° 16,5242' W	20:45:30	1071	red staining, white patches, shrimps

Ship Nr	Ship Latitude	Ship Longitude	Hydrosweep Depth [m]	Subl Latitude	Subl Longitude	Time [UTC]	CTD [m]	Remark
52	62° 11,5482' S	57° 16,5270' W	1099	62° 11,5209' S	57° 16,5049' W	20:46:20	1066	abundant brittle stars, going up hill, cliff
53	62° 11,5515' S	57° 16,5365' W	1099	62° 11,5315' S	57° 16,5054' W	20:47:15	1056	red line (fracture with Fe-oxides?), mottled texture of the sediment, brittle stars
54	62° 11,5614' S	57° 16,5441' W	1098	62° 11,5614' S	57° 16,4983' W	20:51:18	1063	few rocks in 95% sediment with few brittle stars
55	62° 11,5682' S	57° 16,5390' W	1097	62° 11,5737' S	57° 16,4859' W	20:53:01	1054	very steep cliff marking the entrance to the crater
56	62° 11,5932' S	57° 16,5132' W	1096	62° 11,5831' S	57° 16,4707' W	20:57:30	1048	100% sediment
57	62° 11,6021' S	57° 16,4992' W	1105	62° 11,5983' S	57° 16,4705' W	20:59:31	1055	60% rock pebbles; going down hill
58	62° 11,6040' S	57° 16,4955' W	1110	62° 11,5990' S	57° 16,4481' W	21:00:47	1062	rock outcrop with anemones and other small animals attached to the rocks (talus pile)
59	62° 11,6154' S	57° 16,4977' W	1115	62° 11,6052' S	57° 16,4442' W	21:04:14	1074	changed plans; we will go back on a parallel track (100 m to the west)
60	62° 11,6189' S	57° 16,4985' W	1123	62° 11,6213' S	57° 16,4529' W	21:05:49	1082	ship is slowly turning to the new course, OFOS over rock pile with abundant brittle stars
61	62° 11,5879' S	57° 16,5872' W	1097	62° 11,5965' S	57° 16,4959' W	21:10:26	1058	still over rock talus pile with brittle stars
62	62° 11,5817' S	57° 16,6148' W	1100	62° 11,5957' S	57° 16,5034' W	21:11:51	1048	going up hill through sediment with numerous brittle stars
63	62° 11,5786' S	57° 16,6272' W	1100	62° 11,5830' S	57° 16,5425' W	21:12:56	1037	again a talus outcrop
64	62° 11,5693' S	57° 16,6328' W	1100	62° 11,5905' S	57° 16,5575' W	21:15:20	1043	white patches and a stronger temperature anomaly
65	62° 11,5591' S	57° 16,6576' W	1097	62° 11,5677' S	57° 16,5816' W	21:17:36	1058	back to sediment with sea lilies and less abundant brittle stars; it seems that the sulfide (?) talus is restricted to the wall
66	62° 11,5447' S	57° 16,6698' W	1091	62° 11,5537' S	57° 16,6047' W	21:19:39	1057	outcrop of rocks or hydrothermal material
67	62° 11,5382' S	57° 16,6787' W	1083	62° 11,5610' S	57° 16,6011' W	21:20:48	1054	hydrothermal coating on something
68	62° 11,5332' S	57° 16,6850' W	1082	62° 11,5515' S	57° 16,6201' W	21:21:46	1051	temperature spike and red staining on the sediment
69	62° 11,5317' S	57° 16,6880' W	1081	62° 11,5491' S	57° 16,6110' W	21:22:10	1050	white patches with red staining

Ship Nr	Ship Latitude	Ship Longitude	Hydrosweep Depth [m]	Sub1 Latitude	Sub1 Longitude	Time [UTC]	CTD [m]	Remark
70	62° 11,5285' S	57° 16,6936' W	1080	62° 11,5434' S	57° 16,6279' W	21:22:59	1051	more white patches, the right target for a sediment core !!!!!
71	62° 11,5197' S	57° 16,6993' W	1078	62° 11,5371' S	57° 16,6419' W	21:24:53	1050	thick sediment cover with abundant brittle stars
72	62° 11,5145' S	57° 16,7042' W	1078	62° 11,5432' S	57° 16,6463' W	21:26:29	1041	white patches (faint)
73	62° 11,5095' S	57° 16,7106' W	1074	62° 11,5263' S	57° 16,6655' W	21:27:51	1038	white patches; Fe-staining (gravity corer!)
74	62° 11,4980' S	57° 16,7230' W	1079	62° 11,5267' S	57° 16,6624' W	21:29:39	1038	few more white patches
75	62° 11,4927' S	57° 16,7295' W	1078	62° 11,5153' S	57° 16,6685' W	21:30:29	1041	thick sediment pile; very few brittle stars
76	62° 11,4820' S	57° 16,7360' W	1082	62° 11,5157' S	57° 16,6897' W	21:32:43	1046	still in thick sediment
77	62° 11,4762' S	57° 16,7444' W	1085	62° 11,4913' S	57° 16,6927' W	21:34:32	1048	boulder!! in thick sediment
78	62° 11,4610' S	57° 16,7666' W	1088	62° 11,4844' S	57° 16,6935' W	21:37:58	1054	we will move the track 50m to the east and go parallel to both tracks back SE
79	62° 11,4644' S	57° 16,7757' W	1081	62° 11,4797' S	57° 16,7312' W	21:40:20	1054	slide No. 282 in thick sediment while the ship is turning
80	62° 11,4794' S	57° 16,7690' W	1079	62° 11,4723' S	57° 16,7265' W	21:42:39	1050	100% sediment
81	62° 11,4949' S	57° 16,7292' W	1079	62° 11,4820' S	57° 16,7386' W	21:44:53	1048	single rock for the petrology group
82	62° 11,5052' S	57° 16,7033' W	1080	62° 11,5039' S	57° 16,6928' W	21:47:45	1048	thick sediment cover!
83	62° 11,5211' S	57° 16,6972' W	1083	62° 11,5140' S	57° 16,6572' W	21:51:03	1040	white patches with Fe-staining and additional temperature spike (0.08°C)
84	62° 11,5367' S	57° 16,6597' W	1086	62° 11,5213' S	57° 16,6593' W	21:53:31	1037	more white patches with anemones
85	62° 11,5446' S	57° 16,6409' W	1096	62° 11,5276' S	57° 16,6702' W	21:54:46	1047	100% sediment with brittle stars
86	62° 11,5625' S	57° 16,6140' W	1098	62° 11,5358' S	57° 16,6419' W	21:56:58	1051	small rock outcrop
87	62° 11,5697' S	57° 16,6093' W	1100	62° 11,5408' S	57° 16,6265' W	21:57:40	1048	small outcrop with white patches and smaller (0.04°C) T-anomaly
88	62° 11,5827' S	57° 16,5971' W	1097	62° 11,5666' S	57° 16,6067' W	21:59:49	1055	abundant white patches with T-anomaly (0.09°C) and hydrothermal pile (?)

Ship Nr	Ship Latitude	Ship Longitude	Hydrosweep Depth [m]	Subl Latitude	Subl Longitude	Time [UTC]	CTD [m]	Remark
89	62° 11,5845' S	57° 16,5926' W	1096	62° 11,5716' S	57° 16,5809' W	22:01:18	1055	talus slope with white material, T-anomaly
90	62° 11,5922' S	57° 16,5903' W	1093	62° 11,6049' S	57° 16,5488' W	22:04:08	1033	just passed over this small talus (?) pile; terrace
91	62° 11,6047' S	57° 16,5794' W	1091	62° 11,6131' S	57° 16,5644' W	22:07:13	1041	abundant brittle stars
92	62° 11,5968' S	57° 16,5785' W	1097	62° 11,6297' S	57° 16,5469' W	22:10:20	1053	we are turning back to another line covering the ground we have not seen before
93	62° 11,5521' S	57° 16,5937' W	1092	62° 11,5947' S	57° 16,5511' W	22:15:42	1046	T-anomaly (0.14°C), white staining and Fe-oxyhydroxides
94	62° 11,5462' S	57° 16,5986' W	1090	62° 11,5855' S	57° 16,5680' W	22:16:59	1056	still white patches
95	62° 11,5423' S	57° 16,6007' W	1090	62° 11,5781' S	57° 16,5548' W	22:17:58	1055	sulfides (?)
96	62° 11,5339' S	57° 16,6086' W	1092	62° 11,5728' S	57° 16,5706' W	22:19:45	1055	sediment in between talus (at wall) and the white patch within the crater (a bit off the wall)
97	62° 11,5290' S	57° 16,6113' W	1092	62° 11,5608' S	57° 16,5990' W	22:20:54	1053	white patches and grey and red staining on the sediment, small T-anomaly (0.02°C)
98	62° 11,5228' S	57° 16,6127' W	1095	62° 11,5560' S	57° 16,5966' W	22:22:11	1052	crusts and very few white material
99	62° 11,5197' S	57° 16,6138' W	1093	62° 11,5536' S	57° 16,6069' W	22:23:01	1054	old chimney spires (?)
100	62° 11,5165' S	57° 16,6142' W	1093	62° 11,5558' S	57° 16,6173' W	22:23:43	1056	slide 358 = sulfide blocks (?)
101	62° 11,5099' S	57° 16,6152' W	1099	62° 11,5492' S	57° 16,6080' W	22:24:51	1055	octopus
102	62° 11,4850' S	57° 16,6189' W	1104	62° 11,5313' S	57° 16,6013' W	22:27:07	1053	thick sediment
103	62° 11,4519' S	57° 16,6656' W	1103	62° 11,4870' S	57° 16,6167' W	22:32:26	1047	white patches with hydrothermal crusts, Fe-oxyhydroxides (this was not seen before); the temperature anomaly is rather small though (0.06°C)
104	62° 11,4385' S	57° 16,6819' W	1109	62° 11,4743' S	57° 16,6109' W	22:34:38	1057	back to sediment
105	62° 11,4274' S	57° 16,6969' W	1106	62° 11,4612' S	57° 16,6446' W	22:36:21	1039	tape off; OFOS off bottom; we want to move the ship to the next position (the hydrothermal area in the hinge) and drop the OFOS back to the seafloor to add an hour and a half of bottom time

Ship Nr	Ship Latitude	Ship Longitude	Hydrosweep Depth [m]	Subl Latitude	Subl Longitude	Time [UTC]	CTD [m]	Remark
106	62° 11,4163' S	57° 16,7315' W	1099	62° 11,4396' S	57° 16,6671' W	22:39:56	864	the slide counter is on 365
107	62° 12,2736' S	57° 16,1336' W	1572	62° 12,2878' S	57° 16,1588' W	23:59:11	859	tape on for second lowering of the OFOS, fieren to bottom sight
108	62° 12,2859' S	57° 16,1465' W	1574	62° 12,2893' S	57° 16,1818' W	00:02:31	1035	no comment
109	62° 12,3192' S	57° 16,1233' W	1576	62° 12,3104' S	57° 16,2107' W	00:08:40	1371	we just past a plume signal; T stayed high while the OFOS was lowered
110	62° 12,3348' S	57° 16,1342' W	1579	62° 12,3260' S	57° 16,2010' W	00:11:40	1525	bottom sight on fluffy mudball sediment; 100% sediment
111	62° 12,3684' S	57° 16,1154' W	1581	62° 12,3575' S	57° 16,1709' W	00:17:36	1525	fluffy sediment, ship is trying to get around an iceberg to get to the starting point of the profile
112	62° 12,4020' S	57° 16,1113' W	1582	62° 12,3822' S	57° 16,1898' W	00:22:52	1526	still in fluffy sediment; holothurians and polychetes (?)
113	62° 12,4189' S	57° 16,0895' W	1581	62° 12,4039' S	57° 16,1866' W	00:26:00	1529	burrows (shrimp?)
114	62° 12,4367' S	57° 16,0641' W	1582	62° 12,4247' S	57° 16,1677' W	00:29:35	1530	still in fluffy sediment
115	62° 12,4627' S	57° 16,0189' W	1582	62° 12,4593' S	57° 16,1220' W	00:35:51	1531	white patches (clams?)
116	62° 12,4840' S	57° 15,9815' W	1582	62° 12,4650' S	57° 16,0925' W	00:39:50	1533	100% mudball sediment
117	62° 12,4924' S	57° 15,9738' W	1580	62° 12,4776' S	57° 16,0889' W	00:41:04	1533	tape end; changing to tape 2
118	62° 12,5188' S	57° 15,9738' W	1579	62° 12,4920' S	57° 16,0537' W	00:44:59	1532	both tapes are recording
119	62° 12,5369' S	57° 15,9631' W	1572	62° 12,5138' S	57° 16,0469' W	00:48:21	1532	white specks
120	62° 12,5565' S	57° 15,9469' W	1566	62° 12,5379' S	57° 16,0504' W	00:51:26	1532	orange colored mud from underneath; small patches
121	62° 12,5699' S	57° 15,9155' W	1564	62° 12,5590' S	57° 16,0295' W	00:54:31	1532	same stuff
122	62° 12,5713' S	57° 15,9061' W	1562	62° 12,5691' S	57° 16,0170' W	00:55:22	1530	more specks within the mudballs
123	62° 12,5746' S	57° 15,9011' W	1560	62° 12,5703' S	57° 16,0000' W	00:56:20	1523	going uphill in mudball sediment
124	62° 12,5978' S	57° 15,8980' W	1557	62° 12,5830' S	57° 15,9771' W	01:01:06	1505	small outcrop with sponges
125	62° 12,6038' S	57° 15,8953' W	1556	62° 12,5867' S	57° 16,0026' W	01:01:55	1503	linear feature with crust-like appearance

<i>Ship Nr</i>	<i>Ship Latitude</i>	<i>Ship Longitude</i>	<i>Hydrosweep Depth [m]</i>	<i>Sub1 Latitude</i>	<i>Sub1 Longitude</i>	<i>Time [UTC]</i>	<i>CTD [m]</i>	<i>Remark</i>
126	62° 12,6109' S	57° 15,8943' W	1556	62° 12,5911' S	57° 16,0022' W	01:02:59	1502	back to mudball sediments
127	62° 12,6349' S	57° 15,8906' W	1546	62° 12,6168' S	57° 15,9818' W	01:07:03	1496	still the same
128	62° 12,6418' S	57° 15,8922' W	1548	62° 12,6253' S	57° 15,9603' W	01:08:20	1496	slide No. 400
129	62° 12,6689' S	57° 15,8692' W	1542	62° 12,6583' S	57° 15,9389' W	01:14:47	1490	100% mudball sediment
130	62° 12,7198' S	57° 15,8306' W	1538	62° 12,6938' S	57° 15,9243' W	01:21:44	1481	mudball sediments; we are passing the top of the hill in some distance due to the presence of icebergs in the targetted area
131	62° 12,7278' S	57° 15,8334' W	1537	62° 12,7010' S	57° 15,9301' W	01:22:53	1478	slide No. 405, white material on angular piece of ???
132	62° 12,7841' S	57° 15,8464' W	1540	62° 12,7386' S	57° 15,9233' W	01:29:34	1479	still mudballs
133	62° 12,7903' S	57° 15,8461' W	1540	62° 12,7498' S	57° 15,9257' W	01:30:21	1481	single brittle star
134	62° 12,8064' S	57° 15,8471' W	1537	62° 12,7612' S	57° 15,9075' W	01:32:19	1480	white and dark colors (some red) through the sediment
135	62° 12,8258' S	57° 15,8420' W	1539	62° 12,7827' S	57° 15,9023' W	01:34:31	1492	100% mudball sediment
136	62° 12,8879' S	57° 15,8301' W	1535	62° 12,8427' S	57° 15,9215' W	01:41:48	1495	few burrows in mudball sediment
137	62° 12,9215' S	57° 15,8168' W	1530	62° 12,8778' S	57° 15,9083' W	01:45:52	1486	100% mudballs
138	62° 12,9400' S	57° 15,8178' W	1531	62° 12,8939' S	57° 15,9185' W	01:47:55	1487	lost bottom contact; OFOS comes back on deck; end of OFOS; tapes stopped

SONNE - 155



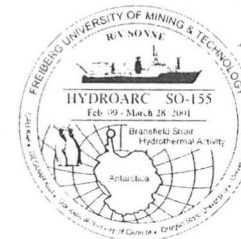
26 Records

SO 155**05 GTVA****Freitag, 2. März 2001**

Ship Nr	Ship Latitude	Ship Longitude	Hydrosweep Depth [m]	Subl Latitude	Subl Longitude	Time [UTC]	CTD [m]	Remark
139	62° 11,5573' S	57° 16,7774' W	0	62° 12,9215' S	57° 15,8712' W	14:02:00	3389	on station 05 GTVA; small scale mapping and then sampling of hydrothermal precipitates in Hook Ridge crater (southern wall)
140	62° 11,5768' S	57° 16,7082' W	0	62° 12,9677' S	57° 15,8118' W	14:19:50	0	TVgrab is off deck
141	62° 11,5538' S	57° 16,6725' W	0	62° 12,9677' S	57° 15,8118' W	14:26:25	0	TVgrab is in the water, fieren to 800 m, then change of the winch operator to the geology lab
142	62° 11,5859' S	57° 16,6673' W	0	62° 11,5913' S	57° 16,7065' W	14:32:09	0	200m
143	62° 11,5677' S	57° 16,6380' W	0	62° 11,5864' S	57° 16,6718' W	14:35:21	0	400m
144	62° 11,5443' S	57° 16,6376' W	0	62° 11,5581' S	57° 16,6504' W	14:38:51	0	600m
145	62° 11,5507' S	57° 16,6185' W	0	62° 11,5554' S	57° 16,6566' W	14:42:07	0	800m, winch operator is coming to geology lab
146	62° 11,5594' S	57° 16,6524' W	0	62° 11,5617' S	57° 16,6669' W	14:43:48	0	lights on; fieren to bottom sight
147	62° 11,5686' S	57° 16,6721' W	0	62° 11,5616' S	57° 16,6789' W	14:44:47	0	tapes (B/W and color) on
148	62° 11,5677' S	57° 16,6544' W	0	62° 11,6048' S	57° 16,7149' W	14:50:23	0	bottom sight in sediment with few brittle stars
149	62° 11,5940' S	57° 16,6122' W	0	62° 11,5764' S	57° 16,6592' W	14:55:07	0	still in sediment, drifting east
150	62° 11,5950' S	57° 16,6151' W	0	62° 11,5978' S	57° 16,6579' W	14:56:26	0	we are a bit too far south
151	62° 11,5922' S	57° 16,6231' W	0	62° 11,6056' S	57° 16,6325' W	14:57:10	0	few talus pieces, more brittle stars
152	62° 11,5792' S	57° 16,5534' W	0	62° 11,5988' S	57° 16,6374' W	14:59:45	0	rock outcrops
153	62° 11,5429' S	57° 16,5618' W	0	62° 11,5849' S	57° 16,5790' W	15:02:32	0	sediment with few white patches next to rock wall

Ship Nr	Ship Latitude	Ship Longitude	Hydrosweep Depth [m]	Subl Latitude	Subl Longitude	Time [UTC]	CTD [m]	Remark
154	62° 11,5115' S	57° 16,5530' W	0	62° 11,5753' S	57° 16,5566' W	15:04:26	0	still white patches
155	62° 11,4916' S	57° 16,5838' W	0	62° 11,5477' S	57° 16,5686' W	15:06:11	0	100% sediment, no indications of hydrothermal activity
156	62° 11,5025' S	57° 16,6214' W	0	62° 11,5144' S	57° 16,6410' W	15:10:32	0	anemones at outcrop
157	62° 11,5065' S	57° 16,6190' W	0	62° 11,5098' S	57° 16,6411' W	15:11:35	0	a lot of white stuff, outcrops (sulfidic?)
158	62° 11,5167' S	57° 16,6410' W	0	62° 11,5286' S	57° 16,6677' W	15:15:36	0	back into rock outcrops with some white patches behind and around them
159	62° 11,4970' S	57° 16,6253' W	0	62° 11,5175' S	57° 16,6420' W	15:22:06	0	grab taken, fieren 10m
160	62° 11,4945' S	57° 16,6013' W	0	62° 11,5433' S	57° 16,6618' W	15:22:56	0	slow heaving, screens are black
161	62° 11,4914' S	57° 16,6107' W	0	62° 11,5634' S	57° 16,6897' W	15:24:13	0	tension reader is not working
162	62° 11,4959' S	57° 16,6258' W	0	62° 11,5065' S	57° 16,6643' W	15:27:41	0	still poor visibility
163	62° 11,4995' S	57° 16,6045' W	0	62° 11,5056' S	57° 16,6866' W	15:28:12	0	heave 5m
164	62° 11,4713' S	57° 16,5921' W	0	62° 11,4855' S	57° 16,5957' W	15:31:21	0	heave 5m

SONNE - 155



107 Records

SO 155**06 GTVA****Freitag, 2. März 2001**

Ship Nr	Ship Latitude	Ship Longitude	Hydrosweep Depth [m]	Sub1 Latitude	Sub1 Longitude	Time [UTC]	CTD [m]	Remark
165	62° 11,4472' S	57° 16,6655' W	0	62° 11,4348' S	57° 16,7274' W	16:53:08	0	water contact
166	62° 11,4790' S	57° 16,6262' W	0	62° 11,4578' S	57° 16,6746' W	17:03:04	0	400m
167	62° 11,4997' S	57° 16,6406' W	0	62° 11,4916' S	57° 16,7152' W	17:09:05	0	800m
168	62° 11,4998' S	57° 16,6472' W	0	62° 11,5097' S	57° 16,7061' W	17:10:08	0	850m
169	62° 11,5278' S	57° 16,6262' W	0	62° 11,5168' S	57° 16,6771' W	17:12:32	0	going down to bottom
170	62° 11,5325' S	57° 16,6450' W	0	62° 11,5061' S	57° 16,6541' W	17:13:40	0	start of the tapes
171	62° 11,5350' S	57° 16,6117' W	0	62° 11,5460' S	57° 16,6655' W	17:17:20	0	1000m
172	62° 11,5134' S	57° 16,6353' W	0	62° 11,5404' S	57° 16,6045' W	17:19:16	0	bottom sight
173	62° 11,5076' S	57° 16,6415' W	0	62° 11,5453' S	57° 16,6445' W	17:19:43	0	sediment, brittle stars, few outcrops?
174	62° 11,5010' S	57° 16,6471' W	0	62° 11,5343' S	57° 16,6382' W	17:20:15	0	white crusts
175	62° 11,4948' S	57° 16,6534' W	0	62° 11,5368' S	57° 16,6444' W	17:20:45	0	white crusts
176	62° 11,4907' S	57° 16,6536' W	0	62° 11,5297' S	57° 16,6474' W	17:21:05	0	white patches, brittle stars in between
177	62° 11,4868' S	57° 16,6543' W	0	62° 11,5148' S	57° 16,6439' W	17:21:25	0	scarp
178	62° 11,4806' S	57° 16,6573' W	0	62° 11,5310' S	57° 16,6662' W	17:22:01	0	back in soft sediment, few brittle stars
179	62° 11,4793' S	57° 16,6544' W	0	62° 11,5163' S	57° 16,6732' W	17:22:26	0	white patches
180	62° 11,4836' S	57° 16,6342' W	0	62° 11,5127' S	57° 16,6924' W	17:22:57	0	soft greyish sediment

Ship Nr	Ship Latitude	Ship Longitude	Hydrosweep Depth [m]	Subl Latitude	Subl Longitude	Time [UTC]	CTD [m]	Remark
181	62° 11,4992' S	57° 16,6046' W	0	62° 11,4984' S	57° 16,6851' W	17:24:46	0	white patches again
182	62° 11,5113' S	57° 16,6245' W	0	62° 11,5070' S	57° 16,6878' W	17:26:28	0	grey soft sediment, whitish patches
183	62° 11,5195' S	57° 16,6299' W	0	62° 11,5215' S	57° 16,6451' W	17:27:18	0	white crusts on sediment?
184	62° 11,5307' S	57° 16,6351' W	0	62° 11,4884' S	57° 16,6054' W	17:28:00	0	white patches
185	62° 11,5366' S	57° 16,6346' W	0	62° 11,5214' S	57° 16,6126' W	17:28:28	0	blocky outcrop, slightly sedimented
186	62° 11,5434' S	57° 16,5920' W	0	62° 11,5372' S	57° 16,6521' W	17:29:56	0	soft sediment
187	62° 11,5131' S	57° 16,5983' W	0	62° 11,5507' S	57° 16,6077' W	17:32:16	0	still soft sediment
188	62° 11,5064' S	57° 16,5967' W	0	62° 11,5406' S	57° 16,6919' W	17:32:42	0	few white patches
189	62° 11,4881' S	57° 16,5968' W	0	62° 11,5283' S	57° 16,6263' W	17:33:58	0	soft sediment
190	62° 11,4810' S	57° 16,5995' W	0	62° 11,4917' S	57° 16,5653' W	17:34:30	0	heading towards the south
191	62° 11,4739' S	57° 16,5736' W	0	62° 11,5230' S	57° 16,6313' W	17:36:26	0	few white patches
192	62° 11,4729' S	57° 16,5772' W	0	62° 11,4989' S	57° 16,6325' W	17:36:41	0	course o. g. is about 300°
193	62° 11,4693' S	57° 16,6111' W	0	62° 11,4650' S	57° 16,6180' W	17:38:04	0	dropstone
194	62° 11,4702' S	57° 16,6204' W	0	62° 11,5186' S	57° 16,6215' W	17:38:31	0	white patches
195	62° 11,4732' S	57° 16,6264' W	0	62° 11,4899' S	57° 16,6406' W	17:39:04	0	sort of lining up of white precipitates
196	62° 11,4880' S	57° 16,6301' W	0	62° 11,4839' S	57° 16,6531' W	17:40:18	0	soft sediment again
197	62° 11,4905' S	57° 16,6454' W	0	62° 11,4858' S	57° 16,6531' W	17:41:18	0	scarp
198	62° 11,4922' S	57° 16,6617' W	0	62° 11,4902' S	57° 16,6711' W	17:43:04	0	soft sediment
199	62° 11,4993' S	57° 16,6536' W	0	62° 11,5068' S	57° 16,6910' W	17:44:49	0	still in soft sediment
200	62° 11,5002' S	57° 16,6388' W	0	62° 11,5216' S	57° 16,6810' W	17:46:37	0	still in soft sediment, no patches
201	62° 11,5050' S	57° 16,6284' W	0	62° 11,5095' S	57° 16,6747' W	17:47:55	0	whitish patches

<i>Ship Nr</i>	<i>Latitude</i>	<i>Ship Longitude</i>	<i>Hydrosweep Depth [m]</i>	<i>Sub1 Latitude</i>	<i>Sub1 Longitude</i>	<i>Time [UTC]</i>	<i>CTD [m]</i>	<i>Remark</i>
202	62° 11,5008' S	57° 16,6548' W	0	62° 11,5052' S	57° 16,6746' W	17:49:08	0	ship has not moved since 15 min
203	62° 11,4927' S	57° 16,6901' W	0	62° 11,4917' S	57° 16,6871' W	17:50:23	0	moving towards the north instead of going south
204	62° 11,5075' S	57° 16,6656' W	0	62° 11,5077' S	57° 16,6679' W	17:52:17	0	soft grey sediment
205	62° 11,5168' S	57° 16,6821' W	0	62° 11,5512' S	57° 16,6755' W	17:55:49	0	heading south again
206	62° 11,5256' S	57° 16,6695' W	0	62° 11,4613' S	57° 16,7583' W	17:57:31	0	brittle stars are back
207	62° 11,5272' S	57° 16,6665' W	0	62° 11,5609' S	57° 16,7827' W	17:57:52	0	white patches
208	62° 11,5372' S	57° 16,6493' W	0	62° 11,5349' S	57° 16,6991' W	17:58:46	0	white rings of white precipitates
209	62° 11,5469' S	57° 16,6407' W	0	62° 11,5180' S	57° 16,6650' W	17:59:39	0	only small white patches
210	62° 11,5472' S	57° 16,6389' W	0	62° 11,5310' S	57° 16,7243' W	17:59:51	0	scarp
211	62° 11,5439' S	57° 16,6413' W	0	62° 11,5485' S	57° 16,6817' W	18:00:34	0	going down the slope
212	62° 11,5398' S	57° 16,6373' W	0	62° 11,5495' S	57° 16,6843' W	18:01:15	0	grey sediment
213	62° 11,5406' S	57° 16,6524' W	0	62° 11,5470' S	57° 16,6594' W	18:04:48	0	brittle stars are back
214	62° 11,5690' S	57° 16,6339' W	0	62° 11,5522' S	57° 16,6946' W	18:07:35	0	few white patches
215	62° 11,5722' S	57° 16,6257' W	0	62° 11,5884' S	57° 16,6970' W	18:08:05	0	white crusts, rocky outcrop
216	62° 11,5715' S	57° 16,6215' W	0	62° 11,5671' S	57° 16,6858' W	18:08:37	0	slope, going down
217	62° 11,5632' S	57° 16,6424' W	0	62° 11,5803' S	57° 16,6639' W	18:09:59	0	soft sediment
218	62° 11,5585' S	57° 16,6293' W	0	62° 11,5743' S	57° 16,6623' W	18:11:19	0	sedimented outcrop
219	62° 11,5542' S	57° 16,6105' W	0	62° 11,5635' S	57° 16,6503' W	18:13:17	0	shrimp
220	62° 11,5537' S	57° 16,6080' W	0	62° 11,5752' S	57° 16,6688' W	18:13:32	0	white patches
221	62° 11,5456' S	57° 16,5960' W	0	62° 11,5666' S	57° 16,6469' W	18:14:37	0	good and distinct white patches
222	62° 11,5393' S	57° 16,5872' W	0	62° 11,5386' S	57° 16,6685' W	18:15:16	0	soft sediment again

<i>Ship Nr</i>	<i>Latitude</i>	<i>Ship Longitude</i>	<i>Hydrosweep Depth [m]</i>	<i>Sub1 Latitude</i>	<i>Sub1 Longitude</i>	<i>Time [UTC]</i>	<i>CTD [m]</i>	<i>Remark</i>
223	62° 11,5372' S	57° 16,5700' W	0	62° 11,5640' S	57° 16,6030' W	18:15:55	0	scarp
224	62° 11,5408' S	57° 16,5522' W	0	62° 11,5645' S	57° 16,6488' W	18:16:30	0	white patches
225	62° 11,5429' S	57° 16,5501' W	0	62° 11,5611' S	57° 16,6280' W	18:16:52	0	chimney-like feature, going down the slope
226	62° 11,5405' S	57° 16,5691' W	0	62° 11,5464' S	57° 16,5908' W	18:18:11	0	sediment
227	62° 11,5410' S	57° 16,5763' W	0	62° 11,5304' S	57° 16,6257' W	18:19:03	0	few small patches, increasing numbre
228	62° 11,5375' S	57° 16,5821' W	0	62° 11,5466' S	57° 16,6169' W	18:20:09	0	good area, white crusts
229	62° 11,5377' S	57° 16,5823' W	0	62° 11,5454' S	57° 16,6151' W	18:20:30	0	grab!, turned over
230	62° 11,5447' S	57° 16,5768' W	0	62° 11,5549' S	57° 16,6177' W	18:22:21	0	grab is empty
231	62° 11,5437' S	57° 16,5856' W	0	62° 11,5591' S	57° 16,5952' W	18:24:45	0	open the grab and next try going towards the south
232	62° 11,5180' S	57° 16,5807' W	0	62° 11,5370' S	57° 16,5767' W	18:28:19	0	bottom sight
233	62° 11,5163' S	57° 16,5894' W	0	62° 11,5282' S	57° 16,6104' W	18:28:38	0	white patches
234	62° 11,5298' S	57° 16,5879' W	0	62° 11,5323' S	57° 16,6159' W	18:30:19	0	soft sediment
235	62° 11,5363' S	57° 16,5754' W	0	62° 11,5335' S	57° 16,6173' W	18:30:54	0	white patches again
236	62° 11,5410' S	57° 16,5824' W	0	62° 11,5748' S	57° 16,6342' W	18:32:52	0	back in our former cloud
237	62° 11,5117' S	57° 16,6570' W	0	62° 11,5316' S	57° 16,6372' W	18:35:54	0	white patches, brittle stars in soft sediment
238	62° 11,5146' S	57° 16,6714' W	0	62° 11,5154' S	57° 16,6438' W	18:37:01	0	patches and rocky/sulfide? outcrops
239	62° 11,5180' S	57° 16,6659' W	0	62° 11,5442' S	57° 16,6358' W	18:37:40	0	big block on a scarp
240	62° 11,5362' S	57° 16,6408' W	0	62° 11,5425' S	57° 16,6787' W	18:39:19	0	white rings again
241	62° 11,5374' S	57° 16,6444' W	0	62° 11,5443' S	57° 16,6916' W	18:40:01	0	white patches
242	62° 11,5809' S	57° 16,5849' W	0	62° 11,5531' S	57° 16,6809' W	18:43:14	0	white patches
243	62° 11,5815' S	57° 16,5862' W	0	62° 11,5527' S	57° 16,6659' W	18:43:22	0	scarp, rock

<i>Ship Nr</i>	<i>Latitude</i>	<i>Ship Longitude</i>	<i>Hydrosweep Depth [m]</i>	<i>Subl Latitude</i>	<i>Subl Longitude</i>	<i>Time [UTC]</i>	<i>CTD [m]</i>	<i>Remark</i>
244	62° 11,5829' S	57° 16,5904' W	0	62° 11,5706' S	57° 16,7636' W	18:44:18	0	small outcrop
245	62° 11,6035' S	57° 16,5405' W	0	62° 11,5816' S	57° 16,6692' W	18:46:05	0	sedimented something, still soft sediment
246	62° 11,6079' S	57° 16,5336' W	0	62° 11,5863' S	57° 16,6124' W	18:46:30	0	sedimented outcrop
247	62° 11,6117' S	57° 16,5324' W	0	62° 11,5754' S	57° 16,6312' W	18:46:58	0	going up to the top
248	62° 11,6094' S	57° 16,5376' W	0	62° 11,6004' S	57° 16,5683' W	18:48:12	0	sedimented talus, no white patches
249	62° 11,5868' S	57° 16,5599' W	0	62° 11,6161' S	57° 16,5643' W	18:49:42	0	moving down again
250	62° 11,5763' S	57° 16,5525' W	0	62° 11,6003' S	57° 16,6079' W	18:51:37	0	white patches again
251	62° 11,5922' S	57° 16,5176' W	0	62° 11,5926' S	57° 16,5833' W	18:52:34	0	grab!
252	62° 11,5995' S	57° 16,5005' W	0	62° 11,6245' S	57° 16,4367' W	18:53:18	0	no grab; collision
253	62° 11,6006' S	57° 16,4994' W	0	62° 11,6293' S	57° 16,5917' W	18:53:32	0	back to the white area
254	62° 11,6058' S	57° 16,4964' W	0	62° 11,6217' S	57° 16,5992' W	18:54:25	0	sedimented talus
255	62° 11,6091' S	57° 16,5057' W	0	62° 11,6138' S	57° 16,5523' W	18:55:43	0	brittle stars in soft sediment
256	62° 11,6239' S	57° 16,5040' W	0	62° 11,6167' S	57° 16,5488' W	18:57:02	0	sedimented outcrop, no white patches, few brittle stars
257	62° 11,6031' S	57° 16,5049' W	0	62° 11,6269' S	57° 16,5462' W	19:00:18	0	soft sediment
258	62° 11,6025' S	57° 16,5016' W	0	62° 11,6265' S	57° 16,5529' W	19:00:37	0	sedimented talus
259	62° 11,5994' S	57° 16,4971' W	0	62° 11,6223' S	57° 16,5414' W	19:01:35	0	terrace, brittle stars in soft sediments, no patches
260	62° 11,5849' S	57° 16,5332' W	0	62° 11,6000' S	57° 16,5602' W	19:03:33	0	scarp
261	62° 11,5760' S	57° 16,5474' W	0	62° 11,6001' S	57° 16,5573' W	19:04:25	0	another scarp, terrace in between
262	62° 11,5730' S	57° 16,5526' W	0	62° 11,5939' S	57° 16,5542' W	19:04:43	0	sedimented talus
263	62° 11,5663' S	57° 16,5587' W	0	62° 11,5688' S	57° 16,5625' W	19:05:16	0	rocky terrain
264	62° 11,5632' S	57° 16,5623' W	0	62° 11,5863' S	57° 16,5527' W	19:05:32	0	white area, patches

<i>Ship Nr</i>	<i>Latitude</i>	<i>Ship Longitude</i>	<i>Hydrosweep Depth [m]</i>	<i>Sub1 Latitude</i>	<i>Sub1 Longitude</i>	<i>Time [UTC]</i>	<i>CTD [m]</i>	<i>Remark</i>
265	62° 11,5499' S	57° 16,5817' W	0	62° 11,5828' S	57° 16,5944' W	19:07:00	0	ridge, single white spot
266	62° 11,5420' S	57° 16,5913' W	0	62° 11,5803' S	57° 16,5623' W	19:07:29	0	another white spot
267	62° 11,5287' S	57° 16,6026' W	0	62° 11,5636' S	57° 16,6096' W	19:09:22	0	ridge, chimney-like
268	62° 11,5105' S	57° 16,6143' W	0	62° 11,5495' S	57° 16,6225' W	19:10:48	0	grab!
269	62° 11,5136' S	57° 16,5542' W	0	62° 11,5240' S	57° 16,6175' W	19:15:13	0	off bottom
270	62° 11,5189' S	57° 16,5364' W	0	62° 11,5267' S	57° 16,5959' W	19:17:55	0	heaving to deck
271	62° 11,5248' S	57° 16,5373' W	0	62° 11,5273' S	57° 16,5940' W	19:19:18	0	tapes off

SONNE - 155



60 Records

SO 155**07 GTVA****Freitag, 2. März 2001**

Ship Nr	Ship Latitude	Ship Longitude	Hydrosweep Depth [m]	Subl Latitude	Subl Longitude	Time [UTC]	CTD [m]	Remark
272	62° 11,5075' S	57° 16,9043' W	0	62° 11,5482' S	57° 16,5960' W	21:03:24	0	TVgrab cable stuck
273	62° 11,5514' S	57° 17,1059' W	0	62° 11,5264' S	57° 17,1609' W	21:16:12	0	TVgrab went into the water, wire out is 60m
274	62° 11,5467' S	57° 17,0722' W	0	62° 11,5546' S	57° 17,1170' W	21:18:14	0	station stopped because of increasingly poor weather conditions !!!
275	62° 11,5679' S	57° 17,0928' W	0	62° 11,5612' S	57° 17,0556' W	21:22:57	0	TVgrab out of the water
276	62° 11,5929' S	57° 17,1768' W	0	62° 11,5612' S	57° 17,0556' W	21:26:24	0	TVgrab on deck, end of station
277	62° 11,5044' S	57° 16,6644' W	0	62° 11,5612' S	57° 17,0556' W	10:59:44	0	TVgrab is prepared for station
278	62° 11,5195' S	57° 16,6075' W	0	62° 11,5214' S	57° 16,6627' W	11:55:48	0	videos turned on, winch operator changed to the geology lab, objectives: to sample barite spire of southern wall of Hook Ridge
279	62° 11,5277' S	57° 16,6195' W	0	62° 11,5144' S	57° 16,6562' W	11:58:05	0	bottom sight next to small rock outcrop with white staining on some of the talus pieces
280	62° 11,5123' S	57° 16,6286' W	0	62° 11,5208' S	57° 16,6814' W	12:00:33	0	abundant white patches on slope facing north, few brittle stars
281	62° 11,5044' S	57° 16,6277' W	0	62° 11,5193' S	57° 16,6861' W	12:01:24	0	thin crusts on top of sediment with silica patches, anemones
282	62° 11,4957' S	57° 16,6286' W	0	62° 11,4990' S	57° 16,6977' W	12:03:10	0	silica along cracks
283	62° 11,5133' S	57° 16,6128' W	0	62° 11,5022' S	57° 16,6775' W	12:05:13	0	ship is turning, and we are now on the same cracks
284	62° 11,5190' S	57° 16,6173' W	0	62° 11,5170' S	57° 16,6858' W	12:09:36	0	heavily sedimented area north of the target
285	62° 11,5282' S	57° 16,6123' W	0	62° 11,5209' S	57° 16,6472' W	12:11:44	0	approaching the target area, some outcrop (small ridge) then back to sediment

<i>Ship Nr</i>	<i>Latitude</i>	<i>Ship Longitude</i>	<i>Hydrosweep Depth [m]</i>	<i>Subl Latitude</i>	<i>Subl Longitude</i>	<i>Time [UTC]</i>	<i>CTD [m]</i>	<i>Remark</i>
286	62° 11,5398' S	57° 16,5798' W	0	62° 11,5204' S	57° 16,6590' W	12:13:06	0	white patches on sedimented terrace
287	62° 11,5456' S	57° 16,5542' W	0	62° 11,5327' S	57° 16,6256' W	12:14:14	0	still same siliceous area, salt and pepper texture
288	62° 11,5449' S	57° 16,5138' W	0	62° 11,5442' S	57° 16,5979' W	12:16:09	0	back into sediment
289	62° 11,5287' S	57° 16,5063' W	0	62° 11,5553' S	57° 16,5620' W	12:17:14	0	protrusions through the sediment, red staining in the sediment
290	62° 11,5045' S	57° 16,5112' W	0	62° 11,5351' S	57° 16,5378' W	12:18:38	0	we are east of the previously mapped area, the sediment shows signs of Fe-oxyhydroxides in circular (burrow) features
291	62° 11,4983' S	57° 16,5133' W	0	62° 11,5230' S	57° 16,5379' W	12:19:24	0	thick sediment with brittle stars and anemones
292	62° 11,4947' S	57° 16,5079' W	0	62° 11,5007' S	57° 16,5689' W	12:20:46	0	ship is turning north to get a second try on the target
293	62° 11,4978' S	57° 16,5194' W	0	62° 11,4918' S	57° 16,5789' W	12:22:17	0	thick sediment within the crater (north of the target)
294	62° 11,5088' S	57° 16,5320' W	0	62° 11,4890' S	57° 16,5790' W	12:23:52	0	sediment, we are approaching the target from NNE (100m to go)
295	62° 11,5099' S	57° 16,5611' W	0	62° 11,4878' S	57° 16,5938' W	12:26:22	0	thick sediment, grab is 100m to the north
296	62° 11,5048' S	57° 16,5930' W	0	62° 11,4935' S	57° 16,6047' W	12:28:26	0	thick sediment, still 75m to go
297	62° 11,5110' S	57° 16,6122' W	0	62° 11,4972' S	57° 16,6135' W	12:29:48	0	first signs of silica precipitates
298	62° 11,5137' S	57° 16,6089' W	0	62° 11,5072' S	57° 16,6322' W	12:30:30	0	the number of brittle stars is increasing as we approach the target
299	62° 11,5157' S	57° 16,6026' W	0	62° 11,5050' S	57° 16,6370' W	12:31:07	0	more white patches and some dark material
300	62° 11,5309' S	57° 16,5709' W	0	62° 11,5165' S	57° 16,6376' W	12:33:26	0	sediment, 50m to go, some brittle stars
301	62° 11,5310' S	57° 16,5485' W	0	62° 11,5298' S	57° 16,6386' W	12:34:58	0	grab is now northwest of the target, getting closer, thick sediment
302	62° 11,5289' S	57° 16,5413' W	0	62° 11,5165' S	57° 16,5976' W	12:37:30	0	still in sediment, grab is north of the target
303	62° 11,5108' S	57° 16,6057' W	0	62° 11,5020' S	57° 16,6191' W	12:41:29	0	white patches
304	62° 11,4981' S	57° 16,6204' W	0	62° 11,4994' S	57° 16,6494' W	12:43:33	0	coming out of the sediment into white material
305	62° 11,4943' S	57° 16,6250' W	0	62° 11,4927' S	57° 16,6649' W	12:45:28	0	white crusts within crusts, dredge target !!!

Ship Nr	Ship Latitude	Ship Longitude	Hydrosweep Depth [m]	Subl Latitude	Subl Longitude	Time [UTC]	CTD [m]	Remark
306	62° 11,5036' S	57° 16,6031' W	0	62° 11,5044' S	57° 16,6838' W	12:47:04	0	it looks as if there is a large hydrothermal cap underneath a thin sediment cover, high T underneath?
307	62° 11,5073' S	57° 16,5859' W	0	62° 11,5059' S	57° 16,6497' W	12:48:16	0	back into sediment
308	62° 11,5100' S	57° 16,5836' W	0	62° 11,4988' S	57° 16,6690' W	12:49:05	0	again some white patches with dark protrusions
309	62° 11,5191' S	57° 16,6051' W	0	62° 11,5129' S	57° 16,6477' W	12:53:59	0	we are still 100m north of our target
310	62° 11,5182' S	57° 16,5500' W	0	62° 11,5129' S	57° 16,6301' W	12:57:40	0	white patches, salty texture (small dotsize)
311	62° 11,5244' S	57° 16,5936' W	0	62° 11,5069' S	57° 16,6091' W	13:02:59	0	abundant brittle stars and few silica patches visible
312	62° 11,5133' S	57° 16,6094' W	0	62° 11,5159' S	57° 16,6482' W	13:06:51	0	thick sediment
313	62° 11,5120' S	57° 16,6077' W	0	62° 11,5142' S	57° 16,6596' W	13:07:18	0	tapes are finished and are being changed
314	62° 11,5297' S	57° 16,5902' W	0	62° 11,5132' S	57° 16,6680' W	13:10:11	0	thick sediment, we are northwest of the target
315	62° 11,5379' S	57° 16,6062' W	0	62° 11,5287' S	57° 16,6598' W	13:13:23	0	white patches with black and white (salt/pepper) texture, linear features might indicate resedimentation
316	62° 11,5292' S	57° 16,6255' W	0	62° 11,5244' S	57° 16,6438' W	13:15:36	0	still in hydrothermally influenced area
317	62° 11,5270' S	57° 16,6220' W	0	62° 11,5299' S	57° 16,6706' W	13:17:39	0	salt and pepper texture with lineations
318	62° 11,5390' S	57° 16,6037' W	0	62° 11,5279' S	57° 16,6646' W	13:22:27	0	the grab is 50 m NW of the target, slowly approaching, be patient
319	62° 11,5400' S	57° 16,6214' W	0	62° 11,5361' S	57° 16,6757' W	13:26:26	0	thick sediment, drifting backwards (westwards)
320	62° 11,5474' S	57° 16,5858' W	0	62° 11,5577' S	57° 16,6384' W	13:30:12	0	rock outcrops, target is very close now
321	62° 11,5461' S	57° 16,5818' W	0	62° 11,5521' S	57° 16,6450' W	13:30:55	0	salt and pepper sediment, hydrothermal blocks and crust
322	62° 11,5426' S	57° 16,5751' W	0	62° 11,5529' S	57° 16,6534' W	13:32:10	0	grab position for dredge target
323	62° 11,5406' S	57° 16,5704' W	0	62° 11,5439' S	57° 16,6363' W	13:34:02	0	white patches in sediment, no outcrop
324	62° 11,5385' S	57° 16,5606' W	0	62° 11,5492' S	57° 16,6153' W	13:35:28	0	getting "hilly"
325	62° 11,5384' S	57° 16,5481' W	0	62° 11,5455' S	57° 16,6182' W	13:36:54	0	back to sediment, with more abundant brittle stars

<i>Ship Nr</i>	<i>Latitude</i>	<i>Ship Longitude</i>	<i>Hydrosweep Depth [m]</i>	<i>Subl Latitude</i>	<i>Subl Longitude</i>	<i>Time [UTC]</i>	<i>CTD [m]</i>	<i>Remark</i>
326	62° 11,5547' S	57° 16,5314' W	0	62° 11,5431' S	57° 16,5921' W	13:39:50	0	the wall, few m up, then brittle stars
327	62° 11,5541' S	57° 16,5388' W	0	62° 11,5428' S	57° 16,5725' W	13:42:10	0	big block
328	62° 11,5537' S	57° 16,5433' W	0	62° 11,5442' S	57° 16,5883' W	13:42:32	0	grab taken, 10 m fieren, red dust shows hydrothermal origin of the sample
329	62° 11,5526' S	57° 16,5595' W	0	62° 11,5374' S	57° 16,5976' W	13:44:30	0	heaving to deck
330	62° 11,5382' S	57° 16,5848' W	0	62° 11,5388' S	57° 16,6365' W	13:49:32	0	tapes turned off
331	62° 11,5407' S	57° 16,5680' W	0	62° 11,5252' S	57° 16,5836' W	14:03:40	0	grab out of the water

SONNE - 155



114 Records

SO 155**08 GTVA****Samstag, 3. März 2001**

<i>Ship Nr</i>	<i>Ship Latitude</i>	<i>Ship Longitude</i>	<i>Hydrosweep Depth [m]</i>	<i>Subl Latitude</i>	<i>Subl Longitude</i>	<i>Time [UTC]</i>	<i>CTD [m]</i>	<i>Remark</i>
332	62° 11,5475' S	57° 16,5792' W	0	62° 11,5311' S	57° 16,6208' W	15:50:15	0	950m cable out
333	62° 11,5531' S	57° 16,5850' W	0	62° 11,5342' S	57° 16,6200' W	15:51:48	0	1000m
334	62° 11,5566' S	57° 16,5880' W	0	62° 11,5372' S	57° 16,6257' W	15:52:58	0	tapes on
335	62° 11,5581' S	57° 16,5874' W	0	62° 11,5364' S	57° 16,6412' W	15:53:52	0	bottom sight
336	62° 11,5581' S	57° 16,5848' W	0	62° 11,5383' S	57° 16,6097' W	15:54:04	0	soft grey sediment, few brittle stars, no patches so far
337	62° 11,5578' S	57° 16,5815' W	0	62° 11,5380' S	57° 16,6454' W	15:54:31	0	about 50m NW of the sample target
338	62° 11,5588' S	57° 16,5789' W	0	62° 11,5443' S	57° 16,6299' W	15:54:55	0	subposition is 50-60m NE of the ship
339	62° 11,5601' S	57° 16,5699' W	0	62° 11,5493' S	57° 16,6100' W	15:55:34	0	first white patches, a sort of lining up
340	62° 11,5596' S	57° 16,5590' W	0	62° 11,5509' S	57° 16,6147' W	15:56:36	0	back to greyish sediment
341	62° 11,5579' S	57° 16,5477' W	0	62° 11,5588' S	57° 16,6033' W	15:57:38	0	rocky outcrop to the left, passed by
342	62° 11,5580' S	57° 16,5418' W	0	62° 11,5590' S	57° 16,5980' W	15:57:59	0	white patches, crusts, some are very blocky in nature
343	62° 11,5552' S	57° 16,5360' W	0	62° 11,5564' S	57° 16,5834' W	15:58:45	0	cliff, going along not upwards, very few white spots
344	62° 11,5528' S	57° 16,5341' W	0	62° 11,5571' S	57° 16,5885' W	15:59:35	0	back to darkgrey sediment, very few white patches
345	62° 11,5505' S	57° 16,5313' W	0	62° 11,5476' S	57° 16,5803' W	15:59:59	0	crusts, rather sedimented talus
346	62° 11,5461' S	57° 16,5325' W	0	62° 11,5473' S	57° 16,5751' W	16:00:49	0	rocky outcrop, blocky in nature, moving down the cliff, small terrace
347	62° 11,5432' S	57° 16,5316' W	0	62° 11,5349' S	57° 16,5820' W	16:01:33	0	back to patchy greyish sediment, brittle stars, no specks

Ship Nr	Ship Latitude	Ship Longitude	Hydrosweep Depth [m]	Subl Latitude	Subl Longitude	Time [UTC]	CTD [m]	Remark
348	62° 11,5436' S	57° 16,5392' W	0	62° 11,5249' S	57° 16,5803' W	16:02:48	0	few white specks again
349	62° 11,5460' S	57° 16,5443' W	0	62° 11,5268' S	57° 16,5715' W	16:03:22	0	sedimented talus; location of 07 GTVA
350	62° 11,5459' S	57° 16,5456' W	0	62° 11,5282' S	57° 16,5766' W	16:05:09	0	blocky sedimented talus; ship is not moving
351	62° 11,5467' S	57° 16,5456' W	0	62° 11,5299' S	57° 16,5706' W	16:06:16	0	subposition is NE of the target; trying to go slowly SW
352	62° 11,5542' S	57° 16,5637' W	0	62° 11,5335' S	57° 16,5694' W	16:07:44	0	cliff again; few white specks in the sediment
353	62° 11,5542' S	57° 16,5688' W	0	62° 11,5334' S	57° 16,5966' W	16:08:58	0	rock talus in soft sediment
354	62° 11,5611' S	57° 16,5736' W	0	62° 11,5395' S	57° 16,5993' W	16:10:23	0	soft sediment, no brittle stars
355	62° 11,5650' S	57° 16,5799' W	0	62° 11,5485' S	57° 16,5908' W	16:11:10	0	crusts, sedimented; subposition is N of the ship
356	62° 11,5628' S	57° 16,5831' W	0	62° 11,5415' S	57° 16,6168' W	16:13:47	0	black patch to the right
357	62° 11,5731' S	57° 16,5788' W	0	62° 11,5558' S	57° 16,6196' W	16:16:36	0	soft grey sediment, number of brittle stars increase
358	62° 11,5722' S	57° 16,5832' W	0	62° 11,5469' S	57° 16,6152' W	16:18:09	0	white specks increase
359	62° 11,5721' S	57° 16,5813' W	0	62° 11,5458' S	57° 16,5989' W	16:19:38	0	still in the spotty area
360	62° 11,5756' S	57° 16,5877' W	0	62° 11,5439' S	57° 16,5900' W	16:21:39	0	larger white spots
361	62° 11,5782' S	57° 16,5937' W	0	62° 11,5550' S	57° 16,5906' W	16:22:07	0	cliff, passed by
362	62° 11,5835' S	57° 16,6011' W	0	62° 11,5593' S	57° 16,5908' W	16:22:56	0	spotty sediment
363	62° 11,5825' S	57° 16,5982' W	0	62° 11,5675' S	57° 16,6078' W	16:23:36	0	white areas increase
364	62° 11,5777' S	57° 16,5918' W	0	62° 11,5539' S	57° 16,6207' W	16:24:39	0	white crusts
365	62° 11,5745' S	57° 16,5889' W	0	62° 11,5609' S	57° 16,6036' W	16:25:27	0	back to the spotty sediment, few brittle stars
366	62° 11,5743' S	57° 16,5849' W	0	62° 11,5489' S	57° 16,6149' W	16:26:02	0	shrimp
367	62° 11,5735' S	57° 16,5856' W	0	62° 11,5561' S	57° 16,5980' W	16:26:13	0	more shrimps
368	62° 11,5729' S	57° 16,5849' W	0	62° 11,5520' S	57° 16,5996' W	16:26:59	0	lining of white specks

<i>Ship Nr</i>	<i>Latitude</i>	<i>Ship Longitude</i>	<i>Hydrosweep Depth [m]</i>	<i>Subl Latitude</i>	<i>Subl Longitude</i>	<i>Time [UTC]</i>	<i>CTD [m]</i>	<i>Remark</i>
369	62° 11,5747' S	57° 16,5838' W	0	62° 11,5414' S	57° 16,5929' W	16:27:36	0	shrimp
370	62° 11,5786' S	57° 16,5825' W	0	62° 11,5601' S	57° 16,6018' W	16:28:39	0	spotty area, few brittle stars
371	62° 11,5824' S	57° 16,5805' W	0	62° 11,5554' S	57° 16,6121' W	16:29:31	0	sedimented crusts
372	62° 11,5851' S	57° 16,5830' W	0	62° 11,5597' S	57° 16,6165' W	16:30:35	0	crusts, base of the cliff
373	62° 11,5871' S	57° 16,5895' W	0	62° 11,5750' S	57° 16,6010' W	16:31:48	0	lots of anemones, sedimented talus
374	62° 11,5915' S	57° 16,6038' W	0	62° 11,5549' S	57° 16,6084' W	16:33:32	0	passing along the cliff, again sedimented talus, no white spots
375	62° 11,5951' S	57° 16,6321' W	0	62° 11,5628' S	57° 16,6187' W	16:35:13	0	still in sedimented talus, obviously going down the slope
376	62° 11,5953' S	57° 16,6503' W	0	62° 11,5719' S	57° 16,6307' W	16:36:24	0	subposition is 50m SW of sample target; N of the ship
377	62° 11,5945' S	57° 16,6642' W	0	62° 11,5640' S	57° 16,6422' W	16:37:35	0	soft grey sediment, single brittle star, anemones
378	62° 11,5829' S	57° 16,6286' W	0	62° 11,5694' S	57° 16,6205' W	16:41:01	0	brittle stars again
379	62° 11,5810' S	57° 16,6208' W	0	62° 11,5631' S	57° 16,5899' W	16:41:28	0	sedimented talus of the cliff
380	62° 11,5771' S	57° 16,6088' W	0	62° 11,5672' S	57° 16,5855' W	16:42:35	0	still the cliff with sedimented talus and outcrops
381	62° 11,5712' S	57° 16,6127' W	0	62° 11,5593' S	57° 16,5876' W	16:44:09	0	back to the sediment; moved along the cliff
382	62° 11,5710' S	57° 16,6183' W	0	62° 11,5535' S	57° 16,5964' W	16:44:47	0	subposition is still N of the ship; 50-60m NE
383	62° 11,5717' S	57° 16,6208' W	0	62° 11,5561' S	57° 16,6044' W	16:45:05	0	altered outcrop, bottom of the cliff; squid; rather a massive block of dacite?!
384	62° 11,5757' S	57° 16,6193' W	0	62° 11,5498' S	57° 16,6200' W	16:46:29	0	back to the soft sediment
385	62° 11,5768' S	57° 16,6065' W	0	62° 11,5581' S	57° 16,6205' W	16:47:24	0	still at the bottom of the cliff; need to go to the S
386	62° 11,5688' S	57° 16,5761' W	0	62° 11,5572' S	57° 16,6314' W	16:49:02	0	soft grey sediment, few brittle stars
387	62° 11,5663' S	57° 16,5654' W	0	62° 11,5618' S	57° 16,6296' W	16:49:53	0	increasing number of brittle stars
388	62° 11,5678' S	57° 16,5604' W	0	62° 11,5540' S	57° 16,6007' W	16:50:18	0	white spotty area

Ship Nr	Ship Latitude	Ship Longitude	Hydrosweep Depth [m]	Sub1 Latitude	Sub1 Longitude	Time [UTC]	CTD [m]	Remark
389	62° 11,5752' S	57° 16,5563' W	0	62° 11,5645' S	57° 16,6082' W	16:51:04	0	ship changes the course
390	62° 11,5790' S	57° 16,5556' W	0	62° 11,5705' S	57° 16,6061' W	16:52:16	0	cliff
391	62° 11,5702' S	57° 16,5484' W	0	62° 11,5496' S	57° 16,6151' W	16:53:31	0	white precipitates
392	62° 11,5716' S	57° 16,5454' W	0	62° 11,5537' S	57° 16,5834' W	16:54:52	0	back to the grey sediment
393	62° 11,5809' S	57° 16,5436' W	0	62° 11,5650' S	57° 16,5831' W	16:55:44	0	white patches
394	62° 11,5941' S	57° 16,5490' W	0	62° 11,5758' S	57° 16,5765' W	16:58:13	0	patchy sediment
395	62° 11,5906' S	57° 16,5453' W	0	62° 11,5652' S	57° 16,5748' W	16:59:24	0	white patchy area
396	62° 11,5926' S	57° 16,5469' W	0	62° 11,5688' S	57° 16,5665' W	17:00:15	0	very highly altered material at the bottom of the cliff
397	62° 11,6133' S	57° 16,5529' W	0	62° 11,5868' S	57° 16,5745' W	17:02:43	0	sedimented talus
398	62° 11,6185' S	57° 16,5580' W	0	62° 11,5872' S	57° 16,5669' W	17:03:18	0	sedimented outcrop; brittle stars
399	62° 11,6253' S	57° 16,5667' W	0	62° 11,5926' S	57° 16,5781' W	17:04:26	0	brittle stars, no patches
400	62° 11,6257' S	57° 16,5727' W	0	62° 11,5945' S	57° 16,5905' W	17:05:45	0	heavily sedimented outcrop, brittle stars around, no patches
401	62° 11,6245' S	57° 16,5775' W	0	62° 11,5964' S	57° 16,5728' W	17:06:38	0	subposition is too far south
402	62° 11,6236' S	57° 16,5806' W	0	62° 11,5949' S	57° 16,5592' W	17:07:16	0	subposition is too far south
403	62° 11,6227' S	57° 16,5840' W	0	62° 11,6045' S	57° 16,5571' W	17:07:36	0	sedimented talus/outcrop
404	62° 11,6295' S	57° 16,6058' W	0	62° 11,6068' S	57° 16,5913' W	17:09:19	0	this feature is a steep ridge
405	62° 11,6363' S	57° 16,6408' W	0	62° 11,6127' S	57° 16,6036' W	17:12:58	0	shrimp
406	62° 11,6155' S	57° 16,6315' W	0	62° 11,6336' S	57° 16,5854' W	17:18:19	0	rocky outcrop and sedimented talus, no white patches
407	62° 11,5920' S	57° 16,6214' W	0	62° 11,6027' S	57° 16,5734' W	17:21:46	0	sedimented ridge
408	62° 11,5880' S	57° 16,6148' W	0	62° 11,5951' S	57° 16,5527' W	17:22:56	0	very few white spots
409	62° 11,5815' S	57° 16,6134' W	0	62° 11,5779' S	57° 16,5722' W	17:26:22	0	few white spots, heavily sedimented talus

Ship Nr	Ship Latitude	Ship Longitude	Hydrosweep Depth [m]	Subl Latitude	Subl Longitude	Time [UTC]	CTD [m]	Remark
410	62° 11,5800' S	57° 16,6228' W	0	62° 11,5630' S	57° 16,5636' W	17:27:57	0	white spots
411	62° 11,5645' S	57° 16,6370' W	0	62° 11,5714' S	57° 16,5837' W	17:29:58	0	back to grey sediment
412	62° 11,5659' S	57° 16,6413' W	0	62° 11,5601' S	57° 16,6050' W	17:33:27	0	still grey sediment
413	62° 11,5511' S	57° 16,6274' W	0	62° 11,5586' S	57° 16,5692' W	17:35:33	0	still grey sediment, few brittle stars; subposition is slightly 50m SE of the ship
414	62° 11,5451' S	57° 16,6238' W	0	62° 11,5432' S	57° 16,5866' W	17:37:49	0	grey sediment, few brittle stars
415	62° 11,5445' S	57° 16,6221' W	0	62° 11,5362' S	57° 16,5696' W	17:38:06	0	white patches, approaching the target
416	62° 11,5482' S	57° 16,6084' W	0	62° 11,5456' S	57° 16,5814' W	17:39:09	0	crusts
417	62° 11,5626' S	57° 16,5804' W	0	62° 11,5432' S	57° 16,5611' W	17:40:41	0	white spots are coming, crusts
418	62° 11,5681' S	57° 16,5709' W	0	62° 11,5431' S	57° 16,5552' W	17:41:39	0	spotty area
419	62° 11,5736' S	57° 16,5778' W	0	62° 11,5481' S	57° 16,5644' W	17:42:37	0	back to the grey sediment
420	62° 11,5768' S	57° 16,6184' W	0	62° 11,5660' S	57° 16,5552' W	17:44:10	0	sedimented talus and outcrop
421	62° 11,5786' S	57° 16,6502' W	0	62° 11,5681' S	57° 16,5764' W	17:46:05	0	increasing number of brittle stars
422	62° 11,5983' S	57° 16,6103' W	0	62° 11,5654' S	57° 16,6038' W	17:47:25	0	sedimented talus, few tiny spots
423	62° 11,6098' S	57° 16,5719' W	0	62° 11,5800' S	57° 16,5999' W	17:49:14	0	black clouds, red staining
424	62° 11,6449' S	57° 16,5573' W	0	62° 11,6057' S	57° 16,5764' W	17:54:28	0	sedimented ridge to the right
425	62° 11,6468' S	57° 16,5712' W	0	62° 11,6194' S	57° 16,5560' W	17:55:40	0	big dacite(?) dome
426	62° 11,6564' S	57° 16,6249' W	0	62° 11,6339' S	57° 16,5882' W	17:59:32	0	back to grey sediment, way to far south; going N
427	62° 11,6531' S	57° 16,6422' W	0	62° 11,6368' S	57° 16,5942' W	18:01:15	0	single rock
428	62° 11,6421' S	57° 16,6460' W	0	62° 11,6380' S	57° 16,5828' W	18:02:43	0	soft sediment
429	62° 11,6258' S	57° 16,6429' W	0	62° 11,6408' S	57° 16,5895' W	18:04:19	0	few rocks

<i>Ship Nr</i>	<i>Ship Latitude</i>	<i>Ship Longitude</i>	<i>Hydrosweep Depth [m]</i>	<i>Subl Latitude</i>	<i>Subl Longitude</i>	<i>Time [UTC]</i>	<i>CTD [m]</i>	<i>Remark</i>
430	62° 11,6157' S	57° 16,6288' W	0	62° 11,6294' S	57° 16,5795' W	18:06:23	0	ridge, brittle stars
431	62° 11,6035' S	57° 16,6326' W	0	62° 11,6020' S	57° 16,5974' W	18:11:20	0	sedimented talus, few brittle stars
432	62° 11,5897' S	57° 16,6466' W	0	62° 11,5937' S	57° 16,6118' W	18:13:55	0	slightly sedimented ridge
433	62° 11,5670' S	57° 16,6454' W	0	62° 11,5673' S	57° 16,5981' W	18:21:39	0	ridge to the right
434	62° 11,5632' S	57° 16,6422' W	0	62° 11,5591' S	57° 16,5928' W	18:24:42	0	soft grey sediment
435	62° 11,5604' S	57° 16,6422' W	0	62° 11,5525' S	57° 16,6020' W	18:32:53	0	brittle stars
436	62° 11,5488' S	57° 16,6540' W	0	62° 11,5548' S	57° 16,6013' W	18:35:07	0	sedimented crusts
437	62° 11,5394' S	57° 16,6556' W	0	62° 11,5471' S	57° 16,6074' W	18:36:31	0	grab
438	62° 11,5369' S	57° 16,6556' W	0	62° 11,5442' S	57° 16,6192' W	18:37:02	0	grab
439	62° 11,5546' S	57° 16,6183' W	0	62° 11,5454' S	57° 16,6207' W	18:40:36	0	grab opened, moving to the next spot
440	62° 11,5387' S	57° 16,6368' W	0	62° 11,5148' S	57° 16,5262' W	18:43:06	0	bottom sight
441	62° 11,5359' S	57° 16,6233' W	0	62° 11,5173' S	57° 16,5789' W	18:46:54	0	ridge, moving upwards
442	62° 11,5364' S	57° 16,6301' W	0	62° 11,5264' S	57° 16,5868' W	18:48:43	0	heaving to clean the grab
443	62° 11,5270' S	57° 16,6347' W	0	62° 11,5262' S	57° 16,5820' W	18:51:06	0	bottom sight
444	62° 11,5274' S	57° 16,6354' W	0	62° 11,5208' S	57° 16,5904' W	18:51:33	0	soft sediment, ridge to the left
445	62° 11,5315' S	57° 16,6327' W	0	62° 11,5173' S	57° 16,6002' W	18:53:26	0	no sight; heaving to deck

SONNE - 155



126 Records

SO 155**41 OFOS****Mittwoch, 7. März 2001**

Ship Nr	Ship Latitude	Ship Longitude	Hydrosweep Depth [m]	Sub1 Latitude	Sub1 Longitude	Time [UTC]	CTD [m]	Remark
451	62° 24,9186' S	58° 23,8614' W	0	62° 11,5495' S	57° 16,6772' W	22:50:02	14	station begins
452	62° 24,9663' S	58° 24,0756' W	0	62° 11,5495' S	57° 16,6772' W	23:00:33	14	problems with the cable
453	62° 25,0014' S	58° 24,0915' W	0	62° 11,5495' S	57° 16,6772' W	23:04:21	17	in the water
454	62° 25,0072' S	58° 24,0974' W	0	62° 24,9964' S	58° 24,1674' W	23:05:19	44	with 1.0 to 700 m fieren
455	62° 24,9798' S	58° 24,0027' W	0	62° 25,0049' S	58° 24,0559' W	23:12:02	428	We start the OFOS in the NE entrance to the crater at a waterdepth of 900 m. We will then head down into the crater. The OFOS will be raised an moved to the southern crater wall (WP3 62°26.75 S / 58°24.90 W) where it will be lowered.
456	62° 24,9387' S	58° 23,9138' W	0	62° 24,9807' S	58° 23,9910' W	23:17:47	706	winch operator changed to the geolab; videos turned on
457	62° 24,9352' S	58° 23,9017' W	0	62° 24,9692' S	58° 23,9749' W	23:18:39	720	350 m west of WP 1 (62°24.90 S / 58°23.60 W), slowly drifting
458	62° 24,9260' S	58° 23,8345' W	0	62° 24,9799' S	58° 23,9366' W	23:22:35	918	bottom sight in sedimented area with brittle stars, mottled texture
459	62° 24,9221' S	58° 23,7911' W	934	62° 24,9798' S	58° 23,8953' W	23:24:57	910	lots of biology on rocky surfaces
460	62° 24,9185' S	58° 23,7687' W	931	62° 24,9687' S	58° 23,8897' W	23:26:12	910	still sedimented with the mottled coarse grained looking texture
461	62° 24,9143' S	58° 23,7365' W	929	62° 24,9756' S	58° 23,8388' W	23:28:41	907	same sediment with brittle stars and golf balls
462	62° 24,9091' S	58° 23,6917' W	928	62° 24,9634' S	58° 23,7973' W	23:31:06	907	the coarse dark material is disappearing, fine sediment is increasing, less brittle stars
463	62° 24,9249' S	58° 23,6742' W	928	62° 24,9507' S	58° 23,7764' W	23:35:08	900	slowly approaching the entrance to the crater, sub is standing still, since ship turned into the track

Ship Nr	Ship Latitude	Ship Longitude	Hydrosweep Depth [m]	Subl Latitude	Subl Longitude	Time [UTC]	CTD [m]	Remark
464	62° 24,9413' S	58° 23,6670' W	927	62° 24,9509' S	58° 23,7629' W	23:36:58	900	slowly climbing upwards, same mottled texture as before, ship is now at the same spot as the OFOS
465	62° 24,9624' S	58° 23,6841' W	930	62° 24,9613' S	58° 23,7401' W	23:39:18	900	large boulder within the sediment
466	62° 24,9696' S	58° 23,6886' W	930	62° 24,9608' S	58° 23,7452' W	23:40:00	901	same sediment as before
467	62° 24,9807' S	58° 23,6900' W	933	62° 24,9681' S	58° 23,7553' W	23:41:00	903	we reached the highest point along this track and are going down into the crater in area of thick sediment
468	62° 24,9911' S	58° 23,6857' W	935	62° 24,9793' S	58° 23,7522' W	23:42:00	905	same sediment
469	62° 25,0107' S	58° 23,6861' W	939	62° 24,9931' S	58° 23,7470' W	23:44:00	908	mottled sediment with fewer dark patches
470	62° 25,0199' S	58° 23,6942' W	942	62° 25,0120' S	58° 23,7587' W	23:45:03	908	same sediment , the steep cliff down is ahead of us
471	62° 25,0334' S	58° 23,7199' W	945	62° 25,0139' S	58° 23,7673' W	23:46:34	909	there seem to be more sea urchins here, also the number of brittle stars seems to have increased
472	62° 25,0430' S	58° 23,7395' W	948	62° 25,0229' S	58° 23,7588' W	23:47:41	909	less brittle stars here
473	62° 25,0505' S	58° 23,7607' W	954	62° 25,0363' S	58° 23,7707' W	23:48:53	913	the water column is a bit murky
474	62° 25,0745' S	58° 23,7739' W	971	62° 25,0534' S	58° 23,8138' W	23:51:05	927	mottled texture in sediment, abundant brittle stars, sediment has darker color
475	62° 25,0939' S	58° 23,7638' W	974	62° 25,0725' S	58° 23,8450' W	23:53:12	937	really going down now
476	62° 25,0977' S	58° 23,7612' W	978	62° 25,0818' S	58° 23,8435' W	23:53:51	941	still sedimented
477	62° 25,1095' S	58° 23,7771' W	992	62° 25,0993' S	58° 23,8448' W	23:55:30	953	mottled sediment with some brittle stars, sea feathers
478	62° 25,1185' S	58° 23,7878' W	1006	62° 25,1106' S	58° 23,8394' W	23:56:29	958	blocky outcrop, dark coarse sediment, still streaky
479	62° 25,1327' S	58° 23,7895' W	1015	62° 25,1269' S	58° 23,8554' W	23:57:59	968	cliff ahead, vertical
480	62° 25,1462' S	58° 23,7772' W	1018	62° 25,1244' S	58° 23,8396' W	23:59:05	984	murky water still going down, at least 30 m vertical, small temperature anomaly
481	62° 25,1546' S	58° 23,7653' W	1014	62° 25,1372' S	58° 23,8558' W	00:00:13	994	still on cliff going down

<i>Ship Nr</i>	<i>Ship Latitude</i>	<i>Ship Longitude</i>	<i>Hydrosweep Depth [m]</i>	<i>Sub1 Latitude</i>	<i>Sub1 Longitude</i>	<i>Time [UTC]</i>	<i>CTD [m]</i>	<i>Remark</i>
482	62° 25,1577' S	58° 23,7650' W	1018	62° 25,1410' S	58° 23,8323' W	00:00:48	1001	dark sediment streaks going down the slope, temperature is still rising although we get deeper
483	62° 25,1697' S	58° 23,7803' W	1038	62° 25,1560' S	58° 23,8460' W	00:02:21	1003	we went 10 more m down, thick sediment, conductivity stayed the same since we entered the crater (unstratified water mass?)
484	62° 25,1751' S	58° 23,8096' W	1056	62° 25,1708' S	58° 23,8291' W	00:03:14	1006	next cliff ahead starting at 1006m
485	62° 25,1820' S	58° 23,8441' W	1079	62° 25,1606' S	58° 23,8211' W	00:04:15	1020	water is very murky, still going down
486	62° 25,2001' S	58° 23,8562' W	1099	62° 25,1779' S	58° 23,8734' W	00:05:48	1046	end of temperature anomaly, but still going down, blocky talus
487	62° 25,2137' S	58° 23,8763' W	1128	62° 25,1897' S	58° 23,8767' W	00:07:29	1070	same blocky talus
488	62° 25,2298' S	58° 23,8839' W	1141	62° 25,2020' S	58° 23,9094' W	00:09:26	1092	still blocky talus slope is not as dramatic any more
489	62° 25,2439' S	58° 23,8645' W	0	62° 25,2269' S	58° 23,9441' W	00:11:23	1106	talus is more heavily sedimented in this area
490	62° 25,2621' S	58° 23,8637' W	0	62° 25,2333' S	58° 23,9307' W	00:13:06	1111	small cliff, abundant biology, very small temperature anomaly, water is murky again
491	62° 25,2884' S	58° 23,8597' W	0	62° 25,2564' S	58° 23,9489' W	00:15:20	1135	going down in sedimented talus material, temperature is rising, cliff ahead
492	62° 25,3033' S	58° 23,8770' W	0	62° 25,2637' S	58° 23,9206' W	00:16:54	1150	water is even more cloudy, steep cliff
493	62° 25,3185' S	58° 23,8873' W	0	62° 25,2844' S	58° 23,9327' W	00:18:34	1177	blocky talus with sediment staining, temperature anomaly (small)
494	62° 25,3231' S	58° 23,8947' W	0	62° 25,2890' S	58° 23,9284' W	00:19:14	1181	black and white sediment with brittle stars
495	62° 25,3305' S	58° 23,9090' W	0	62° 25,3031' S	58° 23,9498' W	00:20:11	1182	the slope is gentle, abundant brittle stars in fine sediment with fewer dark areas
496	62° 25,3378' S	58° 23,9151' W	0	62° 25,3622' S	58° 23,9192' W	00:20:52	1183	its is getting hotter, few rocks
497	62° 25,3474' S	58° 23,9148' W	0	62° 25,3125' S	58° 23,9381' W	00:21:42	1182	sediment pond then rocky again (still 90% sediment though)
498	62° 25,3622' S	58° 23,8996' W	0	62° 25,3269' S	58° 23,9503' W	00:22:58	1179	salt and pepper texture of the sediment, some talus material

<i>Ship Nr</i>	<i>Ship Latitude</i>	<i>Ship Longitude</i>	<i>Hydrosweep Depth [m]</i>	<i>Subl Latitude</i>	<i>Subl Longitude</i>	<i>Time [UTC]</i>	<i>CTD [m]</i>	<i>Remark</i>
499	62° 25,3731' S	58° 23,8834' W	0	62° 25,3358' S	58° 23,9456' W	00:23:54	1174	climbing up the small hill in the northern part of the crater, still salt and pepper
500	62° 25,3829' S	58° 23,8857' W	0	62° 25,3562' S	58° 23,8631' W	00:24:55	1169	salt and pepper, few brittle stars
501	62° 25,3929' S	58° 23,8973' W	0	62° 25,3537' S	58° 23,9547' W	00:26:06	1160	always salt and pepper, temperature spike (small 0.02°C)
502	62° 25,4064' S	58° 23,9079' W	0	62° 25,3692' S	58° 23,9468' W	00:27:19	1155	more coarse grained (?) sediment moving into talus pile
503	62° 25,4145' S	58° 23,9106' W	0	62° 25,3757' S	58° 23,9590' W	00:27:59	1149	temperature is rising during climb
504	62° 25,4332' S	58° 23,9197' W	0	62° 25,4124' S	58° 24,0243' W	00:29:29	1136	in talus material
505	62° 25,4359' S	58° 23,9210' W	0	62° 25,3932' S	58° 23,9579' W	00:29:44	1133	back to salt and pepper textured sediment, still climbing up that small dome (?), temperature is going down
506	62° 25,4547' S	58° 23,9280' W	0	62° 25,4092' S	58° 23,9760' W	00:31:21	1122	temperature on the rise parallel to the depth curve
507	62° 25,4668' S	58° 23,9328' W	0	62° 25,4304' S	58° 24,0177' W	00:32:24	1115	salt and pepper, few brittle stars, more darker material, blocky outcrop
508	62° 25,4747' S	58° 23,9542' W	0	62° 25,4220' S	58° 23,9916' W	00:33:26	1106	parallel dark lines, more brittle stars, few dropstones
509	62° 25,4829' S	58° 23,9803' W	0	62° 25,4442' S	58° 23,9954' W	00:34:24	1104	sediment in washed into small depressions of volcanoclastic material, abundant brittle stars, temperature is dropping
510	62° 25,4958' S	58° 24,0146' W	0	62° 25,4519' S	58° 23,9910' W	00:35:36	1104	water column is getting murky again, we are over the top of the dome (?)
511	62° 25,5083' S	58° 24,0328' W	0	62° 25,4410' S	58° 24,0051' W	00:36:37	1110	sediment with brittle stars, far less dark material
512	62° 25,5147' S	58° 24,0408' W	0	62° 25,4095' S	58° 24,0241' W	00:37:09	1109	thick sediment with abundant urchins and fewer brittle stars
513	62° 25,5238' S	58° 24,0460' W	0	62° 25,4095' S	58° 24,0241' W	00:37:52	1108	slide 243
514	62° 25,5329' S	58° 24,0467' W	0	62° 25,5069' S	58° 23,9818' W	00:38:30	1103	fine grained sediment, black and white
515	62° 25,5532' S	58° 24,0506' W	0	62° 25,4982' S	58° 24,0813' W	00:39:57	1097	thick sediment with brittle stars, some rocky outcrops poking through
516	62° 25,5675' S	58° 24,0536' W	0	62° 25,4900' S	58° 24,0750' W	00:40:57	1097	sediment plain with abundant sea urchins (a lot!)

Ship Nr	Ship Latitude	Ship Longitude	Hydrosweep Depth [m]	Sub1 Latitude	Sub1 Longitude	Time [UTC]	CTD [m]	Remark
517	62° 25,5816' S	58° 24,0634' W	0	62° 25,5515' S	58° 24,0308' W	00:42:02	1097	thick sediment (slide 264)
518	62° 25,5959' S	58° 24,0871' W	0	62° 25,5395' S	58° 24,0966' W	00:43:09	1096	thick sediment with sea urchins, few brittle stars
519	62° 25,6073' S	58° 24,1252' W	0	62° 25,5886' S	58° 24,1060' W	00:44:16	1094	OFOS will be brought up to 500 m and then moved to Waypoint No. 3
520	62° 25,6154' S	58° 24,1516' W	0	62° 25,5623' S	58° 24,1054' W	00:45:03	1071	video stopped
521	62° 26,6735' S	58° 24,9088' W	0	62° 26,6809' S	58° 24,9379' W	02:04:11	509	on station at the southwestern crater rim
522	62° 26,6658' S	58° 24,8960' W	0	62° 26,6711' S	58° 24,9266' W	02:05:07	540	tapes on
523	62° 26,6478' S	58° 24,8711' W	0	62° 26,6790' S	58° 24,8947' W	02:07:32	662	bottom sight
524	62° 26,6454' S	58° 24,8695' W	0	62° 26,6647' S	58° 24,9219' W	02:07:58	667	dark grey sediment, soft, few biology
525	62° 26,6395' S	58° 24,8699' W	0	62° 26,6653' S	58° 24,9125' W	02:08:40	668	sediment is more coarse-grained
526	62° 26,6307' S	58° 24,8777' W	0	62° 26,6616' S	58° 24,9075' W	02:09:21	668	field of brittle stars
527	62° 26,6168' S	58° 24,8733' W	0	62° 26,6470' S	58° 24,9012' W	02:10:25	666	few sea feathers
528	62° 26,6114' S	58° 24,8646' W	0	62° 26,6449' S	58° 24,9069' W	02:11:23	662	still grey coarse-grained sediment
529	62° 26,6104' S	58° 24,8617' W	0	62° 26,6268' S	58° 24,9200' W	02:12:03	660	dropstones with much biology
530	62° 26,5892' S	58° 24,8557' W	0	62° 26,6243' S	58° 24,8837' W	02:14:48	660	still the sediment, amount of biology is increasing
531	62° 26,5834' S	58° 24,8474' W	0	62° 26,6112' S	58° 24,8887' W	02:15:25	665	small cliff
532	62° 26,5697' S	58° 24,8467' W	0	62° 26,6077' S	58° 24,8808' W	02:16:42	675	still going down, same sediment
533	62° 26,5431' S	58° 24,8515' W	0	62° 26,5980' S	58° 24,8823' W	02:19:01	701	still going down, number of brittle stars decrease
534	62° 26,5213' S	58° 24,8399' W	0	62° 26,5928' S	58° 24,8750' W	02:20:52	723	same material
535	62° 26,4968' S	58° 24,8254' W	0	62° 26,5406' S	58° 24,8757' W	02:23:11	751	coarse-grained sediment has slightly changed to sedimented talus
536	62° 26,4854' S	58° 24,8096' W	0	62° 26,5165' S	58° 24,8629' W	02:25:27	773	number of brittle stars increases again
537	62° 26,4787' S	58° 24,8065' W	0	62° 26,4981' S	58° 24,8554' W	02:27:07	787	white critters??

<i>Ship Nr</i>	<i>Ship Latitude</i>	<i>Ship Longitude</i>	<i>Hydrosweep Depth [m]</i>	<i>Sub1 Latitude</i>	<i>Sub1 Longitude</i>	<i>Time [UTC]</i>	<i>CTD [m]</i>	<i>Remark</i>
538	62° 26,4697' S	58° 24,7937' W	0	62° 26,5009' S	58° 24,8383' W	02:28:22	795	rocky outcrop; Fe-oxyhydroxide cone?
539	62° 26,4645' S	58° 24,7815' W	0	62° 26,4848' S	58° 24,8170' W	02:29:05	798	downward the cliff; colonies of brittle stars; small ridge
540	62° 26,4584' S	58° 24,7664' W	0	62° 26,4846' S	58° 24,8661' W	02:29:55	802	again small ridge
541	62° 26,4523' S	58° 24,7547' W	0	62° 26,4808' S	58° 25,0070' W	02:30:39	810	temperature is rising
542	62° 26,4433' S	58° 24,7401' W	0	62° 26,4693' S	58° 24,8019' W	02:31:39	816	sedimented talus
543	62° 26,4296' S	58° 24,7391' W	0	62° 26,4558' S	58° 24,7950' W	02:32:46	825	rocks outcrops, largely sedimented
544	62° 26,4116' S	58° 24,7493' W	0	62° 26,4488' S	58° 24,7734' W	02:33:57	834	relatively steep cliff
545	62° 26,3958' S	58° 24,7266' W	0	62° 26,4529' S	58° 24,7915' W	02:35:22	854	sedimented talus, brittle stars, rocky outcrops
546	62° 26,3887' S	58° 24,7104' W	0	62° 26,4224' S	58° 24,7889' W	02:36:59	867	more fine-grained sediment, number of brittle stars increases again
547	62° 26,3876' S	58° 24,6882' W	0	62° 26,4141' S	58° 24,7635' W	02:38:16	867	flat sedimented terrace, not much biology
548	62° 26,3814' S	58° 24,6592' W	0	62° 26,4059' S	58° 24,7620' W	02:39:34	864	again sedimented talus
549	62° 26,3660' S	58° 24,6379' W	0	62° 26,4069' S	58° 24,7224' W	02:41:12	858	more fine-grained sediments
550	62° 26,3481' S	58° 24,6172' W	0	62° 26,4013' S	58° 24,6889' W	02:42:58	852	big blocks, sedimented
551	62° 26,3449' S	58° 24,6111' W	0	62° 26,3862' S	58° 24,6810' W	02:43:35	848	sedimented talus
552	62° 26,3359' S	58° 24,5836' W	0	62° 26,3693' S	58° 24,6608' W	02:45:44	828	big block, outcrop
553	62° 26,3293' S	58° 24,5647' W	0	62° 26,3543' S	58° 24,5907' W	02:46:48	814	large volcanic ridge
554	62° 26,3258' S	58° 24,5516' W	0	62° 26,3567' S	58° 24,6050' W	02:47:43	806	some volcanics show flow banding, pillow-like shapes
555	62° 26,3074' S	58° 24,5804' W	0	62° 26,3310' S	58° 24,5834' W	02:49:55	800	still sedimented blocky outcrop
556	62° 26,2669' S	58° 24,5638' W	0	62° 26,2948' S	58° 24,6245' W	02:54:23	816	still the same feature
557	62° 26,2526' S	58° 24,5873' W	0	62° 26,2792' S	58° 24,6004' W	02:55:39	824	moving downwards, more talus-like
558	62° 26,2366' S	58° 24,5987' W	0	62° 26,2856' S	58° 24,5919' W	02:57:10	836	getting more blocky again

Ship Nr	Ship Latitude	Ship Longitude	Hydrosweep Depth [m]	Sub1 Latitude	Sub1 Longitude	Time [UTC]	CTD [m]	Remark
559	62° 26,2181' S	58° 24,5315' W	0	62° 26,2470' S	58° 24,6053' W	02:59:48	866	small scarp, increased sediment thickness; slightly more biological activity
560	62° 26,1959' S	58° 24,5605' W	0	62° 26,2279' S	58° 24,5485' W	03:01:29	885	sedimented talus
561	62° 26,1520' S	58° 24,5587' W	0	62° 26,1886' S	58° 24,5867' W	03:05:07	921	sedimented talus
562	62° 26,1477' S	58° 24,5401' W	0	62° 26,1904' S	58° 24,5784' W	03:05:59	927	big block with sponges(?)
563	62° 26,1322' S	58° 24,5009' W	0	62° 26,1538' S	58° 24,5212' W	03:09:42	957	fine-grained sediments, brittle stars, single blocks
564	62° 26,0687' S	58° 24,5259' W	0	62° 26,0837' S	58° 24,5482' W	03:15:18	990	heavily sedimented terrain, talus blocks
565	62° 26,0558' S	58° 24,4559' W	0	62° 26,0774' S	58° 24,5272' W	03:18:58	1008	lava tube?
566	62° 26,0553' S	58° 24,4512' W	0	62° 26,0793' S	58° 24,5215' W	03:19:17	1009	pillow lava with striations
567	62° 26,0511' S	58° 24,4448' W	0	62° 26,0717' S	58° 24,5174' W	03:20:17	1013	nice pillows moving down a small flat cliff
568	62° 26,0392' S	58° 24,4612' W	0	62° 26,0678' S	58° 24,4645' W	03:21:23	1020	big pillows
569	62° 26,0327' S	58° 24,4334' W	0	62° 26,0573' S	58° 24,4903' W	03:22:53	1026	blocky ridge
570	62° 26,0352' S	58° 24,4052' W	0	62° 26,0492' S	58° 24,4874' W	03:23:29	1028	flat sedimented area
571	62° 26,0360' S	58° 24,3941' W	0	62° 26,0606' S	58° 24,4807' W	03:23:48	1028	outcrop/talus again, pillows
572	62° 26,0204' S	58° 24,3977' W	0	62° 26,0340' S	58° 24,4512' W	03:25:46	1033	black sponges/rubber boots
573	62° 25,9969' S	58° 24,3732' W	0	62° 26,0359' S	58° 24,4202' W	03:27:25	1038	flat sedimented area
574	62° 25,9831' S	58° 24,3635' W	0	62° 26,0302' S	58° 24,4372' W	03:28:23	1041	soft fine-grained sediment, few brittle stars
575	62° 25,9499' S	58° 24,3837' W	0	62° 26,0090' S	58° 24,3879' W	03:30:20	1048	the end of OFOS 41; heaving to 900m
576	62° 25,9403' S	58° 24,3618' W	0	62° 25,9935' S	58° 24,4046' W	03:31:20	1033	tapes off

SONNE - 155



106 Records

SO 155**45 OFOS****Freitag, 9. März 2001**

<i>Ship Nr</i>	<i>Ship Latitude</i>	<i>Ship Longitude</i>	<i>Hydrosweep Depth [m]</i>	<i>Sub1 Latitude</i>	<i>Sub1 Longitude</i>	<i>Time [UTC]</i>	<i>CTD [m]</i>	<i>Remark</i>
580	62° 58,3594' S	60° 38,9995' W	113	62° 25,9202' S	58° 24,4129' W	18:30:53	13	on station, OFOS checked
581	62° 58,3621' S	60° 39,0677' W	110	62° 25,9202' S	58° 24,4129' W	18:35:26	13	station begin
582	62° 58,3603' S	60° 38,9846' W	113	62° 25,9202' S	58° 24,4129' W	18:38:05	13	OFOS start point is close to 62°58.5 S and 60°39.0 W and heading on a N course over the implied fault scarps running from Fumarole Bay to Macaroni Point.
583	62° 58,3747' S	60° 38,9922' W	110	62° 25,9202' S	58° 24,4129' W	18:41:52	16	OFOS in the water
584	62° 58,4005' S	60° 38,9692' W	108	62° 58,3843' S	60° 38,8141' W	18:46:13	29	video on, winch operator changed to geology lab
585	62° 58,3944' S	60° 39,0129' W	108	62° 58,3760' S	60° 38,8455' W	18:47:59	0	power failure, station failed, OFOS comes back up
586	62° 58,2154' S	60° 40,2413' W	0	62° 58,3760' S	60° 38,8455' W	21:59:26	13	the focus of this OFOS (at a new target where Rey et al., provide geochemical evidence for hydrothermal mineralization) is at 62°59.00'S / 60°38.00'W. OFOS track is now to the east.
587	62° 59,0146' S	60° 38,1045' W	0	62° 58,3760' S	60° 38,8455' W	22:21:44	13	almost on station
588	62° 59,0145' S	60° 38,0610' W	0	62° 58,3760' S	60° 38,8455' W	22:24:52	14	OFOS in the water
589	62° 58,9891' S	60° 38,0620' W	0	62° 58,9949' S	60° 37,8954' W	22:27:59	27	winch operator changed to the geology lab
590	62° 58,9871' S	60° 38,0854' W	0	62° 58,9946' S	60° 38,1241' W	22:30:44	91	thick sediment, murky water, seastars, blocky pieces
591	62° 58,9918' S	60° 38,0664' W	0	62° 58,9992' S	60° 38,1087' W	22:31:52	92	video on
592	62° 58,9922' S	60° 38,0636' W	0	62° 58,9992' S	60° 38,1087' W	22:32:00	92	abundant urchins (?), actually the floor is covered with them

<i>Ship Nr</i>	<i>Ship Latitude</i>	<i>Ship Longitude</i>	<i>Hydrosweep Depth [m]</i>	<i>SubI Latitude</i>	<i>SubI Longitude</i>	<i>Time [UTC]</i>	<i>CTD [m]</i>	<i>Remark</i>
593	62° 58,9981' S	60° 38,0417' W	0	62° 59,0066' S	60° 38,0812' W	22:33:36	93	still heavily sedimented with abundant urchins and few seastars
594	62° 58,9911' S	60° 38,0238' W	0	62° 59,0042' S	60° 38,0577' W	22:35:48	95	still the same, often white elongated critters
595	62° 58,9916' S	60° 38,0025' W	0	62° 58,9972' S	60° 38,0417' W	22:37:44	97	abundant urchins, few seastars, trace white tubular animals (?)
596	62° 59,0055' S	60° 37,9751' W	0	62° 59,0106' S	60° 38,0202' W	22:39:35	100	minor rock outcrops or ash
597	62° 59,0040' S	60° 37,9383' W	0	62° 59,0175' S	60° 37,9705' W	22:41:04	100	just hit different water mass, temperature went down considerably and then came up again
598	62° 58,9950' S	60° 37,9234' W	0	62° 59,0081' S	60° 37,9591' W	22:42:09	102	several (100) urchins per field of view
599	62° 58,9901' S	60° 37,9072' W	0	62° 58,9966' S	60° 37,9462' W	22:43:53	103	few tube-like white things in a sea of urchins
600	62° 58,9965' S	60° 37,8365' W	0	62° 59,0076' S	60° 37,8690' W	22:47:24	105	sediment with animal clusters (tube?), temperature and conductivity are changing rapidly
601	62° 58,9936' S	60° 37,8117' W	0	62° 59,0004' S	60° 37,8485' W	22:49:46	106	white patches, diffuse; pink holothurians
602	62° 59,0025' S	60° 37,7927' W	0	62° 59,0098' S	60° 37,8261' W	22:51:24	106	larger areas with dark cover (ash?)
603	62° 59,0052' S	60° 37,7782' W	0	62° 59,0146' S	60° 37,8148' W	22:52:13	105	still in a sea of urchins, lots of flocs in the water
604	62° 59,0002' S	60° 37,7557' W	0	62° 59,0147' S	60° 37,7812' W	22:53:56	107	very abundant urchins in thick sediment
605	62° 58,9939' S	60° 37,7329' W	0	62° 59,0048' S	60° 37,7669' W	22:55:44	108	we moved the camera up a bit, the temperature anomalies are not related to a layering of the water masses close to the bottom
606	62° 58,9951' S	60° 37,7160' W	0	62° 59,0028' S	60° 37,7523' W	22:56:33	108	few anemones; there must be some rocks somewhere
607	62° 59,0019' S	60° 37,6899' W	0	62° 59,0123' S	60° 37,7179' W	22:58:24	109	abundant urchins
608	62° 59,0029' S	60° 37,6793' W	0	62° 59,0152' S	60° 37,7018' W	22:59:17	108	clusters of anemones
609	62° 58,9926' S	60° 37,6524' W	0	62° 59,0080' S	60° 37,6845' W	23:01:02	109	same sediment
610	62° 58,9893' S	60° 37,6442' W	0	62° 59,0028' S	60° 37,6777' W	23:01:25	109	fewer urchins for a while, however, the distribution is patchy as well
611	62° 58,9827' S	60° 37,6215' W	0	62° 58,9930' S	60° 37,6525' W	23:02:55	110	the water is getting murkier, OFOS almost stopped

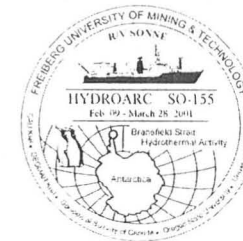
<i>Ship Nr</i>	<i>Ship Latitude</i>	<i>Ship Longitude</i>	<i>Hydrosweep Depth [m]</i>	<i>Subl Latitude</i>	<i>Subl Longitude</i>	<i>Time [UTC]</i>	<i>CTD [m]</i>	<i>Remark</i>
612	62° 58,9905' S	60° 37,6171' W	0	62° 58,9963' S	60° 37,6503' W	23:04:41	111	OFOS seems to go backwards now, just had a small (0.05°C) temperature anomaly; incursion of slightly warmer water
613	62° 59,0048' S	60° 37,5954' W	0	62° 59,0146' S	60° 37,6298' W	23:06:18	109	in sedimented area with less urchins
614	62° 59,0092' S	60° 37,5762' W	0	62° 59,0203' S	60° 37,6110' W	23:07:11	108	back to normal urchin coverage
615	62° 59,0124' S	60° 37,5436' W	0	62° 59,0235' S	60° 37,5834' W	23:08:22	107	climbing (? not really) a small hill, the Mn-mound area should be several 100m away
616	62° 59,0137' S	60° 37,5193' W	0	62° 59,0259' S	60° 37,5528' W	23:09:19	107	warm water incursion again (>0.1°C)
617	62° 59,0125' S	60° 37,5010' W	0	62° 59,0271' S	60° 37,5260' W	23:10:24	107	there goes the hill, going down (very slowly, temperature stays elevated)
618	62° 59,0058' S	60° 37,4704' W	0	62° 59,0184' S	60° 37,5022' W	23:12:20	111	back to urchins in sediment and temperature down, too
619	62° 59,0071' S	60° 37,4512' W	0	62° 59,0183' S	60° 37,4825' W	23:13:28	112	clusters of branching animals
620	62° 59,0056' S	60° 37,4285' W	0	62° 59,0203' S	60° 37,4539' W	23:15:21	112	black patches (due to bioturbation, fewer urchins, more abundant brittle stars; some jellyish pink holothurians)
621	62° 58,9999' S	60° 37,3925' W	0	62° 59,0100' S	60° 37,4271' W	23:17:20	110	corals; black tubular things
622	62° 59,0005' S	60° 37,3797' W	0	62° 59,0108' S	60° 37,4112' W	23:18:09	109	massive urchin assemblage, less brittle stars
623	62° 59,0013' S	60° 37,3641' W	0	62° 59,0122' S	60° 37,3982' W	23:18:54	109	rope, black things
624	62° 59,0008' S	60° 37,3379' W	0	62° 59,0134' S	60° 37,3661' W	23:19:47	110	pink holothurians, anemone, less urchins
625	62° 58,9976' S	60° 37,3132' W	0	62° 59,0106' S	60° 37,3381' W	23:20:50	113	fewer urchins
626	62° 58,9935' S	60° 37,2941' W	0	62° 59,0047' S	60° 37,3215' W	23:22:01	114	the darker patchy (bioturbed) area with few urchins
627	62° 58,9929' S	60° 37,2788' W	0	62° 59,0028' S	60° 37,3103' W	23:22:52	113	britte stars are back on line
628	62° 58,9966' S	60° 37,2602' W	0	62° 59,0050' S	60° 37,2939' W	23:23:47	111	more abundant urchins
629	62° 59,0082' S	60° 37,2499' W	0	62° 59,0143' S	60° 37,2828' W	23:25:12	108	few urchins in thick homogeneous sediment cover

<i>Ship Nr</i>	<i>Latitude</i>	<i>Ship Longitude</i>	<i>Hydrosweep Depth [m]</i>	<i>Subl Latitude</i>	<i>Subl Longitude</i>	<i>Time [UTC]</i>	<i>CTD [m]</i>	<i>Remark</i>
630	62° 59,0135' S	60° 37,2478' W	0	62° 59,0224' S	60° 37,2757' W	23:25:52	107	number of brittle stars is increasing (?)
631	62° 59,0192' S	60° 37,2353' W	0	62° 59,0278' S	60° 37,2694' W	23:26:51	105	no change (despite few bag things floating around)
632	62° 59,0190' S	60° 37,2196' W	0	62° 59,0322' S	60° 37,2504' W	23:27:37	105	urchins and few seastars, have not seen hard rock geology for a while
633	62° 59,0177' S	60° 37,2127' W	0	62° 59,0306' S	60° 37,2446' W	23:27:57	104	pink holothurians
634	62° 59,0151' S	60° 37,2021' W	0	62° 59,0288' S	60° 37,2323' W	23:28:25	104	abundant urchins, some black things
635	62° 59,0092' S	60° 37,1859' W	0	62° 59,0238' S	60° 37,2167' W	23:29:22	105	same sediment
636	62° 59,0027' S	60° 37,1765' W	0	62° 59,0168' S	60° 37,2031' W	23:30:26	107	sediment and urchins
637	62° 58,9993' S	60° 37,1649' W	0	62° 59,0119' S	60° 37,1979' W	23:31:08	110	less urchins
638	62° 58,9982' S	60° 37,1498' W	0	62° 59,0091' S	60° 37,1857' W	23:31:45	111	more brittle stars than urchins
639	62° 59,0054' S	60° 37,0994' W	0	62° 59,0144' S	60° 37,1319' W	23:33:51	109	less urchins, some brittle stars, no pink holothurians
640	62° 59,0088' S	60° 37,0816' W	0	62° 59,0203' S	60° 37,1102' W	23:34:58	107	few urchins in thick sediment
641	62° 59,0059' S	60° 37,0620' W	0	62° 59,0200' S	60° 37,0882' W	23:36:13	107	increasing numbers of urchins
642	62° 58,9980' S	60° 37,0343' W	0	62° 59,0080' S	60° 37,0696' W	23:38:04	107	same sediment
643	62° 59,0067' S	60° 36,9951' W	0	62° 59,0152' S	60° 37,0251' W	23:40:48	107	no change in sedimentation or biology
644	62° 59,0106' S	60° 36,9945' W	0	62° 59,0180' S	60° 37,0246' W	23:41:18	106	few brittle stars, some pink holothurians in groups (?)
645	62° 59,0158' S	60° 36,9619' W	0	62° 59,0305' S	60° 36,9911' W	23:44:28	106	finally a rock, but only a small one then back to the same, urchins and seastars
646	62° 58,9994' S	60° 36,9198' W	0	62° 59,0132' S	60° 36,9453' W	23:46:59	111	undulations in depth seem to represent burried fault scarps. This is also indicated by the small temperature anomalies (leakage?)
647	62° 59,0019' S	60° 36,8802' W	0	62° 59,0123' S	60° 36,9102' W	23:49:14	111	same sediment, same urchins
648	62° 59,0025' S	60° 36,8716' W	0	62° 59,0148' S	60° 36,9004' W	23:49:38	111	more small brittle stars (?)
649	62° 59,0013' S	60° 36,8501' W	0	62° 59,0161' S	60° 36,8711' W	23:50:58	113	cold freshwater incursion (?)

Ship Nr	Ship Latitude	Ship Longitude	Hydrosweep Depth [m]	Subl Latitude	Subl Longitude	Time [UTC]	CTD [m]	Remark
650	62° 58,9986' S	60° 36,8402' W	0	62° 59,0130' S	60° 36,8649' W	23:51:41	114	the black patches (bioturbation?) are back
651	62° 58,9950' S	60° 36,8248' W	0	62° 59,0078' S	60° 36,8531' W	23:52:21	114	clearly less abundant urchins
652	62° 59,0011' S	60° 36,7844' W	0	62° 59,0074' S	60° 36,8154' W	23:54:04	116	still darker patches and less urchins in the sediment
653	62° 59,0088' S	60° 36,7800' W	0	62° 59,0152' S	60° 36,8105' W	23:54:56	115	pink holothurians, still dark patches (bioturbation)
654	62° 59,0189' S	60° 36,7758' W	0	62° 59,0263' S	60° 36,8034' W	23:56:02	114	almost a rocky outcrop
655	62° 59,0225' S	60° 36,7760' W	0	62° 59,0348' S	60° 36,7969' W	23:56:36	114	same dark patches in the sediment
656	62° 59,0240' S	60° 36,7758' W	0	62° 59,0368' S	60° 36,7955' W	23:57:14	114	few urchins and pink holothurians
657	62° 59,0187' S	60° 36,7497' W	0	62° 59,0353' S	60° 36,7739' W	23:58:34	115	few diffuse white patches, some brittle stars, mottled texture
658	62° 59,0112' S	60° 36,7330' W	0	62° 59,0285' S	60° 36,7594' W	23:59:25	116	pink holothurians occur in clusters, increasing number of urchins
659	62° 59,0077' S	60° 36,6797' W	0	62° 59,0153' S	60° 36,7118' W	00:02:22	118	same sediment and biology
660	62° 59,0067' S	60° 36,6206' W	0	62° 59,0203' S	60° 36,6487' W	00:04:00	119	we are trying to turn (port) to get on a NW course. We think we missed the target a bit and went too far south.
661	62° 59,0004' S	60° 36,6201' W	0	62° 59,0158' S	60° 36,6304' W	00:04:55	120	OFOS is turning now, more diffuse white patches on the bottom
662	62° 58,9896' S	60° 36,6209' W	0	62° 59,0113' S	60° 36,6317' W	00:05:40	119	the wind will come from the back, something bush-like just passed by, still mottled dark/light texture
663	62° 58,9638' S	60° 36,6594' W	0	62° 58,9854' S	60° 36,6598' W	00:07:57	121	still mottled sediment, few urchins, anemone
664	62° 58,9572' S	60° 36,6893' W	0	62° 58,9762' S	60° 36,6842' W	00:08:57	121	the water here is clearly not as murky as it was when we began out track
665	62° 58,9431' S	60° 36,7036' W	0	62° 58,9613' S	60° 36,7116' W	00:10:09	121	mottled textured sediment
666	62° 58,9297' S	60° 36,7010' W	0	62° 58,9458' S	60° 36,7188' W	00:11:15	121	pink holothurians cluster in mottled sediment
667	62° 58,9250' S	60° 36,7253' W	0	62° 58,9387' S	60° 36,7399' W	00:12:32	121	mottled sediment few urchins
668	62° 58,9218' S	60° 36,7539' W	0	62° 58,9370' S	60° 36,7607' W	00:13:18	121	dark patch and a rock

<i>Ship Nr</i>	<i>Ship Latitude</i>	<i>Ship Longitude</i>	<i>Hydrosweep Depth [m]</i>	<i>Sub1 Latitude</i>	<i>Sub1 Longitude</i>	<i>Time [UTC]</i>	<i>CTD [m]</i>	<i>Remark</i>
669	62° 58,9124' S	60° 36,7805' W	0	62° 58,9322' S	60° 36,8059' W	00:14:43	121	still mottled sediment with few urchins
670	62° 58,9020' S	60° 36,7933' W	0	62° 58,9199' S	60° 36,8004' W	00:16:15	121	huge cluster of pink holothurians
671	62° 58,8962' S	60° 36,8019' W	0	62° 58,9143' S	60° 36,8214' W	00:17:04	121	no change
672	62° 58,8908' S	60° 36,8026' W	0	62° 58,9007' S	60° 36,8289' W	00:18:38	121	mottled sediment, few urchins and pink holothurians
673	62° 58,9072' S	60° 36,8654' W	0	62° 58,9059' S	60° 36,8960' W	00:21:08	121	no change, mottled sediment
674	62° 58,9203' S	60° 36,8797' W	0	62° 58,9223' S	60° 36,9010' W	00:22:01	120	sediment thickness is increasing, dark patches dissappear
675	62° 58,9273' S	60° 36,8910' W	0	62° 58,9266' S	60° 36,9211' W	00:22:33	121	another one of theses bushes
676	62° 58,9442' S	60° 36,8886' W	0	62° 58,9490' S	60° 36,9181' W	00:23:35	119	slight temperature increase, more urchins
677	62° 58,9697' S	60° 36,9057' W	0	62° 58,9825' S	60° 36,9210' W	00:26:22	117	thicker sediment, bush, increasing number of brittle stars
678	62° 58,9745' S	60° 36,9456' W	0	62° 58,9906' S	60° 36,9539' W	00:28:32	117	rocky outcrop, have we seen this one before? We are very close to our original track!
679	62° 58,9713' S	60° 36,9596' W	0	62° 58,9879' S	60° 36,9671' W	00:29:20	117	more brittle stars in sediment
680	62° 58,9619' S	60° 36,9868' W	0	62° 58,9805' S	60° 36,9898' W	00:30:45	117	more brittle stars
681	62° 58,9424' S	60° 37,0204' W	0	62° 58,9626' S	60° 37,0228' W	00:32:47	118	mottled sediment with pink holothurians cluster
682	62° 58,9332' S	60° 37,0430' W	0	62° 58,9529' S	60° 37,0443' W	00:33:44	119	more urchins coming this way, mottled sediment
683	62° 58,9172' S	60° 37,0457' W	0	62° 58,9282' S	60° 37,0695' W	00:35:44	118	mottled sediment
684	62° 58,9190' S	60° 37,1301' W	0	62° 58,9376' S	60° 37,1296' W	00:40:03	120	OFOS off bottom, video turned off, OFOS will be taken up and than ship and OFOS are moved to the second track.
685	62° 58,0134' S	60° 39,0779' W	0	62° 58,9334' S	60° 37,1594' W	01:09:46	13	on station (for station 46-OFOS)

SONNE - 155



42 Records

SO 155**46 OFOS****Samstag, 10. März 2001**

Ship Nr	Ship Latitude	Ship Longitude	Hydrosweep Depth [m]	Subl Latitude	Subl Longitude	Time [UTC]	CTD [m]	Remark
686	62° 58,0077' S	60° 39,0437' W	0	0	0	01:16:16	142	bottom sight in thick sediment, urchins
687	62° 58,0105' S	60° 39,0411' W	0	0	0	01:18:18	142	snow blower
688	62° 57,9951' S	60° 39,0316' W	0	0	0	01:22:00	144	heavy sediment on seafloor; lots of particulate in water column
689	62° 57,9796' S	60° 39,0257' W	0	0	0	01:25:24	148	black patterns on the seafloor
690	62° 57,9637' S	60° 39,0199' W	0	0	0	01:27:24	150	a small rock
691	62° 57,9409' S	60° 39,0153' W	0	0	0	01:30:40	155	black patterns on seafloor (ash bombs and tephra)
692	62° 57,9085' S	60° 39,0296' W	0	0	0	01:34:11	163	more black tephra, ash bombs
693	62° 57,9021' S	60° 39,0298' W	0	0	0	01:35:04	165	some kind of sea bush; within sediments
694	62° 57,8975' S	60° 39,0327' W	0	0	0	01:35:39	165	some pink holothurians
695	62° 57,8813' S	60° 39,0293' W	0	0	0	01:37:35	170	more black patterns (tephra or ash bombs); lots of material in the water column
696	62° 57,8757' S	60° 39,0231' W	0	0	0	01:38:21	171	weight just dragged the bottom, very dark material kicked up, fine ash?
697	62° 57,8675' S	60° 39,0195' W	0	0	0	01:39:31	170	white pathes in the midst of the black patches
698	62° 57,8604' S	60° 39,0257' W	0	0	0	01:40:41	170	more white and black patches
699	62° 57,8426' S	60° 39,0402' W	0	0	0	01:42:50	171	slight increase in temperature and conductivity, constant depth
700	62° 57,8386' S	60° 39,0407' W	0	0	0	01:43:15	170	mix of white and dark patches continues, white patches perhaps bacteria?

<i>Ship Nr</i>	<i>Ship Latitude</i>	<i>Ship Longitude</i>	<i>Hydrosweep Depth [m]</i>	<i>Subl Latitude</i>	<i>Subl Longitude</i>	<i>Time [UTC]</i>	<i>CTD [m]</i>	<i>Remark</i>
701	62° 57,8292' S	60° 39,0329' W	0	0	0	01:44:23	170	sudden drop in temperature and conductivity, depth constant
702	62° 57,8174' S	60° 39,0097' W	0	0	0	01:47:10	170	minor white patches amongst black ones, variable temperature and conductivity, due to cold freshwater input
703	62° 57,7997' S	60° 39,0141' W	0	0	0	01:49:41	170	a fair amount of bioluminescent organisms in the water column
704	62° 57,7818' S	60° 39,0208' W	0	0	0	01:51:22	170	still more black patches within thick sediment, some minor white patches
705	62° 57,7591' S	60° 39,0310' W	0	0	0	01:53:22	170	slight increase in white patches, dark sediment (ash) kicked up by weight
706	62° 57,7203' S	60° 39,0222' W	0	0	0	01:58:06	170	white patches amongst dark sediment patches
707	62° 57,7120' S	60° 39,0221' W	0	0	0	01:59:28	170	very dark sediment kicked up by weight
708	62° 57,7089' S	60° 39,0220' W	0	0	0	01:59:53	170	starfish
709	62° 57,6857' S	60° 39,0163' W	0	0	0	02:02:30	170	more dark sediment kicked up by weight
710	62° 57,6647' S	60° 39,0086' W	0	0	0	02:05:07	170	very dark sediment kicked up by weight
711	62° 57,6580' S	60° 39,0069' W	0	0	0	02:06:00	170	heavy particulate action in the water column
712	62° 57,6506' S	60° 39,0067' W	0	0	0	02:06:49	170	sharper drop in conductivity than water temperature
713	62° 57,6412' S	60° 39,0071' W	0	0	0	02:07:55	170	very murky water column, bottom not easily perceptible, rare sea bush
714	62° 57,6251' S	60° 38,9961' W	0	0	0	02:09:55	171	sediment less dark when kicked up by weight
715	62° 57,6227' S	60° 38,9928' W	0	0	0	02:10:15	171	dark patch, kinda all by itself amongst typical greyish sediment
716	62° 57,6155' S	60° 38,9867' W	0	0	0	02:11:20	170	dark patches, stringy white elongate object, soupy water
717	62° 57,5916' S	60° 39,0143' W	0	0	0	02:14:34	169	very very murky water column
718	62° 57,5828' S	60° 39,0171' W	0	0	0	02:15:30	170	bottom barely perceptible, small particulate dominates the water column

<i>Ship Nr</i>	<i>Ship Latitude</i>	<i>Ship Longitude</i>	<i>Hydrosweep Depth [m]</i>	<i>Subl Latitude</i>	<i>Subl Longitude</i>	<i>Time [UTC]</i>	<i>CTD [m]</i>	<i>Remark</i>
719	62° 57,5627' S	60° 39,0058' W	0	0	0	02:17:35	170	bottom pretty much imperceptible
720	62° 57,5512' S	60° 38,9988' W	0	0	0	02:19:02	170	lowest conductivity and temperature, so far
721	62° 57,5367' S	60° 38,9849' W	0	0	0	02:21:12	170	elongate stringy white material
722	62° 57,5261' S	60° 38,9739' W	0	0	0	02:23:13	170	still in very murky water
723	62° 57,4880' S	60° 38,9897' W	0	0	0	02:27:49	170	more white elongate tubular material
724	62° 57,4652' S	60° 38,9960' W	0	0	0	02:30:09	170	dark sediment kicked up by weight
725	62° 57,4492' S	60° 38,9909' W	0	0	0	02:32:49	170	still very murky water column
726	62° 57,4439' S	60° 38,9896' W	0	0	0	02:33:42	170	more stringy tubular material
727	62° 57,4048' S	60° 38,9791' W	0	0	0	02:38:45	165	end dive